UNIVERSITEIT GENT

FACULTEIT GENEESKUNDE EN GEZONDHEIDSWETENSCHAPPEN

Modulation of the reactivity of the vessel wall by local substances derived from the endothelium and perivascular nerves

Thesis submitted in fulfilment of the requirements for the degree of "Doctor in de Biomedische Wetenschappen"

Joke Breyne

Promotor: Prof. Dr. Bert Vanheel

Table of contents

Abbreviations

$[Ca^{2+}]_i$	intracellular Ca^{2+} concentration
$[K^+]_o$	extracellular potassium concentration
AM	acetoxymethyl
ATP	adenosine triphosphate
BK_{Ca} channel	large conductance Ca^{2+} activated K^+ channel
CB_1	type 1 cannabinoid receptor
CB_2	type 2 cannabinoid receptor
CB_x	non-CB_1/non-CB_2 receptor
CGRP	calcitonine gene-related peptide
CNP	C-type natriuretic peptide
COX	cyclooxygenase
Cx	connexin
CYP	cytochrome P450 epoxygenase
DMSO	dimethylsulfoxide
EDCF	endothelium-derived contracting factor
EDHF	endothelium-derived hyperpolarizing factor
EDRF	endothelium-derived relaxing factor
EET	epoxyeicosatrienoic acid
E_m	membrane potential
eNOS	endothelial nitric oxide synthase
GPCR	G-protein-coupled receptor
H_2O_2	hydrogen peroxide
HBSS-HEPES	Hanks' balanced salt solution buffered with 25 mM HEPES
IEL	internal elastic lamina
IK_{Ca} channel	intermediate conductance Ca^{2+} activated K^+ channel
iNOS	inducible nitric oxide synthase
IP_3	inositoltrisphosphate
K_{120}	Krebs-Ringer bicarbonate solution containing 120 mM K^+
K_{30}	Krebs-Ringer bicarbonate solution containing 30 mM K^+

K_{ATP} channel	ATP sensitive K^+ channel
K_{Ca} channel	Ca^{2+} activated K^+ channels
K_{IR} channel	inwardly rectifying K^+ channel
KRB solution	Krebs-Ringer bicarbonate solution
L-NA	N^{ω}-nitro-L-arginine
L-NAME	N^{ω}-nitro-L-arginine methyl ester
NKA	neurokinin A
NKB	neurokinin B
nNOS	neuronal nitric oxide synthase
NO	nitric oxide
NOR	norepinephrine
NOS	nitric oxide synthase
NPY	neuropeptide Y
PGI_2	prostacyclin
PSS	physiological salt solution
PVN	perivascular nerves
SACC	stretch activated Ca^{2+} channel
SERCA	sarco/endoplasmic reticulum Ca^{2+} ATPase
sGC	soluble guanylate cyclase
SK_{Ca} channel	small conductance Ca^{2+} activated K^+ channel
TEA	tetraethylammoniumchloride
THC	tetrahydrocannabinol
$TRPV_1$	type 1 vanilloid receptor
$TRPV_4$	type 4 vanilloid receptor
VIP	vasoactive intestinal peptide

Chapter

1

General introduction

1.1. THE CARDIOVASCULAR SYSTEM: THE BODY'S LIFELINE

The cardiovascular circulation delivers blood to the individual organs and tissues and therefore is of utmost importance to maintain body function and survival. The blood flow is set to some degree by the number and size of arteries feeding the organ, but also varies according to the metabolic needs of the tissue in order to maintain homeostasis. Furthermore, it carries out compensatory adjustments to challenges faced in everyday life (e.g. gravitational changes or exercise) or in disease (e.g. inflammation, shock or hypertension). One of the most important ways to control the blood flow through a vascular bed is by alteration of the diameter of the resistance vessels. Neural, humoral or local chemical mechanisms dilate or constrict the vessels of a tissue, thereby regulating the regional blood supply. The systemic circulation is made up of numerous circuits in parallel, which permits such wide regional variations in blood flow without affecting the total systemic flow.

In the present study, we concentrated on small mesenteric or gastric arteries, two vessels belonging to the splanchnic circulation (figure 1). The splanchnic circulation refers to the vascular system which brings blood to and from the major abdominal organs. It is one of the major blood reservoirs of the body, containing between 20 % (under resting conditions) and 40 % (after food intake) of total blood volume. The blood flow to the abdominal organs is arranged in a series of parallel circuits, with all the blood from the stomach, intestines, pancreas and spleen draining via the portal vein to the liver. From the liver, the blood continues via the hepatic veins to the inferior vena cava.

The gastrointestinal vasculature consists of intramural and extramural components. The intramural system contains plexuses in the different layers from the wall of the digestive tract and contains specialisations adapted to the functions of the different organs. The extramural arterial supply to the abdominal organs is provided by three major arteries arising from the thoracic aorta: the celiac trunk and the superior and inferior mesenteric arteries (figure 1). The branches of these vessels form an arcade network, providing a rich blood supply to the different organs. The main arterial blood supply to the stomach, for example, arises from the celiac axis. The common hepatic artery branches into the gastroduodenal artery and the right gastric artery, which then joins the left gastric artery along the lesser curvature of the stomach. Short gastric arteries and the right and left gastroepiploic arteries provide the blood supply along the greater curvature of the stomach. The intestines, on the other hand, are supplied by a series of parallel circulations via branches of the superior and inferior mesenteric arteries (figure 1).

Gastrointestinal blood flow varies locally along the alimentary canal. Several factors are implicated in the regulation of splanchnic circulation, e.g. neurohumoral or paracrine substances or food intake. The gastrointestinal blood flow can be regulated by changes in metabolism, but is also controlled by the autonomous nervous system.

Furthermore, some pathological conditions in the gastrointestinal system are associated with abnormalities in the splanchnic circulation. Gastrointestinal ischemia results from the obstruction of one of the major arteries of the splanchnic circulation. Collaterals open immediately to compensate for the resulting decrease in arterial pressure. The bowel may tolerate remarkable reductions in blood flow without damage. However,

below a certain crucial flow level ischemic damage will occur as a result of hypoxia. Regions with abundant collateral circulation, such as the stomach, duodenum and rectum, show a decreased risk for ischemic injury. Portal hypertension is one of the major complications of cirrhosis and results from increased resistance to portal blood flow. It is characterized by a pathologic increase in portal venous pressure that leads to the formation of an extensive network of collaterals that divert a large part of the portal blood to the systemic circulation, omitting the liver. In the later state, increased portal venous inflow, promoted by an increased splanchnic circulation, contributes to maintenance and aggravation of portal hypertension.

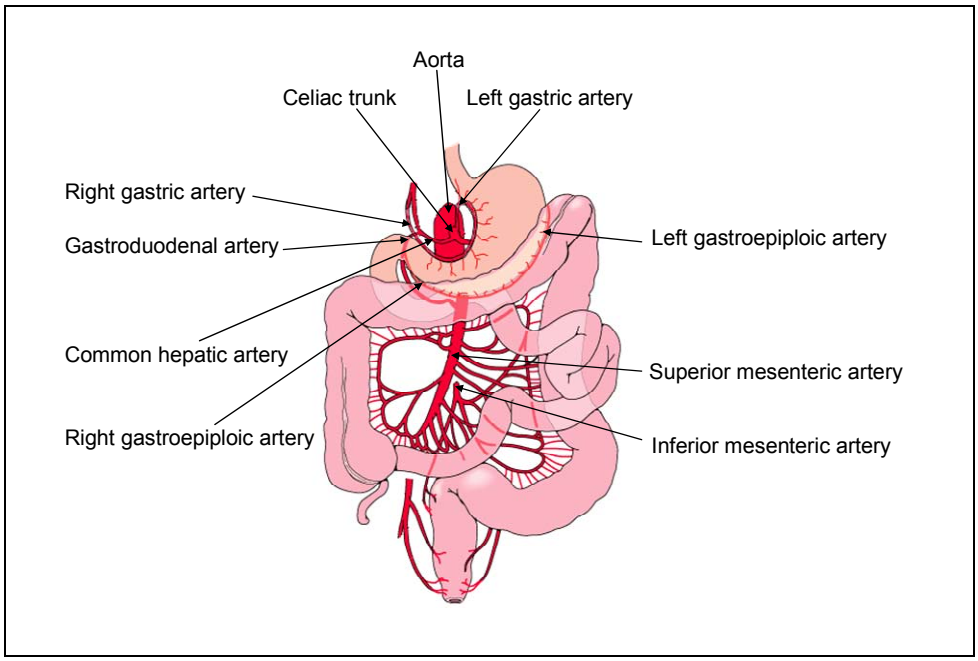

Figure 1: *Schematic overview of the splanchnic circulation, showing the most important arteries.*

Blood flow (F) through a vascular bed is directly proportional to the pressure gradient (ΔP) over the vascular bed and inversely proportional to the resistance (R) of the system to blood flow ($F \sim \Delta P/R$). In conditions of laminar flow, vascular resistance (R) is inversely related to the fourth power of the radius (r) of the blood vessel, as expressed in the equation of Poiseuille: $R = 8L\eta/\pi r^4$ (with L being the length of the vessel and η the viscosity of the blood). Consequently, blood flow is markedly affected by small changes in diameter of the vessels.

1.2. CARDIOVASCULAR LOCAL CONTROL MECHANISMS

As mentioned above, local control mechanisms match the perfusion of a given organ with its metabolic demands, despite variations in blood pressure. Blood flow in a vascular bed is regulated in part by autoregulation. Additionally, it is controlled by circulating or locally produced vasoactive metabolites and affected by substances secreted by the endothelium or the nerves innervating the vessel. All of these mechanisms influence blood flow by altering the diameter of the vessels.

1.2.1. Autoregulation

Most vascular beds have the intrinsic capacity to compensate for moderate changes in perfusion pressure by changing the vascular resistance, thereby keeping the blood flow relatively constant. This is referred to as autoregulation, a mechanism of which the importance varies among different vascular beds and seems to depend on the diameter of the arteries. It has been shown to be well developed in the kidney [1] and has

also been observed in cerebral and coronary arteries and the mesenteric vascular bed [2-5].

The exact mechanism by which autoregulation takes place is still elusive, but it has been proposed to rely on both myogenic and metabolic mechanisms. An increase in perfusion pressure (and thus also an increase in transmural pressure) distends the blood vessel wall causing contraction of the smooth muscle cells. Similar myogenic control has been shown to contribute significantly to autoregulation in different vascular beds such as the mesenteric, skeletal muscle, cerebral, renal and coronary circulation [1-4, 6, 7]. However, the exact mechanism responsible for this myogenic response remains unclear. Evidence suggests that it is accompanied by depolarisation of the membrane potential and an increase of the intracellular Ca^{2+} concentration of the vascular smooth muscle cells via activation of voltage operated Ca^{2+} channels [8, 9]. In case of metabolic regulation, changes in the concentration of local metabolites contribute to the autoregulation. For example, a decrease in perfusion of the vascular bed results in accumulation of metabolically produced vasodilatory substances and the subsequent dilatation of the blood vessel.

1.2.2. Vasoactive factors released by the endothelium

A single layer of endothelial cells lines the entire vascular system. The cell structure and functional integrity are important in the maintenance of the vessel wall and circulatory function. The endothelium is strategically located between the blood components on one hand and vascular smooth muscle cells in the blood vessel wall on the other. In 1980 Furchgott and Zawadzki reported that the relaxation response to acetylcholine and other agonists of

the muscarine receptor critically depended on the presence of a functional endothelium and hence demonstrated the existence of an endothelium-derived relaxing factor (EDRF) [10]. This pivotal observation in isolated rabbit arteries has since been extended to a wide range of arteries from different species including human [11]. At present it is known that the endothelium produces different vasodilating and vasoconstricting mediators, both under basal conditions and in response to different chemical or mechanical stimuli. The endothelial cells are activated by a number of agonists acting on G-protein-coupled receptors (GPCR), including acetylcholine, bradykinin, substance P and histamine or by physical stimuli such as shear stress or changes in oxygen levels. The former leads to the activation of stretch activated non-selective cation channels [12]. Activation of the endothelial cells results in an increase in their intracellular Ca^{2+} concentration ($[Ca^{2+}]_i$), triggering the release of several vasoactive mediators from the endothelium. The most important among them are discussed below.

1.2.2.1. Nitric oxide

A few years after the discovery of the EDRF, the agent responsible for a large portion of the endothelium-dependent relaxation has been identified as nitric oxide (NO) [13-15]. NO is synthesised from L-arginine by an enzyme known as nitric oxide synthase (NOS), which exists in three distinct isoforms: the constitutive enzymes endothelial NOS (eNOS) and neuronal NOS (nNOS) and the inducible NOS (iNOS). The endothelial eNOS catalyses within seconds the formation of small amounts (pM) of NO, required to maintain cardiovascular homeostasis. It is a Ca^{2+} - and calmodulin-dependent enzyme and requires a high intracellular Ca^{2+}

concentration [16]. The other constitutive enzyme, nNOS, is found in the central and the peripheral nervous system [17] and has similar characteristics as eNOS. Finally, the inducible isoform iNOS is especially found in inflamed or damaged tissues and catalyses the formation of large amounts (nM) of NO. Its activation does not require Ca^{2+} and the release of NO may continue for several hours or days.

Upon stimulation of the endothelial cells, the increased free $[Ca^{2+}]_i$ activates eNOS and thus the production of NO (figure 2). Subsequently, NO diffuses to the adjacent vascular smooth muscle cells where it interacts with soluble guanylate cyclase (sGC) causing an increase in cytosolic cGMP. cGMP subsequently reduces the intracellular Ca^{2+} concentration through multiple signaling pathways, finally causing relaxation (figure 2).

Several mechanisms are involved in this, each requiring a cGMP-dependent protein kinase. For example, cGMP activates plasma membrane Ca^{2+} ATPases, reducing the intracellular Ca^{2+} concentration [18-20]. On the other hand, $[Ca^{2+}]_i$ is lowered by stimulation of the Ca^{2+} reuptake in the endoplasmic reticulum through activation of the sarco/endoplasmic reticulum Ca^{2+} ATPase (SERCA) [21]. Additionally, cGMP causes Ca^{2+} desensitization of the contractile apparatus by activating myosin light chain phosphatases [22].

On the other hand, NO can also directly activate Ca^{2+}-dependent potassium channels in the vascular smooth muscle cells, promoting vasodilation through a cGMP-independent decrease in $[Ca^{2+}]_i$ [23, 24]. NO has also been reported to activate other K^+-channels [25-27] and Na^+/K^+-ATPases [28]. These pathways may be of crucial importance in atherosclerotic arteries, in which, according to some authors [23, 29], the cGMP-dependent pathway of

relaxation is compromised (although other studies report a reduced NO bioavailability which can be caused by a lack of L-arginine or cofactors or a reduced expression of NOS [30, 31]).

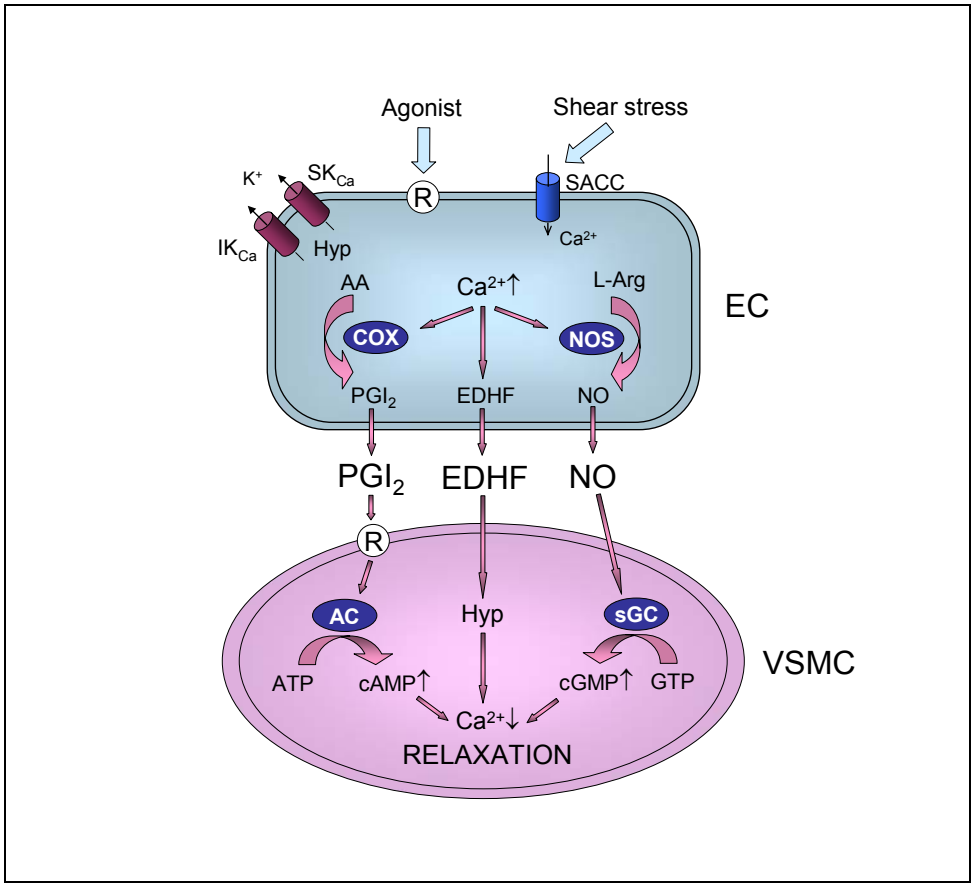

Figure 2: *Schematic overview of the different endothelium-derived relaxing factors. EC = endothelial cell; VSMC = vascular smooth muscle cell; R = receptor; SACC = stretch activated cation channel; L-Arg = L-arginine; NOS = nitric oxide synthase; NO = nitric oxide; sGC = soluble guanylate cyclase; AA = arachidonic acid; COX = cyclooxygenase; PGI_2 = prostacyclin; AC = adenylate cyclase; EDHF = endothelium-derived hyperpolarizing factor; SK_{Ca} = small conductance Ca^{2+} activated K^+ channels; IK_{Ca} = intermediate conductance Ca^{2+} activated K^+ channels; hyp = hyperpolarization.*

Since the discovery of the NO-pathway, several NOS inhibitors have been described and used to study the role of NO in endothelium-dependent relaxations. The production of NO can be inhibited by calmodulin antagonists in most arteries. However, these substances did not affect relaxations mediated by NO and evoked by agonists in canine and porcine coronary arteries [32]. The synthesis of NO can also be inhibited by analogues of L-arginine (e.g. N^{ω}-nitro-L-arginine (L-NA) and its methyl ester (L-NAME)) or inhibitors for the required cofactors of eNOS (e.g. flavoprotein inhibitors or depletors of tetrahydrobiopterin). More recently, selective inhibition of the endothelial NO production was obtained in mutant $eNOS^{-/-}$ mice where the gene encoding for eNOS was disrupted [33-35].

1.2.2.2. Prostaglandins

Prostaglandins are derivatives of arachidonic acid which are formed in various parts of the vascular wall in a reaction catalysed by cyclooxygenase (COX). Currently, two COX isoforms are known: COX-1 and COX-2. Both enzymes act basically in the same fashion. COX-1 is a constitutive enzyme and is expressed in a large number of cells. On the other hand, COX-2 is regarded as an inducible enzyme, undetectable in most normal tissues, which becomes abundant in activated macrophages and other cells at sites of inflammation. However, recent reports about the atherothrombotic side effects of some selective COX-2 inhibitors (coxibs), together with experimental and clinical studies, have shown that COX-2 can also be constitutively expressed in a variety of tissues. For example, constitutive expression of COX-2 has been reported in brain, kidney, gastrointestinal tissues and vascular endothelium [36-38].

Once activated by chemical or mechanical stimuli, the enzyme phospholipase A_2 in the endothelial cells of the vascular wall converts membrane phospholipids to arachidonic acid. COX converts arachidonic acid to prostaglandin H_2 which is then acted upon by various synthases resulting in the production of potent vasoactive prostaglandins. Prostacyclin (PGI_2) is the major vasodilator prostaglandin produced by the endothelium [39, 40] and causes relaxation predominantly through the adenylyl cyclase/cAMP transduction pathway (figure 2) [41, 42]. The formed cAMP activates protein kinase A to phosphorylate selective target proteins, thereby causing vasorelaxation [43]. Furthermore, several other vasoactive prostaglandins are produced by the endothelium upon activation of cyclooxygenase, such as the vasodilators PGE_2 [44] and PGD_2.

The production of prostaglandins can be blocked by the use of cyclooxygenase inhibitors such as indomethacin [45]. Recent studies obtained specific inhibition of prostacyclin synthesis with COX knock-out mice, in which the gene encoding for the COX-1 isoform was disrupted [34]. The fact that blood pressure is little affected in these mice, suggests that in normal physiological circumstances, prostaglandins play little role.

1.2.2.3. Endothelium-derived hyperpolarizing factor

In many vessels the pharmacological inhibition of both NOS (with L-arginine analogues) and cyclooxygenase (for example with indomethacin) does not result in the total loss of endothelium-dependent relaxations to chemical and mechanical stimulation, indicating the involvement of another vasodilator mechanism. The cellular action of this putative non-NO/non-PGI_2 vasodilator system is usually associated with a hyperpolarization of

the membrane potential of the vascular smooth muscle cells (figure 2) [46, 47]. There are two primary mechanisms that can account for endothelium-derived hyperpolarization. On one hand, hyperpolarization of the smooth muscle cells can be attributed to the release of a diffusible substance from the endothelium, also called the endothelium-derived hyperpolarizing factor or EDHF. The identity of this EDHF is still controversial and during the past years several candidates have been put forward, such as residual NO, H_2O_2, K^+-ions, epoxyeicosatrienoic acids (EETs) and anandamide (figure 3) [48-52]. Therefore, it has been suggested that EDHF is not a single substance and that its nature and cellular targets may show considerable tissue and species variability [53, 54]. An alternative pathway for endothelium-dependent hyperpolarization is transmission of the agonist-induced hyperpolarization of the endothelial cells to the vascular smooth muscle via myoendothelial gap junctions (figure 3). This heterocellular coupling allows the spread of an electrical current or the transfer of small hydrophilic messenger molecules such as cAMP or IP_3 and ions (e.g. Ca^{2+}) [55-58].

It is, however, generally accepted that the action of EDH(F) is dependent on the endothelial release of intracellular Ca^{2+} and the activation of a specific set of K^+-channels. The EDH(F)-mediated responses are completely blocked by the combination of apamin (a selective inhibitor of small conductance Ca^{2+} sensitive K^+-channels (SK_{Ca})) and charybdotoxin (inhibitor of intermediate and large conductance K_{Ca}-channels (IK_{Ca} and BK_{Ca}, respectively) [59], but not by iberiotoxin (selective inhibitor of BK_{Ca} channels) [59, 60], suggesting that activation of IK_{Ca}- and SK_{Ca}-channels on the endothelium is involved. This has more recently been confirmed in rat carotid and mesenteric arteries by using apamin in combination with the new and selective inhibitors of IK_{Ca} TRAM-34 and TRAM-39 [61-63].

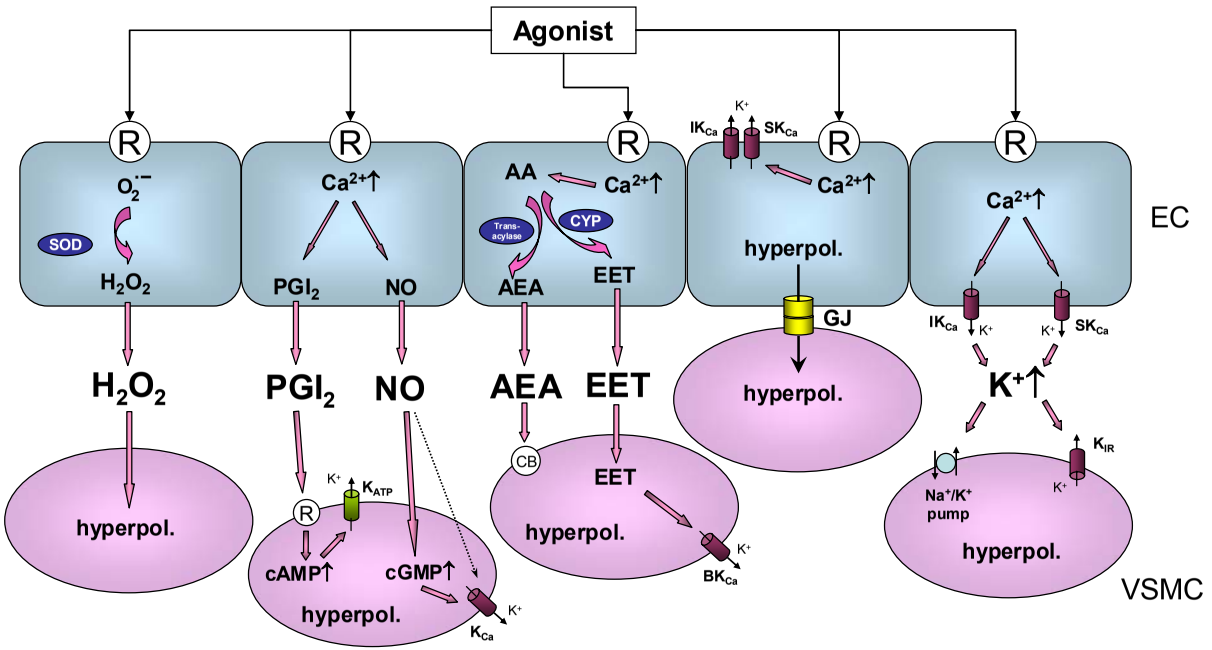

Figure 3: *Overview of the different mechanisms proposed for EDH(F). Agonists such as acetylcholine, bradykinin or substance P increase the intracellular Ca^{2+} concentration in the endothelial cells through activation of their respective receptors. This eventually leads to endothelium-derived hyperpolarization. EC = endothelial cell; VSMC = vascular smooth muscle cell; R = receptor; NO = nitric oxide; NOS = NO synthase; SOD = superoxide dismutase; H_20_2 = hydrogen peroxide; $O_2^{\cdot-}$ = superoxide anion; hyperpol. = hyperpolarization; PGI_2 = prostacyclin; K_{ATP} = ATP sensitive K^+ channels; K_{Ca} = Ca^{2+} activated K^+ channels; AA = arachidonic acid; CYP = cytochrome P450 epoxygenase; EET = epoxyeicosatrienoic acid; AEA = anandamide; CB = cannabinoid receptor; GJ = gap junction; SK_{Ca} = small conductance K_{Ca}; IK_{Ca} = intermediate conductance K_{Ca}; BK_{Ca} = large conductance K_{Ca}; K_{IR} = inward rectifying K^+ channel.*

It has been established that a change in the membrane potential of the smooth muscle cells with a few mV can result in a substantial change in vessel diameter [64, 65]. Furthermore, hyperpolarization of the vascular smooth muscle cells produces a rapid effect on contractile tone, compared to the relaxation mediated by second messengers. Together with the observation that the relative contribution of the endothelium-dependent hyperpolarization augments with decreasing vessel diameter [66-68], it is now generally accepted that changes in the synthesis or release of EDHF or in the magnitude of EDH are of critical importance in the regulation of organ blood flow and contribute to pathophysiological states such as hypertension [69].

1.2.2.4. Endothelium-derived contracting factor

In most vascular diseases, the vasodilator function of the endothelium is attenuated or even abolished. It has been reported that under pathological conditions the endothelium can induce contractile responses in certain vessels. For example, contraction of canine arteries arising during anoxia was markedly reduced after removal of the endothelium [70]. Therefore, it was concluded that under certain, mostly pathological, conditions, the endothelium can produce endothelium-derived contracting factors (EDCF). The identity of the released EDCFs, however, can differ strongly among species, but also among different vascular beds [71]. Over the years, several EDCFs have been identified, such as vasoconstricting prostaglandins (e.g. thromboxane A_2) [72], endoperoxides [73], endothelin [74] and superoxide anions [75], which can be produced by the endothelium in response to various stimuli such as stretch, acetylcholine, angiotensin I and II, arachidonic acid, ADP, ATP, substance P and noradrenaline.

The most potent vasoconstrictor peptide released from the endothelium described today is endothelin. Under normal circumstances, endothelin plays only a minor role in vascular homeostasis. Any tendency to (over)produce the peptide in healthy endothelial cells will be offset by an increased release of NO and possibly also of PGI_2 and EDHF, which themselves reduce the production of endothelin [76, 77]. Only when the endothelium looses its ability to generate EDRFs, endothelin can be produced in sufficient amounts and may contribute to vascular disease [78].

1.2.3. Vasoactive factors released from sensory nerves

Sensory nerves are a type of neurons regulating vascular blood flow. All sensory neurons have their cell bodies in the dorsal root ganglia. Their function is primary afferent as they send nerve impulses to the spinal cord. However, the impulses initiated in sensory nerves can also be relayed antidromically down collateral branches of these nerve fibres which directly innervate blood vessels. This local neural mechanism is called the axon reflex. Through the release of a number of vasoactive peptides including substance P, neurokinin A (NKA), neurokinin B (NKB) and calcitonin gene-related peptide (CGRP), the sensory nerves can produce immediate local responses. This phenomenon plays an important role in the reaction to skin injury. When the skin is hurt, the axon reflex will cause an immediate dilatation of the local capillaries and an increase in their permeability, respectively leading to typical reddening (red reaction) and swelling (wheal) at the site of injury. Dilatation of the arterioles is responsible for the redness spreading out from the injury (flare). Sensory nerves are capsaicin-sensitive. Capsaicin is a naturally occurring substance derived from hot chilli peppers and interacts with vanilloid ($TRPV_1$) receptors on

sensory afferents. Chronic exposure to capsaicin stimulates the $TRPV_1$ receptor and causes local depletion of neuropeptides.

The perivascular sensory nerves may contain different combinations of neuropeptides, which usually induce vasodilatation [79]. In general, substance P, NKA and NKB induce endothelium-dependent vasodilatation through the release of NO and EDHF [80, 81]. However, contractile responses to these peptides have been demonstrated, resulting from the activation of smooth muscle receptors [82, 83]. CGRP is a potent vasodilator in a number of vascular preparations [84]. The effects of CGRP are generally due to direct activation of receptors on the vascular smooth muscle and a decrease in intracellular Ca^{2+} regulated by adenylate cyclase [85]. However, CGRP has also been reported to activate ATP-sensitive K^+-channels in arterial smooth muscle [86], while in rat aorta the CGRP-mediated vasodilatation is endothelium-dependent and involves the release of NO [87, 88].

1.3. ENDOTHELIUM-DERIVED HYPERPOLARIZATION

As mentioned above, several hypotheses have been suggested with regard to the mechanism of action and the nature of EDH(F). As outlined in the previous chapter, two principle mechanisms have been proposed by which EDH(F) can cause smooth muscle cell hyperpolarization, namely the transfer of a diffusible factor (EDHF) across the extracellular space and the transmission of endothelial hyperpolarization (EDH) via myoendothelial gap junctions. A schematic overview of the different mechanisms proposed for EDH(F) is depicted in figure 3.

1.3.1. Diffusible factors

In several arteries, EDHF was reported to be a diffusible factor released from the endothelium which initiates hyperpolarization and relaxation of the smooth muscle cells by activation of specific smooth muscle cell receptors or ion channels. The identity of EDHF is still elusive, but different putative candidates have been proposed. Residual NO, H_2O_2, K^+, EETs, anandamide, C-type natriuretic peptide (CNP), carbon monoxide and L-citrulline have all been suggested as an EDHF in certain vascular beds [49, 51, 52, 89-91]. The most important candidates are discussed below.

1.3.1.1. Residual NO

As mentioned above, NO is now accepted to be the major mediator of endothelium-dependent smooth muscle relaxation. However, whether or not NO can account for the endothelium-dependent hyperpolarization is controversial. At least in some vessels such as the guinea-pig uterine artery, rabbit aorta and rat small mesenteric artery, exogenous NO caused hyperpolarization of the vascular smooth muscle cells [23-25, 92]. Also prostacyclin has been described to cause hyperpolarization [93]. Therefore, EDHF responses should always be measured in the continuous presence of both inhibitors of NOS and cyclooxygenase.

In rabbit carotid arteries stimulated with acetylcholine, it was shown that the application of L-NAME, in a concentration originally considered to be sufficient to completely inhibit NOS in most tissues (30 µM), decreased but did not completely inhibit the release of NO. The additional application of L-NA, another inhibitor of NO, further reduced the release of NO and the hyperpolarization and relaxation of these vessels to acetylcholine.

Therefore, it was suggested that NO was the mediator of both endothelium-dependent relaxation and hyperpolarization [48]. Correspondingly, in several other vascular beds it was shown that, although NOS was inhibited with L-arginine analogues, there was still some resistant NO released from the endothelium [53, 91]. In rat superior mesenteric arteries [91], acetylcholine still evoked relaxations in the presence of L-nitroarginine (L-NA). Since the NO scavenger oxyhaemoglobin further reduced these L-NA resistant relaxations, it was suggested that they were due to residual NO, which could be derived from a source other than L-arginine. However, in studies using both NOS-inhibitors and NO-scavengers a large part of the endothelium-derived hyperpolarization persists.

Moreover, if indeed NO fully accounts for the endothelium-dependent hyperpolarization in the presence of NOS-inhibitors, exogenous NO should be able to evoke comparable hyperpolarizations when applied in physiological concentrations. In rat aorta, nitroglycerin (10 µM) induced only a hyperpolarization of about 2 mV [94]. Similarly, application of other NO-donors only caused a fraction of the membrane potential change induced by acetylcholine [94]. Comparable observations were found in the main mesenteric artery [95, 96]. Moreover, while the membrane potential of the smooth muscle cells of these arteries showed comparable sensitivity to exogenous NO, the EDHF-induced hyperpolarization was much more expressed in the mesenteric artery than in the rat aorta [94-96]. Taken together, these findings suggest that although residual NO might be present in some conditions and contribute to some minor extent in EDH, a separate but NO-unrelated EDHF exists [53, 97,98].

1.3.1.2. Hydrogen peroxide

H_2O_2 may be produced in the endothelium from superoxide anions via superoxide dismutase and has been implicated as an EDHF, namely in human and mouse mesenteric and porcine coronary arteries [49, 99, 100]. This hypothesis arose from the report that catalase, an enzyme that dismutates H_2O_2 to water and oxygen, inhibited the EDHF-mediated hyperpolarization and subsequent relaxation [49, 99, 100]. However, this was not consistent with several other studies in the same vascular beds, where catalase had no effect on the EDHF-response [101, 102]. Similarly, in other vascular preparations, catalase was unable to inhibit the EDHF response [103, 104]. In contrast to the reports about its vasodilating action, several studies have shown that H_2O_2 can cause a vasoconstriction and suggested that it might act as an EDCF in some vessels [105]. Therefore, the physiological relevance of H_2O_2 as an EDHF is questioned.

1.3.1.3. Potassium ions

In some arteries such as the rat hepatic and small mesenteric arteries, K^+ was proposed as an EDHF [50]. More specifically, acetylcholine was shown to stimulate the opening of SK_{Ca} and IK_{Ca} channels of the endothelial cells, thereby causing hyperpolarization. The resulting K^+ efflux would cause a raise in the extracellular K^+ concentration ($[K^+]_o$) in the restricted myoendothelial space [50]. In turn, this increase would activate Na^+/K^+-ATPases and inwardly rectifying K^+-channels (K_{IR} channels) located on the adjacent vascular smooth muscle cells, resulting in a hyperpolarization of these latter [50]. The evidence for the involvement of these mechanisms is mainly derived from studies using ouabain and Ba^{2+}, respective blockers of Na^+/K^+-ATPases and K_{IR} channels. In these studies, it has been shown that

the hyperpolarization and relaxation induced by small increases in $[K^+]_o$ could be inhibited by these blockers, administered either alone or in combination [50, 106, 107].

More recently, however, it was reported that exogenous increases in $[K^+]_o$ elicited relaxation in only 30-40% of preconstricted rat small mesenteric arteries, while responses to acetylcholine were always present [108]. Moreover, the relaxations caused by a raise in $[K^+]_o$ were endothelium-dependent and significantly smaller than the acetylcholine responses [108]. Correspondingly, in small mesenteric arteries from the same species mounted isometrically, a raise in $[K^+]_o$ caused no relaxation of endothelium intact and denuded arteries, whereas acetylcholine only failed to relax endothelium denuded preparations [109]. Furthermore, in pressurised arteries, raising $[K^+]_o$ dilated only 30% of the arteries, while the acetylcholine-response was consistently present in all vessels [109].

The absence of K^+-induced hyperpolarization in endothelium-denuded rat small mesenteric arteries was confirmed after stimulating the vessels with phenylephrine [110]. Blockers of vascular smooth muscle delayed rectifier and large conductance Ca^{2+}-sensitive K^+-channels (4-aminopyridine and iberiotoxin, respectively) were able to restore the hyperpolarizations in these stimulated vessels. It was suggested, therefore, that activation of the smooth muscle with phenylephrine, which is known to increase K^+ efflux from the myocytes by opening of smooth muscle K^+ channels [111], resulted in a K^+-cloud in the myoendothelial spaces, preventing the vasodilator action of exogenous added K^+ [110]. This explains the observation that the K^+-channel blockers could restore the K^+-induced hyperpolarization in stimulated vessels. A key component in the K^+-induced responses is the smooth muscle Na^+/K^+-ATPase [112], a family of proteins of which the

different isoforms display different affinities for $[K^+]_o$. The α_1-containing isoforms would perform a 'housekeeping' role, and are fully activated at physiological concentrations of $[K^+]_o$. α_2- and α_3-containing isoforms, on the other hand, are not saturated at normal $[K^+]_o$ and might be further activated by small increases in $[K^+]_o$ [113, 114]. Therefore, it was suggested that the observed K^+-induced effects under resting conditions are due to stimulation of Na^+/K^+-ATPases containing α_2- and/or α_3-subunits. However, extracellular accumulation of K^+ ions as the result of activation of the smooth muscle cells with phenylephrine (the K^+-cloud), would fully activate and saturate the Na^+/K^+ pumps containing α_2- and α_3-subunits [110, 115, 116], favouring the alternative gap junctional pathway for endothelium-dependent smooth muscle hyperpolarization [110, 116]. The hyperpolarization of the endothelial cells thereby is transferred to the underlying smooth muscle cells through gap junctional coupling (as discussed in § 1.3.2).

1.3.1.4. Epoxyeicosatrienoic acids

A number of enzymes can metabolise arachidonic acid into a variety of metabolites, all of which are able to influence smooth muscle tone. EETs are cytochrome *P450* (CYP) epoxygenase metabolites of arachidonic acid which have been shown to activate smooth muscle BK_{Ca} [117, 118], resulting in hyperpolarization and subsequent relaxation of cerebral, coronary and renal arteries of several species [119-121].

A number of studies suggest that EETs may account for EDHF in a number of vascular preparations. They reported that the EDHF response could be inhibited by CYP inhibitors [122-125] and was also associated with the release of EETs from endothelial cells [51]. In addition, in porcine coronary arteries the EDHF mediated response was precisely mimicked by 11,12-EET [126].

Furthermore, the vasodilator potency of EETs seems to increase with decreasing vessel diameter [127], a typical characteristic of EDHF.

However, considerable evidence also argues against the role of EETs as "universal" EDHF. Some of the CYP inhibitors used are now known to exert non-specific effects. For example, proadifen, clotrimazole and the antimycotic imidazole can directly inhibit vascular smooth muscle K^+-channels [128-130]. Moreover, in rat hepatic, guinea-pig carotid and porcine coronary arteries, chemically unrelated inhibitors of CYP had no effect whatsoever on the EDHF-mediated responses [131-133]. EETs seem to hyperpolarize vascular smooth muscle cells via the activation of iberiotoxin-sensitive BK_{Ca}-channels [117, 134]. Taken together, these observations clearly show that the hypothesis that EETs represent EDHF, requires further investigation and certainly can not be a universal one.

1.3.1.5. Anandamide

The endogenous cannabinoid anandamide (N-arachidonylethanolamine) is another arachidonic acid derivative which is formed via the action of a transacylase enzyme and has been shown to exert potent vasodilatory effects in a number of vascular preparations [52, 135-139]. The properties of the endogenous cannabinoids (also called endocannabinoids) are discussed in more detail in a next paragraph (§ 1.4., p25).

In the perfused mesenteric bed of the rat, where anandamide caused endothelium-independent vasodilatation, the cannabinoid receptor antagonist SR141716A inhibited the EDHF-mediated response induced by carbachol [52]. Moreover, the investigators found that anandamide and EDHF

exerted similar characteristics in these preparations [140], suggesting they were identical.

Nonetheless, a number of later studies could not confirm this proposal and proved that anandamide and EDHF did not share the same pharmacological and physiological profile [60, 139, 141-145]. Further doubt about the early reports arose with the report that SR141716A, besides blocking cannabinoid receptors, also exerted additional, non-selective effects such as disrupting myoendothelial gap junctional communication [146] or influencing Ca^{2+} influx initiated by agonists [147].

1.3.2. Gap junctional coupling

An alternative pathway for endothelium-dependent hyperpolarization is transmission of the agonist-induced hyperpolarization of the endothelial cells to the adjacent smooth muscle cells via gap junctions. Gap junctions are formed by docking of two connexons or hemichannels, supplied by the two interacting cells at points of cell-cell contact. They form an aqueous pore allowing the spread of electrical current or the transfer of small hydrophilic molecules (< 1 kDa), including cAMP, cGMP, IP_3, as well as inorganic ions, such as Ca^{2+} [55-57, 148]. Gap junctions are seen in virtually all cells that contact other cells in tissues. In the vascular wall gap junctions can occur between cells of the same type, such as between endothelial cells or between smooth muscle cells and are hence called homocellular gap junctions. On the other hand, gap junctions can also be formed between endothelial cells and vascular smooth muscle cells. These heterocellular gap junctions are referred to as myoendothelial gap junctions. In many arteries, the endothelial cell layer is coupled to the

smooth muscle cell layer by pentalaminar myoendothelial gap junctions located at the end of thin projections that originate from the endothelial cells [149, 150].

Each connexon is constructed from six connexin (Cx) protein subunits traversing the cell membrane [151, 152]. Several Cx isotypes have been identified [153, 154] and are named according to their predicted molecular weights in kDa. A hemichannel may be comprised of a single Cx isotype or multiple isotypes, resulting in the formation of homomeric or heteromeric connexons, respectively. Complete gap junction channels may be either homotypic, if comprised of two identical hemichannels, or heterotypic if the hemichannels supplied by each cell are different [155]. Changes in Cx composition can have significant effects on the properties of gap junctions present in a tissue. This explains why different Cx are observed in different tissues, providing their distinct characteristics.

Within the vascular tissue, four connexins have been reported so far: Cx37, Cx40, Cx43 and Cx45 [156]. The endothelial cells lining the arterial lumen are well coupled and have been found to express Cx37, Cx40 and Cx43. Cx37, Cx40 are the most abundant connexins and have been detected in endothelial cells of most vessels, while Cx43 is the least well expressed and is even absent in some vessels such as the intramural coronary arteries [156, 157]. In the vascular smooth muscle Cx43 is the most abundant, followed by Cx40 and 45 [158]. Cx37 is usually thought to be restricted to the endothelial cells, but it has also been found in smooth muscle cells [159]. Although the exact Cx isotype present in myoendothelial gap junctions remains unknown, recent evidence suggest that Cx40 plays a critical role in heterocellular signalling [160].

It has been hypothesised that myoendothelial gap junctions are more important in resistance than in conduit arteries [161, 162], which may explain the predominance of EDH in the resistance vasculature. However, the role of myoendothelial gap junctions in the EDH remains controversial since the specificity of the gap junction uncouplers used in most studies was questioned. Indeed, agents such as heptanol, 18α- and 18ß-glycyrrhetinic acid and carbenoxolone all have been shown to exert non-specific effects in a dose- and tissue-dependent manner [163-165]. Therefore, a more specific inhibitor has been designed, based on the amino acid sequence of a portion of the extracellular loop of Cx43. This peptide, Gap 27, contains 11 amino acids and prevents the formation of the connexon hemichannel [163, 166, 167]. Another problem in the study of gap junctional coupling is that none of the used uncouplers, including Gap 27, can selectively inhibit the myoendothelial cell coupling versus coupling between adjacent endothelial cells or smooth muscle cells [168, 169]. Therefore, additional studies are required before the contribution of myoendothelial gap junctions in endothelium-derived hyperpolarizations can be further established.

1.4. ENDOCANNABINOIDS

The hemp plant (*Cannabis sativa*) has been used for millennia as a medicine and for social and religious purposes. The term cannabis is generally used to describe a single entity. However, research in the past century has revealed that cannabis is the source of more than 60 different compounds, collectively referred to as cannabinoids [170, 171]. Cannabinol was the first of these plant cannabinoids to be isolated and described. The most abundant cannabinoid, primarily responsible for the psychotropic effects of cannabis, is Δ^9-tetrahydrocannabinol (THC). Other, well described naturally

occurring cannabinoids are Δ^8-THC and cannabidiol [172]. Compared to Δ^9-THC, cannabinol has much more lower potency as a psychotropic agent, whereas cannabidiol lacks any psychotropic activity. At first, cannabinoid experiments focused mainly on the psychotropic properties. However, later studies showed that cannabinoids could also exert potent cardiovascular effects [173, 174].

To date, two distinct receptor subtypes for cannabinoids have been identified and cloned. Type 1 cannabinoid (CB_1) receptors [175] are mainly localised on neurons but are also present in some peripheral tissues including heart, lung and gastrointestinal tissues and in vasculature [136, 176-178]. On the other hand, type 2 cannabinoid (CB_2) receptors [179] are primarily expressed in immune cells, although there is some evidence that these receptors are also expressed by neuronal tissue [180]. In several arteries, the vasorelaxant effect of cannabinoids has been reported to be mediated by stimulation of CB_1 receptors, since SR141716A, a CB_1 receptor antagonist, inhibits relaxations by anandamide [52, 136, 181]. Recently, it was suggested that in some vessels the vasodilator response to cannabinoids is mediated by stimulation of a novel, not yet identified, non-CB_1/CB_2 receptor located on the endothelium [182-184].

In the early 1990's, endogenous cannabinoids have been identified. The first of these endocannabinoids described was anandamide [185]. In addition to their neurobehavioral effects, they have a profound influence on the cardiovascular system [173]. Both, endogenous and synthetic cannabinoids have potent vasodilatory effects in a variety of isolated vascular preparations [52, 135, 136, 186]. Their precise mechanisms of action, however, are still unknown and seem to vary with species, vessel type and size [139, 187]. Also the site of action, whether they act on the endothelial cells, the

vascular smooth muscle cells or the perivascular nerves of the vessel wall is still elusive (figure 4).

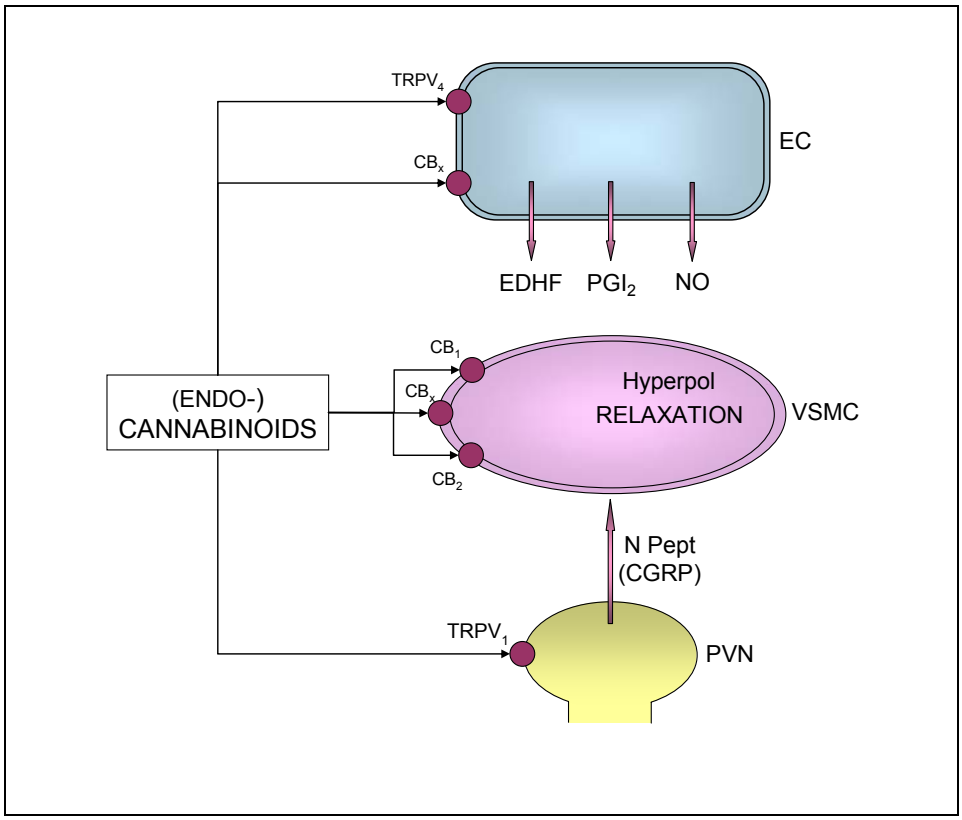

Figure 4: *Schematic presentation of the possible mechanisms of action of (endo)cannabinoids in the vessel wall. EC = endothelial cell; VSMC = vascular smooth muscle cell; PVN = perivascular nerves; EDHF = endothelium-derived hyperpolarizing factor; PGI_2 = prostacyclin; NO = nitric oxide; hyperpol = hyperpolarization; NPept = neuropeptides; CGRP = calcitonin gene-related peptide; CB_1 = type 1 cannabinoid receptor; CB_2 = type 2 cannabinoid receptor; CB_x = non-CB_1/non-CB_2 cannabinoid receptor; $TRPV_1$ = type 1 vanilloid receptor; $TRPV_4$ = type 4 vanilloid receptor.*

In some vascular preparations, the anandamide-induced responses have been shown to be entirely endothelium-dependent [137, 146, 183], and associated with the release of prostanoids [135, 188], NO [136] or EDHF [146]. Most studies, however, have shown that the vasorelaxations caused by anandamide are completely [52] or partly [146] endothelium-independent.

The endothelium-independent pathway by which cannabinoids induce vasodilatation is still elusive. Some studies report that cannabinoids directly stimulate cannabinoid receptors on the vascular smooth muscle cells [52, 136, 146]. Moreover, some studies demonstrated that, in the isolated perfused mesenteric bed of the rat, the endothelium-dependent vasodilator response of bradykinin was also inhibited by the CB_1 inhibitor SR141716A and concluded that anandamide could be EDHF in these arteries [52]. However, later studies have provided convincing evidence against this hypothesis, so that it is now generally accepted that EDHF and anandamide are different factors with other physiological and pharmacological properties [60, 139, 141, 143, 189, 190].

Besides as an endocannabinoid, anandamide could also act as an endovanilloid in a number of vascular preparations. Indeed, the vasorelaxant influence of cannabinoids has been reported to be due to stimulation of vanilloid $TRPV_1$ receptors on the perivascular sensory nerves and the subsequent release of sensory neuropeptides such as the powerful vasodilator calcitonin gene related peptide (CGRP). It has been shown that anandamide binds and activates $TRPV_1$ receptors. Moreover, its vasorelaxant response was antagonised by the $TRPV_1$ receptor antagonist capsazepine and the CGRP receptor antagonist $CGRP_{(8-37)}$, but not by the CB1 receptor antagonist SR141716A [138]. The picture is further complicated by more recent studies that identified endocannabinoids as potential

activators of the vanilloid $TRPV_4$ receptor [191]. This receptor is highly expressed on vascular endothelial cells, and its stimulation enhances Ca^{2+} influx, an essential trigger to release various vasoactive factors including NO, prostaglandins and the EDHF mechanism [192]. Moreover, the $TRPV_4$ receptor was recently also found in the myocytes of cerebral arteries, and its activation was shown to cause smooth muscle cell hyperpolarization via BK_{Ca} channel activation [193]. The endocannabinoids stimulate the $TRPV_4$ receptor indirectly, after conversion to its metabolite 5',6'-epoxyeicosatrienoic acid [191].

1.5. STUDY AIM

During the past 25 years, the important paracrine role of the vascular endothelium in the regulation of blood vessel tone and blood flow has become increasingly clear. While the role of the endothelium-derived vasorelaxing factors nitric oxide (NO) and prostacyclin (PGI_2) is well established, the mechanism underlying the endothelium-dependent hyperpolarization in various vessels is still debated. Several hypotheses have been put forward and there seem to be considerable tissue and species differences. The starting point of this work was to further explore the identity and the characteristics of the endothelium-derived hyperpolarizing factor (EDHF).

In resting rat hepatic and small mesenteric arteries, K^+ was proposed as EDHF [50, 116]. On the other hand, the endothelium-derived hyperpolarization in stimulated rat hepatic and mesenteric arteries seemed to rely more on gap junctional coupling [115, 116]. It was proposed, therefore, that the increased K^+ efflux from the myocytes upon activation of the smooth

muscle with phenylephrine, resulted in a K^+-cloud in the myoendothelial space. This process would saturate Na^+/K^+-pumps and favour the gap junctional pathway for smooth muscle hyperpolarization [110, 116]. In **chapter 3** we further explore the functional consequences of modulation of basal smooth muscle K^+ efflux for endothelium-dependent hyperpolarizations. We more specifically investigate the involvement of gap junctional coupling, Na^+/K^+-ATPases and inward rectifying K^+ (K_{IR}) channels in the acetylcholine-induced hyperpolarization of smooth muscle cells of rat small mesenteric arteries.

Previous tension measurements performed in our lab revealed the existence of endothelium-dependent, but NO- and PGI_2-independent vasorelaxations in rat gastric arteries stimulated with acetylcholine [194]. However, as far as we knew, no data were available of endothelium-derived membrane potential responses in these arteries. In **chapter 4** we extend these observations by directly measuring the membrane potential responses of the gastric arteriolar smooth muscle cells to acetylcholine. We further characterise the observed endothelium-dependent hyperpolarizations by investigating the involvement of K_{IR}-channels and Na^+/K^+-ATPases.

Since the discovery of the existence of EDHF, several candidates have been proposed and their properties were intensively investigated and compared with those of EDHF. The endogenous cannabinoid anandamide, a derivative of arachidonic acid, has also been suggested as EDHF [52]. Later studies, however, found convincing evidence against this hypothesis and it is now generally accepted that anandamide and EDHF are different factors. Nonetheless, endocannabinoids are potent vasodilators in a variety of vascular preparations. Previous work showed that anandamide and its

stable analogue methanandamide exert potent hyperpolarizing effects in rat mesenteric arteries, possibly through the activation of vanilloid $TRPV_1$ receptors on perivascular nerves and the subsequent release of the vasodilatory neuropeptide calcitonin gene-related peptide (CGRP) [139]. In **chapter 5** we examine the influence of these cannabinoids on the membrane potential in isolated small gastric arteries and compare this with the responses to exogenous CGRP. We further investigate the involvement of $TRPV_1$ receptors in the cannabinoid responses using the specific antagonist capsazepine. **Chapter 6** explores the relaxant effects of cannabinoids in small gastric arteries. More specifically, we characterise the relaxation induced by methanandamide and compared this with the response to exogenous CGRP. We assess the involvement of $TRPV_1$ receptors and the different types of cannabinoid receptors in the methanandamide response. Finally, we test the hypothesis that the relaxation induced by methanandamide could be due to an inhibitory action on voltage activated Ca^{2+} channels.

The processes of vasorelaxation and vasoconstriction of arteries involves changes in intracellular Ca^{2+} concentration in the vascular smooth muscle cells. In **chapter 7** we attempt to visualise and characterise changes in the intracellular Ca^{2+} concentration in smooth muscle cells of isolated small mesenteric arteries in response to different vasorelaxing and vasoconstricting substances using microscope Ca^{2+} imaging techniques.

1.6. REFERENCES

1. Persson PB. Renal blood flow autoregulation in blood pressure control. *Curr Opin Nephrol Hypertens.* 2002;11(1):67-72.

2. Johnson PC. The myogenic response in the microcirculation and its interaction with other control systems. *J Hypertens.* 1989;7:S33-S40.

3. Muller JM, Davis MJ, Chilian WM. Integrated regulation of pressure and flow in the coronary microcirculation. *Cardiovasc Res.* 1996;32(4):668-78.

4. Faraci FM, Baumbach GL, Heistad DD. Myogenic mechanisms in the cerebral circulation. *J Hypertens.* 1989;7:S61-S65.

5. Dole WP. Autoregulation of the coronary circulation. *Progr Cardiovasc Dis.* 1987;29(4):293-323.

6. Roman RJ, Harder DR. Cellular and ionic signal transduction mechanisms for the mechanical activation of renal arterial vascular smooth muscle. *J Am Soc Nephrol.* 1993;4(4):986-96.

7. Shin HK, Hong KW. Importance of calcitonin gene-related peptide, adenosine and reactive oxygen species in cerebral autoregulation under normal and diseased conditions. *Clin Exp Pharmacol Physiol.* 2004;31(1-2):1-7.

8. Knot HJ, Nelson MT. Regulation of membrane potential and diameter by voltage-dependent K^+ channels in rabbit myogenic cerebral arteries. *Am J Physiol.* 1995;38(1):H348-H355.

9. Knot HJ, Nelson MT. Regulation of arterial diameter and wall [Ca^{2+}] in cerebral arteries of rat by membrane potential and intravascular pressure. *J Physiol.* 1998;508(1):199-209.

10. Furchgott RF, Zawadzki JV. The obligatory role of endothelial cells in the relaxation of arterial smooth muscle by acetylcholine. *Nature.* 1980;288(5789):373-6.

11. Furchgott RF, Vanhoutte PM. Endothelium-derived relaxing and contracting factors. *FASEB J.* 1989;3(9):2007-18.

12. Vanhoutte PM. Endothelium and control of vascular function - state of the art lecture. *Hypertension.* 1989;13(6):658-67.

13. Palmer RMJ, Ferrige AG, Moncada S. Nitric oxide release accounts for the biological activity of endothelium-derived relaxing factor. *Nature.* 1987;327(6122):524-6.

14. Ignarro LJ, Buga GM, Wood KS, Byrns RE, Chaudhuri G. Endothelium-derived relaxing factor produced and released from

artery and vein is nitric oxide. *Proc Natl Acad Sci U S A.* 1987;84(24):9265-9.

15. Palmer RMJ, Ashton DS, Moncada S. Vascular endothelial cells synthesize nitric oxide from L-arginine. *Nature.* 1988;333(6174):664-6.

16. Moncada S, Higgs EA. Molecular mechanisms and therapeutic strategies related to nitric oxide. *FASEB J.* 1995;9(13):1319-30.

17. Hobbs AJ, Higgs A, Moncada S. Inhibition of nitric oxide synthase as a potential therapeutic target. *Annu Rev Pharmacol Toxicol.* 1999;39:191-220.

18. Schmidt HH, Lohmann SM, Walter U. The nitric oxide and cGMP signal transduction system: regulation and mechanism of action. *Biochim Biophys Acta.* 1993;1178(2):153-75.

19. Lincoln TM, Cornwell TL. Intracellular cyclic GMP receptor proteins. *FASEB J*. 1993;7(2):328-38.

20. Cornwell TL, Lincoln TM. Regulation of intracellular Ca^{2+} levels in cultured vascular smooth muscle cells. Reduction of Ca^{2+} by atriopeptin and 8-bromo-cyclic GMP is mediated by cyclic GMP-dependent protein kinase. *J Biol Chem.* 1989;264(2):1146-55.

21. Zhang Q, Scholz PM, He Y, Tse J, Weiss HR. Cyclic GMP signaling and regulation of SERCA activity during cardiac myocyte contraction. *Cell Calcium.* 2005;37(3):259-66.

22. Lee MR, Li L, Kitazawa T. Cyclic GMP causes Ca^{2+} desensitization in vascular smooth muscle by activating the myosin light chain phosphatase. *J Biol Chem.* 1997;272(8):5063-8.

23. Bolotina VM, Najibi S, Palacino JJ, Pagano PJ, Cohen RA. Nitric oxide directly activates calcium-dependent potassium channels in vascular smooth muscle. *Nature.* 1994;368(6474):850-3.

24. Mistry DK, Garland CJ. Nitric oxide (NO)-induced activation of large conductance Ca^{2+}-dependent K^+ channels (BK_{Ca}) in smooth muscle cells isolated from the rat mesenteric artery. *Br J Pharmacol.* 1998;124(6):1131-40.

25. Garland JG, McPherson GA. Evidence that nitric oxide does not mediate the hyperpolarization and relaxation to acetylcholine in the rat small mesenteric artery. *Br J Pharmacol.* 1992;105(2):429-35.

26. Tare M, Parkington HC, Coleman HA. EDHF, NO and a prostanoid: hyperpolarization-dependent and -independent relaxation in guinea-pig arteries. *Br J Pharmacol.* 2000;130(3):605-18.

27. Murphy ME, Brayden JE. Nitric oxide hyperpolarizes rabbit mesenteric arteries via ATP-sensitive potassium channels. *J Physiol.* 1995;486 (Pt 1):47-58.

28. Gupta S, McArthur C, Grady C, Ruderman NB. Stimulation of vascular Na^+/K^+-ATPase activity by nitric oxide: a cGMP-independent effect. *Am J Physiol.* 1994;266(5 Pt 2):H2146-H2151.

29. Najibi S, Cowan CL, Palacino JJ, Cohen RA. Enhanced role of potassium channels in relaxations to acetylcholine in hypercholesterolemic rabbit carotid artery. *Am J Physiol.* 1994;266(5 Pt 2):H2061-H2067.

30. Cooke JP, Dzau VJ. Derangements of the nitric oxide synthase pathway, L-arginine, and cardiovascular diseases. *Circulation.* 1997;96(2):379-82.

31. Cosentino F, Katusic ZS. Tetrahydrobiopterin and dysfunction of endothelial nitric oxide synthase in coronary arteries. *Circulation.* 1995;91(1):139-44.

32. Illiano S, Nagao T, Vanhoutte PM. Calmidazolium, a calmodulin inhibitor, inhibits endothelium-dependent relaxations resistant to nitro-L-arginine in the canine coronary artery. *Br J Pharmacol.* 1992;107(2):387-92.

33. Chataigneau T, Feletou M, Huang PL, Fishman MC, Duhault J, Vanhoutte PM. Acetylcholine-induced relaxation in blood vessels from endothelial nitric oxide synthase knockout mice. *Br J Pharmacol.* 1999;126(1):219-26.

34. Scotland RS, Madhani M, Chauhan S, Moncada S, Andresen J, Nilsson H, Hobbs AJ, Ahluwalia A. Investigation of vascular responses in endothelial nitric oxide synthase/cyclooxygenase-1 double-knockout mice - Key role for endothelium-derived hyperpolarizing factor in the regulation of blood pressure in vivo. *Circulation.* 2005;111(6):796-803.

35. Huang PL, Huang ZH, Mashimo H, Bloch KD, Moskowitz MA, Bevan JA, Fishman MC. Hypertension in mice lacking the gene for endothelial nitric oxide synthase. *Nature.* 1995;377(6546):239-42.

36. Krotz F, Schiele TM, Klauss V, Sohn HY. Selective COX-2 inhibitors and risk of myocardial infarction. *J Vasc Res.* 2005;42(4):312-24.

37. Porcher C, Horowitz B, Ward SM, Sanders KM. Constitutive and functional expression of cyclooxygenase 2 in the murine proximal colon. *Neurogastroenterol Motil.* 2004;16(6):785-99.

38. Hinz B, Brune K. Cyclooxygenase-2--10 years later. *J Pharmacol Exp Ther.* 2002;300(2):367-75.

39. Moncada S, Gryglewski R, Bunting S, Vane JR. An enzyme isolated from arteries transforms prostaglandin endoperoxides to an unstable substance that inhibits platelet aggregation. *Nature.* 1976;263(5579):663-5.

40. Moncada S, Herman AG, Higgs EA, Vane JR. Differential formation of prostacyclin (PG_X or PGI_2) by layers of the arterial wall. An explanation for the anti-thrombotic properties of vascular endothelium. *Thromb Res.* 1977;11(3):323-44.

41. Kukovetz WR, Holzmann S, Wurm A, Poch G. Prostacyclin increases cAMP in coronary arteries. *J Cyclic Nucleotide Res.* 1979;5(6):469-76.

42. Ignarro LJ, Harbison RG, Wood KS, Wolin MS, McNamara DB, Hyman AL, Kadowitz PJ. Differences in responsiveness of intrapulmonary artery and vein to arachidonic acid: mechanism of arterial relaxation involves cyclic guanosine 3':5'-monophosphate and cyclic adenosine 3':5'-monophosphate. *J Pharmacol Exp Ther.* 1985;233(3):560-9.

43. Tang DG, Grossi IM, Tang KQ, Diglio CA, Honn KV. Inhibition of TPA and 12(S)-HETE stimulated tumor cell adhesion by prostacyclin and its stable analogs - Rationale for their antimetastatic effects. *Int J Cancer.* 1995;60(3):418-25.

44. Astin M. Effects of prostaglandin E-2, F-2 alpha, and latanoprost acid on isolated ocular blood vessels in vitro. *J Ocular Pharmacol Ther.* 1998;14(2):119-28.

45. Vane JR. Inhibition of prostaglandin synthesis as a mechanism of action for aspirin-like drugs. *Nat New Biol.* 1971;231(25):232-5.

46. Cohen RA, Vanhoutte PM. Endothelium-dependent hyperpolarization. Beyond nitric oxide and cyclic GMP. *Circulation.* 1995;92(11):3337-49.

47. McGuire JJ, Ding H, Triggle CR. Endothelium-derived relaxing factors: a focus on endothelium-derived hyperpolarizing factor(s). *Can J Physiol Pharmacol.* 2001;79(6):443-70.

48. Cohen RA, Plane F, Najibi S, Huk I, Malinski T, Garland CJ. Nitric oxide is the mediator of both endothelium-dependent relaxation and hyperpolarization of the rabbit carotid artery. *Proc Natl Acad Sci U S A.* 1997;94(8):4193-8.

49. Matoba T, Shimokawa H, Nakashima M, Hirakawa Y, Mukai Y, Hirano K, Kanaide H, Takeshita A. Hydrogen peroxide is an endothelium-derived hyperpolarizing factor in mice. *J Clin Invest.* 2000;106(12):1521-30.

50. Edwards G, Dora KA, Gardener MJ, Garland CJ, Weston AH. K^+ is an endothelium-derived hyperpolarizing factor in rat arteries. *Nature.* 1998;396(6708):269-72.

51. Campbell WB, Gebremedhin D, Pratt PF, Harder DR. Identification of epoxyeicosatrienoic acids as endothelium-derived hyperpolarizing factors. *Circ Res.* 1996;78(3):415-23.

52. Randall MD, Alexander SPH, Bennett T, Boyd EA, Fry JR, Gardiner SM, Kemp PA, McCulloch AI, Kendall DA. An endogenous cannabinoid as an endothelium-derived vasorelaxant. *Biochem Biophys Res Commun.* 1996;229(1):114-20.

53. Kemp BK, Cocks TM. Evidence that mechanisms dependent and independent of nitric oxide mediate endothelium-dependent relaxation to bradykinin in human small resistance-like coronary arteries. *Br J Pharmacol.* 1997;120(5):757-62.

54. Triggle CR, Dong H, Waldron GJ, Cole WC. Endothelium-derived hyperpolarizing factor(s): species and tissue heterogeneity. *Clin Exp Pharmacol Physiol.* 1999;26(2):176-9.

55. Yamamoto Y, Imaeda K, Suzuki H. Endothelium-dependent hyperpolarization and intercellular electrical coupling in guinea-pig mesenteric arterioles. *J Physiol.* 1999;514 (Pt 2):505-13.

56. Hutcheson IR, Chaytor AT, Evans WH, Griffith TM. Nitric oxide-independent relaxations to acetylcholine and A23187 involve different routes of heterocellular communication. Role of Gap junctions and phospholipase A_2. *Circ Res.* 1999;84(1):53-63.

57. Coleman HA, Tare M, Parkington HC. EDHF is not K^+ but may be due to spread of current from the endothelium in guinea pig arterioles. *Am J Physiol.* 2001;280(6):H2478-H2483.

58. Coleman HA, Tare M, Parkington HC. Myoendothelial electrical coupling in arteries and arterioles and its implications for endothelium-derived hyperpolarizing factor. *Clin Exp Pharmacol Physiol.* 2002;29(7):630-7.

59. Zygmunt PM, Hogestatt ED. Role of potassium channels in endothelium-dependent relaxation resistant to nitroarginine in the rat hepatic artery. *Br J Pharmacol.* 1996;117(7):1600-6.

60. Chataigneau T, Feletou M, Thollon C, Villeneuve N, Vilaine JP, Duhault J, Vanhoutte PM. Cannabinoid CB_1 receptor and endothelium-dependent hyperpolarization in guinea-pig carotid, rat mesenteric and porcine coronary arteries. *Br J Pharmacol.* 1998;123(5):968-74.

61. Wulff H, Miller MJ, Hansel W, Grissmer S, Cahalan MD, Chandy KG. Design of a potent and selective inhibitor of the intermediate-conductance Ca^{2+}-activated K^+ channel, IK_{Ca1}: a potential immunosuppressant. *Proc Natl Acad Sci U S A.* 2000;97(14):8151-6.

62. Eichler I, Wibawa J, Grgic I, Knorr A, Brakemeier S, Pries AR, Hoyer J, Kohler R. Selective blockade of endothelial Ca^{2+}-activated small- and intermediate-conductance K^+-channels suppresses EDHF-mediated vasodilation. *Br J Pharmacol.* 2003;138(4):594-601.

63. Hinton JM, Langton PD. Inhibition of EDHF by two new combinations of K^+-channel inhibitors in rat isolated mesenteric arteries. *Br J Pharmacol.* 2003;138(6):1031-5.

64. Nelson MT, Quayle JM. Physiological roles and properties of potassium channels in arterial smooth muscle. *Am J Physiol.* 1995;268(4 Pt 1):C799-C822.

65. Brayden JE, Nelson MT. Regulation of arterial tone by activation of calcium-dependent potassium channels. *Science.* 1992;256(5056):532-5.

66. Shimokawa H, Yasutake H, Fujii K, Owada MK, Nakaike R, Fukumoto Y, Takayanagi T, Nagao T, Egashira K, Fujishima M, Takeshita A. The importance of the hyperpolarizing mechanism

increases as the vessel size decreases in endothelium-dependent relaxations in rat mesenteric circulation. *J Cardiovasc Pharmacol*.1996;28(5):703-11.

67. Nagao T, Illiano S, Vanhoutte PM. Heterogeneous distribution of endothelium-dependent relaxations resistant to NG-nitro-L-arginine in rats. *Am J Physiol.* 1992;263(4 Pt 2):H1090-H1094.

68. Hoeffner U, Boulanger C, Vanhoutte PM. Proximal and distal dog coronary arteries respond differently to basal EDRF but not to NO. *Am J Physiol.* 1989;256(3 Pt 2):H828-H831.

69. Shimokawa H. Endothelial dysfunction in hypertension. *J Atheroscler Thromb.* 1998;4(3):118-27.

70. De Mey JG, Vanhoutte PM. Contribution of the endothelium to the response to anoxia in the canine femoral artery. *Arch Int Pharmacodyn Ther.* 1981;253(2):325-6.

71. Katusic ZS, Shepherd JT. Endothelium-derived vasoactive factors: II. Endothelium-dependent contraction. *Hypertension.* 1991;18(Suppl 5):III86-III92.

72. Taddei S, Vanhoutte PM. Endothelium-dependent contractions to endothelin in the rat aorta are mediated by thromboxane A_2. *J Cardiovasc Pharmacol.* 1993;22 (Suppl 8):S328-S331.

73. Ge T, Hughes H, Junquero DC, Wu KK, Vanhoutte PM, Boulanger CM. Endothelium-dependent contractions are associated with both augmented expression of prostaglandin H synthase-1 and hypersensitivity to prostaglandin H2 in the SHR aorta. *Circ Res.* 1995;76(6):1003-10.

74. Yanagisawa M, Kurihara H, Kimura S, Tomobe Y, Kobayashi M, Mitsui Y, Yazaki Y, Goto K, Masaki T. A novel potent vasoconstrictor peptide produced by vascular endothelial cells. *Nature.* 1988;332(6163):411-5.

75. Katusic ZS, Vanhoutte PM. Superoxide anion is an endothelium-derived contracting factor. *Am J Physiol*.1989;257(1 Pt 2):H33-H37.

76. Boulanger C, Luscher TF. Release of endothelin from the porcine aorta. Inhibition by endothelium-derived nitric oxide. *J Clin Invest.* 1990;85(2):587-90.

77. Luscher TF, Boulanger CM, Dohi Y, Yang ZH. Endothelium-derived contracting factors. *Hypertension.* 1992;19(2):117-30.

78. Boulanger CM, Tanner FC, Bea ML, Hahn AW, Werner A, Luscher TF. Oxidized low density lipoproteins induce mRNA expression and release of endothelin from human and porcine endothelium. *Circ Res.* 1992;70(6):1191-7.

79. Morris JL, Gibbins IL, Kadowitz PJ, Herzog H, Kreulen DL, Toda N, Claing A. Roles of peptides and other substances in cotransmission from vascular autonomic and sensory neurons. *Can J Physiol Pharmacol.* 1995;73(5):521-32.

80. Kuroiwa M, Aoki H, Kobayashi S, Nishimura J, Kanaide H. Mechanism of endothelium-dependent relaxation induced by substance P in the coronary artery of the pig. *Br J Pharmacol.* 1995;116(3):2040-7.

81. Mizuta A, Takano Y, Honda K, Saito R, Matsumoto T, Kamiya H. Nitric oxide is a mediator of tachykinin NK_3 receptor-induced relaxation in rat mesenteric artery. *Br J Pharmacol.* 1995;116(7):2919-22.

82. Stephenson JA, Burcher E, Summers RJ. Autoradiographic demonstration of endothelium-dependent ^{125}I-Bolton-Hunter substance P binding to dog carotid artery. *Eur J Pharmacol.* 1986;124(3):377-8.

83. Kummer W, Shigemoto R, Haberberger R. Smooth muscle cells are the site of neurokinin-1 receptor localization in the arterial supply of the rat sciatic nerve. *Neurosci Lett.* 1999;259(2):119-22.

84. Kawasaki H, Takasaki K, Saito A, Goto K. Calcitonin gene-related peptide acts as a novel vasodilator neurotransmitter in mesenteric resistance vessels of the rat. *Nature.* 1988;335(6186):164-7.

85. Bell D, McDermott BJ. Calcitonin gene-related peptide in the cardiovascular system: characterization of receptor populations and their (patho)physiological significance. *Pharmacol Rev.* 1996;48(2):253-88.

86. Quayle JM, Bonev AD, Brayden JE, Nelson MT. Calcitonin gene-related peptide activated ATP-sensitive K^+ currents in rabbit arterial smooth muscle via protein kinase A. *J Physiol.* 1994;475(1):9-13.

87. Brain SD, Williams TJ, Tippins JR, Morris HR, MacIntyre I. Calcitonin gene-related peptide is a potent vasodilator. *Nature.* 1985;313(5997):54-6.

88. Gray DW, Marshall I. A pharmacological profile of the endothelium-derived relaxant factor released by calcitonin gene-related peptide in rat aorta. *Ann N Y Acad Sci.* 1992;657:517-8.

89. Edwards G, Weston AH. Endothelium-derived hyperpolarizing factor--a critical appraisal. *Prog Drug Res.* 1998;50:107-33.

90. Chauhan SD, Nilsson H, Ahluwalia A, Hobbs AJ. Release of C-type natriuretic peptide accounts for the biological activity of endothelium-derived hyperpolarizing factor. *Proc Natl Acad Sci U S A.* 2003;100(3):1426-31.

91. Simonsen U, Wadsworth RM, Buus NH, Mulvany MJ. In vitro simultaneous measurements of relaxation and nitric oxide concentration in rat superior mesenteric artery. *J Physiol.* 1999;516 (Pt 1):271-82.

92. Tare M, Parkington HC, Coleman HA, Neild TO, Dusting GJ. Hyperpolarization and relaxation of arterial smooth muscle caused by nitric oxide derived from the endothelium. *Nature.* 1990;346(6279):69-71.

93. Parkington HC, Tare M, Tonta MA, Coleman HA. Stretch revealed three components in the hyperpolarization of guinea-pig coronary artery in response to acetylcholine. *J Physiol.* 1993;465:459-76.

94. Vanheel B, Van de Voorde J, Leusen I. Contribution of nitric oxide to the endothelium-dependent hyperpolarization in rat aorta. *J Physiol.* 1994;475(2):277-84.

95. Vanheel B, Van de Voorde J. Nitric oxide induced membrane hyperpolarization in the rat aorta is not mediated by glibenclamide-sensitive potassium channels. *Can J Physiol Pharmacol.* 1997;75(12):1387-92.

96. Vanheel B, Van de Voorde J. Differential influence of extracellular and intracellular pH on K^+ accumulation in ischaemic mammalian cardiac tissue. *J Mol Cell Cardiol.* 1995;27(7):1443-55.

97. Ge ZD, Zhang XH, Fung PC, He GW. Endothelium-dependent hyperpolarization and relaxation resistance to N(G)-nitro-L-arginine

and indomethacin in coronary circulation. *Cardiovasc Res.* 2000;46(3):547-56.

98. Vanheel B, Van de Voorde J. EDHF and residual NO: different factors. *Cardiovasc Res.* 2000;46(3):370-5.

99. Matoba T, Shimokawa H, Kubota H, Morikawa K, Fujiki T, Kunihiro I, Mukai Y, Hirakawa Y, Takeshita A. Hydrogen peroxide is an endothelium-derived hyperpolarizing factor in human mesenteric arteries. *Biochem Biophys Res Commun.* 2002;290(3):909-13.

100. Matoba T, Shimokawa H. Hydrogen peroxide is an endothelium-derived hyperpolarizing factor in animals and humans. *J Pharmacol Sci.* 2003;92(1):1-6.

101. Beny JL, der Weid PY. Hydrogen peroxide: an endogenous smooth muscle cell hyperpolarizing factor. *Biochem Biophys Res Commun.* 1991;176(1):378-84.

102. Pomposiello S, Rhaleb NE, Alva M, Carretero OA. Reactive oxygen species: role in the relaxation induced by bradykinin or arachidonic acid via EDHF in isolated porcine coronary arteries. *J Cardiovasc Pharmacol.* 1999;34(4):567-74.

103. Hamilton CA, McPhaden AR, Berg G, Pathi V, Dominiczak AF. Is hydrogen peroxide an EDHF in human radial arteries? *Am J Physiol.* 2001;280(6):H2451-H2455.

104. McNeish AJ, Wilson WS, Martin W. Ascorbate blocks endothelium-derived hyperpolarizing factor (EDHF)-mediated vasodilatation in the bovine ciliary vascular bed and rat mesentery. *Br J Pharmacol.* 2002;135(7):1801-9.

105. Gao YJ, Lee RM. Hydrogen peroxide induces a greater contraction in mesenteric arteries of spontaneously hypertensive rats through thromboxane A(2) production. *Br J Pharmacol.* 2001;134(8):1639-46.

106. Beny JL, Schaad O. An evaluation of potassium ions as endothelium-derived hyperpolarizing factor in porcine coronary arteries. *Br J Pharmacol.* 2000;131(5):965-73.

107. Crane GJ, Walker SD, Dora KA, Garland CJ. Evidence for a differential cellular distribution of inward rectifier K^+ channels in the rat isolated mesenteric artery. *J Vasc Res.* 2003;40(2):159-68.

108. Lacy PS, Pilkington G, Hanvesakul R, Fish HJ, Boyle JP, Thurston H. Evidence against potassium as an endothelium-derived hyperpolarizing factor in rat mesenteric small arteries. *Br J Pharmacol.* 2000;129(3):605-11.

109. Doughty JM, Boyle JP, Langton PD. Potassium does not mimic EDHF in rat mesenteric arteries. *Br J Pharmacol.* 2000;130(5):1174-82.

110. Richards GR, Weston AH, Burnham MP, Feletou M, Vanhoutte PM, Edwards G. Suppression of K^+-induced hyperpolarization by phenylephrine in rat mesenteric artery: relevance to studies of endothelium-derived hyperpolarizing factor. *Br J Pharmacol.* 2001;134(1):1-5.

111. Bolton TB, Clapp LH. The diverse effects of noradrenaline and other stimulants on ^{86}Rb and ^{42}K efflux in rabbit and guinea-pig arterial muscle. *J Physiol.* 1984;355:43-63.

112. Prior HM, Webster N, Quinn K, Beech DJ, Yates MS. K^+-induced dilation of a small renal artery: no role for inward rectifier K^+ channels. *Cardiovasc Res.* 1998;37(3):780-90.

113. Blanco G, Mercer RW. Isozymes of the Na^+/K^+-ATPase: heterogeneity in structure, diversity in function. *Am J Physiol.* 1998;275(5 Pt 2):F633-F650.

114. Crambert G, Hasler U, Beggah AT, Yu C, Modyanov NN, Horisberger JD, Lelievre L, Geering K. Transport and pharmacological properties of nine different human Na^+/K^+-ATPase isozymes. *J Biol Chem.* 2000;275(3):1976-86.

115. Edwards G, Feletou M, Gardener MJ, Thollon C, Vanhoutte PM, Weston AH. Role of gap junctions in the responses to EDHF in rat and guinea-pig small arteries. *Br J Pharmacol.* 1999;128(8):1788-94.

116. Busse R, Edwards G, Feletou M, Fleming I, Vanhoutte PM, Weston AH. EDHF: bringing the concepts together. *Trends Pharmacol Sci.* 2002;23(8):374-80.

117. Archer SL, Gragasin FS, Wu X, Wang S, McMurtry S, Kim DH, Platonov M, Koshal A, Hashimoto K, Campbell WB, Falck JR, Michelakis ED. Endothelium-derived hyperpolarizing factor in human internal mammary artery is 11,12-epoxyeicosatrienoic acid

and causes relaxation by activating smooth muscle BK_{Ca} channels. *Circulation.* 2003;107(5):769-76.

118. Zhang Y, Oltman CL, Lu T, Lee HC, Dellsperger KC, VanRollins M. EET homologs potently dilate coronary microvessels and activate BK_{Ca} channels. *Am J Physiol.* 2001;280(6):H2430-H2440.

119. Pratt PF, Li P, Hillard CJ, Kurian J, Campbell WB. Endothelium-independent, ouabain-sensitive relaxation of bovine coronary arteries by EETs. *Am J Physiol.* 2001;280(3):H1113-H1121.

120. Campbell WB, Harder DR. Endothelium-derived hyperpolarizing factors and vascular cytochrome P450 metabolites of arachidonic acid in the regulation of tone. *Circ Res.* 1999;84(4):484-8.

121. Fleming I, Fisslthaler B, Michaelis UR, Kiss L, Popp R, Busse R. The coronary endothelium-derived hyperpolarizing factor (EDHF) stimulates multiple signalling pathways and proliferation in vascular cells. *Pflugers Arch.* 2001;442(4):511-8.

122. Hecker M, Bara AT, Bauersachs J, Busse R. Characterization of endothelium-derived hyperpolarizing factor as a cytochrome P450-derived arachidonic acid metabolite in mammals. *J Physiol.* 1994;481 (Pt 2):407-14.

123. Chen G, Cheung DW. Modulation of endothelium-dependent hyperpolarization and relaxation to acetylcholine in rat mesenteric artery by cytochrome P450 enzyme activity. *Circ Res.* 1996;79(4):827-33.

124. Fulton D, Mahboubi K, McGiff JC, Quilley J. Cytochrome P450-dependent effects of bradykinin in the rat heart. *Br J Pharmacol.* 1995;114(1):99-102.

125. Dong H, Waldron GJ, Galipeau D, Cole WC, Triggle CR. NO/PGI_2-independent vasorelaxation and the cytochrome P450 pathway in rabbit carotid artery. *Br J Pharmacol.* 1997;120(4):695-701.

126. Fisslthaler B, Popp R, Kiss L, Potente M, Harder DR, Fleming I, Busse R. Cytochrome P450 2C is an EDHF synthase in coronary arteries. *Nature.* 1999;401(6752):493-7.

127. Rosolowsky M, Campbell WB. Role of PGI_2 and epoxyeicosatrienoic acids in relaxation of bovine coronary arteries to arachidonic acid. *Am J Physiol.* 1993;264(2 Pt 2):H327-H335.

128. Vanheel B, Van de Voorde J. Evidence against the involvement of cytochrome P450 metabolites in endothelium-dependent hyperpolarization of the rat main mesenteric artery. *J Physiol.* 1997;501 (Pt 2):331-41.

129. Vanheel B, Calders P, Van den Bossche I, Van de Voorde J. Influence of some phospholipase A_2 and cytochrome P450 inhibitors on rat arterial smooth muscle K^+ currents. *Can J Physiol Pharmacol.* 1999;77(7):481-9.

130. Edwards G, Zygmunt PM, Hogestatt ED, Weston AH. Effects of cytochrome P450 inhibitors on potassium currents and mechanical activity in rat portal vein. *Br J Pharmacol.* 1996;119(4):691-701.

131. Corriu C, Feletou M, Canet E, Vanhoutte PM. Inhibitors of the cytochrome P450 monooxygenase and endothelium-dependent hyperpolarizations in the guinea-pig isolated carotid artery. *Br J Pharmacol.* 1996;117(4):607-10.

132. Zygmunt PM, Edwards G, Weston AH, Davis SC, Hogestatt ED. Effects of cytochrome P450 inhibitors on EDHF-mediated relaxation in the rat hepatic artery. *Br J Pharmacol.* 1996;118(5):1147-52.

133. Graier WF, Holzmann S, Hoebel BG, Kukovetz WR, Kostner GM. Mechanisms of L-NG nitroarginine/indomethacin-resistant relaxation in bovine and porcine coronary arteries. *Br J Pharmacol.* 1996;119(6):1177-86.

134. Zhang Y, Oltman CL, Lu T, Lee HC, Dellsperger KC, VanRollins M. EET homologs potently dilate coronary microvessels and activate BK_{Ca} channels. *Am J Physiol.* 2001;280(6):H2430-H2440.

135. Ellis EF, Moore SF, Willoughby KA. Anandamide and delta 9-THC dilation of cerebral arterioles is blocked by indomethacin. *Am J Physiol.* 1995;269(6 Pt 2):H1859-H1864.

136. Deutsch DG, Goligorsky MS, Schmid PC, Krebsbach RJ, Schmid HHO, Das SK, Dey SK, Arreaza G, Thorup C, Stefano G, Moore LC. Production and physiological actions of anandamide in the vasculature of the rat kidney. *J Clin Invest.* 1997;100(6):1538-46.

137. Pratt PF, Hillard CJ, Edgemond WS, Campbell WB. N-arachidonylethanolamide relaxation of bovine coronary artery is not mediated by CB_1 cannabinoid receptor. *Am J Physiol.* 1998;43(1):H375-H381.

138. Zygmunt PM, Petersson J, Andersson DA, Chuang HH, Sorgard M, Di Marzo V, Julius D, Hogestatt ED. Vanilloid receptors on sensory nerves mediate the vasodilator action of anandamide. *Nature.* 1999;400(6743):452-7.

139. Vanheel B, Van de Voorde J. Regional differences in anandamide- and methanandamide-induced membrane potential changes in rat mesenteric arteries. *J Pharmacol Exp Ther.* 2001;296(2):322-8.

140. Randall MD, Kendall DA. Endocannabinoids: a new class of vasoactive substances. *Trends Pharmacol Sci.* 1998;19(2):55-8.

141. Plane F, Holland M, Waldron GJ, Garland CJ, Boyle JP. Evidence that anandamide and EDHF act via different mechanisms in rat isolated mesenteric arteries. *Br J Pharmacol.* 1997;121(8):1509-11.

142. White R, Hiley CR. Comparison of the vasorelaxation caused by endothelium-derived hyperpolarizing factor (EDHF) and anandamide in the small mesenteric artery of the rat. *Br J Pharmacol.* 1997;122:23.

143. Zygmunt PM, Hogestatt ED, Waldeck K, Edwards G, Kirkup AJ, Weston AH. Studies on the effects of anandamide in rat hepatic artery. *Br J Pharmacol.* 1997;122(8):1679-86.

144. Zygmunt PM, Sorgard M, Petersson J, Johansson R, Hogestatt ED. Differential actions of anandamide, potassium ions and endothelium-derived hyperpolarizing factor in guinea-pig basilar artery. *Naunyn-Schmiedebergs Arch Pharmacol.* 2000;361(5):535-42.

145. Fulton D, Quilley J. Evidence against anandamide as the hyperpolarizing factor mediating the nitric oxide-independent coronary vasodilator effect of bradykinin in the rat. *J Pharmacol Exp Ther.* 1998;286(3):1146-51.

146. Chaytor AT, Martin PE, Evans WH, Randall MD, Griffith TM. The endothelial component of cannabinoid-induced relaxation in rabbit mesenteric artery depends on gap junctional communication. *J Physiol.* 1999;520 (Pt 2):539-50.

147. Mombouli JV, Schaeffer G, Holzmann S, Kostner GM, Graier WF. Anandamide-induced mobilization of cytosolic Ca^{2+} in endothelial cells. *Br J Pharmacol.* 1999;126(7):1593-600.

148. Emerson GG, Segal SS. Electrical coupling between endothelial cells and smooth muscle cells in hamster feed arteries: role in vasomotor control. *Circ Res.* 2000;87(6):474-9.

149. Dora KA, Sandow SL, Gallagher NT, Takano H, Rummery NM, Hill CE, Garland CJ. Myoendothelial gap junctions may provide the pathway for EDHF in mouse mesenteric artery. *J Vasc Res.* 2003;40(5):480-90.

150. Spagnoli LG, Villaschi S, Neri L, Palmieri G. Gap junctions in myo-endothelial bridges of rabbit carotid arteries. *Experientia.* 1982;38(1):124-5.

151. Kumar NM, Gilula NB. The gap junction communication channel. *Cell.* 1996;84(3):381-8.

152. Perkins GA, Goodenough DA, Sosinsky GE. Formation of the gap junction intercellular channel requires a 30 degree rotation for interdigitating two apposing connexons. *J Mol Biol.* 1998;277(2):171-7.

153. Kumar NM, Gilula NB. Cloning and characterization of human and rat liver cDNAs coding for a gap junction protein. *J Cell Biol.* 1986;103(3):767-76.

154. Willecke K, Eiberger J, Degen J, Eckardt D, Romualdi A, Guldenagel M, Deutsch U, Sohl G. Structural and functional diversity of connexin genes in the mouse and human genome. *Biol Chem.* 2002;383(5):725-37.

155. Goodenough DA, Goliger JA, Paul DL. Connexins, connexons, and intercellular communication. *Annu Rev Biochem.* 1996;65:475-502.

156. Hill CE, Phillips JK, Sandow SL. Heterogeneous control of blood flow amongst different vascular beds. *Med Res Rev.* 2001;21(1):1-60.

157. Severs NJ, Rothery S, Dupont E, Coppen SR, Yeh HI, Ko YS, Matsushita T, Kaba R, Halliday D. Immunocytochemical analysis of connexin expression in the healthy and diseased cardiovascular system. *Microsc Res Tech.* 2001;52(3):301-22.

158. Brink PR. Gap junctions in vascular smooth muscle. *Acta Physiol Scand.* 1998;164(4):349-56.

159. Hill CE, Rummery N, Hickey H, Sandow SL. Heterogeneity in the distribution of vascular gap junctions and connexins: implications for function. *Clin Exp Pharmacol Physiol.* 2002;29(7):620-5.

160. Mather S, Dora KA, Sandow SL, Winter P, Garland CJ. Rapid endothelial cell-selective loading of connexin 40 antibody blocks endothelium-derived hyperpolarizing factor dilation in rat small mesenteric arteries. *Circ Res.* 2005;97(4):399-407.

161. Sandow SL, Hill CE. Incidence of myoendothelial gap junctions in the proximal and distal mesenteric arteries of the rat is suggestive of a role in endothelium-derived hyperpolarizing factor-mediated responses. *Circ Res.* 2000;86(3):341-6.

162. Beny JL, Pacicca C. Bidirectional electrical communication between smooth muscle and endothelial cells in the pig coronary artery. *Am J Physiol.* 1994;266(4 Pt 2):H1465-H1472.

163. Chaytor AT, Evans WH, Griffith TM. Peptides homologous to extracellular loop motifs of connexin 43 reversibly abolish rhythmic contractile activity in rabbit arteries. *J Physiol.* 1997;503 (Pt 1):99-110.

164. Taylor HJ, Chaytor AT, Evans WH, Griffith TM. Inhibition of the gap junctional component of endothelium-dependent relaxations in rabbit iliac artery by 18-alpha glycyrrhetinic acid. *Br J Pharmacol.* 1998;125(1):1-3.

165. Santicioli P, Maggi CA. Effect of 18beta-glycyrrhetinic acid on electromechanical coupling in the guinea-pig renal pelvis and ureter. *Br J Pharmacol.* 2000;129(1):163-9.

166. Chaytor AT, Evans WH, Griffith TM. Central role of heterocellular gap junctional communication in endothelium-dependent relaxations of rabbit arteries. *J Physiol.* 1998;508 (Pt 2):561-73.

167. Dora KA, Duling BR. Use of fluorescent reporters in the quantitation of microvascular function. *Microcirculation.* 1998;5(2-3):95-100.

168. Fleming I. Myoendothelial gap junctions: the gap is there, but does EDHF go through it? *Circ Res.* 2000;86(3):249-50.

169. Edwards G, Feletou M, Gardener MJ, Glen CD, Richards GR, Vanhoutte PM, Weston AH. Further investigations into the endothelium-dependent hyperpolarizing effects of bradykinin and

substance P in porcine coronary artery. *Br J Pharmacol.* 2001;133(7):1145-53.

170. Hall W, Solowij N. Adverse effects of cannabis. *Lancet.* 1998;352(9140):1611-6.

171. Robson P. Cannabis. *Arch Dis Child.* 1997;77(2):164-6.

172. Hirst RA, Lambert DG, Notcutt WG. Pharmacology and potential therapeutic uses of cannabis. *Br J Anaesth.* 1998;81(1):77-84.

173. Hillard CJ. Endocannabinoids and vascular function. *J Pharmacol Exp Ther.* 2000;294(1):27-32.

174. Randall MD, Harris D, Kendall DA, Ralevic V. Cardiovascular effects of cannabinoids. *PharmacolTher.* 2002;95(2):191-202.

175. Matsuda LA, Lolait SJ, Brownstein MJ, Young AC, Bonner TI. Structure of a cannabinoid receptor and functional expression of the cloned cDNA. *Nature.* 1990;346(6284):561-4.

176. Germano MP, D'Angelo V, Mondello MR, Pergolizzi S, Capasso F, Capasso R, Izzo AA, Mascolo N, De Pasquale R. Cannabinoid CB_1-mediated inhibition of stress-induced gastric ulcers in rats. *Naunyn Schmiedebergs Arch Pharmacol.* 2001;363(2):241-4.

177. Liu J, Gao B, Mirshahi F, Sanyal AJ, Khanolkar AD, Makriyannis A, Kunos G. Functional CB_1 cannabinoid receptors in human vascular endothelial cells. *Biochem J.* 2000;346:835-40.

178. Sugiura T, Kodaka T, Nakane S, Kishimoto S, Kondo S, Waku K. Detection of an endogenous cannabimimetic molecule, 2-arachidonoylglycerol, and cannabinoid CB_1 receptor mRNA in human vascular cells: Is 2-arachidonoylglycerol a possible vasomodulator? *Biochem Biophys Res Commun.* 1998;243(3):838-43.

179. Munro S, Thomas KL, Abu-Shaar M. Molecular characterization of a peripheral receptor for cannabinoids. *Nature.* 1993;365(6441):61-5.

180. Griffin G, Fernando SR, Ross RA, McKay NG, Ashford ML, Shire D, Huffman JW, Yu S, Lainton JA, Pertwee RG. Evidence for the presence of CB_2-like cannabinoid receptors on peripheral nerve terminals. *Eur J Pharmacol.* 1997;339(1):53-61.

181. White R, Ho WSV, Bottrill FE, Ford WR, Hiley CR. Mechanisms of anandamide-induced vasorelaxation in rat isolated coronary arteries. *Br J Pharmacol.* 2001;134(4):921-9.

182. Jarai Z, Wagner JA, Varga K, Lake KD, Compton DR, Martin BR, Zimmer AM, Bonner TI, Buckley NE, Mezey E, Razdan RK, Zimmer A, Kunos G. Cannabinoid-induced mesenteric vasodilation through an endothelial site distinct from CB_1 or CB_2 receptors. *Proc Natl Acad Sci U S A.* 1999;96(24):14136-41.

183. Wagner JA, Varga K, Jarai Z, Kunos G. Mesenteric vasodilation mediated by endothelial anandamide receptors. *Hypertension.* 1999;33(1):429-34.

184. Offertaler L, Mo FM, Batkai S, Liu J, Begg M, Razdan RK, Martin BR, Bukoski RD, Kunos G. Selective ligands and cellular effectors of a G protein-coupled endothelial cannabinoid receptor. *Mol Pharmacol.* 2003;63(3):699-705.

185. Devane WA, Hanus L, Breuer A, Pertwee RG, Stevenson LA, Griffin G, Gibson D, Mandelbaum A, Etinger A, Mechoulam R. Isolation and structure of a brain constituent that binds to the cannabinoid receptor. *Science.* 1992;258(5090):1946-9.

186. Zygmunt PM, Plane F, Paulsson M, Garland CJ, Hogestatt ED. Interactions between endothelium-derived relaxing factors in the rat hepatic artery: focus on regulation of EDHF. *Br J Pharmacol.* 1998;124(5):992-1000.

187. O'Sullivan SE, Kendall DA, Randall MD. Heterogeneity in the mechanisms of vasorelaxation to anandamide in resistance and conduit rat mesenteric arteries. *Br J Pharmacol.* 2004;142(3):435-42.

188. Fleming I, Schermer B, Popp R, Busse R. Inhibition of the production of endothelium-derived hyperpolarizing factor by cannabinoid receptor agonists. *Br J Pharmacol.* 1999;126(4):949-60.

189. White R, Hiley CR. A comparison of EDHF-mediated and anandamide-induced relaxations in the rat isolated mesenteric artery. *Br J Pharmacol.* 1997;122(8):1573-84.

190. White R, Hiley CR. The actions of the cannabinoid receptor antagonist, SR 141716A, in the rat isolated mesenteric artery. *Br J Pharmacol.* 1998;125(4):689-96.

191. Watanabe H, Vriens J, Prenen J, Droogmans G, Voets T, Nilius B. Anandamide and arachidonic acid use epoxyeicosatrienoic acids to activate $TRPV_4$ channels. *Nature.* 2003;424(6947):434-8.

192. Yao XQ, Garland CJ. Recent developments in vascular endothelial cell transient receptor potential channels. *Circ Res.* 2005;97(9):853-63.

193. Earley S, Heppner TJ, Nelson MT, Brayden JE. $TRPV_4$ forms a novel Ca^{2+} signaling complex with ryanodine receptors and BK_{Ca} channels. *Circ Res.* 2005;97(12):1270-9.

194. Van de Voorde J, Vanheel B. EDHF-mediated relaxation in rat gastric small arteries: influence of ouabain/Ba^{2+} and relation to potassium ions. *J Cardiovasc Pharmacol.* 2000;35(4):543-8.

Chapter

2

Materials & methods

2.1. INTRODUCTION

Vasodilatation plays an important role in the regulation of blood flow and blood supply to the organs. Several techniques have been developed to study the pharmacodynamics of isolated small resistance arteries. Such *in vitro* experiments with segments of isolated arteries offer a useful approach to analyse the influence of local mechanisms controlling blood flow, without other interfering with other regulatory mechanisms as may be present in *in vivo* experiments.

In the studies composing this work, different techniques have been used to study the mechanism of action of endothelium derived hyperpolarizing factor and endocannabinoids. Membrane potentials of the vascular smooth muscle cells were measured using electrophysiological microelectrode techniques. Tension measurements were performed in a wire myograph to study relaxation and contractile responses. Finally, intracellular Ca^{2+} changes were monitored using fluorescent dyes and confocal microscopy.

2.2. TISSUE PREPARATION

All experiments were performed on isolated arterial ring segments from adult female Wistar rats (180 – 280 g) and were approved by the ethical committee on animal research of Ghent University. The animals were anesthetized by a lethal dose (200 mg kg^{-1}) of pentobarbitone and killed by cervical dislocation.

For the studies described in this thesis, small mesenteric or gastric arteries were used. Therefore, the mesentery or the stomach, as appropriate, were rapidly excised and placed in cold (4°C) Krebs-Ringer bicarbonate (KRB)

solution. Second and third order branches of the arteries were dissected free and transferred to fresh KRB solution, gassed with 5% CO_2 in O_2 (pH 7.4). Then the vessels were cleaned from surrounding connective tissue. For the electrophysiological and tension measurements, the isolated vessels were cut into segments of about 4 mm in length and transferred to the respective experimental chambers. For the Ca^{2+} imaging studies, larger segments were used. These vessel segments were cannulated with a thin glass capillary (borosilicate glass, Hilgenberg, Malsfeld, Germany) with flame polished tip that was inserted into the lumen over the entire segment length. The diameter of the glass capillary was slightly (~15 %) larger than the vessel lumen diameter and cannulation was done to stabilize the preparation against possible movement upon stimulation with low concentrations of norepinephrine.

2.3. ELECTROPHYSIOLOGICAL EXPERIMENTS

Hyperpolarization of the vascular smooth muscle cells is one of the possible ways to induce vasorelaxation and subsequent vasodilation. It is generally accepted that a change in the membrane potential of a few mV can result in a substantial change in vessel diameter [1, 2]. Furthermore, hyperpolarization of the vascular smooth muscle cells produces a rapid effect on blood flow. Therefore, membrane potential measurements are of great importance in the study of vasodilatation.

2.3.1. Experimental setup

The experimental set-up for membrane potential measurements is depicted in figure 1. A small cut-away (with a volume of approximately 5 ml) in a

Perspex block (6 x 8 x 8 cm), heated by a Lauda bath (37 °C, Haake, Berlin, Germany), forms the experimental chamber. Since vibration is to be avoided to allow cell impalements for an extended period, the whole experimental set-up is mounted on a pneumatic vibration isolation table.

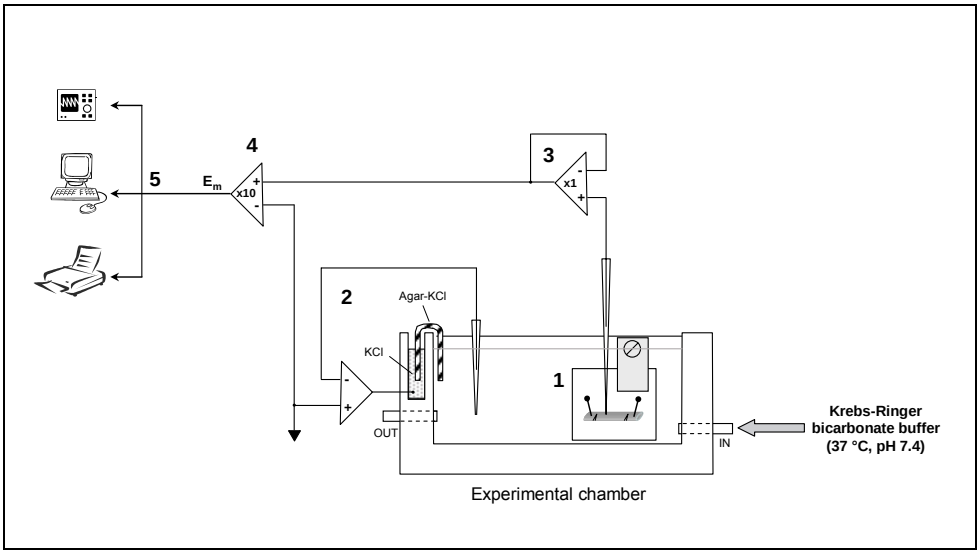

Figure 1: *Experimental set-up for membrane potential measurements: (1) vessel segment pinned down to a silicone base with insect pins and fixed to the bottom of the experimental chamber; (2) bath-clamp; (3) pre-amplifier for impedance compensation; (4) amplifier; (5) the measured membrane potential is monitored on an oscilloscope and a computer and traced with a pen recorder.*

The isolated arterial rings are pinned down to a silicone base using two small insect pins. Small incisions are made at the distal endings to facilitate diffusion of added vasoactive agents to the lumenal side. The preparations are then fixed on the bottom of the experimental chamber under an angle of 45°, permitting visualisation from the front with a binocular microscope, the penetrating microelectrode being in focus with the preparation. The chamber is perfused with warmed KRB solution (35 °C), gassed with 95% O_2 and 5% CO_2 in an external bath. A roller pump (minipuls 2, Gilson)

transfers the solution through a polyethylene tubing to the experimental chamber at a flow rate of 5 ml/min. Before reaching the vessel segment, the solution passes a spiral shaped glass tubing at the bottom of the experimental block, to compensate for possible cooling during the transfer. The volume in the organ chamber is kept as low as necessary just to cover the vessel by adjusting the outflow, facilitating impalements and visualisation of the preparations through the binocular microscope. After mounting in the experimental chamber, the arteries are equilibrated for at least 60 minutes before starting the microelectrode impalements.

2.3.2. Membrane potential measurements

The experimental bath was continuously clamped at ground potential using a bath clamp circuit. The operational amplifier of this circuit is connected at the non-inverting input with the virtual ground, while the inverting input is connected to the bath through an Ag/AgCl electrode. The output of the amplifier is connected back to the experimental bath fluid via an agar-KCl bridge. Hereby, possible fluctuations of the ground potential are immediately corrected by supplying the appropriate current to the bath. Hence, the bath potential is always clamped at the same virtual ground level.

Transmembrane potentials of the vascular smooth muscle cells are measured by penetrating the cells with conventional microelectrodes pulled with a vertical pipette puller (David Kopf, Tujunga, CA) from filamented borosilicate glass tubings (1 mm o.d., Hilgenberg, Malsfeld, Germany). The microelectrodes are filled with 1 M KCl and fixed on a preamplifier which is mounted on an oil driven micromanipulator (Narishige MO-388, Nikon) . A

short Ag/AgCl wire provides electrical contact between the preamplifier and the solution in the electrode. The electrical resistance of the microelectrodes, measured in normal KRB solution, ranges from 40 – 80 MΩ. The used preamplifiers have high impedance compared with the microelectrode (MOS/FET operational amplifier with an impedance of 1.5 x 10^3 MΩ) and hence serve for impedance compensation. The electrodes and the pre-amplifier are shielded by an aluminium plate, protecting them from environmental electrostatic influences (Faraday cage). The output of the preamplifier is connected to an amplifier where the bath potential is subtracted from the measured potential. The resulting potential is monitored on an oscilloscope and followed on a computer monitor after AD-conversion using a data acquisition processor board (Microstar Laboratories) with appropriate software (DAPview Plus 1.10; Microstar Laboratories). The measured potential is also traced with a pen recorder at low speed. In some experiments, the recorded pen traces are digitized off-line with a digitizing tablet connected to a PC.

The micromanipulator allows advancing the electrodes in very small steps until stable cell penetration is reached. Successful impalements of the vascular smooth muscle cells are characterised by an extremely sharp voltage deflection on entering the cell and a fast return to the baseline on exit of the microelectrode from the cell. Absolute values for the membrane potential (E_m) are taken as the difference of the stabilised potential after cell impalement and the zero potential as obtained upon electrode dislodgement. During a successful impalement, membrane potential responses produced by vasoactive substances are measured under control conditions and after preincubation with inhibitors. All drugs are added into a know volume in the outside mixing chamber and perfused at known concentrations into the experimental chamber.

2.4. TENSION MEASUREMENTS

The mechanical properties of ring segments of small resistance vessels were investigated using a wire myograph. This technique allows the study of the contractile reactivity of isolated arteries. It is based on the methods developed by Mulvany and Halpern (1976) [3]. Briefly, vessel segments are mounted in the organ chamber of a wire myograph onto two thin (40 µm diameter) wires (figure 2). One of the wires is connected to a force transducer, which allows measurement of isometric tension changes of the ring segments.

2.4.1. The wire myograph

For the tension measurements, a manual wire myograph was used constructed by the technical staff of our laboratory (Mr. Dirk De Gruytere and Mr. Cyriel Mabilde). Each preparation is mounted under a dissecting microscope onto two thin stainless steel wires that are fixed at two holders. One holder is connected to a micrometer which is used to change the distance between the wires in the beginning of the experiment, in order to apply a passive force on the vessel. The other holder was connected to a force-displacement transducer that measures the isometric tension changes in the vessel segment (figure 2).

2.4.2. Mounting of a ring segment

Before mounting, the first thin wire is cut to length (approximately 2.5 cm) and is clamped between the two holders in the organ bath (figure 3A). The

far end of the wire is then fixed on the left holder with a screw. The near end, pointing towards the operator, is kept free so that a ring segment can be slipped over it (figure 3B and C). Next, using a pair of extra fine tweezers, the arterial ring is pulled over the free end of the wire, taking care not to injure the endothelium (figure 3D). The holders are then set apart and the vessel is drawn further over the wire, until it is situated between the holders (figure 3E). The near end of the wire can then be fixed with a screw to the other side of the left holder (figure 3F).

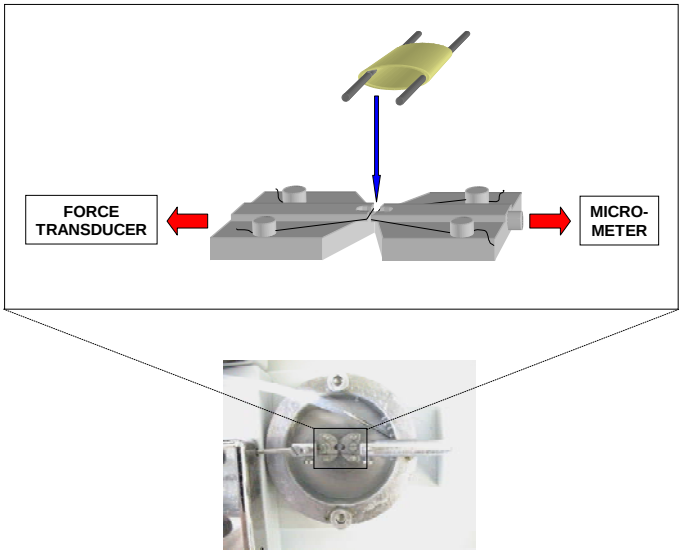

Figure 2: *A photograph of the organ bath of the wire myograph and a schematic detail of a pair of holders. Arterial segments are mounted on two thin wires, fixed on the two holders in the organ bath. One holder is connected to a micrometer which is used to change the distance between the wires. The other holder is connected to a force transducer which allows measurement of isometric tension changes in the vessel segment*

The second wire can now be guided carefully through the lumen of the artery (figure 3G). The holders are brought together, and both ends of the

second wire are fixed on the right holder. It should be noted that wires must be levelled, so that they both lay in the same horizontal plane (figure 3H and I). Once the vessel is mounted, the length of the segment (l) is measured with a micrometer eyepiece (Zeiss, Germany). The preparations are then allowed to equilibrate for at least 30 minutes in gassed KRB solution (pH 7.4) at 37 °C before proceeding with the experiment.

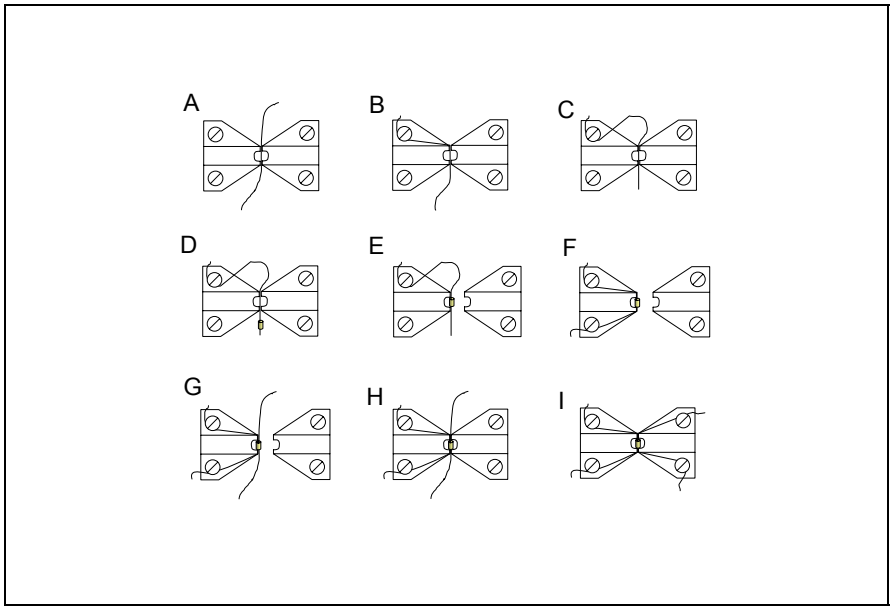

Figure 3: *Schematic presentation of the different steps involved in the mounting of an arterial segment on two thin stainless steel wires, fixed on the holders*

2.4.3. The normalisation procedure

In small arteries, the vascular smooth muscle cells are circumferentially arranged. Hence, stretching the vessel will influence the length of these smooth muscle cells [4]. Since active force development of a muscle cell depends on its length [4, 5], the vessels must be distended to bring the actin-

myosin fibres into alignment for optimal force development. It is generally accepted that the active force development in vascular tissue peaks at a certain internal circumference or diameter, which corresponds to a particular length of the smooth muscle cell. Therefore, at the beginning of each experiment, the vessels should be stretched to their optimal lumen diameter, affording optimal experimental conditions.

It has been found experimentally, that active force production is maximal when the internal circumference is 0.9 times the internal diameter that the relaxed vessel would have under a transmural pressure of 100 mmHg (IC_{100}). The normalisation procedure allows us to calculate the IC_{100} for the mounted vessel and to determine the position of the holders stretching the segment to its ideal internal circumference. Additionally, the size of the vessel can be calculated through this normalisation procedure. The size of a vessel is defined as its size when fully relaxed and under a transmural pressure of 100 mmHg.

Prior to the normalisation procedure, the micrometer setting corresponding to a force of 0 mN is determined. Therefore, the holders are brought together until the two wires touch. This is characterized by a negative force registered by the transducer. The holders are then gently pulled back until the registered force returns to baseline. At this point, the force registered by the transducer is 0 mN (y_0) and the distance between the two wires is 0 µm. The corresponding micrometer setting is x_0.

During the normalisation procedure the vessel is stretched in steps by moving the micrometer as required to drift the wires apart. One minute after each step (i), the corresponding micrometer setting (x_i) and force (y_i) are registered. These measurements allow the calculation of the internal

circumference (IC_i) and the wall tension (T_i). With these values, the transmural pressure (P_i) can be calculated that would yield this IC_i in the ring segment.

- *Calculation of the internal circumference (IC_i)*

  The IC_i is calculated from the distance between the wires ($x_i - x_0$) and the diameter of the mounting wires (40 µm) (figure 4):

  $IC_i = 2 \times ((2\pi \times 20\ \mu m) / 2) + 4 \times 20\ \mu m + 2 \times (x_i - x_0)$
  $= 205.66\ \mu m + 2 \times (x_i - x_0)$

- *Calculation of the wall tension (T_i)*

  The T_i is the measured force (y_i) divided by the length of the vessel wall. Since there is both an upper and a lower wall, the total length of the vessel wall equals two times the length of the vessel as measured with the micrometer eyepiece (l) after mounting.

  $T_i = y_i / (2 \times l)$

- *Calculation of the transmural pressure (P_i)*

  The pressure (P_i) leading to the calculated IC_i can be deduced from the law of Laplace, which states that in a cylinder, wall tension is proportional to the pressure times the radius of the cylinder. Since the radius (r) can be calculated from the IC_i ($IC_i = 2\pi\ r$), the P_i can be determined with the following formula:

  $P_i = T_i / (IC_i / 2\pi)$

It should be noted that the calculated pressure is only an estimate for the intraluminal pressure that would be necessary to stretch the vessel to the measured IC_i.

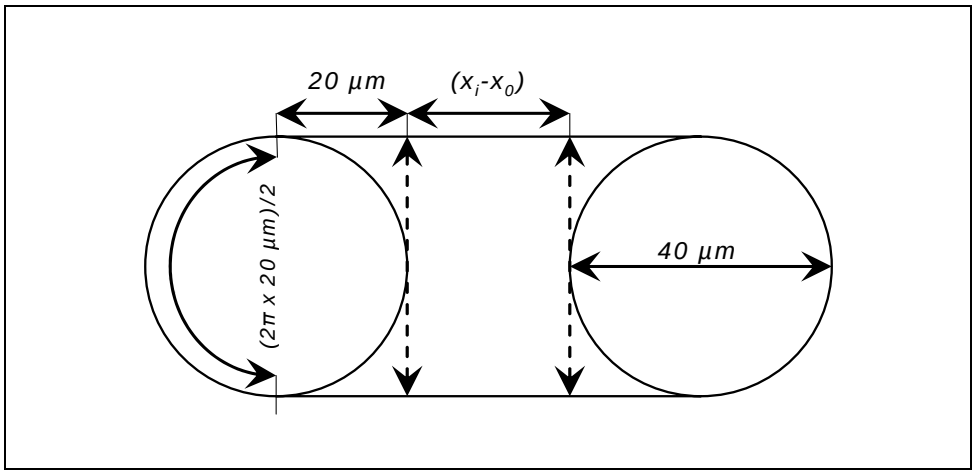

Figure 4: *A schematic representation of the blood vessel after distention i.*

For each pair of readings (x_i and y_i), the corresponding pressure is calculated. The stepwise stretching of the vessel segments is stopped when the pressure exceeds 100 mm Hg (= 13.3 kPa). Subsequently, a graph is constructed expressing the pressure in function of the corresponding internal circumference. The points are fitted on an exponential curve of the form $y = a.e^{bx}$ (figure 5). On this curve, the point corresponding with a pressure of 100 mm Hg represents the IC_{100}. Next, the ideal position of the holders to obtain an internal circumference of 0.9 x IC_{100} can be calculated by inserting this value in the formula for IC_i. At the end of the normalisation procedure, the holders are set in this position and the experiment can be started. Furthermore, the IC_{100} value allows us to

calculate the diameter the ring segment would have when exposed to a transmural pressure of 100 mm Hg (IC = 2π r).

2.4.4. A detailed example of a normalisation procedure

The following example shows the different steps in the normalisation procedure for a rat gastric artery with a length of 2.52 mm.

Starting parameters:

y_0 = 0.00 mN (force registered by the transducer at the beginning of the normalisation procedure)

x_0 = 3611 µm (position of the micrometer when the distance between the two wires is 0 µm)

P_0 = 0.00 kPa (at the start of the normalisation procedure, there is no force on the wall of the vessel, so there is no pressure)

1 minute after the first distension:

y_1 = 3.92 mN

x_1 = 3889 µm

$x_1 - x_0$ (distance between the wires) = 278 µm

From these values, we can calculate the following parameters:

IC_1 = 205.66 µm + (2 x ($x_1 - x_0$)) µm = 761.66 µm

T_1 = y_1 / (2 x l) = 3.92 mN / (2 x 2.52 mm) = 0.778 mN/mm

P_1 = T_1 / (IC_1 / 2π) = 0.778 mN/mm /(0.121 mm) = 6.42 kPa

The same calculations were made for the following distensions. The readings of x_i and y_i, obtained 1 minute after each distension, and the calculated values of IC_i, T_i and P_i are summarized in table 1.

Table 1: *values of y_i, x_i, x_i-x_0, IC_i, T_i and P_i for each distension step in the normalisation procedure of a rat gastric artery with a length of 2.52 mm.*

Step (i)	y_i (mN)	x_i (µm)	x_i-x_0 (µm)	IC_i (µm)	T_i (mN/mm)	P_i (kPa)
1	3.92	3889	278	761.66	0.778	6.42
2	6.44	3940	329	863.66	1.278	9.30
3	8.68	3971	360	925.66	1.722	11.69
4	10.64	3993	382	969.66	2.111	13.68

The relation between the internal circumference and the pressure is then expressed in an exponential curve, presented in figure 5. On this curve, the point corresponding with a pressure of 13.3 kPa corresponds with an IC_{100} of 961.6 µm. With this value, both the ideal position of the holders and the size of the artery can be calculated:

The ideal internal circumference IC_{90} = 0.9 x IC_{100} = 865.44 µm

The ideal micrometersetting (x_1') yielding this IC90 can be calculated with the following equation: IC90 = 205.66 µm + (2 x (x_1' – x_0)) µm

$\Rightarrow$ x_1' = ((IC90 -205.66 µm)/2) + x0 µm = 3941 µm

The diameter of the ring segment, when it would be exposed to a transmural pressure of 13.3 kPa **(I100)** can also be calculated:

I100 = IC100 / π = 306.1 µm

Before the start of the experiment, the micrometer is set at 3941 µm.

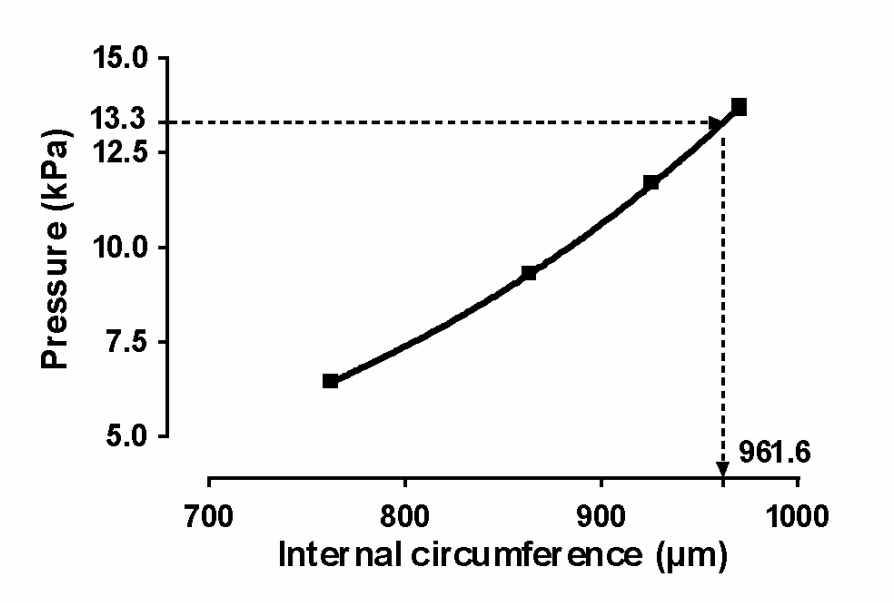

Figure 5: *Relation between the internal circumference of the ring segment and the corresponsding intraluminal pressure necessary to extend the vessel to this internal circumference. The calculated points are fitted on an exponential curve (The equation for the curve in this example is: $y=0.40048.e^{0.00364264x}$). From this curve, the internal circumference can be deduced corresponding to a pressure of 13.3 kPa.*

2.4.5. The experiment

After the normalisation procedure, the preparations are repeatedly activated with KRB solution containing 120 mM K^+ (K_{120}) and 10^{-5} M norepinephrine.

During the actual experiments, the arterial segments are contracted by adding 10^{-5} M norepinephrine to the organ bath or by replacing the standard KRB solution in the organ bath by a KRB solution containing 120 mM K^+. When a stable contraction is obtained, concentration-response curves are constructed by cumulative addition of an agonist under control

conditions or in the presence of an antagonist. The presence of functional endothelium is assessed at the start of each experiment by the ability of 10^{-5} M acetylcholine to induce more than 80 % relaxation.

In some experiments, the influence of methanandamide on the influx of extracellular Ca^{2+} through plasma membrane Ca^{2+} channels is studied. Therefore, intracellular Ca^{2+} stores are first depleted by washing the vessels with nominally Ca^{2+}-free KRB solution (same composition as normal KRB solution, but without added $CaCl_2$), exposing them subsequently to Ca^{2+}-free, EGTA (1 mM) containing solution, and repeatedly challenging the vessels to 10^{-5} M norepinephrine. After thoroughly washing the preparations with Ca^{2+}-free KRB solution, norepinephrine (10^{-5} M) is added and a concentration-contraction curve for $CaCl_2$ (10^{-5} to 10^{-2} M) is constructed in control conditions and after 30 min preincubation with 10^{-5} M methanandamide. Contractions are expressed as a percentage of the maximum contraction induced by $CaCl_2$ in control conditions.

In some experiments the endothelium has to be removed from the vessels. For this purpose, the arteries are first unstretched in the myograph. Then, an L-shaped micropipette is placed at the proximal end of the segment and gas (95 % O_2 and 5 % CO_2) is bubbled through the lumen of the preparations for 2 min. Subsequently, the vessels were again stretched to their optimal lumen diameter. After an equilibration period of 30 min, the absence of functional endothelium was confirmed by the lack of relaxation to acetylcholine.

2.5. CALCIUM IMAGING

In the Ca^{2+} imaging experiments, Ca^{2+} responses are studied in the smooth muscle cells of intact small mesenteric arteries using confocal microscopy. Briefly, the vessel preparations are loaded with the Ca^{2+} indicator fluo-3 (fluo-3) which is essentially non-fluorescent unless bound to Ca^{2+}. This allows us to visualize changes in free intracellular Ca^{2+} concentration upon addition of several agonists by measuring changes in fluorescence. Differences in efficiency of loading between different reparations were annihilated by setting baseline fluorescence as 100% and expressing changes in fluorescence as percentage of this baseline.

2.5.1. Confocal microscopy

Conventional light microscopes are probably the most well-known and used research tools, affording an easy and direct method for studying cells. Using transillumination or epifluorescence microscopy, one is able to obtain a lot of information from a single layer of cells. However, when studying for example cell-cell interactions in living cells or Ca^{2+} dynamics in tissues, these microscopes are unusable. Furthermore, images obtained with these microscopes often appear blurred and have poor contrast, due to light scattered around the image. A confocal laser scanning microscope is capable of observing selected thin layers of a thick specimen. Such microscope is not only able to produce three dimensional reconstructions of preparations, but it also creates sharp images of a specimen that would be hazy when viewed with a conventional microscope.

If light is incident on a molecule, it may absorb the light and subsequently emit light of a different colour. This process is known as fluorescence. In

the experiments performed for this thesis, excitation was done with the 488 nm line of an argon-laser (blue light). When a molecule of the fluorescent dye loaded in the cells of the preparation absorbs a photon of this high energetic light, its energy increases, subsequently bringing it to an electronically excited state (S_1 in figure 6). Some of the absorbed energy is quickly lost internally through collisions with surrounding molecules, which brings the molecule to a lower energy level (S_1' in figure 6). Finally, the molecule can fall back to its original energetic state (S_0 in figure 6), thereby causing spontaneous emission of light with a larger wavelength than the excitation light (λ=520 nm, corresponding with green light).

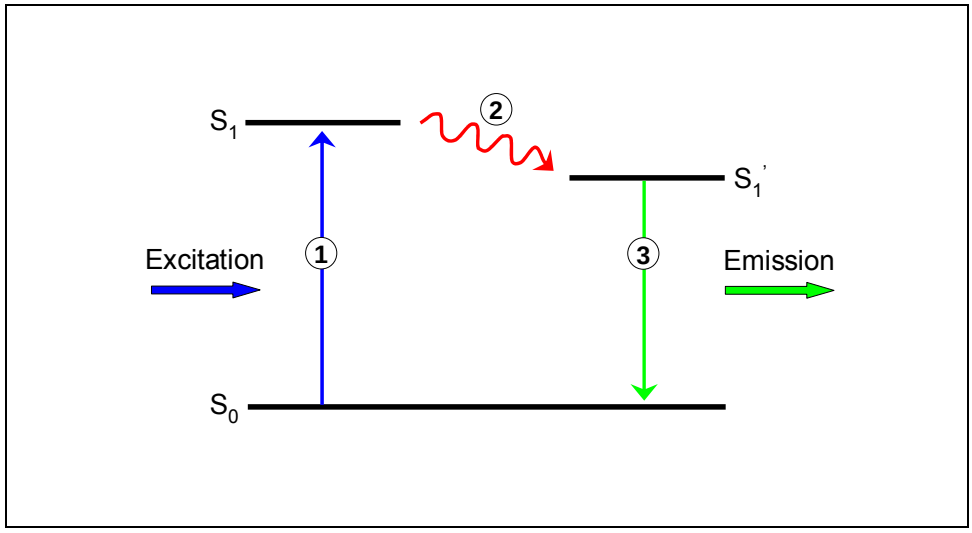

Figure 6: *Single photon excitation of a fluorescent probe. The fluorescent probe may absorb a photon of light (blue light, λ=488 nm), increasing the energy of the molecules and causing an electron to jump to a singlet excited state (1). The electron jumps from a lower, but stable energy level (S_0) to a higher unstable level (S_1). The molecule quickly loses some of the absorbed energy through collisions with neighbouring molecules, causing the electron to drop (2) to a lower energy level (S_1'). Finally, the electron returns (3) to its ground state (S_0), thereby losing the remaining energy by emitting light of a longer wavelength (green light, λ=520 nm).*

The term “confocal” refers to the fact that only light from the focal point of the objective lens is used to construct the image. This is obtained using a pinhole (figure 7) which only allows light from the focal point to pass, resulting in a sharper image (figure 8).

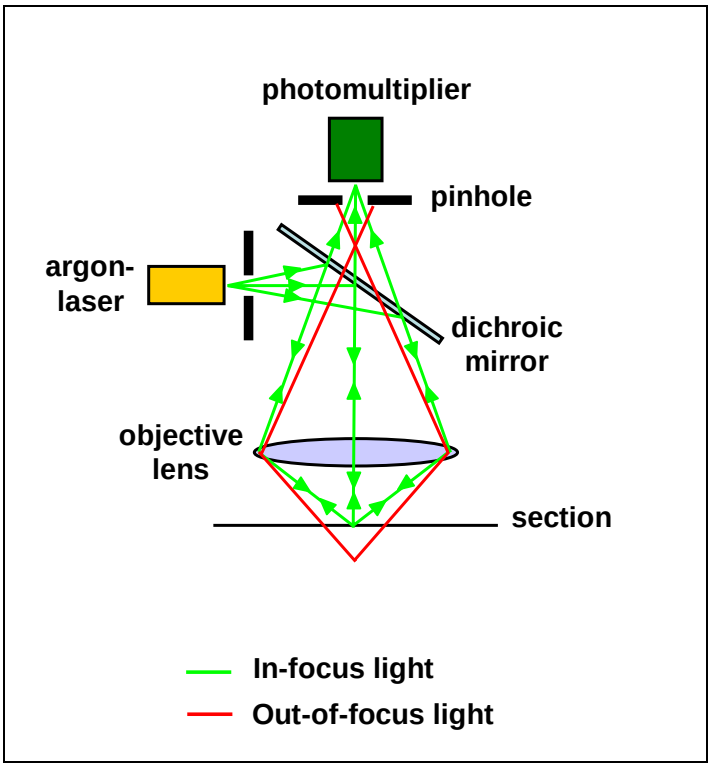

***Figure** 7: Diagram showing the principle of confocal microscopy. Light from a laser reflects off a dichroic mirror directing it through the objective lens to the preparation. The dye in the preparation is excited by the laser light and fluoresces. The returning fluorescent light of longer wavelength is allowed to pass through the dichroic mirror. The light that makes it through the pinhole is measured by the photomultiplier.*

Using this principle, it is possible to view one cell layer in a multilayer preparation, namely the layer situated in the focus of the objective lens. By changing the depth of scanning, different cell layers can be focused separately. Under optimal conditions, preparations of about 100 µm thick

can be visualised. When the preparation depth is larger than 100 µm, the intensity of the excitation light is insufficient to produce enough emission light, gradually decreasing the quality of the captured images.

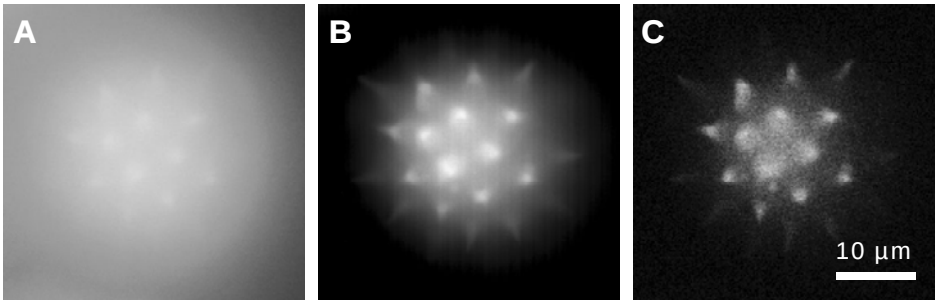

Figure 8: *Image of a fluorescein-labeled pollen grain (taken from a slice containing mixed fluorescent pollen grains (30-4264; Carolina Biological Supply)). Comparison of the images obtained with a conventional epifluorescence microscope (A) and a confocal microscope (B&C) (x 40 oil immersion objective, NA 1.30). (A) Image obtained in epifluorescence mode (excitation at 470 nm (bandpass, 40 nm bandwidth); emission at 520 nm (longpass)). In epifluorescence mode, out-of-focus light significantly blurs the image and reduces the contrast. (B & C) Images of the same preparation taken with the confocal microscope (excitation at 488 nm; emission at 522 nm (bandpass, 25 nm bandwidth)), using a large and a very small pinhole, respectively. The spiculae protruding from the spherical soma of the pollen grain can be best appreciated in C. The focal plane was situated close to the spherical soma surface.*

Briefly, the laser light reflects off a dichroic mirror, which directs it through the objective lens to the preparation. The dye in the specimen (Fluo-3 in our experiments) is excited by the laser light and fluoresces. Returning fluorescent (green) light is of longer wavelength and is allowed to pass through the dichroic mirror. Thereafter, it is focused onto a pinhole. Only light from the focal point of the objective lens can make it through the pinhole and is measured by a detector such as a photomultiplier. For visualisation, the detector is coupled to a computer which builds up the image pixel per pixel.

2.5.2. Calcium imaging

In our experiments we use laser scanning confocal microscopy in combination with the fluorescent Ca^{2+} probe Fluo-3 (figure 9A) to measure the free Ca^{2+} concentration. Fluo-3 is part of a group of Ca^{2+} indicators which are excitable by visible light. Figure 9B shows its Ca^{2+}-dependent emission spectrum for excitation at 488 nm (argon-laser sources) [6]. Fluorescent Ca^{2+} indicators excited with visible light offer several advantages over UV light-excitable indicators (e.g. Fura-2 and indo-1). For example, they show efficient excitation with most laser-based instrumentation and exhibit less cellular photodamage and light scatter. Also, there is a reduced interference from sample autofluorescence and due to stronger absorption by the dye, lower concentrations may be used, reducing phototoxicity. Fluo-3 is essentially non-fluorescent unless bound to Ca^{2+} and exhibits a K_d for Ca^{2+} of 390 nM. It shows a very large increase in fluorescence intensity in response to Ca^{2+} binding, resulting in sensitive detection of Ca^{2+} transients. The Fluo-3 used in the present experiments exhibits an at least 100-fold Ca^{2+}-dependent increase in fluorescence. The acetoxymethyl (AM) ester derivative of Fluo-3 is an uncharged molecule that can easily permeate the cell membranes. The intact acetoxymethyl (AM) ester derivative of fluo-3 is also non-fluorescent, unlike the AM esters of fura-2. Once inside the cells, the molecule is cleaved by non-specific esterases resulting in a charged form able to bind Ca^{2+} ions.

The cannulated arterial segments are loaded with the Ca^{2+} dye by incubation overnight at 4°C in a loading buffer (Hanks' balanced salt solution buffered with 25 mM HEPES (HBSS-HEPES)) containing 20 µM Fluo-3-AM and 0.05 % pluronic. The morning of the experiments, the preparations are transferred to loading buffer (same fluo-3-AM

concentration) now at 37°C and incubated for 90 min. The arteries are then washed in HEPES-buffered physiological salt solution (PSS, pH 7.4).

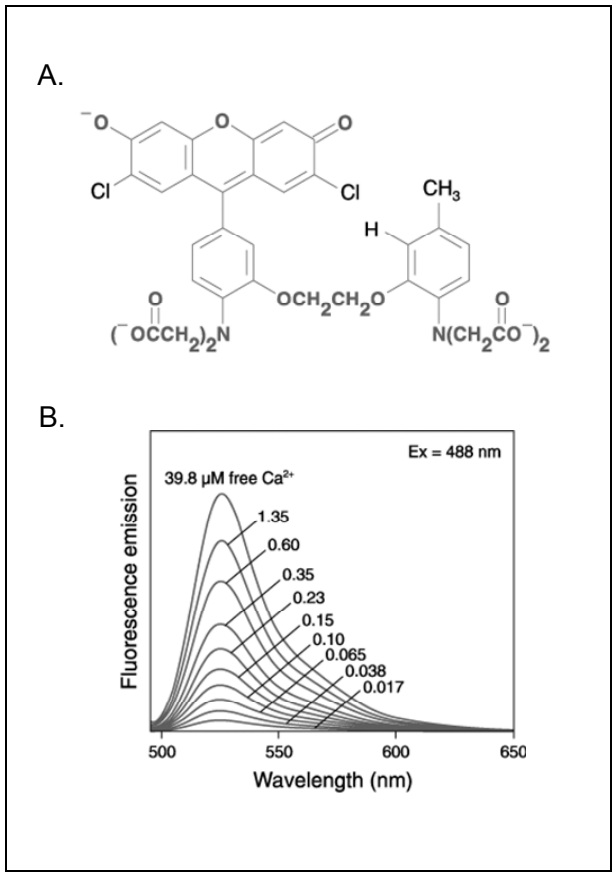

Figure 9: *(A) Structure formula of the visible light-excitable Ca^{2+} indicator Fluo-3. (B) Ca^{2+} dependent Fluorescence emission spectra of Fluo-3 at various levels of free $[Ca^{2+}]_i$. (From: Invitrogen/Molecular Probes – A Guide to Fluorescent Probes and Labeling Technologies)*

Ca^{2+} imaging is done with a custom developed real-time laser scanning microscope built around a Nikon Eclipse TE300 (Analis, Ghent, Belgium) [7] and a x40 oil immersion objective with high numeric aperture (CFI Plan Fluo, Nikon - 1.4 NA). A cannulated vessel segment is placed on a glass

coverslip and immobilized by covering it with a fine nylon mesh attached to a ring. The coverslip with the vessel is placed on the stage of the inverted microscope and is continuously superfused in situ with PSS at a rate of 1 ml/min. Excitation is done with the 488 nm line of an argon-laser (type 543R-AP-A01, Melles Griot, Carlsbad, CA, U.S.A.), the dichroic is a dual-wavelength dichroic XF2043 (490-550DBDR) and the emission light is bandpass filtered at 522 nm (25 nm bandwidth - all filters from Omega Optical, Brattleboro, VT, U.S.A. - details can be found in Leybaert et al., J.Microscopy [7]). Images of an optical section of the arterial wall (~ 123 µm x 93 µm and containing about 30-40 cells) are obtained at 2 frames s^{-1} and transferred directly to a PC equipped with an image acquisition and processing board (DT3155, Data translation, Marlboro, MA, USA). Off-line image analysis is done with software (Fluoframes) developed in Microsoft Visual C.

2.5.3. Experimental procedures and analysis

The experiments are performed at room temperature. After recording 2 min (240 images) in control conditions, norepinephrine (10^{-6} M) is added to the superfusate and recording is continued for another 3 min (360 images). Thereafter, still in the presence of norepinephrine, the tissues are exposed to various pharmacological agents and the responses are monitored over another 8 min (960 images) or 3 min (360 images), as appropriate. The first stage image analysis consists of counting the number of cells showing clear Ca^{2+} responses under control conditions, in the presence of norepinephrine and in the presence of the various pharmacological substances. The responding cells are subdivided in those showing oscillatory spiking activity upon stimulation with norepinephrine and those

reacting with an increase in fluorescence relative to the baseline level. In a second stage of the analysis, the number of Ca^{2+} spikes per cell, the spiking frequency (over the last 240 frames, expressed as spikes per minute) and the change in fluorescence relative to the baseline level is calculated (from the last 150 frames, baseline level was assumed 100 %).

2.6. REFERENCES

1. Nelson MT, Quayle JM. Physiological roles and properties of potassium channels in arterial smooth muscle. *Am J Physiol.* 1995;268(4 Pt 1):C799-C822.
2. Brayden JE, Nelson MT. Regulation of arterial tone by activation of calcium-dependent potassium channels. *Science.* 1992;256(5056):532-5.
3. Mulvany MJ, Halpern W. Mechanical properties of vascular smooth muscle cells in situ. *Nature.* 1976;260(5552):617-9.
4. Mulvany MJ, Warshaw DM. Active tension-length curve of vascular smooth muscle related to its cellular components. *J Gen Physiol.* 1979;74(1):85-104.
5. Gordon AM, Huxley AF, Julian FJ. The variation in isometric tension with sarcomere length in vertebrate muscle fibres. *J Physiol.* 1966;184(1):170-92.
6. Minta A, Kao JP, Tsien RY. Fluorescent indicators for cytosolic calcium based on rhodamine and fluorescein chromophores. *J Biol Chem.* 1989;264(14):8171-8.
7. Leybaert L, de Meyer A, Mabilde C, Sanderson MJ. A simple and practical method to acquire geometrically correct images with resonant scanning-based line scanning in a custom-built video-rate laser scanning microscope. *J Microsc.* 2005;219(Pt 3):133-40.

Chapter

3

Role of Ba^{2+}-resistant K^+ channels in endothelium-dependent hyperpolarization of rat small mesenteric arteries

Joke Breyne & Bert Vanheel
Department of physiology & physiopathology

Can J Physiol Pharmacol 2004; 82: 65-71

Abstract

In rat small mesenteric arteries, the influence of modulation of basal smooth muscle K^+-efflux on the mechanism of endothelium-dependent hyperpolarization was investigated. The membrane potentials of the vascular smooth muscle cells were measured using conventional microelectrode techniques. Incubation of resting arteries with the gap junction uncoupler carbenoxolone (20 µM) decreased the endothelium-dependent hyperpolarization elicited by a submaximal concentration of acetylcholine (3 µM) to about 65 % of the control. In the presence of Ba^{2+} (200 µM), which depolarized the membrane potential by 10 mV, the acetylcholine-induced membrane potential response was doubled in magnitude, reaching values not different from control. Moreover, the hyperpolarization was more resistant to carbenoxolone in these conditions. Finally, both in the absence and in the presence of carbenoxolone, the combined application of Ba^{2+} and ouabain (0.5 mM) did not abolish the acetylcholine response. These results suggest that gap junctional coupling plays a role in endothelium-dependent hyperpolarization of smooth muscle cells of resting rat small mesenteric arteries. Additionally, these findings show that the hyperpolarization does not rely on activation of inward rectifying K^+ channels. Although a minor contribution of Na/K-pumping cannot be excluded, the Ba^{2+} experiments show that the membrane electrical response is mediated by activation of a Ba^{2+}-resistant K^+ conductance.

Keywords: *EDHF, carbenoxolone, potassium channels, vascular smooth muscle cell membrane potential, vasodilation*

3.1. INTRODUCTION

Agonists such as acetylcholine dilate blood vessels through several endothelium-dependent mechanisms. These include the synthesis and release of nitric oxide (NO) and prostacyclin by the endothelial cells. Moreover, in various arteries an endothelium-dependent vasodilation resistant to inhibitors of NO synthases and cyclooxygenases has been demonstrated. This type of relaxation of the vascular tissue is associated with a hyperpolarization of the smooth muscle cells [1,2].

Earlier evidence suggested that the NO- and prostacyclin-independent smooth muscle hyperpolarization is caused by a factor diffusing from the endothelial cells. This humoral substance has been termed endothelium-derived hyperpolarizing factor (EDHF). As yet, the identity of EDHF is still elusive. Epoxyeicosatrienoic acids (EETs), K^+ ions, anandamide, H_2O_2 and C-type natriuretic peptide have all been suggested as an EDHF in certain vascular beds [3-7]. An alternative pathway for endothelium-dependent hyperpolarization is transmission of the agonist-induced hyperpolarization of the endothelial cells to the vascular smooth muscle via myoendothelial gap junctions. This heterocellular coupling, which is also documented in rat mesenteric arteries [8], allows the spread of electrical current or the transfer of a small hydrophilic messenger molecule such as cAMP [9-12].

In rat hepatic and small mesenteric arteries, K^+ was proposed as EDHF [5]. More specifically, acetylcholine was shown to stimulate the opening of apamin- and charybdotoxin-sensitive K^+-channels in the endothelial cell membrane (causing hyperpolarization), and the resulting K^+ efflux would transiently raise the extracellular K^+-concentration ($[K+]_o$) in the restricted myoendothelial spaces within the vessel wall [5]. In turn, this increase would

activate the Na/K-ATPases and inwardly rectifying K^+ channels (K_{IR} channels) in the membrane of the adjacent smooth muscle cells, as is documented for exogenous small increases in $[K^+]_o$ in some vessels [13,14]. This activation results in the hyperpolarization of the vascular smooth muscle cells [5]. More recently, however, it was reported that exogenous increases in $[K^+]_o$ elicited relaxation in only 30% - 40% of preconstricted rat small mesenteric arteries, while all vessels relaxed in response to acetylcholine [15]. Moreover, relaxations caused by a rise in $[K^+]_o$ were significantly smaller than the acetylcholine-responses and were absent after removal of the endothelium [15]. In another study, raising $[K^+]_o$ similarly dilated only 30% of pressurized rat small mesenteric arteries, while all vessels dilated to acetylcholine [16]. Moreover, in this study an increase in $[K^+]_o$ caused no relaxation of preconstricted arteries that were isometrically mounted, either with or without destroyed endothelium [16].

The absence of K^+-induced hyperpolarization in endothelium-denuded rat small mesenteric arteries was confirmed after stimulating the vessels with phenylephrine [17]. Since blockers of vascular smooth muscle K^+ channels restored hyperpolarizations in these stimulated vessels, it was suggested that activation of the smooth muscle, which is known to increase K^+ efflux from the myocytes [18], resulted in a K^+ cloud in the myoendothelial spaces. This extracellular accumulation of K^+ ions would saturate Na/K-pumps [17,19,20] and favour the alternative gap junctional pathway for smooth muscle hyperpolarization [17,20].

In this paper, we further explore the possible existence of local depletions and (or) accumulations of extracellular K^+ within the vessel wall, and assessed the functional consequences of modulation of basal smooth muscle K^+ efflux for endothelium-dependent hyperpolarization. More

specifically, we measured the acetylcholine-induced hyperpolarization of the smooth muscle cells in rat mesenteric arteries, and investigated the separate and combined influence of inhibition of gap junctional coupling with carbenoxolone and of membrane Na/K-ATPases with ouabain in the absence and the presence of the K_{IR} channel inhibitor Ba^{2+}. Low concentrations of Ba^{2+} are known to specifically block K_{IR} currents [21], and blocking tonically open K_{IR} channels is expected to reduce resting K^+ efflux and consequently, diminish the K^+ load in the myoendothelial spaces.

3.2. MATERIALS AND METHODS

3.2.1. Preparations

Small mesenteric arteries from female Wistar rats (180 – 230 g) were used. The animals were treated in accordance with the principles and guidelines of the Canadian Council on Animal Care for the use of laboratory animals. Experiments were approved by the ethical committee on animal research of Gent University. The rats were killed by cervical dislocation. Branches of the mesenteric arteries were rapidly removed and placed in cold (4°C) Krebs-Ringer bicarbonate solution containing the following (in mM): NaCl, 135; KCl, 5; $NaHCO_3$, 20; $CaCl_2$, 2.5; $MgSO_4.7H_2O$, 1.3; KH_2PO_4, 1.2; EDTA, 0.026; glucose, 10. The solution was bubbled with 95% O_2 – 5% CO_2.

Second and third order arteries were cleaned from surrounding connective tissue and cut into segments of about 4 mm in length. The vessels were pinned down to the bottom of an experimental chamber and were continuously superfused with the Krebs-Ringer solution (37 °C) of the

above composition, supplemented with N^G-nitro-L-arginine (L-NA)(10^{-4} M) and indomethacin (5×10^{-5} M) to avoid interference from NO and prostacyclin, respectively. The solution was continuously gassed with a 95% O_2 – 5% CO_2 gas mixture (pH ~ 7.4). The preparation was allowed to equilibrate for at least 60 min.

3.2.2. Electrophysiological measurements

Membrane potentials of the vascular smooth muscle cells were measured with sharp microelectrodes, pulled from filamented borosilicate glass tubings (Hilgenberg, Malsfeld, Germany) with a vertical pipette puller (David Kopf Instruments, Tujunga California, USA), and filled with 1 M KCl. Electrical signals were monitored on an oscilloscope and recorded with a pen recorder. Successful cell impalements were characterized by an extremely sharp voltage deflection on entering the cell and a fast return to the baseline upon withdrawal of the microelectrode. Values of the transmembrane potential (E_m) were taken as the difference between the stabilized membrane potential after cell impalement and the zero potential upon dislodgement of the electrode from the cell. Changes in membrane potential produced by exposing the cells to acetylcholine in control conditions and after incubation with various substances (Ba^{2+}, carbenoxolone, ouabain) were measured.

Ba^{2+} was added to the superfusate for at least 10 min before application of acetylcholine to the preparations. In the experiments where the influence of carbenoxolone and the combined influence of carbenoxolone and ouabain were tested, the preparation was pre-exposed for at least 20 min to these drugs.

3.2.3. Drugs

Acetylcholine chloride, carbenoxolone, indomethacin, L-NA, ouabain and $BaCl_2$ were obtained from Sigma Chemical Co. (St. Louis, Mo). All concentrations mentioned are the final molar concentrations in the experimental chamber. Stock solutions of 10^{-2} M acetylcholine were made in 50 mM potassium hydrogen phthalate buffer, pH 4.0. Further dilutions (1:10 or 1:1000) were made in the control fluid. L-NA, $BaCl_2$, and carbenoxolone were dissolved in water while stock solutions of indomethacin were made in anhydrous ethanol. Ouabain was added as a solid directly to the superfusate.

3.2.4. Statistics

Results are expressed as means ± SEM. Statistical evaluation was performed using student's *t* test for paired or unpaired data, as appropriate. Values of $P < 0.05$ were considered significantly different. The number of preparations, each obtained from a different rat, is indicated as *n*.

3.3. RESULTS

In control conditions (in the presence of L-NA and indomethacin), the resting membrane potential of the mesenteric artery smooth muscle cells averaged -60.3 ± 0.9 mV (n = 30). Preliminary experiments showed that acetylcholine (3 µM) evoked submaximal hyperpolarizations of the membrane potential in these vessels. In endothelium-denuded arteries, the membrane potential does not appreciably change after application of acetylcholine [22].

3.3.1. Influence of carbenoxolone

In a first series of experiments (n=10), we compared the hyperpolarization elicited by acetylcholine (3 µM) in the absence and in the presence of the gap junction inhibitor carbenoxolone (figure 1). In control conditions, the addition of the endothelium-dependent vasodilator to the superfusate induced a hyperpolarization of the smooth muscle cell membrane potential, averaging 7.8 ± 0.6 mV, to a peak value of -68.9 ± 1.9 mV (n = 10). After reaching this peak change, the membrane potential slowly recovered towards its control level, recovery of which was accelerated by washout of the agonist (figure 1).

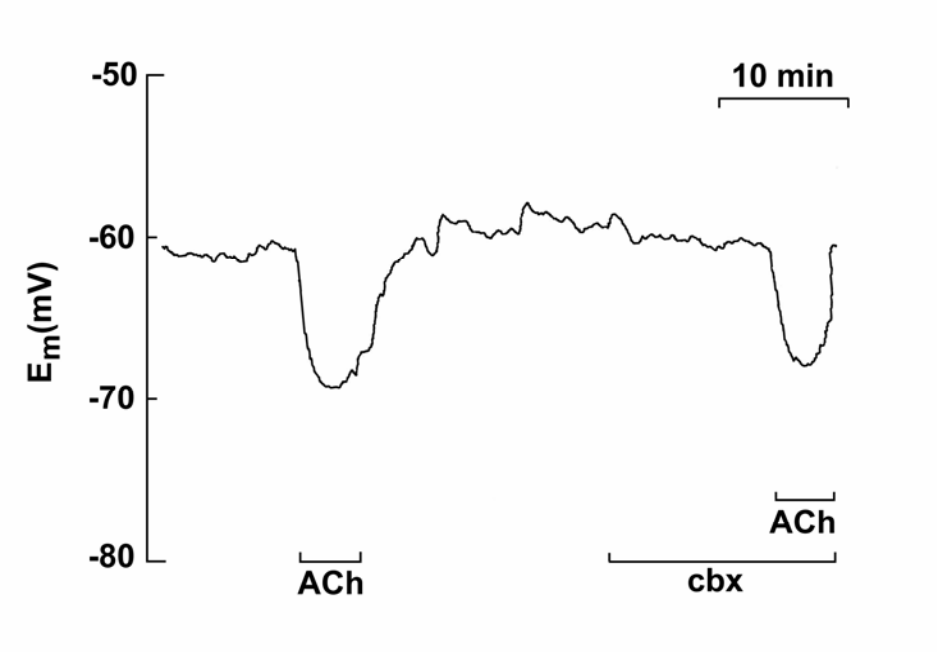

Figure 1: *Tracing of rat mesenteric artery smooth muscle cell membrane potential (E_m) responses to application of acetylcholine (ACh, 3 µM) in control conditions and after pre-exposure to carbenoxolone (cbx, 20 µM).*

Pre-exposure to carbenoxolone (20 µM) did not significantly change the resting membrane potential (-61.9 ± 1.8 mV vs -61.6 ± 1.8 mV in this subset of experiments, n=10). In the presence of carbenoxolone, the hyperpolarization elicited by acetylcholine was significantly decreased. The membrane potential reached a peak value of -67.0 ± 1.9 mV, significantly different from -68.9 ± 1.9 mV ($P < 0.05$). The average value for the hyperpolarization in the presence of the gap junction inhibitor, 5.1 ± 0.7 mV ($P < 0.001$), represents a reduction to 64.4 ± 6.8 % of that in control conditions.

3.3.2. Influence of Ba^{2+} and of Ba^{2+}/carbenoxolone

In the next series of experiments, the influence of carbenoxolone was tested after inhibition of the inward rectifying K^+ channels with Ba^{2+}. Pre-exposure to 200 µM Ba^{2+} depolarized the resting E_m to -50.5 ± 1.1 mV (mean depolarization of 9.5 ± 0.8 mV, n = 20). In the presence of the K_{IR} inhibitor, the amplitude of the hyperpolarization caused by acetylcholine was more than doubled (-17.0 ± 1.0 mV as compared with -7.8 mV; n = 20)(figure 2). A mean peak value of -67.4 ± 1.3 mV (n=20) was reached, being not significantly different from the membrane potential reached in the control acetylcholine exposures (-68.9 ± 1.9 mV, $P = 0.51$).

After additional pre-exposure to carbenoxolone (20 µM), the hyperpolarization induced by acetylcholine was significantly reduced. The mean hyperpolarization (-15.4 ± 1.2 mV, n = 7, $P < 0.005$ from that in Ba^{2+} alone) represents 79.5 ± 3.2 % of the membrane potential response to acetylcholine in Ba^{2+} alone (figure 3). The mean peak value of -64.0 ± 3.0

mV was slightly but not significantly less negative than that reached in the control exposures (-68.9 ± 1.9 mV) or in Ba^{2+} alone (-67.4 ± 1.3 mV).

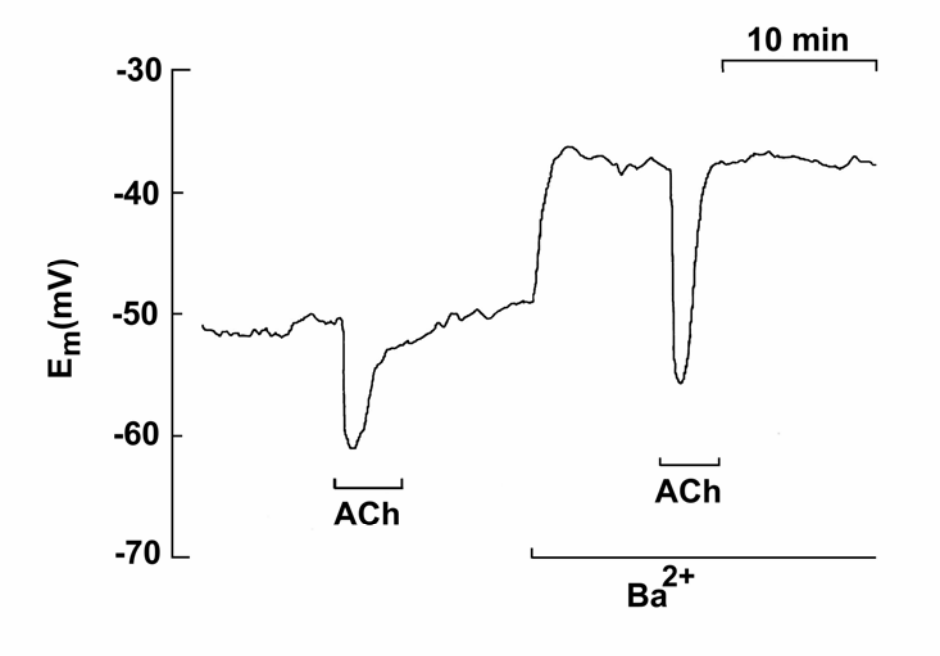

Figure 2: *Smooth muscle cell membrane potential (E_m) hyperpolarization induced by acetylcholine (ACh, 3 µM) in control conditions and after pre-exposure to Ba^{2+} (200 µM).*

Since carbenoxolone apparently had less influence after inhibition of the K_{IR} channels, a next series of experiments was performed with a higher concentration of the gap junction inhibitor.

Application of 100 µM carbenoxolone in the continuous presence of Ba^{2+} increased the membrane potential by 3.4 ± 1.2 mV to -57.1 ± 0.7 mV (n=7). In the combined presence of 200 µM Ba^{2+} and 100 µM carbenoxolone, the

peak hyperpolarization induced by acetylcholine was reduced from 14.7 ± 0.5 mV to 9.7 ± 0.9 mV (n = 7; *P* < 0.001; figure 4), or to 65.3 ± 5.0 % of the peak change observed in the absence of carbenoxolone in Ba^{2+}. This degree of inhibition is comparable to that observed with the lower concentration of carbenoxolone in the absence of Ba^{2+} (cf. figure 3). The peak E_m value reached after addition of acetylcholine in the presence of carbenoxolone and Ba^{2+} (-66.8 ± 1.1 mV, n = 7) was not significantly different from that in Ba^{2+} alone (-67.4 ± 1.3 mV).

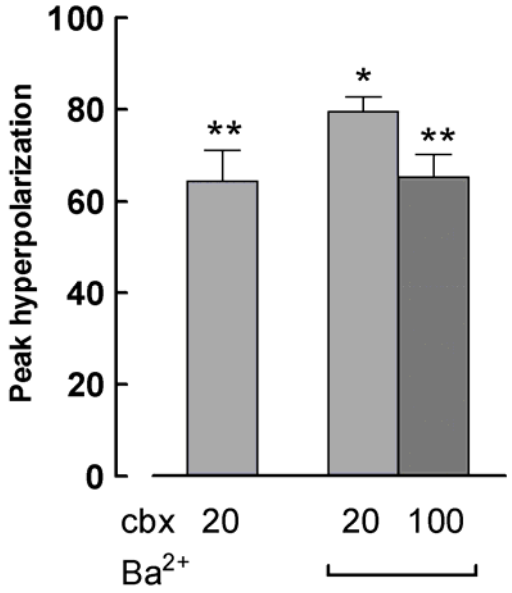

Figure 3: *Comparison of the influence of carbenoxolone in the absence and the presence of Ba^{2+}. The columns represent the hyperpolarization obtained in the presence of 20 µM or 100 µM carbenoxolone (cbx 20 or 100) before and after pre-treatment with 200 µM Ba^{2+}, as indicated by the lower horizontal bar. Values are means ± SEM of 7 to 10 experiments. In each experiment, the hyperpolarization observed in the absence of carbenoxolone served as the control reference (100%). * P<0.005; ** P<0.001).*

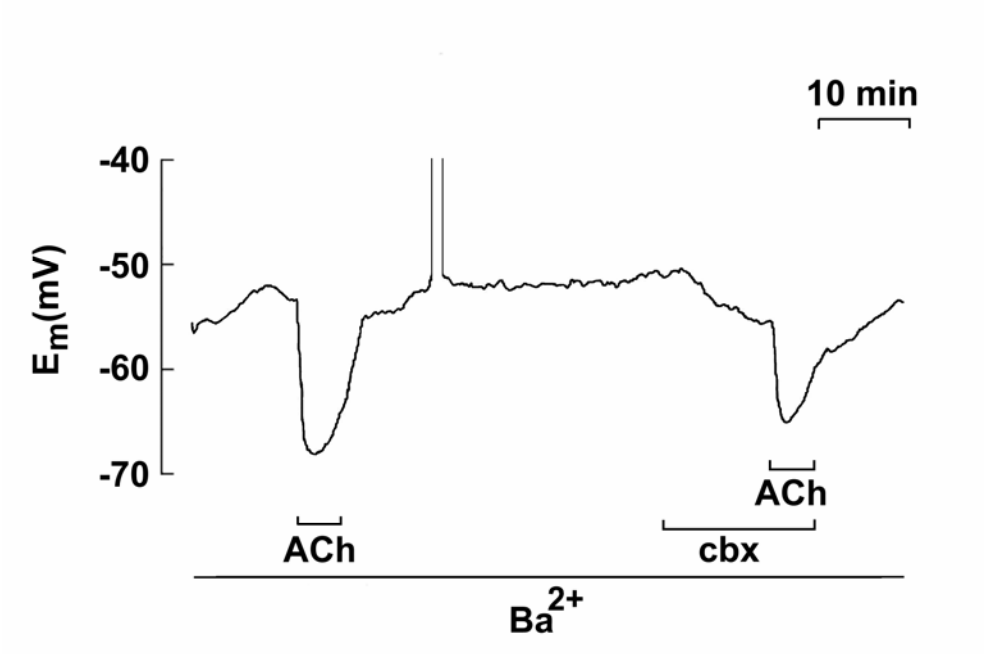

Figure 4: *Recording of the membrane potential (E_m) responses to acetylcholine (ACh, 3 µM) in the presence of Ba^{2+} (200 µM) and in the combined presence of Ba^{2+} and carbenoxolone (cbx, 100 µM). Parallel vertical deflections in the trace indicate a moment of microelectrode dislodgement and reimpalement.*

3.3.3. Influence of ouabain and of ouabain + carbenoxolone

In the next series of experiments, the influence of ouabain (0.5 mM) on the acetylcholine-induced hyperpolarization was investigated. In the presence of Ba^{2+}, the additional application of ouabain depolarized the membrane potential by 4.0 $\pm$ 0.8 mV (n = 4). In the combined presence of Ba^{2+} and ouabain, the peak E_m change elicited by acetylcholine was reduced to 10.0 $\pm$ 1.6 mV as compared with 13.1 $\pm$ 1.0 mV in Ba^{2+} alone.

Simultaneous application of ouabain and carbenoxolone (20 µM) in the continuous presence of Ba^{2+} depolarized the smooth muscle cells by 5.7 ± 0.6 mV (n = 5). In the combined presence of Ba^{2+}, ouabain and carbenoxolone, the acetylcholine-induced hyperpolarization was significantly reduced to 10.4 ± 2.0 mV (n = 6, $P < 0.001$) as compared with the amplitude measured in the presence of Ba^{2+} alone (-16.8 ± 2.7 mV, n = 6). A representative experiment is depicted in figure 5. The peak E_m value reached after addition of acetylcholine in the combined presence of ouabain, carbenoxolone and Ba^{2+} (-55.8 ± 3.5 mV, n = 6) was significantly different ($P < 0.02$) from that in Ba^{2+} alone (-67.4 ± 1.3 mV).

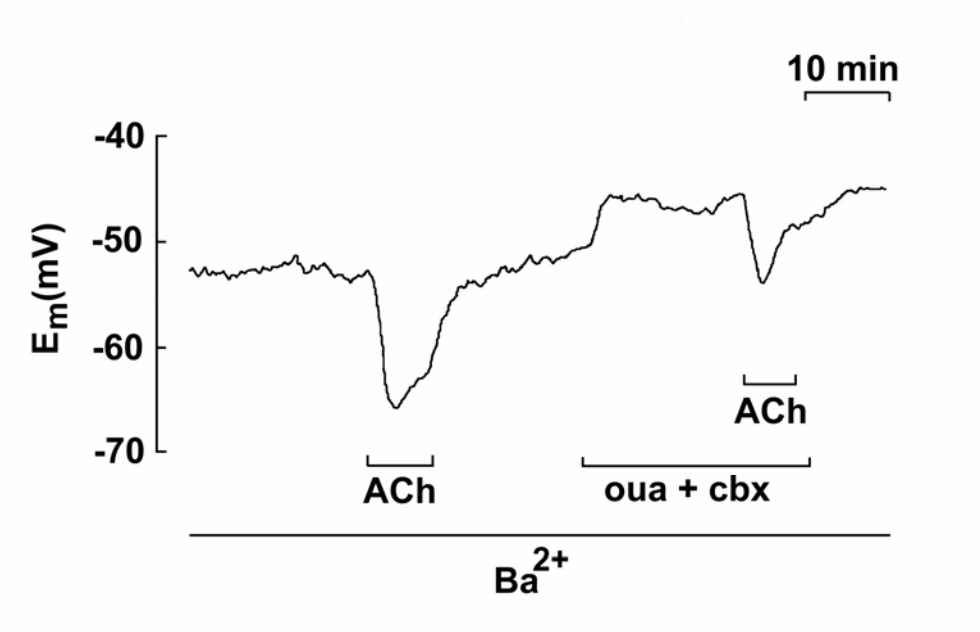

Figure 5: *Tracing of the smooth muscle cell membrane potential (E_m) responses to acetylcholine (ACh, 3 µM) in the presence of Ba^{2+} and in the combined presence of Ba^{2+}, ouabain (oua, 0.5 mM) and carbenoxolone (cbx, 20 µM).*

3.4. DISCUSSION

In the present study, we used the K_{IR} channel inhibitor Ba^{2+} as a possible modulator of myoendothelial extracellular K^+ concentration, and examined the contribution of gap junctional coupling to the acetylcholine-induced hyperpolarization. The main findings of the present study are that: (1) carbenoxolone partially inhibited the endothelium-dependent hyperpolarization elicited by acetylcholine, (2) after inhibition of the K_{IR} channels, the acetylcholine-induced membrane potential response was more resistant to carbenoxolone, and (3) the combined application of Ba^{2+} and ouabain, either in the absence or in the presence of the gap junction inhibitor, did not abolish the acetylcholine-response.

It is generally accepted that the mechanism of endothelium-dependent hyperpolarization is heterogeneous and varies among different species and vascular beds [1,2]. Furthermore, the state of activation of a vessel might influence the way hyperpolarization comes about [23]. In resting rat hepatic and small mesenteric arteries, K^+ was proposed as the diffusible EDHF [5,20], while stimulated hepatic and mesenteric vessels would rely more on gap junctional coupling [5,20]. Other studies, however, reported that gap junctions play a critical role in endothelium-dependent hyperpolarization of resting rat mesenteric arteries [24,25].

In the present findings, carbenoxolone (20 µM) did not abolish the acetylcholine-induced membrane potential response to acetylcholine, but decreased the peak hyperpolarization by about 35 %. This is consistent with earlier relaxation experiments in rat mesenteric arteries [26], in which 100 µM of the gap junction uncoupler 18α-glycyrhetinic acid (18α-GA) had no dramatic inhibitory effect on the endothelium-dependent relaxation. In

these arteries a depressed dilatation in response to acetylcholine was found with the uncouplers Gap27 (300 µM) and 18α-GA (100 µM) [16]. Also membrane potential measurements confirm the rather limited effect of gap junctional uncouplers on the response to acetylcholine in this vessel. Thus, a small reduction (by about 25 %) of the acetylcholine-induced hyperpolarization of the vascular smooth muscle cells of resting rat small mesenteric arteries was observed with 100 µM of carbenoxolone [19]. In this vessel the amplitude of the EDHF-mediated hyperpolarization was reduced to 33 % of the control after incubation with 300 µM Gap27 [24]. Another study recently described that 100 µM 18α-GA partially inhibited, while 300 µM carbenoxolone completely abolished the acetylcholine-induced hyperpolarization [25]. However, since the endothelium-independent hyperpolarization in response to levcromakalim, a direct opener of ATP-dependent K^+ channels, was also inhibited by 300 µM carbenoxolone but not by 100 µM 18α-GA [25], the possibility that higher concentrations (300 µM) of carbenoxolone have non-specific effects might be considered [12,27].

In resting rat hepatic and mesenteric arteries, the endothelium-dependent hyperpolarization was described to be largely insensitive to carbenoxolone and Gap27 [19], and completely inhibited by the combined application of Ba^{2+} and ouabain [19], indicating the importance of stimulation of K_{IR} channels and Na/K-pumps by K^+ ions liberated from the endothelium. Molecular experiments using the RT-PCR technique indicated that messenger RNA encoding for a K_{IR} isoform ($K_{IR}2.1$) is present in rat mesenteric vascular smooth muscle cells [28]. In a second series of experiments, therefore, we examined the influence of Ba^{2+}. Low concentrations of Ba^{2+} are known to block the K_{IR}-current [21] and correspondingly, in the present study, the addition of 200 µM Ba^{2+} significantly depolarized the smooth muscle cell membrane. After inhibition of the K_{IR} channels, the magnitude of the

acetylcholine-induced hyperpolarization was doubled. This is consistent with earlier results from our laboratory [29]. Inhibition of the K_{IR} channels of the vascular smooth muscle cells is expected to increase the membrane resistance and, therefore, to enlarge the impact of any hyperpolarizing current on the membrane potential. However, this decrease in membrane conductance is unlikely to double the amplitude of the acetylcholine-induced hyperpolarization. An additional increase, therefore, results from the Ba^{2+}-induced depolarization of the membrane potential, enlarging the driving force on K^+. This depolarization is unlikely to drastically influence Na/K-pump activity since both the inwardly directed Na^+ and the outwardly directed K^+ electrochemical gradients are simultaneously altered. Therefore, the substantially increased acetylcholine-induced hyperpolarization in the presence of Ba^{2+} indicates that an EDHF acts by opening of a Ba^{2+}-insensitive conductance rather than by pump stimulation. The additional application of ouabain, indeed, did not abolish the EDHF response, although it was somewhat decreased. These results are fully consistent with activation of an outwardly rectifying K^+ current, insensitive to Ba^{2+} and (or) ouabain, underlying the hyperpolarization due to EDHF [12].

After stimulation of hepatic and mesenteric arteries with phenylephrine, endothelium-dependent membrane potential responses became more sensitive to gap junction inhibitors [19]. It was proposed, therefore, that the activation of Na/K-ATPases and K_{IR} channels was hampered by a presumed K^+-cloud in the vessel wall, originating from an increased basal K^+-efflux from the smooth muscle cells in these conditions, and making the endothelium-dependent hyperpolarization more dependent on the alternative pathway, gap junctional coupling. In the present experiments with Ba^{2+}, the reverse might be expected. Thus, on assuming a restricted diffusion of extracellular K^+-ions within the vessel wall, blocking tonically

open K_{IR} channels (as shown by the evoked membrane depolarization) by pre-exposure to Ba^{2+} might be expected to lower the steady state extracellular K^+ concentration around the smooth muscle cells and, hence, to increase any K^+ efflux dependent hyperpolarizing mechanism that is Ba^{2+}-insensitive when switched on by EDHF. The present finding that, after pre-exposure to Ba^{2+}, carbenoxolone was less efficient at inhibiting the acetylcholine-response is fully consistent with the view that in these conditions the endothelium-dependent hyperpolarization relies to less extent on gap junctional coupling. Therefore, the substantially potentiated EDHF-mediated hyperpolarization in the continuous presence of Ba^{2+} might also be due, in addition to the above mentioned influence on membrane conductance and on membrane potential, to a decreased steady state extracellular K^+ concentration in the vessel wall. This would both enlarge the outward driving force on K^+ ions and make more Na/K-pumps available for activation by EDHF. However, the experiments in which we additionally applied ouabain preclude a substantial role for Na/K-pump activation in the response to EDHF. To inhibit all Na/K-ATPase isoforms, high concentrations (0.5 mM) of the inhibitor were used [30,31]. In the presence of Ba^{2+}, the application of ouabain reduced acetylcholine-responses to the level observed in control conditions. Also after inhibition of both the gap junctional and the membrane inward rectifying K^+ conductances by simultaneous treatment with carbenoxolone and Ba^{2+}, the additional application of ouabain did not abolish endothelium-dependent hyperpolarization. These findings are not consistent with Na/K-pump activation by endothelially derived K^+ ions being the main gap junction-independent hyperpolarizing mechanism in these resting vessels. In this respect, increasing extracellular K^+ concentration by 4 or 5 mM was previously found to consistently and reproducibly depolarize the smooth muscle cells of rat mesenteric arteries at rest [29].

Besides some possible contribution of increased Na/K-pumping to the EDHF-mediated hyperpolarization, several alternatives might underlie the somewhat diminished hyperpolarization after pre-exposure to ouabain. First, ouabain might cause a depolarization of the endothelial cell membrane, which decreases the driving force for Ca^{2+} entry upon stimulation with the agonist [32,33]. Because it is generally accepted that a rise in intracellular Ca^{2+} is a crucial step in the release of endothelial factors [34,35], a smaller response might be expected under these conditions. A second possibility for the inhibitory action of ouabain on the acetylcholine-response arises from the reported attenuation of intercellular gap junctional communication exerted by this substance [36]. Furthermore, besides decreasing the intracellular K^+ concentration, ouabain pre-exposure eventually might increase the steady state extracellular K^+ concentration in the vessel wall, both of which influence the outward gradient for K^+ efflux.

In conclusion, we found that gap junctions play some role in the endothelium-dependent hyperpolarization of rat small mesenteric arteries. Our data also demonstrate that this endothelium-derived hyperpolarization does not rely on the activation of K_{IR} channels. Although a minor contribution of activation of Na/K-ATPases can not be excluded, our results rather point to the activation of an as yet unidentified but Ba^{2+}-resistant conductance underlying a significant fraction of the endothelium-dependent hyperpolarization. Furthermore, our results are consistent with the hypothesis that basal K^+ efflux might influence local extracellular K^+ concentration within the vessel wall, pointing toward K^+ channels mediating the endothelium-dependent hyperpolarization. It is stressed, however, that presumed local accumulations or depletions of extracellular K^+ will not only influence the steady state activity of the Na/K-pumps (and their capacity to

respond to EDHF), but are likely to affect all transmembrane potassium fluxes.

3.5. ACKOWLEDGEMENTS

We are grateful to Eliane De Wulf, Dirk De Gruytere, Julien Dupont, Marc Gillis and Cyriel Mabilde for unfailing technical assistance.

3.6. REFERENCES

1. Cohen RA, Vanhoutte PM. Endothelium-dependent hyperpolarization. Beyond nitric oxide and cyclic GMP. *Circulation*. 1995;92:3337-3349.

2. McGuire JJ, Ding H, Triggle CR. Endothelium-derived relaxing factors: a focus on endothelium-derived hyperpolarizing factor(s). *Can J Physiol Pharmacol*. 2001;79:443-470.

3. Campbell WB, Gebremedhin D, Pratt PF, Harder DR. Identification of epoxyeicosatrienoic acids as endothelium-derived hyperpolarizing factors. *Circ Res*. 1996;78:415-423.

4. Randall MD, Alexander SPH, Bennett T, Boyd EA, Fry JR, Gardiner SM, Kemp PA, McCulloch AI, Kendall DA. An endogenous cannabinoid as an endothelium-derived vasorelaxant. *Biochem Biophys Res Commun*. 1996;229:114-120.

5. Edwards G, Dora KA, Gardener MJ, Garland CJ, Weston AH. K^+ is an endothelium-derived hyperpolarizing factor in rat arteries. *Nature*. 1998;396:269-272.

6. Matoba T, Shimokawa H, Nakashima M, Hirakawa Y, Mukai Y, Hirano K, Kanaide H, Takeshita A. Hydrogen peroxide is an endothelium-derived hyperpolarizing factor in mice. *J Clin Invest*. 2000;106:1521-1530.

7. Chauhan SD, Nilsson H, Ahluwalia A, Hobbs AJ. Release of C-type natriuretic peptide accounts for the biological activity of

endothelium-derived hyperpolarizing factor. *Proc Natl Acad Sci USA*. 2003;100:1426-1431.

8. Sandow SL, Hill CE. Incidence of myoendothelial gap junctions in the proximal and distal mesenteric arteries of the rat is suggestive of a role in endothelium-derived hyperpolarizing factor-mediated responses. *Circ Res*. 2000;86:341-346.

9. Hutcheson IR, Chaytor AT, Evans WH, Griffith TM. Nitric oxide-independent relaxations to acetylcholine and A23187 involve different routes of heterocellular communication. Role of gap junctions and phospholipase A2. *Circ Res*. 1999;84:53-63.

10. Yamamoto Y, Imaeda K, Suzuki H. Endothelium-dependent hyperpolarization and intercellular electrical coupling in guinea-pig mesenteric arterioles. *J Physiol*. 1999;514:505-513.

11. Emerson GG, Segal SS. Electrical coupling between endothelial cells and smooth muscle cells in hamster feed arteries: role in vasomotor control. *Circ Res*. 2000;87:474-479.

12. Coleman HA, Tare M, Parkington HC. K^+ currents underlying the action of endothelium-derived hyperpolarizing factor in guinea-pig, rat and human blood vessels. *J Physiol*. 2001;531:359-373.

13. Knot HJ, Zimmermann PA, Nelson MT. Extracellular K^+-induced hyperpolarizations and dilatations of rat coronary and cerebral arteries involve inward rectifier K^+ channels. *J Physiol*. 1996;492:419-430.

14. Prior HM, Webster N, Quinn K, Beech DJ, Yates MS. K^+-induced dilation of a small renal artery: no role for inward rectifier K^+ channels. *Cardiovasc Res*. 1998;37:780-790.

15. Lacy PS, Pilkington G, Hanvesakul R, Fish HJ, Boyle JP, Thurston H. Evidence against potassium as an endothelium-derived hyperpolarizing factor in rat mesenteric small arteries. *Br J Pharmacol*. 2000;129:605-611.

16. Doughty JM, Boyle JP, Langton PD. Potassium does not mimic EDHF in rat mesenteric arteries. *Br J Pharmacol*. 2000;130:1174-1182.

17. Richards GR, Weston AH, Burnham MP, Feletou M, Vanhoutte PM, Edwards G. Suppression of K^+-induced hyperpolarization by phenylephrine in rat mesenteric artery: relevance to studies of

endothelium-derived hyperpolarizing factor. *Br J Pharmacol*. 2001;134:1-5.

18. Bolton TB, Clapp LH. The diverse effects of noradrenaline and other stimulants on ^{86}Rb and ^{42}K efflux in rabbit and guinea-pig arterial muscle. *J Physiol*. 1984;355:43-63.

19. Edwards G, Feletou M, Gardener MJ, Thollon C, Vanhoutte PM, Weston AH. Role of gap junctions in the responses to EDHF in rat and guinea-pig small arteries. *Br J Pharmacol*. 1999;128:1788-1794.

20. Busse R, Edwards G, Feletou M, Fleming I, Vanhoutte PM, Weston AH. EDHF: bringing the concepts together. *Trends Pharmacol Sci*. 2002;23:374-380.

21. Nelson MT, Quayle JM. Physiological roles and properties of potassium channels in arterial smooth muscle. *Am J Physiol*. 1995;268:C799-C822.

22. Vanheel B, Van de Voorde J. Regional differences in anandamide- and methanandamide-induced membrane potential changes in rat mesenteric arteries. *J Pharmacol Exp Ther*. 2001;296:322-328.

23. Félétou M, Vanhoutte PM. Third pathway: Endothelium-dependent hyperpolarization. *Drug Developm Res*. 2003;58:18-22.

24. Sandow SL, Tare M, Coleman HA, Hill CE, Parkington HC. Involvement of myoendothelial gap junctions in the actions of endothelium-derived hyperpolarizing factor. *Circ Res*. 2002;90:1108-1113.

25. Goto K, Fujii K, Kansui Y, Abe I, Iida M. Critical role of gap junctions in endothelium-dependent hyperpolarization in rat mesenteric arteries. *Clin Exp Pharmacol Physiol*. 2002;29:595-602.

26. Tanaka Y, Otsuka A, Tanaka H, Shigenobu K. Glycyrrhetinic acid-sensitive mechanism does not make a major contribution to non-prostanoid, non-nitric oxide mediated endothelium-dependent relaxation of rat mesenteric artery in response to acetylcholine. *Res Commun Mol Pathol Pharmacol*. 1999;103:227-239.

27. Davidson JS, Baumgarten IM. Glycyrrhetinic acid derivatives: a novel class of inhibitors of gap-junctional intercellular communication. Structure-activity relationships. *J Pharmacol Exp Ther*. 1988;246:1104-1107.

28. Bradley KK, Jaggar JH, Bonev AD, Heppner TJ, Flynn ERM, Nelson MT, Horowitz B. K(ir)2.1. encodes the inward rectifier potassium channel in rat arterial smooth muscle cells. *J Physiol*. 1999;515:639-651.

29. Vanheel B, Van de Voorde J. Barium decreases endothelium-dependent smooth muscle responses to transient but not to more prolonged acetylcholine applications. *Pflugers Archiv Eur J Physiol*. 1999;439:123-129.

30. Noel F, Godfraind T. Heterogeneity of ouabain specific binding sites and (Na^+/K^+)-ATPase inhibition in microsomes from rat heart. *Biochem Pharmacol*. 1984;33:47-53.

31. Adeagbo ASO, Malik KU. Endothelium-dependent and Brl-34915-induced vasodilatation in rat isolated perfused mesenteric arteries: role of G-proteins, K^+ and calcium channels. *Br J Pharmacol*. 1990;100:427-434.

32. Adams DJ, Barakeh J, Laskey R, Vanbreemen C. Ion channels and regulation of intracellular calcium in vascular endothelial cells. *FASEB J*. 1989;3:2389-2400.

33. Schilling WP. Effect of membrane potential on cytosolic calcium of bovine aortic endothelial cells. *Am J Physiol*. 1989;257:H778-H784.

34. Chen GF, Suzuki H. Calcium Dependency of the endothelium-dependent hyperpolarization in smooth muscle cells of the rabbit carotid artery. *J Physiol*. 1990;421:521-534.

35. Lückhoff A, Busse R. Calcium influx into endothelial cells and formation of endothelium-derived relaxing factor is controlled by the membrane potential. *Pflugers Archiv Eur J Physiol*. 1990;416:305-311.

36. Harris D, Martin PE, Evans WH, Kendall DA, Griffith TM, Randall MD. Role of gap junctions in endothelium-derived hyperpolarizing factor responses and mechanisms of K^+-relaxation. *Eur J Pharmacol*. 2000;402:119-128.

Chapter

4

Endothelium-dependent hyperpolarization in small gastric arteries

Bert Vanheel & Joke Breyne
Department of physiology & physiopathology

Cardiovasc Res 2004; 63: 331-337

Abstract

***Objective**: In many blood vessels, stimulation of the endothelium with various vasoactive substances induces, besides the nitric oxide (NO) and prostacyclin pathways, a third mechanism evoking dilatation. It is based on hyperpolarization of the vascular smooth muscle cell membrane. In the present study, we investigated the existence of endothelium-dependent hyperpolarization in small gastric arteries of the rat and explored its underlying mechanism. **Methods**: Membrane potentials were recorded by conventional microelectrode techniques in isolated segments of small gastric arteries, the normalized diameter of which was determined from the passive wall tension-internal circumference characteristics as measured with a myograph. **Results**: After blocking NO and prostaglandin synthesis, application of acetylcholine (3×10^{-7} M) resulted in a membrane hyperpolarization in endothelium intact but not in endothelium-denuded arteries. This membrane potential change was increased by pre-exposure to a low concentration (30 μM) of Ba^{2+}, which selectively inhibits inward rectifying potassium channels. Moreover, the acetylcholine-induced hyperpolarization was unaffected by additional pre-exposure to high concentrations (0.5 mM) of the Na^+/K^+- ATPase inhibitor ouabain, which by itself caused a secondary slow endothelium-independent hyperpolarization after an initial peak depolarization. **Conclusions**: We conclude that acetylcholine produces endothelium-dependent hyperpolarization in gastric small arteries, which does not rely on activation of smooth muscle cell inward rectifying K^+ channels or Na^+/K^+-pumps, and might prove to be another important regulator of gastric mucosal blood flow.*

***Keywords**: blood flow, vascular smooth muscle membrane potential, vasoactive agents, endothelial factors*

4.1. INTRODUCTION

Gastric mucosal blood flow is of primary importance in maintaining the integrity of the mucosa. The blood provides oxygen, nutrients and gastrointestinal hormones to maintain mucosal function and turnover. The production and secretion of mucus, and the secretion of bicarbonate ions which protect the mucosa, are fully dependent on this blood flow. Moreover, the circulating blood removes waste materials and back-diffusing hydrogen ions. Therefore, disturbances in the mucosal microcirculation can result in mucosal injury and influence the development of peptic ulcers [1].

An increase in gastric mucosal blood flow is brought about by dilation of submucosal arterioles. Systemic as well as local factors such as prostaglandins, leukotrienes and other endogenous chemical mediators of the mucosa influence arteriolar tone. Moreover, gastric blood flow is substantially increased by stimulation of cholinergic vasodilator nerves, within seconds [2], and the reduction in blood flow immediately after vagotomy suggests a basal vasodilatory tone exerted by the vagus nerve [3]. Often, the vasodilators act primarily on the arteriolar endothelial cells to stimulate the production of endothelium derived relaxing substances.

During the last two decades, the important paracrine role of the vascular endothelium in regulation of blood vessel tone has become increasingly clear. Nitric oxide (NO), formed by the constitutive NO synthase (NOS) in response to stimulation by acetylcholine and other vasodilators, is a well known endothelium-dependent relaxing factor [4,5], also involved in the regulation of the gastric mucosal blood flow [6-8]. Besides NO, prostacyclin (PGI_2) is liberated by the endothelial cells upon stimulation with various agonists, similarly eliciting vasorelaxation [9]. Moreover, in the presence of

inhibitors of NOS and prostaglandin synthesis, endothelium-dependent dilation persists in most arteries. This NO- and PGI_2-independent relaxation is associated with a hyperpolarization of the membrane of the vascular smooth muscle cells [10,11]. Hyperpolarization of the membrane potential immediately brings about dilatation of blood vessels [12]. It decreases the open probability of voltage dependent Ca^{2+} channels, lowering Ca^{2+} influx [13]. In addition, it reduces Ca^{2+} release from internal stores [14] and also diminishes the impact of intracellular Ca^{2+} on the contractile proteins by altering their Ca^{2+} sensitivity [15].

The mechanism underlying the endothelium-dependent hyperpolarization in various vessels is still debated (for recent reviews, see refs. [16-18]. In hepatic and small mesenteric arteries of the rat, a transient rise in K^+ concentration in the restricted myoendothelial extracellular space, resulting from K^+ efflux through agonist-induced activation of Ca^{2+}-dependent K^+ channels on the endothelial cells, was reported [19,20] to act as endothelium derived hyperpolarizing factor (EDHF). Indeed, in some vessels, small increases in extracellular K^+ might influence the inward rectifier and stimulate the Na^+/K^+-ATPases of vascular smooth muscle cells, producing the expected membrane potential change. In the superior mesenteric artery of the rabbit, however, it was shown that acetylcholine-induced EDHF-mediated relaxation requires the transfer of a cytosolic factor from the endothelial cells to the smooth muscle cells via heterocellular gap junctions [21]. In smaller arteries, such as intestinal submucosal arterioles, the flow through gap junctions of hyperpolarizing current from endothelial cells might be sufficient to hyperpolarize the electrotonically coupled smooth muscle cells [22,23]. It appears, therefore, that different hyperpolarizing mechanisms may exist in different vascular beds. Moreover, the smooth muscle cells of some

arteries such as the femoral artery of the rat are devoid of endothelium-dependent hyperpolarization responses [24].

In previous tension measurements, we showed endothelium-dependent, NO- and PGI_2-independent vasorelaxations to occur in isolated small gastric arteries stimulated with acetylcholine [25]. In the present study, we extended these observations by directly measuring the membrane potential responses of the gastric arteriolar smooth muscle cells to acetylcholine using electrophysiological techniques. Moreover, the endothelium-dependent hyperpolarization was further characterized by investigating the involvement of inward rectifying K^+ channels and Na^+/K^+-ATPases by the use of the blockers Ba^{2+} and ouabain, respectively. To the best of our knowledge, this study reports the first detailed measurements of endothelium-dependent membrane potential responses in small gastric arteries.

4.2. MATERIALS AND METHODS

4.2.1. Animals

Young female Wistar rats (200-250 g body weight) were purchased from Iffa Credo (Brussels, Belgium). The animals were treated in accordance with the Guide for the Care and Use of Laboratory Animals published by the US National Institutes of Health (NIH Publication No 85-23, revised 1996).

4.2.2. Preparation

Experiments were approved by the ethical committee on animal research of Ghent University. Animals were killed with an intraperitoneal injection of a lethal dose (200 mg/kg) of pentobarbitone and laparotomized. The stomach was rapidly excised and transferred to a chilled medium of the following composition (mM): NaCl 135, KCl 5, $NaHCO_3$ 20, $CaCl_2$ 2.5, $MgSO_4.7H_2O$ 1.3, KH_2PO_4 1.2, EDTA 0.026 and glucose 10, gassed with 95% O_2, 5% CO_2. Several segments of first and second order branches of the gastric artery were dissected and transferred to fresh oxygenated medium. After removal of the adherent tissue, one of these segments was reduced to 1.5 mm, taking care not to injure the endothelium, and transferred to a small recording chamber where it was continuously superfused at 35 °C with control fluid. The control fluid consisted of the isolation medium supplemented with N^G-nitro-L-arginine (10^{-4} M) and indomethacin (5×10^{-5} M), to exclude interference from NO and prostanoids, respectively. In some experiments, the endothelium was removed from the arteries by rubbing the intimal surface.

For electrophysiological recordings, the preparation was pinned down to the silicone bottom of the experimental chamber using small pins. Near both attachment sides, the vessel was incised such as to facilitate later access of acetylcholine to the endothelium. After mounting, the vessel segment was allowed to equilibrate for at least 60 min before starting the microelectrode impalements. Microelectrode penetrations were performed from the adventitial side. At the end of the experiments, some representative vessels were moved to an automated wire myograph (model 500A, JP Trading, Aarhus, Denmark) in order to calculate their internal diameter. For this purpose, two stainless steel wires were guided through the lumen, one

was connected to a force transducer and the other fixed to a micrometer, and the passive wall tension-internal circumference characteristics were determined. From this relation, the mean internal diameter of these vessels at an effective transmural pressure of 100 mm Hg was calculated according to the method of Mulvany and Halpern [26].

4.2.3. Electrophysiological measurements

Transmembrane potentials were measured with standard microelectrode techniques, as described previously [27,28]. Briefly, conventional micro-electrodes were pulled with a vertical pipette puller (David Kopf, model 750, Tujunga, CA) from 1 mm o.d. filamented glass tubings (Hilgenberg, Germany). Micropipettes were filled with 1 M KCl and connected to the input stage of a laboratory made MOS/FET operational amplifier. The electrical resistance of the microelectrodes, measured in the normal Krebs-Ringer solution, ranged from 40 to 80 MΩ. The measured potential was followed on an oscilloscope and traced with a pen recorder at low speed. Absolute values of membrane potential were taken as the difference of the stabilized potential after cell impalement and the zero potential upon withdrawal of the microelectrode from the cell. Changes in membrane potential produced by applications of acetylcholine in control conditions and after experimental intervention (Ba^{2+}, ouabain) were usually measured in the same cell during continuous recordings. Barium chloride was added to the superfusate for at least 10 min before challenging the preparations with acetylcholine. With ouabain, pre-exposure time was minimally 5 min but varied between experiments, as described in the Results. Exposures to Ba^{2+} and acetylcholine were made by addition of these substances from the appropriate stock solutions to the superfusion solution.

4.2.4. Chemicals

Indomethacin, L-NA, acetylcholine chloride, ouabain and barium chloride were obtained from Sigma (St. Louis, MO). All concentrations are expressed as final molar concentrations in the superfusion chamber. Stock solutions of L-NA and $BaCl_2$ were made in pure water, indomethacin was dissolved in anhydrous ethanol. Acetylcholine was dissolved in 50 mM potassium hydrogen phthalate buffer, pH 4.0, as a 10^{-2} M solution. Further dilutions (1:10 or 1:100) were made in the control fluid immediately before addition of aliquots to the superfusate. Ouabain was dissolved directly in the warmed superfusion solution.

4.2.5. Statistics

Results are expressed as means $\pm$ SEM. Statistical significance was evaluated using Student's *t* test for paired or unpaired observations, as appropriate, a *P* value < 0.05 indicating a significant difference; n indicates the number of preparations, each obtained from a different animal.

4.3. RESULTS

The small gastric arteries used in this study had an average normalized diameter (at a transmural pressure of 100 mm Hg) of 214 $\pm$ 26 μm, as determined in 4 preparations at the end of the experiments (see Materials and Methods). Smooth muscle cells of such arteries, superfused wih the normal L-NA (10^{-4} M) and indomethacin ($5x10^{-5}$ M) containing Krebs-Ringer solution, had a stable resting membrane potential with a mean value of -64.5 $\pm$ 1.3 mV (n=15).

Exposure of intact vessels to a submaximal concentration of acetylcholine ($3x10^{-7}$ M), a concentration previously shown to relax norepinephrine preconstricted gastric arteries by about 50% of the developed active tension, induced a transient peak hyperpolarization of 5.1 ± 0.6 mV (n=14). In the continuous presence of the vasodilator, the membrane potential slowly recovered towards its control level. Recovery was accelerated by washout of the agonist (figure 1A).

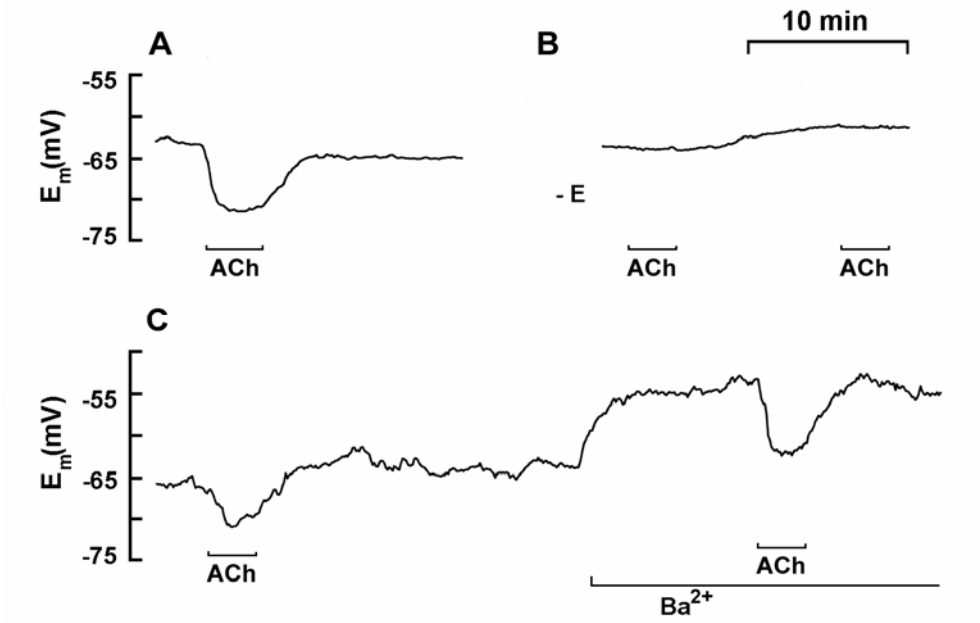

Figure 1: *Endothelium-dependent hyperpolarization induced by acetylcholine (ACh). Typical tracings of the membrane potential (E_m) recorded in smooth muscle cells from small gastric arteries during application of 0.3 μM ACh in the presence (A, C) and the absence (B) of a functional endothelium (E) and after pre-exposure to 30 μM of Ba^{2+}, an inhibitor of inward rectifying K^+ channels (C). Notice the larger endothelium-dependent membrane potential response in the presence of Ba^{2+}.*

In endothelium-denuded arteries (cf. figure 1B) the smooth muscle cells had a mean resting membrane potential not significantly different from the control vessels (-65.0 ± 3.1 mV, n=4). Hyperpolarization of the membrane potential did not occur after exposing endothelium-denuded arteries to acetylcholine.

In a next series of experiments (n=8), the influence on the membrane potential and its response to acetylcholine of pre-exposure to low concentrations of Ba^{2+}, known to inhibit the inward rectifying K^+ channels, was tested. Figure 1C shows an original trace from a representative experiment. Superfusion with 30 μM Ba^{2+} containing fluid caused a depolarization of the resting membrane potential by 5.6 ± 0.5 mV. Pre-exposure to this inhibitor, however, did not decrease the magnitude of the endothelium-dependent hyperpolarization elicited by acetylcholine. Conversely, in this series of experiments an increase of the endothelium-dependent hyperpolarization was observed. The peak hyperpolarization induced by acetylcholine in the presence of Ba^{2+} averaged 6.2 ± 0.8 mV, *vs*. 4.7 ± 0.6 mV in control conditions in this subset of arteries. This difference is statistically significant ($p < 0.05$).

Application of a large concentration (0.5 mM) of ouabain in the continuous presence of Ba^{2+} produced a transient peak depolarization followed by a slow return of the membrane potential towards baseline. Traces from two succesfull long-term impalements in which the microelectrode was kept in a cell for several hours are shown in figure 2A and 2B. Due to the more compressed time scale used to construct these figures, acetylcholine-induced hyperpolarizations merely appear as inverted peaks.

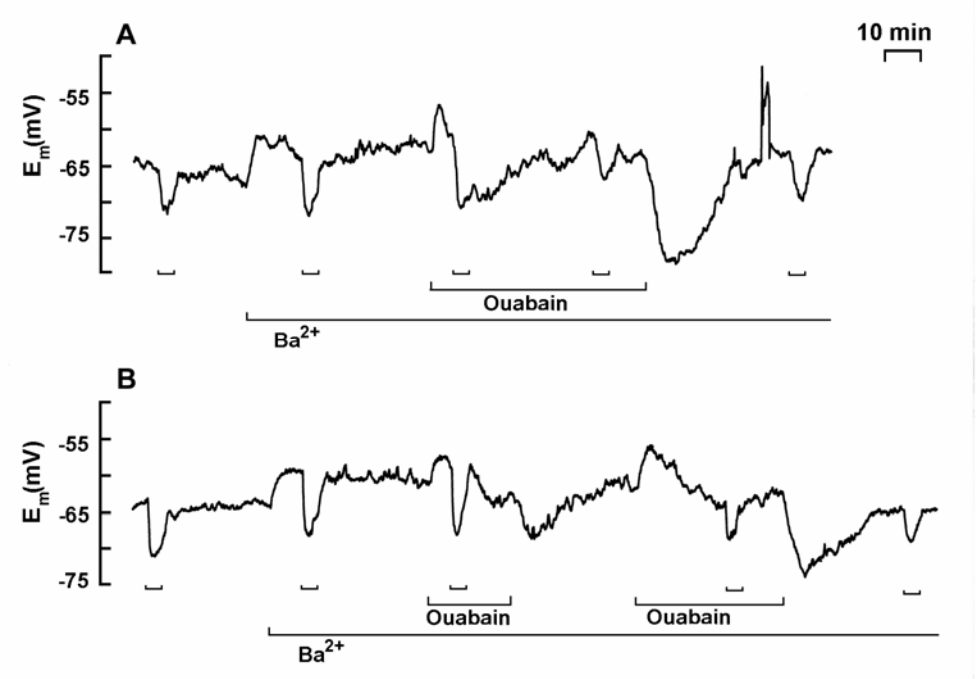

Figure 2: *Influence of additional pre-exposure to the Na^+/K^+-ATPase inhibitor ouabain. Original recordings of the membrane potential (E_m) recorded in smooth muscle cells of small gastric arteries, showing its responses to superfusion with acetylcholine (0.3 μM) containing fluid (as indicated by the short horizontal lines) in control conditions, in the presence of Ba^{2+} (30 μM), and during and after additional exposure to ouabain (0.5 mM).*

Ouabain depolarized the smooth muscle cells by 6.4 ± 0.7 mV (n=8). When acetylcholine was applied shortly after exposure to ouabain, at a time when the membrane potential was still more depolarized with respect to its level in Ba^{2+} alone (cf. figure 2A and 2B), the endothelium-dependent hyperpolarization averaged 7.0 ± 1.7 mV (n=4), a value not significantly different from that observed in the absence of ouabain. After prolonged pre-exposure to ouabain, acetylcholine still evoked membrane hyperpolarization, averaging 4.3 ± 0.8 mV (n=4), a value slightly but not significantly smaller than that observed in the absence of ouabain. Effective inhibition of the Na^+/K^+-pump by ouabain was additionally demonstrated by

the transient hyperpolarizations of the smooth muscle cells after washout of the drug, being, evidently, more important with increasing exposure time to the inhibitor (figure 2A and 2B). From all ouabain experiments, the mean values for the resting membrane potential before application of acetylcholine and for the magnitude of the peak vasodilator-induced hyperpolarization are summarized in figure 3. In the combined presence of Ba^{2+} and ouabain, the endothelium-dependent hyperpolarization evoked by acetylcholine was not significantly different from that in Ba^{2+} alone, or from that in control conditions.

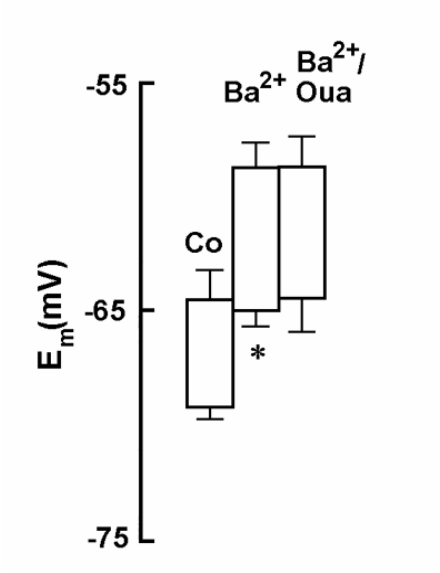

Figure 3: *Acetylcholine-induced hyperpolarizations of gastric artery smooth muscle cells in control conditions (Co), in the presence of barium (Ba^{2+}, 30 μM) and after additional application of ouabain (Ba^{2+}/ouabain). Data are means $\pm$ SEM (n=8) and represent the membrane potential (E_m) values before and after application of acetylcholine. * Significantly different from control value (P<0.05).*

It might be argued that the rather unexpected secondary hyperpolarization of the membrane potential in the continuous presence of 0.5 mM ouabain is due to incomplete inhibition of all membrane Na^+/K^+-ATPases, some

residual pump activity being stimulated by the rise in intracellular sodium concentration caused by the inhibited pumps. To test this possibility, the ouabain concentration was doubled during the slow hyperpolarization phase in some experiments. Increasing the concentration of the glycoside from 0.5 to 1 mM did not further depolarize the membrane or otherwise modify the course of the slow hyperpolarization (figure 4A). Moreover, the slow membrane potential change in the presence of ouabain was independent of an intact endothelium, as depicted in figure 4B (n=4).

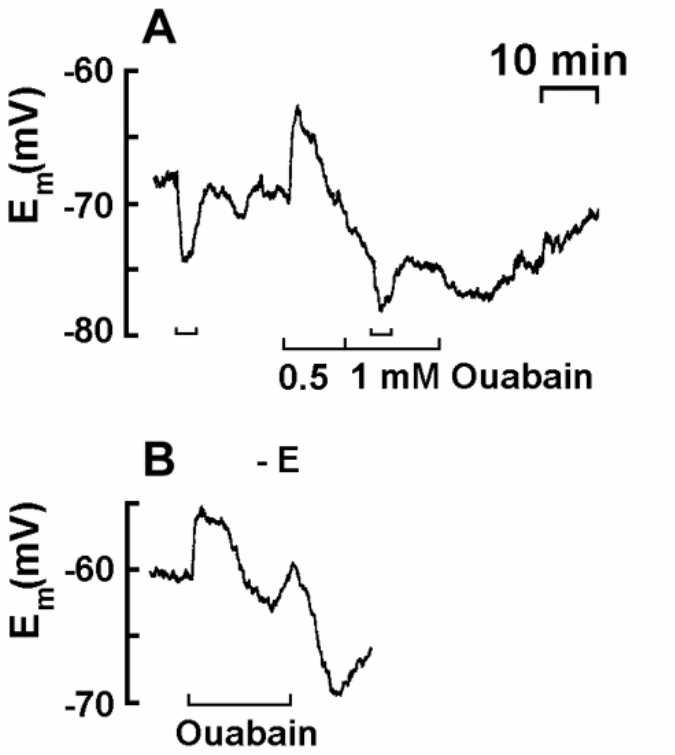

Figure 4: *Typical tracings showing the effect of doubling the ouabain concentration (A) and of endothelium (E) removal (B) on the membrane potential (E_m) of gastric artery smooth muscle cells. Vessels were exposed to Ba^{2+} (30 μM) throughout. Short horizontal lines in A show times of application of acetylcholine (0.3 μM).*

4.4. DISCUSSION

The membrane potential of the smooth muscle cells is an important determinant of arterial tone [12]. In this study, the resting membrane potential of smooth muscle cells of small gastric arteries was measured, and the membrane response to cholinergic stimulation of the intact vessel was quantified and characterized.

A physiological concentration ($3x10^{-7}$ M) of acetylcholine, previously shown to relax norepinephrine-stimulated arteries in an NO- and prostacyclin-independent way to about 50 % of their preconstriction level, caused a 5 mV hyperpolarizing shift of the smooth muscle cell membrane potential from a resting level of about -65 mV. The experiments with the endothelium-denuded arteries showed that the acetylcholine-induced hyperpolarization was completely endothelium-dependent, and that the agonist did not exert a direct depolarizing action on the smooth muscle cells as has been reported for some arteries. These direct measurements, therefore, confirm the existence of endothelium-dependent hyperpolarization in gastric arteries, as has been suggested from earlier tension measurements [25,29].

The magnitude of the membrane potential response to the submaximal acetylcholine concentration might seem relatively small. However, it should be noted that a change in membrane potential of just a few millivolts can result in a substantial change in vessel diameter [30]. In rat mesenteric arteries in the presence of N^G-nitro-L-arginine, an acetylcholine induced hyperpolarization of 1 mV corresponded to a 4.3 % decrease of the induced tone [31]. This implies, therefore, that the endothelium-dependent hyperpolarization as measured in the present study makes an important

contribution to the regulation of the diameter of small gastric arteries in situ. Moreover, alterations of the membrane potential generally evoke faster changes in arteriolar diameter than those mediated by second messengers, which more slowly influence gastric blood flow.

Low concentrations of Ba^{2+} are known to specifically block the inward rectifier K^+ current in vascular tissue. In the present conditions, we found 30 μM of Ba^{2+} to significantly depolarize the smooth muscle cells of small gastric arteries, indicating that the inward rectifier contributes to the setting of the resting membrane potential in these vessels. After inhibition of the inward rectifyer, however, endothelium-dependent smooth muscle cell responses to submaximal concentrations of acetylcholine were not inhibited but significantly increased. This excludes a role for inward rectifying K^+ channels in the acetylcholine-induced endothelium-dependent hyperpolarization of small gastric arteries. It also suggests that in tonically contracted vessels, in which the membrane potential is similarly depolarized with respect to resting conditions, endothelium-dependent hyperpolarization might be larger than observed in the resting arteries as used in the present study. The increased response might be due to the enhanced driving force on intracellular K^+ after Ba^{2+}-induced depolarization, or to the diminished total membrane conductance after blocking the open K^+ channels with Ba^{2+}, enlarging the impact of any hyperpolarizing current on the smooth muscle cell membrane potential. With submaximal concentrations of acetylcholine, this current is not expected to drive the membrane potential to values as negative as E_K, explaining the less negative absolute level of membrane potential after the Ba^{2+}-induced depolarization. Similarly, in smooth muscle cells from guinea-pig coronary arteries, 100 μM $BaCl_2$ increased EDHF-attributed hyperpolarization [32], while in cells of ilial submucosal arterioles and of mesenteric arterioles of

the same species 500 μM Ba^{2+} was used to depolarize the membrane potential away from the K^+ equilibrium potential in order to observe significant endothelium-dependent hyperpolarizations after application of acetylcholine [22,33].

In gastric arteries, the additional inhibition of the Na^+/K^+-pump with 0.5 mM ouabain further depolarized the smooth muscle cells, as expected from the sudden loss of electrogenic pump activity. Since the K_d value for ouabain of the ubiquitous low affinity α_1-isoform containing Na^+/K^+-ATPase in rat tissue is about 15 μM [34], and the other isoenzymes are much more sensitive to the cardiotonic steroid [35], it can reasonably be assumed that in the present conditions all pump isoenzymes are effectively inhibited by 0.5 mM of the cardiotonic steroid. In mesenteric arteries of the rat, the vasodilation occurring on readmission of K^+ ions after K^+-free perfusion was completely inhibited by 100 μM of ouabain [36]. Moreover, in the present study the complete inhibition of Na^+/K^+-ATPase activity by 0.5 mM ouabain was directly verified by the lack of additional depolarization on doubling the ouabain concentration.

In the combined presence of barium and ouabain, the magnitude of the endothelium-dependent hyperpolarization induced by acetylcholine was not significantly changed. These observations strongly suggest that small gastric artery smooth muscle cells do not rely on their inward rectifiers and Na^+/K^+-pumps to produce this hyperpolarization. In a previous study, it was found that small increases in extracellular K^+ concentration were unable to consistently relax preconstricted gastric arteries [25]. Taken together, these findings argue against a role for extracellular K^+ to act as an EDHF in this preparation.

In the prolonged presence of ouabain, the membrane potential slowly became more hyperpolarized than before exposure to the cardiotonic glycoside, in an endothelium-independent way. A plausible explanation for this observed shift is that the ouabain-induced rise in intracellular Na^+ concentration leads, via an influence on the Na/Ca exchanger, to a secondary rise in intracellular Ca^{2+} concentration, as has been documented in several cell types. This raised Ca^{2+} is expected to subsequently open the Ca^{2+}-dependent K^+ channels of the smooth muscle cell. In the pancreatic B-cell, e.g., ouabain was shown to increase ^{86}Rb (used as a tracer for K^+) outflow [37]. Thus, a gradually increasing membrane K^+ conductance might explain both the slow hyperpolarization as well as the observed tendency for the endothelium-dependent hyperpolarization to decrease in magnitude after prolonged ouabain exposure.

In a previous study, shorter exposures to ouabain were found to inhibit the EDHF-mediated relaxation of gastric arteries [25]. The present measurements showing that the endothelium-dependent hyperpolarization of the vascular smooth mucle cells is not affected by the pump inhibitor suggest, therefore, a defective coupling between the change in membrane potential and the mechanical response, presumably involving a hampered Ca^{2+} extrusion. Moreover, they stress the importance of electrophysiological measurements when studying the EDHF phenomenon [38].

In summary, we have shown that acetylcholine hyperpolarizes the membrane potential of the vascular smooth muscle cells of small gastric arteries. This electrical change, expected to exert a substantial influence on vessel tone and resistance, is entirely dependent on an intact endothelium, but independent from the endothelial NO/prostacyclin pathways. The mechanism underlying the endothelium-dependent hyperpolarization does

not seem to rely on the stimulation of inward rectifying K^+ channels or Na^+/K^+-pumps, as was shown for rat hepatic arteries. Endothelium-dependent hyperpolarization might prove to be another important and rapid regulator of gastric mucosal blood flow, of utmost importance in the maintenance of mucosal function and integrity.

4.5. REFERENCES

1. Kawano S, Tsuji S. Role of mucosal blood flow: A conceptional review in gastric mucosal injury and protection. *J Gastroenterol Hepatol.*. 2000;15:D1-D6.
2. Morishita T, Guth PH. Vagal nerve stimulation causes noncholinergic dilatation of gastric arterioles. *Am J Physiol*. 1986;250:G660-G664.
3. Abdel-Salam OM, Czimmer J, Debreceni A, Szolcsanyi J, Mozsik G. Gastric mucosal integrity: gastric mucosal blood flow and microcirculation. An overview. *J Physiol (Paris)*. 2001;95:105-127.
4. Furchgott RF, Zawadzki JV. The obligatory role of endothelial cells in the relaxation of arterial smooth muscle by acetylcholine. *Nature*. 1980;288:373-376.
5. Palmer RMJ, Ferrige AG, Moncada S. Nitric oxide release accounts for the biological activity of endothelium-derived relaxing factor. *Nature*. 1987;327:524-526.
6. Holzer P. Neural emergency system in the stomach. *Gastroenterol*. 1998;114:823-839.
7. Abe Y, Itoh K, Arakawa Y. Altered vascular response to acetylcholine in conditions of endothelial damage in the isolated perfused rat stomach. *J Gastroenterol*. 2000;35:93-98.
8. Helmer KS, West SD, Shipley GL, Chang L, Cui Y, Mailman D, Mercer DW. Gastric nitric oxide synthase expression during endotoxemia: implications in mucosal defense in rats. *Gastroenterol*. 2002;123:173-186.

9. Furchgott RF, Vanhoutte PM. Endothelium-derived relaxing and contracting factors. *FASEB J*. 1989;3:2007-2018.

10. Chen G, Suzuki H, Weston AH. Acetylcholine releases endothelium-derived hyperpolarizing factor and EDRF from rat blood vessels. *Br J Pharmacol*. 1988;95:1165-1174.

11. Taylor SG, Weston AH. Endothelium-derived hyperpolarizing factor: a new endogenous inhibitor from the vascular endothelium. *Trends Pharmacol Sci*. 1988;9:272-274.

12. Kuriyama H, Kitamura K, Nabata H. Pharmacological and physiological significance of ion channels and factors that modulate them in vascular tissues. *Pharmacol Rev*. 1995;47:387-573.

13. Nelson MT, Patlak JB, Worley JF, Standen NB. Calcium channels, potassium channels, and voltage dependence of arterial smooth muscle tone. *Am J Physiol*. 1990;259:C3-18.

14. Itoh T, Seki N, Suzuki S, Ito S, Kajikuri J, Kuriyama H. Membrane hyperpolarization inhibits agonist-induced synthesis of inositol 1,4,5-trisphosphate in rabbit mesenteric artery. *J Physiol*. 1992;451:307-328.

15. Okada Y, Yanagisawa T, Taira N. Brl-38227 (Levcromakalim)-induced hyperpolarization reduces the sensitivity to Ca^{2+} of contractile elements in canine coronary artery. *Naunyn-Schmiedebergs Arch Pharmacol* 1993;348:348.

16. McGuire JJ, Ding H, Triggle CR. Endothelium-derived relaxing factors: a focus on endothelium-derived hyperpolarizing factor(s). *Can J Physiol Pharmacol*. 2001;79:443-470.

17. Busse R, Edwards G, Feletou M, Fleming I, Vanhoutte PM, Weston AH. EDHF: bringing the concepts together. *Trends Pharmacol Sci*. 2002;23:374-380.

18. Triggle CR, Ding H. Endothelium-derived hyperpolarizing factor: Is there a novel chemical mediator? *Clin Exp Pharmacol Physiol*. 2002;29:153-160.

19. Edwards G, Dora KA, Gardener MJ, Garland CJ, Weston AH. K^+ is an endothelium-derived hyperpolarizing factor in rat arteries. *Nature*. 1998;396:269-272.

20. Weston AH, Richards GR, Burnham MP, Feletou M, Vanhoutte PM, Edwards G. K^+-induced hyperpolarization in rat mesenteric artery: identification, localization and role of Na^+/K^+-ATPases. *Br J Pharmacol*. 2002;136:918-926.

21. Hutcheson IR, Chaytor AT, Evans WH, Griffith TM. Nitric oxide-independent relaxations to acetylcholine and A23187 involve different routes of heterocellular communication. Role of Gap junctions and phospholipase A2. *Circ Res*. 1999;84:53-63.

22. Yamamoto Y, Imaeda K, Suzuki H. Endothelium-dependent hyperpolarization and intercellular electrical coupling in guinea-pig mesenteric arterioles. *J Physiol*. 1999;514 (Pt 2):505-513.

23. Imaeda K, Yamamoto Y, Fukuta H, Koshita M, Suzuki H. Hyperpolarization-induced dilatation of submucosal arterioles in the guinea-pig ileum. *Br J Pharmacol*. 2000;131:1121-1128.

24. Sandow SL, Tare M, Coleman HA, Hill CE, Parkington HC. Involvement of myoendothelial gap junctions in the actions of endothelium-derived hyperpolarizing factor. *Circ Res*. 2002;90:1108-1113.

25. Van de Voorde J, Vanheel B. EDHF-mediated relaxation in rat gastric small arteries: influence of ouabain/Ba^{2+} and relation to potassium ions. *J Cardiovasc Pharmacol*. 2000;35:543-548.

26. Mulvany MJ, Halpern W. Contractile properties of small arterial resistance vessels in spontaneously hypertensive and normotensive rats. *Circ Res*. 1977;41:19-26.

27. Vanheel B, VandeVoorde J. Evidence against the involvement of cytochrome P450 metabolites in endothelium-dependent hyperpolarization of the rat main mesenteric artery. *J Physiol*. 1997;501:331-341.

28. Breyne J, Vanheel BJ. Role of Ba^{2+}-resistant K^+ channels in endothelium-dependent hyperpolarization of rat small mesenteric arteries. *Can J Physiol Pharmacol*. 2004;82:65-71.

29. Kawabata A, Nakaya Y, Kuroda R, Wakisaka M, Masuko T, Nishikawa H, Kawai K. Involvement of EDHF in the hypotension and increased gastric mucosal blood flow caused by PAR-2 activation in rats. *Br J Pharmacol*. 2003;140:247-254.

30. Nelson MT, Quayle JM. Physiological roles and properties of potassium channels in arterial smooth muscle. *Am J Physiol*. 1995;268:C799-C822.

31. Cheung DW, Chen G, MacKay MJ, Burnette E. Regulation of vascular tone by endothelium-derived hyperpolarizing factor. *Clin Exp Pharmacol Physiol*. 1999;26:172-175.

32. Nishiyama M, Hashitani H, Fukuta H, Yamamoto Y, Suzuki H. Potassium channels activated in the endothelium-dependent hyperpolarization in guinea-pig coronary artery. *J Physiol*. 1998;510 (Pt 2):455-465.

33. Hashitani H, Suzuki H. K^+ channels which contribute to the acetylcholine-induced hyperpolarization in smooth muscle of the guinea-pig submucosal arteriole. *J Physiol*. 1997;501 (Pt 2):319-329.

34. Noel F, Godfraind T. Heterogeneity of ouabain specific binding sites and Na^+/K^+-ATPase inhibition in microsomes from rat heart. *Biochem Pharmacol*. 1984;33:47-53.

35. Blanco G, Mercer RW. Isozymes of the Na^+/K^+-ATPase: heterogeneity in structure, diversity in function. *Am J Physiol*. 1998;275:F633-F650.

36. Adeagbo AS, Malik KU. Endothelium-dependent and BRL 34915-induced vasodilatation in rat isolated perfused mesenteric arteries: role of G-proteins, K^+ and calcium channels. *Br J Pharmacol*. 1990;100:427-434.

37. Lebrun P, Malaisse WJ, Herchuelz A. Na^+/K^+-pump activity and the glucose-stimulated Ca^{2+}-sensitive K^+ permeability in the pancreatic B-cell. *J Membr Biol*. 1983;74:67-73.

38. Edwards G, Weston AH. EDHF - are there gaps in the pathway? *J Physiol*. 2001;531:299.

Chapter

5

Methanandamide hyperpolarizes gastric arteries by stimulation of TRPV1 receptors on perivascular CGRP containing nerves

Joke Breyne & Bert Vanheel
Department of physiology & physiopathology

J Cardiovasc Pharmacol 2006; 47: 303-309

Abstract

Endogenous as well as synthetic cannabinoids have potent vasodilatory actions in a variety of vascular preparations. Their precise mechanism of action is as yet unclear but several studies point to the activation of type 1 vanilloid ($TRPV_1$) receptors on primary afferent perivascular nerves, stimulating the release of calcitonin gene-related peptide (CGRP). Given the documented gastroprotective function of these nerves, and the various gastrointestinal effects reported for cannabinoids, we explored a possible link between these systems in the gastric circulation by comparing responses of small gastric arteries to cannabinoids and to CGRP using conventional microelectrode techniques. Exposure of small gastric arteries to the stable endocannabinoid analogue methanandamide caused a hyperpolarization of the vascular smooth muscle cells, which was completely abolished by the vanilloid receptor antagonist capsazepine ($p<0.01$). Exposure to exogenous CGRP evoked fully reproducible ($p>0.05$) hyperpolarizations with similar time course, unaffected by capsazepine. Preincubation with glibenclamide, an inhibitor of ATP-sensitive potassium (K_{ATP}) channels, reversed both responses to methanandamide ($p<0.01$) and CGRP ($p<0.05$). Similar results were found in rat mesenteric arteries. These findings show that cannabinoids stimulate $TRPV_1$ receptors, presumably causing the release of CGRP, which hyperpolarizes the smooth muscle cells by activation of K_{ATP} channels. Since membrane hyperpolarization is a powerful mediator of vasorelaxation, this novel pathway might prove to be an important mechanism affording gastroprotection.

Keywords: *vascular smooth muscle membrane potential, vasoactive agents, endothelial factors, blood flow, cannabinoids*

5.1. INTRODUCTION

Plant derived, synthetic as well as endogenous cannabinoids have a pronounced influence on gastrointestinal motility and secretion [1-4]. Effects reported for stimulation of type I cannabinoid receptors (CB_1) include inhibition of gastric acid secretion and reduction of the development of stress-induced gastric ulcers in rats [5,6]. The integrity of the gastric mucosa, however, also depends on an appropriate microcirculatory blood flow. Indeed, the production and secretion of mucus, and the secretion of bicarbonate ions which protect the mucosa, are fully dependent on this circulation. Moreover, the blood removes waste materials and back-diffusing hydrogen ions. Disturbances in the mucosal microcirculation therefore lead to mucosal injury and peptic ulcers [7]. Among the defence mechanisms, a group of sensory neurons originating from the dorsal root ganglia constitute a separate alarm system in the stomach [8]. They express type 1 vanilloid ($TRPV_1$) receptors, which are activated by noxious stimuli including molecules with a vanillyl moiety such as capsaicin, but also by heat and protons. Stimulation of this receptor triggers the local release of neuropeptides from their peripheral endings, the most important of which is the powerful vasodilator calcitonin gene related peptide (CGRP) [9]. CGRP containing nerves are also present in the human gastric mucosa, and with increased density at the margin of ulcers [10]. The gastroprotective role of CGRP released from sensory nerves has been shown in various studies, and results from the rise in mucosal blood flow the peptide produces[11-13]. CGRP might act directly on the vascular smooth muscle cells and/or stimulate the endothelium to release relaxing substances such as nitric oxide (NO), prostacyclin and the as yet unidentified endothelium-derived hyperpolarizing factor (EDHF) [14,15].

Since the original observation that vasorelaxation by cannabinoids can be mediated by stimulation of $TRPV_1$ receptors on CGRP containing perivascular nerves [16], several recent studies have documented $TRPV_1$ stimulation by the endogenous CB_1 agonist anandamide, and stressed that the agent should be considered both an endocannabinoid and an endovanilloid [17,18]. In a previous study, we showed that the cannabinoids anandamide and its stable derivative methandamide produce a substantial hyperpolarization of smooth muscle cells of isolated small mesenteric rat arteries, an effect attributed to cannabinoid-induced release of CGRP from the perivascular nerves [19]. CGRP-induced hyperpolarization of vascular smooth muscle cells, indeed, immediately brings about dilation of the blood vessels.

Given the documented important role played by primary afferent nerves in the gastric mucosa, we explored the influence of cannabinoids on the membrane potential of smooth muscle cells in isolated small gastric arteries, compared this with their response to exogenous CGRP, and investigated the involvement of $TRPV_1$ receptors using the specific antagonist capsazepine. Their effect was compared with that of the endothelium-dependent vasodilator acetylcholine. To the best of our knowledge, this study reports the first detailed measurements of membrane potential responses to cannabinoids and to CGRP in gastric arteries. It shows that cannabinoids locally stimulate $TRPV_1$ receptors releasing a substance like CGRP, which hyperpolarizes the blood vessels by opening ATP-dependent potassium channels. This local action of cannabinoids might prove to constitute an alternative pathway affording gastroprotection.

5.2. MATERIALS AND METHODS

5.2.1. Preparations

Small gastric and mesenteric arteries from female Wistar rats (180 – 280 g) were used. The animals were treated in accordance with the Guiding Principles in the Care and Use of Animals and the experiments were approved by the ethical committee on animal research of Ghent University. The animals were anesthetized by a lethal dose (200 mg kg^{-1}) of pentobarbitone and killed by cervical dislocation. Both the stomach and the mesentery were rapidly excised and placed in cold (4°C) normal Krebs-Ringer bicarbonate solution, bubbled with a 95% O_2 – 5% CO_2 gas mixture. Second and third order branches of the gastric and mesenteric arteries were dissected free and transferred to fresh and gassed medium, where they were cleaned from surrounding connective tissue and cut into segments of about 2 mm in length.

5.2.2. Tension measurements

For tension measurements, the arterial segments were mounted into the organ bath of an automated dual small-vessel myograph (model 500 A; J. P. Trading, Aarhus, Denmark), filled with 10 ml Krebs-Ringer bicarbonate solution. Two stainless steel wires (40 µm in diameter) were guided through the lumen of the segments. Each wire was fixed to a holder of the myograph: one holder was connected to a micrometer which was used to change the distance between the wires, the other holder was connected to a force-displacement transducer to measure the isometric tension changes. After mounting, the preparations were allowed to equilibrate for at least 30 min in warmed (37 °C), oxygenated (5% CO_2 in O_2; pH 7.4) Krebs-Ringer

bicarbonate solution. At the start of each experiment the vessels were stretched to their optimal lumen diameter for active force development, as calculated on the basis of the passive wall tension-internal circumferences relationship [20]. Subsequently, the arteries were repeatedly activated with a Krebs-Ringer bicarbonate solution containing 120 mM K^+ and 10^{-5} M norepinephrine to assess maximal contractility. After this preparation procedure, the gastric arteries were contracted by adding 10^{-5} M norepinephrine to the standard Krebs-Ringer bicarbonate solution in the organ bath. When a stable contraction was reached, a concentration-response curve was constructed by cumulative additions of methanandamide.

5.2.3. Electrophysiological measurements

For the membrane potential measurements, the isolated segments were pinned down to the silicone bottom of an experimental chamber and were continuously superfused with warmed (35 °C), oxygenated (5% CO_2 in O_2; pH 7.4) Krebs-Ringer solution, supplemented with N^G-nitro-L-arginine (L-NA, 10^{-4} M) and indomethacin (5×10^{-5} M) to rule out the interference of NO and prostanoids, respectively. After mounting, the preparations were allowed to equilibrate for at least 60 min before starting the electrophysiological measurements.

Membrane potentials of the vascular smooth muscle cells were measured using standard microelectrode techniques as described previously [21,22]. Conventional sharp microelectrodes were pulled from filamented borosilicate glass tubings (Hilgenberg, Germany) with a vertical pipette puller (David Kopf Instruments, Tujunga California). Micropipettes were

filled with 1 M KCl. Their electrical resistance, measured in normal Krebs-Ringer solution, ranged from 40 to 80 MΩ. The measured potential was monitored on an oscilloscope and traced with a pen recorder. Successful impalements of the vascular smooth muscle cells were characterized by a sharp voltage deflection on entering the cell and a fast return to the baseline upon dislodgement of the microelectrode from the cell. Absolute values for the membrane potential (E_m) were taken as the difference of the stabilized potential after cell impalement and the zero potential as obtained upon electrode dislodgement. At the beginning of each experiment, the presence of a functional endothelium was assessed by the ability of acetylcholine (3 µM) to induce a substantial hyperpolarization. Changes in membrane potential produced by application of anandamide (10 µM), methanandamide (10 µM), CGRP (3×10^{-9} M) or acetylcholine (3 µM) in control conditions and in the presence of various inhibitors (capsazepine, 3 µM; glibenclamide, 10 µM) were measured. Given the technical difficulty of the experiments and the limited time period a cell impalement could be maintained, only one concentration of the respective dilator was tested. Glibenclamide was added to the superfusate for at least 10 min before application of a vasodilator, whereas in the experiments in which the influence of capsazepine was tested, pre-exposure time was minimally 20 min. All tested agents were added from the appropriate stock solutions to the superfusate.

5.2.4. Chemicals

All experiments were performed in a Krebs-Ringer bicarbonate solution of the following composition (in mM): NaCl 135, KCl 5, $NaHCO_3$ 20, $CaCl_2$ 2.5, $MgSO_4.7H_2O$ 1.3, KH_2PO_4 1.2, EDTA 0.026 and glucose 10. Acetylcholine

chloride, anandamide, indomethacin, L-NA, norepinephrine, capsazepine and glibenclamide were purchased from Sigma-Aldrich (St. Louis, MO). Methanandamide was obtained from two different sources: Research Biochemicals International (Natick, MA) and Tocris (Bristol, UK). CGRP was obtained from Tocris (Bristol, UK). Acetylcholine was dissolved in 50 mM potassium hydrogen phtalate buffer, pH 4.0. L-NA, norepinephrine and CGRP were dissolved in water; indomethacin, anandamide, methanandamide and capsazepine in anhydrous ethanol and glibenclamide in dimethyl sulfoxide. All concentrations mentioned are expressed as final molar concentrations in the experimental chamber.

5.2.5. Statistics

Data were computed as means ± S.E.M. and evaluated statistically using student's *t*-test for paired or unpaired samples or repeated measures ANOVA with Bonferroni's post hoc test when appropriate. A p value < 0.05 indicates a significant difference. *n* represents the number of preparations tested, each obtained from a different rat. In the tension measurements, relaxation is expressed as the percentage decrease in norepinephrine-induced tone.

5.3. RESULTS

5.3.1. Tension measurements

The small gastric arteries as used in the present relaxation measurements had a mean normalized diameter of 307.4 ± 28.5 µm (n=5). After norepinephrine (10^{-5} M) had induced a stable contraction (10.2 ± 1.8 mN;

n=5), cumulative addition of the anandamide analogue methanandamide (from 10^{-7} M to 10^{-5} M) elicited concentration-dependent relaxations (n=5; figure 1). Since hyperpolarization is one mechanism to induce relaxation, we further performed electrophysiological measurements to investigate and characterize the influence of the cannabinoid on the smooth muscle membrane potential of gastric arteries.

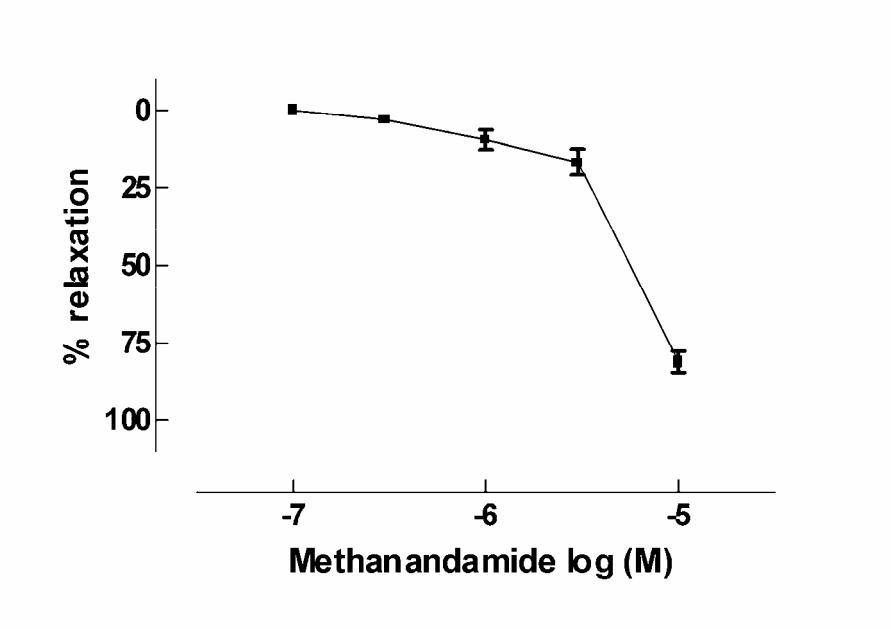

Figure 1: *Relaxation induced by methanandamide in rat gastric arteries. Concentration-response curve for methanandamide (n=5) in arteries precontracted with norepinephrine. Relative responses are expressed as the percentage relaxation induced by the cannabinoid.*

5.3.2. Electrophysiological measurements

5.3.2.1. Characterization of the membrane electrical response to the cannabinoid methanandamide and to CGRP

In the continuous presence of L-NA (10^{-4} M) and indomethacin (5×10^{-5} M), smooth muscle cells of rat small gastric arteries had a stable resting membrane potential with a mean value of –54.7 ± 1.2 mV (n=23).

The addition of acetylcholine (3 µM) evoked hyperpolarizations peaking within the first 2 min of application at a mean level 7.9 ± 1.4 mV (n=7) more negative than the resting membrane potential. In the presence of acetylcholine, membrane potential slowly recovered towards its control level. A typical tracing is depicted in figure 2.

After washout of the agonist, the membrane potential quickly recovered to its initial level. After exposure of intact vessels to methanandamide (10 µM), the membrane potential rather slowly hyperpolarized by a mean value of 8.5 ± 1.2 mV. The maximal change was reached 8.8 ± 0.9 min (n=4) after application of the cannabinoid. As can be seen more clearly in figure 3A, in which continuous recordings from the same cell are shown, the membrane potential recovered very slowly from exposure to methanandamide. Moreover, a second application of the cannabinoid after a washout period of at least 30 min hardly evoked any electrical response (+1.3 ± 1.3 mV upon second exposure vs –3.7 ± 0.5 mV at first exposure in this subset of 3 experiments; $p<0.05$).

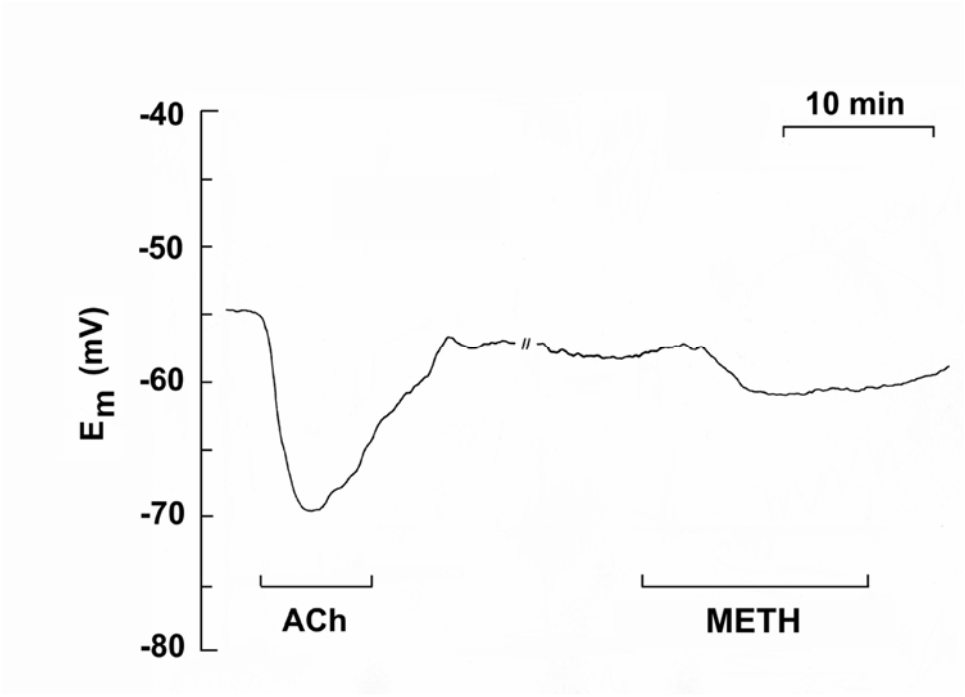

Figure 2: *Original tracing of the membrane potential (E_m) recorded in a vascular smooth muscle cell of a small gastric artery, showing the different time course of the hyperpolarization elicited by acetylcholine (ACh, 3×10^{-6} M)and methanandamide (METH, 10^{-5} M). During the break in the trace, the artery was continuously superfused with the control fluid for about 30 min without dislodgement of the microelectrode from the cell.*

The application of calcitonin gene related peptide to the vessels produced hyperpolarizations of the membrane potential comparable to those obtained with methanandamide (figure 3B). With 3×10^{-9} M a mean change of -8.8 ± 1.8 mV (n=5) was observed. As was observed with the cannabinoid, the membrane potential slowly recovered toward its control level after washout of the peptide. However, the effect of CGRP was fully reproducible. A second exposure of the preparations to CGRP, after a washout period of at least 20 min, caused a hyperpolarization of -8.5 ± 0.7 mV (n=5; $p>0.05$) (figure 3B). CGRP also hyperpolarized vessels which were previously

exposed to methanandamide. A representative tracing is shown in figure 3A.

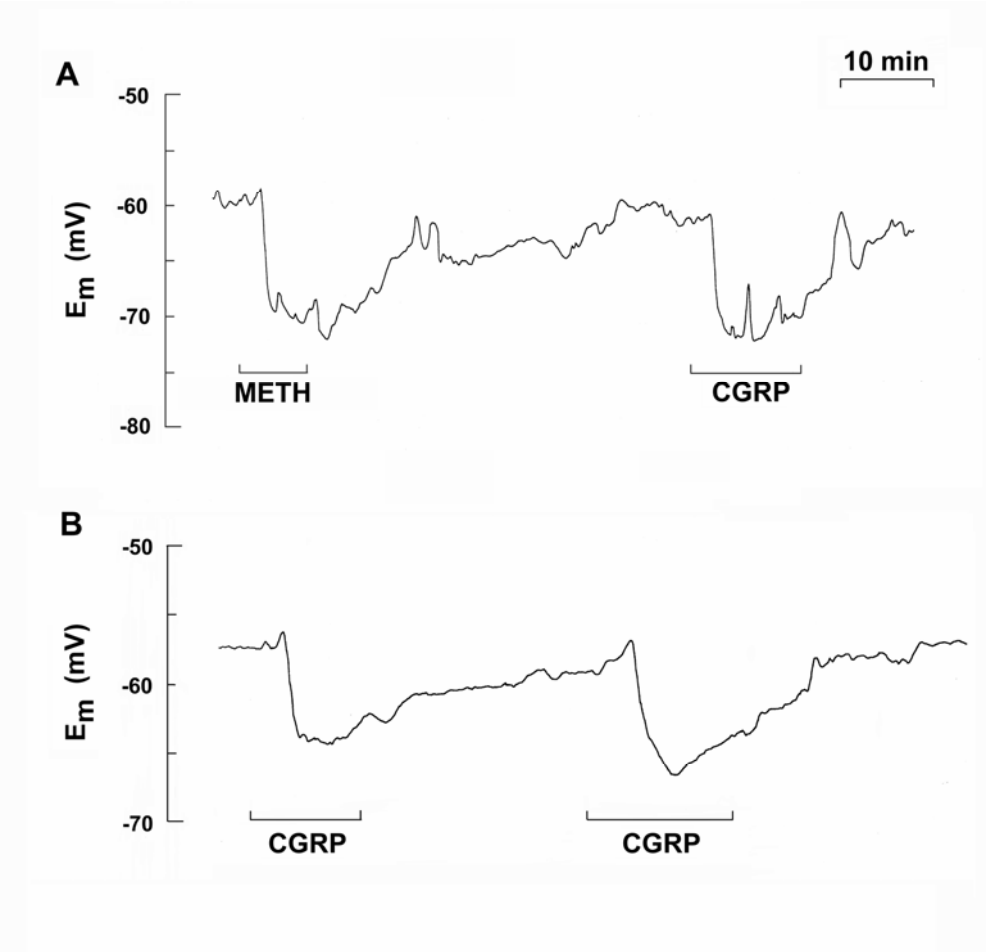

Figure 3: *Original long-term recordings of the membrane potential (E_m) recorded in vascular smooth muscle cells of small gastric arteries, showing substantial hyperpolarization in response to CGRP (3×10^{-9} M) after a first application and washout of (A) methanandamide (METH, 10^{-5} M) or (B) CGRP (3×10^{-9} M). Notice the reproducibility of the response to CGRP.*

5.3.2.2. Influence of blocking the $TRPV_1$ receptor

In a next series of experiments, we investigated the influence of capsazepine, a selective antagonist of the $TRPV_1$ receptors, on hyperpolarizations induced by methanandamide and CGRP. Incubation with capsazepine (3 µM) slightly depolarized the resting membrane potential of the vascular smooth muscle cells (1.3 ± 1.3 mV). In the presence of the antagonist, the response to methanandamide was completely abolished (0.0 ± 0.0 mV; n=4; $p<0.01$). A representative tracing is shown in figure 4A, while the mean values are given in figure 5A. The hyperpolarization induced by acetylcholine in these preparations was completely unaffected (-7.0 ± 2.7 mV; n=4) (figure 4A, 5A). In contrast to the methanandamide-induced response, the hyperpolarization induced by exogenous CGRP was totally unaffected by preincubation with capsazepine (-6.9 ± 1.1 mV vs –6.8 ± 1.2 mV in control conditions; n=4; $p>0.05$; or vs –7.3 ± 0.8 mV in all control experiments; n=14; $p>0.05$) (figure 4A, 5A).

5.3.2.3. Effect of glibenclamide

In a separate series of experiments, the role of ATP-sensitive potassium (K_{ATP}) channels in the membrane electrical response to CGRP, methanandamide and acetylcholine was investigated using the selective inhibitor glibenclamide (10 µM). In the presence of glibenclamide, the hyperpolarizing responses to CGRP and to methanandamide were completely abolished (figure 4B). In fact, the mean membrane potential change obtained from 4 experiments in which CGRP was tested (figure 5B) was a slight depolarization of the resting potential (2.1 ± 1.2 mV, $p<0.05$).

Similar findings were obtained with methanandamide. In the presence of glibenclamide, the cannabinoid significantly ($p<0.01$) depolarized the smooth muscle cells (1.1 ± 0.4 mV, n=4, figure 5B). Conversely, hyperpolarizations in response to acetylcholine were not affected (figure 4B).

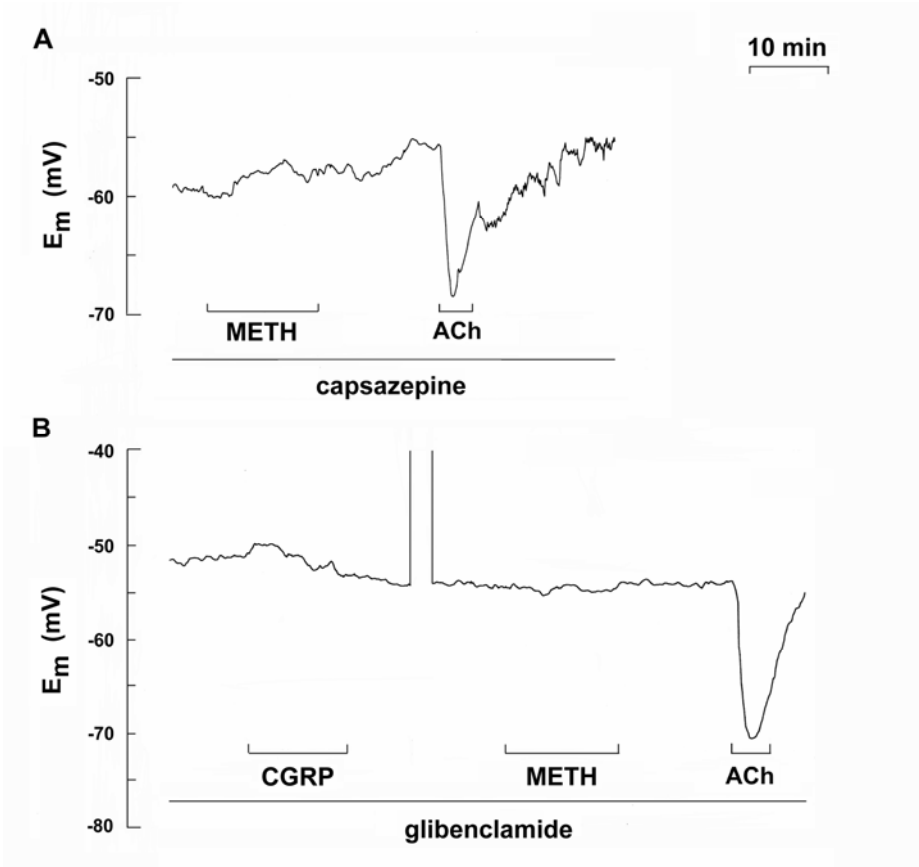

Figure 4: *(A) Tracing of rat gastric artery smooth muscle cell membrane potential (E_m) responses to application of methanandamide (METH, 10^{-5} M), acetylcholine (ACh, 3×10^{-6} M) and exogenous CGRP (3×10^{-9} M) after pre-exposure to capsazepine (3×10^{-6} M), a selective vanilloid receptor antagonist. The latter trace was obtained from a different preparation. (B) Influence of CGRP (3×10^{-9} M), methanandamide (METH, 10^{-5} M) and acetylcholine (ACh, 3×10^{-6} M) on the membrane potential in the presence of glibenclamide, a K_{ATP} channel inhibitor.*

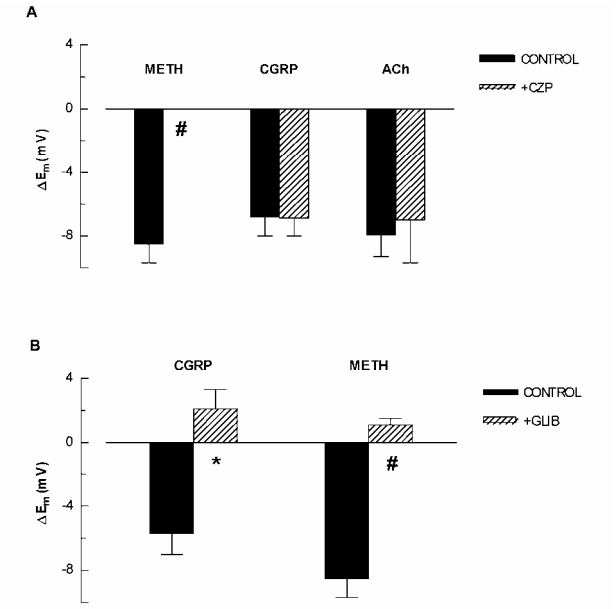

Figure 5: *(A) Influence of capsazepine (CZP, 3×10^{-6} M) on the membrane potential response of gastric artery smooth muscle cells to methanandamide (METH, 10^{-5} M), CGRP (3×10^{-9} M) and acetylcholine (ACh, 3×10^{-6} M). (B) Influence of glibenclamide (GLIB, 10^{-5} M) on the membrane potential response of gastric artery smooth muscle cells to CGRP (3×10^{-9} M) and methanandamide (10^{-5} M). Data are means ± SEM and represent the change in membrane potential from the resting level (ΔE_m) before and after application of the inhibitors. *, p<0.05; #, p<0.01.*

Essentially similar results were obtained in small mesenteric arteries. Thus the application of anandamide or methanandamide produced slowly developing hyperpolarizations averaging 9.6 ± 1.3 mV (n=7) and 3.9 ± 0.6 mV (n=7), respectively (figure 6). The acetylcholine-induced hyperpolarizations in these subsets of experiments averaged –11.4 ± 2.0 mV (n=3) and –9.6 ± 1.3 mV (n=7), respectively. While the responses to the cannabinoids desensitized, exogenous CGRP caused fully reproducible hyperpolarizations displaying a similar time course (-7.0 ± 0.3 mV and –6.5 ± 0.7 mV after a washout period of at least 20 min, n=3, p>0.05) (figure 7A).

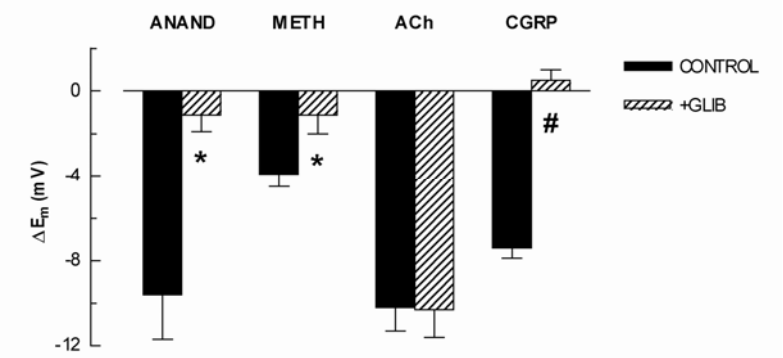

Figure 6: *Comparison of the influence of glibenclamide on the hyperpolarization induced by anandamide (ANAND, 10^{-5} M), methanandamide (METH, 10^{-5} M), acetylcholine (ACh, 3×10^{-6} M) and CGRP (3×10^{-9} M) in small mesenteric arteries. The columns represent the hyperpolarization before and after preincubation with glibenclamide (10^{-5} M). Values are means ± SEM. *, p<0.05; #, p<0.01.*

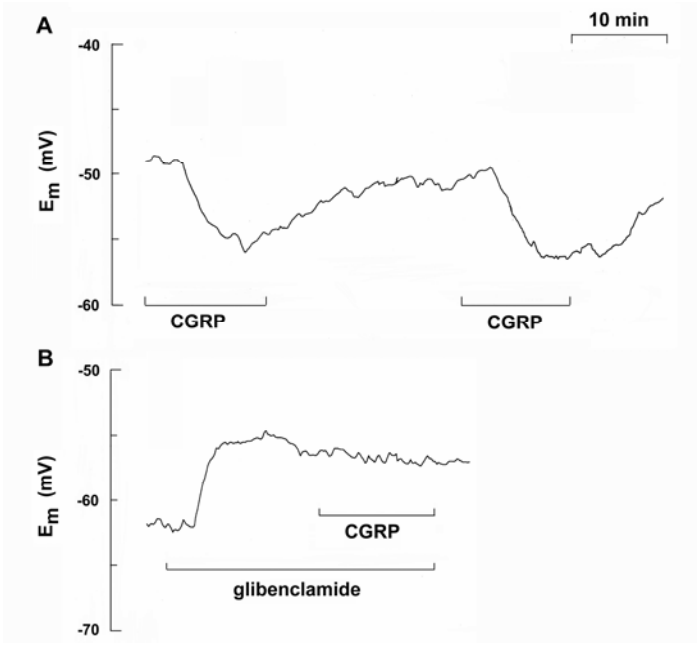

Figure 7: *Typical tracings of the membrane potential (E_m) of rat small mesenteric arteries smooth muscle cells showing (A) the responses to two successive applications of CGRP (3×10^{-9} M), and (B) the effect of preincubation with glibenclamide (10^{-5} M), an inhibitor of K_{ATP} channels, on the response to CGRP (3×10^{-9} M).*

After pre-exposure to the K_{ATP} channel inhibitor glibenclamide the membrane potential responses to anandamide and methanandamide were significantly inhibited (-1.1 ± 0.8 mV, n=5, $p<0.05$ and -1.1 ± 0.9 mV, n=6, $p<0.05$, respectively) while there was no effect on the hyperpolarizations to acetylcholine in these preparations (respectively -13.0 ± 1.0 mV, n=4, $p>0.05$ and -8.0 ± 1.6 mV, n=5, $p>0.05$ in these subsets of experiments). Moreover, the hyperpolarizations to CGRP were completely abolished by glibenclamide (+0.5 ± 0.5 mV vs 7.4 ± 0.5 mV in control conditions, n=4, $p<0.01$) (figure 6, figure 7B).

5.4. DISCUSSION

In the present study, we explored the influence of cannabinoids on the membrane potential of small gastric artery smooth muscle cells, compared it with that observed in mesenteric arteries, and investigated their mechanism of action. The main new findings are that (1) in gastric arteries, methanandamide hyperpolarizes the smooth muscle cells; (2) this effect is mediated by stimulation of vanilloid $TRPV_1$ receptors since completely inhibited by capsazepine; (3) CGRP causes a comparable, but reproducible hyperpolarization in both rat small gastric and mesenteric arteries; (4) both the responses to CGRP and to methanandamide are completely abolished by glibenclamide, in gastric as well as in mesenteric arteries.

In this study, we found methanandamide to induce concentration-dependent relaxation of small gastric arteries of the rat, consistent with the known potent vasodilatory effect described for cannabinoids in a variety of other vascular preparations [16,23-26]. Since in rat small mesenteric and guinea-pig carotid arteries, anandamide and methanandamide have been

shown to hyperpolarize the membrane potential of the smooth muscle cells [19,27], a change absent in some vessels which fail to show tension responses to these cannabinoids [27], it was reasonable to assume that at least part of the observed vasorelaxation is due to the associated membrane potential change. Besides confirming the potent hyperpolarizing action of anandamide and methanandamide in small mesenteric arteries [19], the present study reports a similar electrical response in small gastric arteries. To the best of our knowledge, gastric artery smooth muscle cell membrane potential changes to cannabinoids have not been reported before either.

The mechanism by which cannabinoids induce vasodilation is as yet unclear. While some studies propose a direct activation of CB_1 receptors on the vascular smooth muscle [24,25,28-32], several others report an indirect action, either by activation of endothelial receptors stimulating the release of vasorelaxing substances such as NO or EDHF [25,27,33], or by activation of $TRPV_1$ receptors on perivascular sensory nerves, causing the release of vasodilatory neuropeptides such as CGRP [16,31,32,34]. Moreover, recent evidence suggests that the vasodilation to cannabinoids is mediated by stimulation of a novel non CB_1/CB_2 receptor [35-38]. Earlier membrane potential measurements in rat mesenteric arteries showed that the hyperpolarization was abolished by capsaicin pre-treatment and blocked by capsazepine [19], supporting the involvement of $TRPV_1$ receptors on perivascular nerves in the electrical response to anandamide [19]. In the present membrane potential measurements in gastric arteries, we similarly found that the methanandamide-induced hyperpolarization was completely inhibited by capsazepine. Unless the used agonists/antagonists have unknown or aspecific actions, this shows the central role of the perivascular nerve $TRPV_1$ receptor in promoting the cannabinoid-induced hyperpolarization in these vessels.

Exogenous application of CGRP similarly produced a substantial hyperpolarization of the membrane potential, both in small gastric and mesenteric arteries. The time-course of this response was comparable to that of the cannabinoids, both in onset and recovery. In contrast to the cannabinoid response, the hyperpolarization induced by exogenous CGRP was completely unaffected by preincubation with capsazepine.

Whereas exogenous CGRP caused fully reproducible hyperpolarizations, a second application of cannabinoids failed to affect the membrane potential. Consistent with the expected desensitizing influence of cannabinoids on peptidergic primary afferent nerves in isolated vessel preparations [39], our findings suggest that the irreversibility of methanandamide-induced hyperpolarization in the present in vitro experiments might be due to depletion of CGRP and/or desensitization of $TRPV_1$ receptors of the perivascular nerves, and further confirm the role of these nerves in the hyperpolarization to cannabinoids.

Glibenclamide fully abolished or even reversed the CGRP-induced membrane potential change in gastric and in mesenteric arteries, suggesting that activation of K_{ATP} channels is responsible for the hyperpolarization induced by the peptide. This is consistent with literature reports on the action of CGRP. In rabbit mesenteric arteries, glibenclamide similarly blocked the CGRP-induced membrane potential change [40]. In rats, an increase in gastric mucosal blood flow was reported after administration of exogenous CGRP, sensitive to glibenclamide [41]. In the present study, also the hyperpolarizations to methanandamide were found to be abolished in the presence of glibenclamide in small mesenteric as well as in gastric arteries, extending earlier observations with anandamide in mesenteric arteries [27]. Therefore, the similar mechanism of hyperpolarization induced

by cannabinoids and by CGRP at the level of the smooth muscle cells further corroborates the view that the former stimulate $TRPV_1$ receptors on perivascular nerves, thereby releasing CGRP which activates the smooth muscle K_{ATP} channels.

Several vasodilators such as acetylcholine relax arteries by releasing vasoactive substances from the endothelium, such as NO, prostacyclin and an as yet unidentified EDHF. In some arteries, also CGRP induces endothelium-dependent relaxation [15,42]. To exclude the involvement of NO and prostanoids, the present experiments were all performed in the combined presence of L-NA and indomethacin. The hyperpolarization caused by acetylcholine, therefore, might be totally attributed to EDHF. This hyperpolarization, however, which had a completely different time course than that observed with the cannabinoids or with exogenous CGRP, was found to be resistant to glibenclamide, both in mesenteric and gastric arteries. These findings exclude a role for EDHF in the membrane electrical response to CGRP or cannabinoids in these vessels. For the mesenteric artery, this is consistent with earlier reports showing that the hyperpolarization or the relaxation induced by cannabinoids [19], by CGRP [43,44] or by activating the primary afferent nerves [14,43] is entirely endothelium-independent. The present findings suggest a similar direct action of CGRP on the vascular smooth muscle cells in gastric arteries. Moreover, they show that in gastric arteries the endocannabinoid anandamide is not an EDHF, as was reported for other vessels [19,30,45].

5.5. CONCLUSION

In summary, we have shown that methanandamide hyperpolarizes the membrane potential of the vascular smooth muscle cells of rat isolated small gastric and mesenteric arteries. This hyperpolarization is due to activation of K_{ATP} channels of the vascular smooth muscle cells and the response is mimicked by exogenous CGRP. The similarity of the membrane potential changes induced by exogenous CGRP, their similar sensitivity to glibenclamide, the desensitizing action of the cannabinoids and their full inhibition by capsazepine all point to stimulation of $TRPV_1$ receptors on perivascular CGRP containing nerves as primary cause for the cannabinoid-induced hyperpolarization of the arteries. Since membrane hyperpolarization is a powerful mediator of vasorelaxation, this local action of the cannabinoids might prove to be a novel mechanism providing gastroprotection.

5.6. ACKNOWLEDGEMENTS

We are grateful to Julien Dupont, Dirk De Gruytere, Marc Gillis and Cyriel Mabilde for unfailing technical assistance.

5.7. REFERENCES

1. Pertwee RG. Cannabinoids and the gastrointestinal tract. *Gut*. 2001;48:859-867.
2. Izzo AA, Mascolo N, Capasso F. The gastrointestinal pharmacology of cannabinoids. *Curr Opin Pharmacol*. 2001;1:597-603.

3. Krowicki ZK, Moerschbaecher JM, Winsauer PJ, Digavalli SV, Hornby PJ. Delta9-tetrahydrocannabinol inhibits gastric motility in the rat through cannabinoid CB_1 receptors. *Eur J Pharmacol*. 1999;371:187-196.

4. Lehmann A, Blackshaw LA, Branden L, Carlsson A, Jensen J, Nygren E, Smid SD. Cannabinoid receptor agonism inhibits transient lower esophageal sphincter relaxations and reflux in dogs. *Gastroenterology*. 2002;123:1129-1134.

5. Germano MP, D'Angelo V, Mondello MR, Pergolizzi S, Capasso F, Capasso R, Izzo AA, Mascolo N, De Pasquale R. Cannabinoid CB_1-mediated inhibition of stress-induced gastric ulcers in rats. *Naunyn Schmiedebergs Arch Pharmacol*. 2001;363:241-244.

6. Coruzzi G, Adami M, Coppelli G, Frati P, Soldani G. Inhibitory effect of the cannabinoid receptor agonist WIN 55,212-2 on pentagastrin-induced gastric acid secretion in the anaesthetized rat. *Naunyn Schmiedebergs Arch Pharmacol*. 1999;360:715-718.

7. Kawano S, Tsuji S. Role of mucosal blood flow: A conceptional review in gastric mucosal injury and protection. *J Gastroenterol Hepatol*. 2000;15:D1-D6.

8. Holzer P. Neural emergency system in the stomach. *Gastroenterology*. 1998;114:823-839.

9. Holzer P, Pabst MA. Visceral afferent neurons: role in gastric mucosal protection. *News Physiol Sci*. 1999;14:201-206.

10. Tani N, Miyazawa M, Miwa T, Shibata M, Yamaura T. Immunohistochemical localization of calcitonin gene-related peptide in the human gastric mucosa. *Digestion*. 1999;60:338-343.

11. Mizuguchi S, Ohno T, Hattori Y, Kamata K, Arai K, Saeki T, Saigenji K, Hayashi I, Kuribayashi Y, Majima M. Calcitonin gene-related peptide released by capsaicin suppresses myoelectrical activity of gastric smooth muscle. *J Gastroenterol Hepatol*. 2005;20:611-618.

12. Holzer P, Lippe IT. Stimulation of afferent nerve endings by intragastric capsaicin protects against ethanol-induced damage of gastric mucosa. *Neuroscience*. 1988;27:981-987.

13. Kinoshita Y, Inui T, Chiba T. Calcitonin gene-related peptide: a neurotransmitter involved in capsaicin-sensitive afferent nerve-

mediated gastric mucosal protection. *J Clin Gastroenterol*. 1993;17 Suppl 1:S27-S32.

14. Li YJ, Duckles SP. Effect of endothelium on the actions of sympathetic and sensory nerves in the perfused rat mesentery. *Eur J Pharmacol*. 1992;210:23-30.

15. Gray DW, Marshall I. Human alpha calcitonin gene-related peptide stimulates adenylate cyclase and guanylate cyclase and relaxes rat thoracic aorta by releasing nitric oxide. *Br J Pharmacol*. 1992;107:691-696.

16. Zygmunt PM, Petersson J, Andersson DA, Chuang HH, Sorgard M, Di Marzo V, Julius D, Hogestatt ED. Vanilloid receptors on sensory nerves mediate the vasodilator action of anandamide. *Nature*. 1999;400:452-457.

17. Ralevic V. Cannabinoid modulation of peripheral autonomic and sensory neurotransmission. *Eur J Pharmacol*. 2003;472:1-21.

18. Ahluwalia J, Urban L, Bevan S, Nagy I. Anandamide regulates neuropeptide release from capsaicin-sensitive primary sensory neurons by activating both the cannabinoid 1 receptor and the vanilloid receptor 1 in vitro. *Eur J Neurosci*. 2003;17:2611-2618.

19. Vanheel B, Van de Voorde J. Regional differences in anandamide- and methanandamide-induced membrane potential changes in rat mesenteric arteries. *J Pharmacol Exp Ther*. 2001;296:322-328.

20. Mulvany MJ, Halpern W. Contractile properties of small arterial resistance vessels in spontaneously hypertensive and normotensive rats. *Circ Res*. 1977;41:19-26.

21. Vanheel B, Van de Voorde J. Evidence against the involvement of cytochrome P450 metabolites in endothelium-dependent hyperpolarization of the rat main mesenteric artery. *J Physiol*. 1997;501 (Pt 2):331-341.

22. Breyne J, Vanheel BJ. Role of Ba^{2+}-resistant K^+ channels in endothelium-dependent hyperpolarization of rat small mesenteric arteries. *Can J Physiol Pharmacol*. 2004;82:65-71.

23. Ellis EF, Moore SF, Willoughby KA. Anandamide and delta 9-THC dilation of cerebral arterioles is blocked by indomethacin. *Am J Physiol*. 1995;269:H1859-H1864.

24. Randall MD, Alexander SPH, Bennett T, Boyd EA, Fry JR, Gardiner SM, Kemp PA, McCulloch AI, Kendall DA. An endogenous cannabinoid as an endothelium-derived vasorelaxant. *Biochem Biophys Res Commun*. 1996;229:114-120.

25. Deutsch DG, Goligorsky MS, Schmid PC, Krebsbach RJ, Schmid HHO, Das SK, Dey SK, Arreaza G, Thorup C, Stefano G, Moore LC. Production and physiological actions of anandamide in the vasculature of the rat kidney. *J Clin Invest*. 1997;100:1538-1546.

26. Pratt PF, Hillard CJ, Edgemond WS, Campbell WB. N-arachidonylethanolamide relaxation of bovine coronary artery is not mediated by CB_1 cannabinoid receptor. *Am J Physiol*. 1998;43:H375-H381.

27. Chataigneau T, Feletou M, Thollon C, Villeneuve N, Vilaine JP, Duhault J, Vanhoutte PM. Cannabinoid CB_1 receptor and endothelium-dependent hyperpolarization in guinea-pig carotid, rat mesenteric and porcine coronary arteries. *Br J Pharmacol*. 1998;123:968-974.

28. White R, Hiley CR. A comparison of EDHF-mediated and anandamide-induced relaxations in the rat isolated mesenteric artery. *Br J Pharmacol*. 1997;122:1573-1584.

29. Fulton D, Quilley J. Evidence against anandamide as the hyperpolarizing factor mediating the nitric oxide-independent coronary vasodilator effect of bradykinin in the rat. *J Pharmacol Exp Ther*. 1998;286:1146-1151.

30. Chaytor AT, Martin PE, Evans WH, Randall MD, Griffith TM. The endothelial component of cannabinoid-induced relaxation in rabbit mesenteric artery depends on gap junctional communication. *J Physiol*. 1999;520 Pt 2:539-550.

31. Ross RA, Gibson TM, Brockie HC, Leslie M, Pashmi G, Craib SJ, Di Marzo V, Pertwee RG. Structure-activity relationship for the endogenous cannabinoid, anandamide, and certain of its analogues at vanilloid receptors in transfected cells and vas deferens. *Br J Pharmacol*. 2001;132:631-640.

32. Ellington HC, Cotter MA, Cameron NE, Ross RA. The effect of cannabinoids on capsaicin-evoked calcitonin gene-related peptide (CGRP) release from the isolated paw skin of diabetic and non-diabetic rats. *Neuropharmacology*. 2002;42:966-975.

33. Mombouli JV, Schaeffer G, Holzmann S, Kostner GM, Graier WF. Anandamide-induced mobilization of cytosolic Ca^{2+} in endothelial cells. *Br J Pharmacol*. 1999;126:1593-1600.

34. Roberts LA, Christie MJ, Connor M. Anandamide is a partial agonist at native vanilloid receptors in acutely isolated mouse trigeminal sensory neurons. *Br J Pharmacol*. 2002;137:421-428.

35. Jarai Z, Wagner JA, Varga K, Lake KD, Compton DR, Martin BR, Zimmer AM, Bonner TI, Buckley NE, Mezey E, Razdan RK, Zimmer A, Kunos G. Cannabinoid-induced mesenteric vasodilation through an endothelial site distinct from CB_1 or CB_2 receptors. *Proc Natl Acad Sci USA*. 1999;96:14136-14141.

36. O'Sullivan SE, Kendall DA, Randall MD. Heterogeneity in the mechanisms of vasorelaxation to anandamide in resistance and conduit rat mesenteric arteries. *Br J Pharmacol*. 2004;142:435-442.

37. Ford WR, Honan SA, White R, Hiley CR. Evidence of a novel site mediating anandamide-induced negative inotropic and coronary vasodilatator responses in rat isolated hearts. *Br J Pharmacol*. 2002;135:1191-1198.

38. Wagner JA, Varga K, Jarai Z, Kunos G. Mesenteric vasodilation mediated by endothelial anandamide receptors. *Hypertension*. 1999;33:429-434.

39. Holzer P. Capsaicin - Cellular targets, mechanisms of action, and selectivity for thin sensory neurons. *Pharmacol Rev*. 1991;43:143-201.

40. Nelson MT, Huang Y, Brayden JE, Hescheler J, Standen NB. Arterial dilations in response to calcitonin gene-related peptide involve activation of K^+ channels. *Nature*. 1990;344:770-773.

41. Doi K, Nagao T, Kawakubo K, Ibayashi S, Aoyagi C, Yano YJ, Yamamoto C, Kanamoto K, Iida M, Sadoshima S, Fujishima M. Calcitonin gene-related peptide affords gastric mucosal protection by activating potassium channel in Wistar rat. *Gastroenterology*. 1998;114:71-76.

42. Brain SD, Williams TJ, Tippins JR, Morris HR, MacIntyre I. Calcitonin gene-related peptide is a potent vasodilator. *Nature*. 1985;313:54-56.

43. Kawasaki H, Takasaki K, Saito A, Goto K. Calcitonin gene-related peptide acts as a novel vasodilator neurotransmitter in mesenteric resistance vessels of the rat. *Nature*. 1988;335:164-167.

44. Dunn WR, Hardy TA, Brock JA. Electrophysiological effects of activating the peptidergic primary afferent innervation of rat mesenteric arteries. *Br J Pharmacol*. 2003;140:231-238.

45. Zygmunt PM, Hogestatt ED, Waldeck K, Edwards G, Kirkup AJ, Weston AH. Studies on the effects of anandamide in rat hepatic artery. *Br J Pharmacol*. 1997;122:1679-1686.

Chapter

6

Characterisation of the vasorelaxation to methanandamide in rat gastric arteries

Joke Breyne, Johan Van de Voorde & Bert Vanheel
Department of physiology & physiopathology

Can J Physiol Pharmacol 2006; In Press

Abstract

In the present study, the relaxant effect of the cannabinoid methanandamide was explored in rat gastric arteries. Since in some vessels cannabinoids have been shown to release CGRP from perivascular nerves, the influence of methanandamide was compared with that of exogenous CGRP. Methanandamide and CGRP elicited concentration-dependent, endothelium-independent relaxations. Methanandamide-induced relaxations were unaffected by the CB_1 receptor antagonist AM251, the CB_2 receptor antagonists AM630 and SR144528 and combined pre-exposure to AM251 and SR144528. Pre-exposure to O-1918, an antagonist of a novel non-CB_1/CB_2 cannabinoid receptor, did not influence the relaxations to methanandamide. Capsaicin or capsazepine treatment slightly inhibited methanandamide-induced relaxations. Preincubation with 30 mM extracellular K^+ or TEA had no significant effect on the responses elicited by methanandamide, but reduced CGRP-induced relaxations. Relaxation to 10^{-5} M methanandamide was significantly blunted by Bay-K8644 and by preincubation with nifedipine. Furthermore, 10^{-5} M methanandamide significantly inhibited $CaCl_2$-induced contractions in norepinephrine-stimulated vessels previously depleted of intra- and extracellular Ca^{2+}. Finally, preincubation with 10^{-5} M methanandamide almost completely abolished high K^+-induced contractions. These findings suggest that the vasorelaxant action of methanandamide in rat gastric arteries is not mediated by stimulation of known cannabinoid receptors, and only partly related to stimulation of $TRPV_1$ receptors on perivascular nerves. At high concentrations, methanandamide might induce relaxation by reducing Ca^{2+} entry into the smooth muscle cells.

***Keywords**: vasoactive agents, endothelial factors, vasorelaxation, cannabinoid receptors, vanilloid receptors*

6.1. INTRODUCTION

Plant derived cannabinoids have been used for centuries for their psychoactive properties. In the early 1990s, endogenous cannabinoids were described. The first of these endocannabinoids identified was N-arachidonoylethanolamide (anandamide) [1]. Since their discovery, the effects of both synthetic and endogenous cannabinoids have been extensively examined. In addition to their neurobehavioral effects, they have a profound influence on the cardiovascular system [2]. Moreover, they influence gastrointestinal function. Reported effects include inhibition of gastrointestinal motility and of gastric acid secretion [3]. In rats, cannabinoids were accordingly found to reduce stress-induced gastric ulceration [4].

Mucosal injury and peptic ulcers may also result from disturbances in gastric mucosal blood flow. The production and secretion of mucus, the secretion of bicarbonate ions which protect the mucosal barrier, and the removal of back-diffusing protons all depend on an appropriate mucosal microcirculation. The influence of cannabinoids on mucosal blood flow, however, has not been studied yet.

In a variety of isolated vascular preparations, potent vasodilatory effects of synthetic and endogenous cannabinoids have been shown [5-8]. Their mechanisms of action, however, are complex and seem to vary with species, vessel type and even size [9, 10]. To date, two distinct receptor subtypes for cannabinoids have been identified and cloned. CB_1 receptors are mainly localized on neurons but are also present in some peripheral tissues including heart, lung and gastrointestinal tissues and in vasculature [11]. In contrast, CB_2 receptors are primarily expressed in immune cells, although there is some evidence that these receptors are also expressed

by neuronal tissue [11]. Both receptor types are coupled through G-proteins to adenylyl cyclase and mitogen activated protein kinase. Cannabinoids reduce the cAMP concentration via pertussis toxin-sensitive G-proteins [12, 13].

In several arteries, the vasorelaxant effect of cannabinoids is mediated by stimulation of CB_1 receptors. Indeed, SR141716A, a CB_1 receptor antagonist, inhibits relaxations by anandamide in rat mesenteric arteries, coronary arteries and kidney arterioles [6, 7, 14] and in cat cerebral arteries [15]. However, recent evidence suggests that, at least in some vessels, the vasodilator response of cannabinoids is caused by stimulation of an as yet unidentified non-CB_1/CB_2 receptor [10, 16, 17]. On the other hand, the vasorelaxant influence of cannabinoids has also been reported to be due to stimulation of vanilloid $TRPV_1$ receptors on primary afferent perivascular nerves and the subsequent release of sensory neuropeptides such as the powerful vasodilator calcitonin gene related peptide (CGRP). In rat hepatic and small mesenteric arteries, the vasorelaxant influence of anandamide was antagonised by the $TRPV_1$ receptor antagonist capsazepine and the CGRP receptor antagonist CGRP(8-37), but not by the CB_1 receptor antagonist SR141716A [8]. The picture is further complicated by more recent studies that identified endocannabinoids as potential activators of the endothelial vanilloid $TRPV_4$ receptor [18].

Stimulation of the CB_1 receptor modulates the activity of several types of ion channels via G-proteins. For example, it has been shown that (endo)cannabinoids block voltage gated N-, L- and P/Q-type Ca^{2+}-channels [15, 19-21] and stimulate inwardly rectifying K^+-channels [20, 22]. Moreover, endocannabinoids can directly target and inhibit voltage gated Ca^{2+}-

channels [23-26], Na^+-channels [27] and various types of K^+-channels [28-31], although usually at higher concentrations.

In the present study, we analysed the influence of methanandamide on isolated small gastric arteries. This cannabinoid is a stable derivative of anandamide with slightly higher affinity for the CB_1 receptor (Anandamide: K_i=89 nM and 371 nM at CB_1 and CB_2 receptors respectively; methanandamide: K_i=20 nM and 815 nM at CB_1 and CB_2 receptors respectively [32-34]). Since CGRP containing sensory neurons were described in the gastric mucosa [35], we compared the response to methanandamide with that exerted by exogenous CGRP to assess a possible action of the cannabinoid via stimulation of perivascular nerves. Furthermore, by using selective agonists and antagonists, we investigated the involvement of CB_1, CB_2, non CB_1/CB_2 and $TRPV_1$ receptors in the observed vasorelaxation to methanandamide. This vasorelaxation, however, was found to be endothelium-independent and largely independent from an action at the classical cannabinoid, the non CB_1/CB_2 or the $TRPV_1$ receptor, but probably related to reduction of Ca^{2+} influx into vascular smooth muscle cells.

6.2. MATERIALS AND METHODS

6.2.1. Preparations

The investigation conforms to *the Guide for the Care and Use of Laboratory Animals* (1996, published by National Academy Press, 2101 Constitution Ave. NW, Washington, DC 20055, USA). The experiments were performed on isolated small gastric artery ring segments taken from female Wistar rats

(180 – 280 g). Experiments were approved by the ethical committee on animal research of Ghent University. After the rats were killed by cervical dislocation, the stomach was rapidly excised and placed in cold (4°C) normal Krebs-Ringer bicarbonate (KRB) solution, bubbled with a 95% O_2 – 5% CO_2 gas mixture. Second and third order branches of the gastric artery were dissected free and transferred to fresh oxygenated and chilled fluid, where they were cleaned from surrounding connective tissue and cut into segments of about 2 mm in length.

6.2.2. Tension measurements

The arterial segments were mounted into the organ bath of a small-vessel myograph, filled with 10 ml KRB solution. Two stainless steel wires (40 µm in diameter) were guided through the lumen of the segments. Each wire was fixed to a holder of the myograph: one holder was connected to a micrometer which was used to change the distance between the wires, the other holder was connected to a force-displacement transducer to measure the isometric tension changes. After mounting, the preparations were allowed to equilibrate for at least 30 min in warmed (37 °C), oxygenated (5% CO_2 in O_2; pH 7.4) KRB solution. The arteries were then normalised to obtain optimal conditions for active force development [36]. The optimal lumen diameter of the vessels was calculated on the basis of the passive wall tension-internal circumferences relationship [36]. At the start of each experiment the vessels were stretched to their optimal lumen diameter (316.3 $\pm$ 6.6 µm, n=151). Subsequently, all segments were repeatedly activated with a KRB solution containing 120 mM K^+ (K_{120}) and 10^{-5} M norepinephrine.

Thereafter, the gastric arteries were contracted by adding 10^{-5} M norepinephrine to the organ bath or by replacing the standard KRB solution in the organ bath by a KRB solution containing 120 mM K^+. When a stable contraction was obtained, concentration-response curves were made by cumulative addition of an agonist under control conditions or in the presence of an antagonist. The presence of functional endothelium was assessed by the ability of 10 µM acetylcholine to provoke more than 80 % relaxation. It was noted that after a first application of methanandamide (from 10^{-7} to 10^{-5} M), norepinephrine (10^{-5} M) was unable to induce a substantial contraction level in most preparations tested. Therefore, all vessels were exposed to methanandamide only once and the experiments were performed unpaired.

In some experiments, the influence of methanandamide on the influx of extracellular Ca^{2+} through plasma membrane Ca^{2+} channels was studied. For this purpose, intracellular Ca^{2+} stores were first depleted by washing the vessels with nominally Ca^{2+}-free KRB solution (same composition as normal KRB solution, but without added $CaCl_2$), exposing them subsequently to Ca^{2+}-free, EGTA (1 mM) containing solution, and repeatedly challenging the vessels to 10^{-5} M norepinephrine. After thoroughly washing the preparations with Ca^{2+}-free KRB solution, norepinephrine (10^{-5} M) was added and a concentration-contraction curve for $CaCl_2$ (10^{-5} to 10^{-2} M) was constructed in control conditions and after 30 min preincubation with 10^{-5} M methanandamide. Contractions were expressed as a percentage of the maximum contraction induced by $CaCl_2$ in control conditions (in the presence of norepinephrine).

In some experiments the endothelium was removed from the vessels. For this purpose, the arteries were first unstretched in the myograph. Then, an

L-shaped micropipette was placed at the proximal end of the segment and gas (95 % O_2 and 5 % CO_2) was bubbled through the lumen of the preparations for 2 min. Subsequently, the vessels were again stretched to their optimal lumen diameter. After an equilibration period of 30 min, the absence of functional endothelium was confirmed by the lack of relaxation to acetylcholine.

6.2.3. Drugs

All experiments were performed in a Krebs-Ringer bicarbonate solution of the following composition (in mM): NaCl 135, KCl 5, $NaHCO_3$ 20, $CaCl_2$ 2.5, $MgSO_4.7H_2O$ 1.3, KH_2PO_4 1.2, EDTA 0.026 and glucose 10. A KRB solution containing 30 mM or 120 mM K^+ (K_{30} or K_{120} respectively) was obtained by equimolar substitution of NaCl with KCl. Acetylcholine chloride, N^{ω}-nitro-L-arginine (L-NA), indomethacin, norepinephrine, glibenclamide, capsazepine, EGTA, (S)-(−)-1,4-dihydro-2,6-dimethyl-5-nitro-4-[2-(trifluoromethyl)phenyl]-3-pyridinecarboxylic acid methyl ester ((S)-(−)-Bay K8644), nifedipine and tetraethyl ammonium chloride (TEA) were purchased from Sigma-Aldrich (St. Louis, MO). Noladin ether, (R)-(+)-methanandamide, (-)-cannabidiol, levcromakalim, calcitonin gene-related peptide (CGRP Rat), JWH-015, AM251 and AM630 were obtained from Tocris (Bristol, UK). E-Capsaicin was purchased from Calbiochem (La Jolla, CA), AM1241 from Alexis Benelux (Zandhoven, Belgium) and O-1918 from Cayman Chemical (Ann Arbor, MI). SR144528 was a kind gift from Sanofi-Synthélabo Recherche (Montpellier, France).

For stock solutions, acetylcholine was dissolved in 50 mM potassium hydrogen phtalate buffer, pH 4.0. L-NA, CGRP, TEA and norepinephrine were dissolved in water; indomethacin, methanandamide, noladin ether,

cannabidiol, capsaicin, capsazepine and Bay K8644 in anhydrous ethanol; glibenclamide, levcromakalim, JWH-015, AM251, AM630, AM1241, SR144528 and nifedipine in dimethyl sulfoxide and O-1918 in methyl acetate. The final concentration of ethanol or dimethyl sulfoxide in the organ bath never exceeded 0.1%. All concentrations mentioned are expressed as final molar concentrations in the experimental chamber.

6.2.4. Statistics

Data were computed as means ± S.E.M. and evaluated statistically using Student's *t* test for paired or unpaired data or repeated measures ANOVA with Bonferroni's post hoc test, as appropriate. A P value < 0.05 indicates a significant difference. *n* represents the number of preparations tested, each obtained from a different rat. Relaxations are expressed as the percentage decrease in active tone.

6.3. RESULTS

6.3.1. Characterisation of vasorelaxing responses to methanandamide and CGRP

In endothelium-intact norepinephrine-precontracted small gastric arteries, methanandamide (from 10^{-7} M to 10^{-5} M) elicited concentration-dependent relaxations (figure 1A). Similarly, the addition of exogenous CGRP (from 10^{-10} M to 10^{-8} M) concentration-dependently relaxed precontracted arteries (figure 1B).

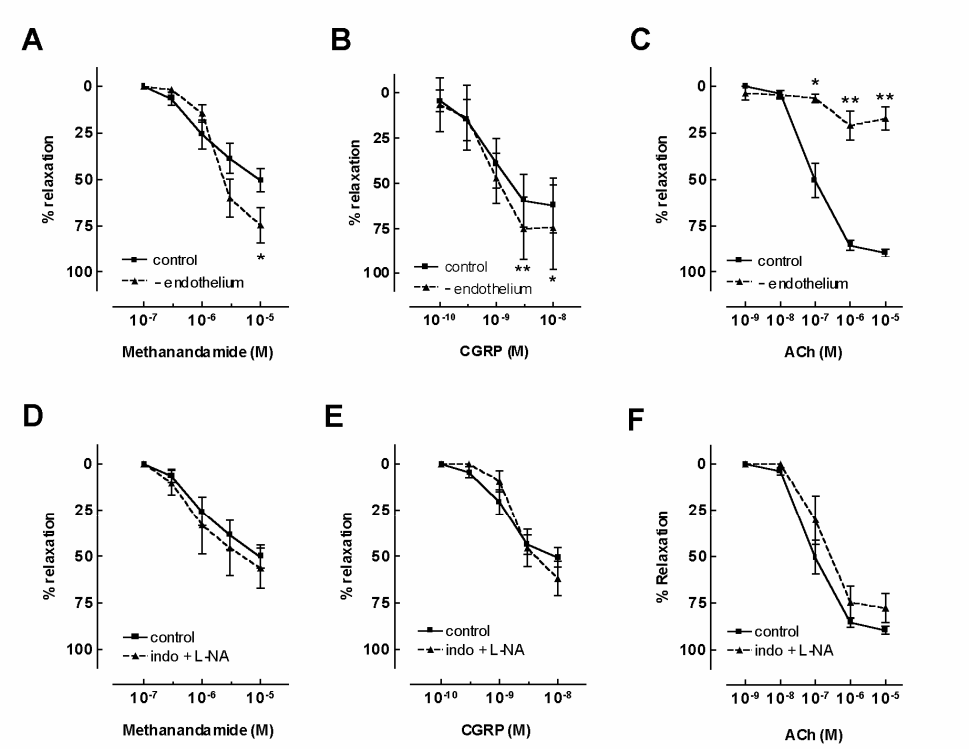

Figure 1: *Effects of endothelium removal on the vasorelaxant responses to (A) methanandamide (control: n=10, -endothelium: n=5), (B) exogenous CGRP (n=5) and (C) acetylcholine (n=5). Effect of the combined exposure to indomethacin and L-NA on the vasorelaxant responses to (D) methanandamide (control: n=10, indo + L-NA: n=5), (E) CGRP (n=7) and (F) acetylcholine (n=5). Data are expressed as the percentage decrease of the tone induced by 10 µM norepinephrine (* p<0.05, **p<0.01).*

Removal of the endothelium, which significantly inhibited the relaxations induced by acetylcholine (10^{-9} M to 10^{-5} M, figure 1C), did not affect the responses to methanandamide or CGRP. Both, the relaxations elicited by methanandamide and CGRP were even larger after removal of the endothelium (figure 1A and B). Similarly, relaxing responses to both methanandamide and CGRP were not affected by pre-exposure of the vessels to the combination of L-NA (10^{-4} M) and indomethacin (10^{-5} M) to block the formation of NO and prostanoids respectively (figure 1D and E).

Although these inhibitors tended to decrease the responses to acetylcholine, this effect was not statistically significant (figure 1F).

6.3.2. Role of cannabinoid receptors in the methanandamide-induced vasorelaxation

In contrast to methanandamide, the selective CB_1 receptor agonist noladin ether (10^{-7} M to 10^{-5} M) only weakly affected tone of precontracted gastric arteries, suggesting a minor importance of CB_1 receptors in these preparations (figure 2A). JWH-015 and AM1241, two selective agonists of the CB_2 receptor, caused concentration-dependent relaxations similar to those elicited by methanandamide (figure 2A). Preincubation with the CB_1 receptor antagonist AM251 (10^{-6} M for 10 min; K_i = 7.49 nM at CB_1) [37] did not significantly affect the relaxations elicited by methanandamide (figure 2B). Pre-exposure to the CB_2 receptor antagonists AM630 (10^{-5} M for 10 min; K_i = 31.2 nM at CB_2) [38] or SR144528 (10^{-5} M for 10 min; K_i = 0.3 nM) [39] did not inhibit the relaxation response to methanandamide (figure 2C and D). Correspondingly, relaxing responses to methanandamide were not affected by pre-exposure of the vessels to the combination of AM251 and SR144528 to block both types of cannabinoid receptors (figure 2E).

Preincubation with O-1918 (10^{-5} M), an antagonist of the novel non-CB_1/non-CB_2 cannabinoid receptor which does not bind to CB_1 or CB_2 receptors at concentrations up to 3×10^{-5} M [40], did not influence the relaxations induced by methanandamide (figure 2F). The influence of another reported antagonist of this receptor, cannabidiol, could not be tested on methanandamide-induced relaxations since the substance (3×10^{-7} M to 10^{-5} M) relaxed the gastric arteries by itself.

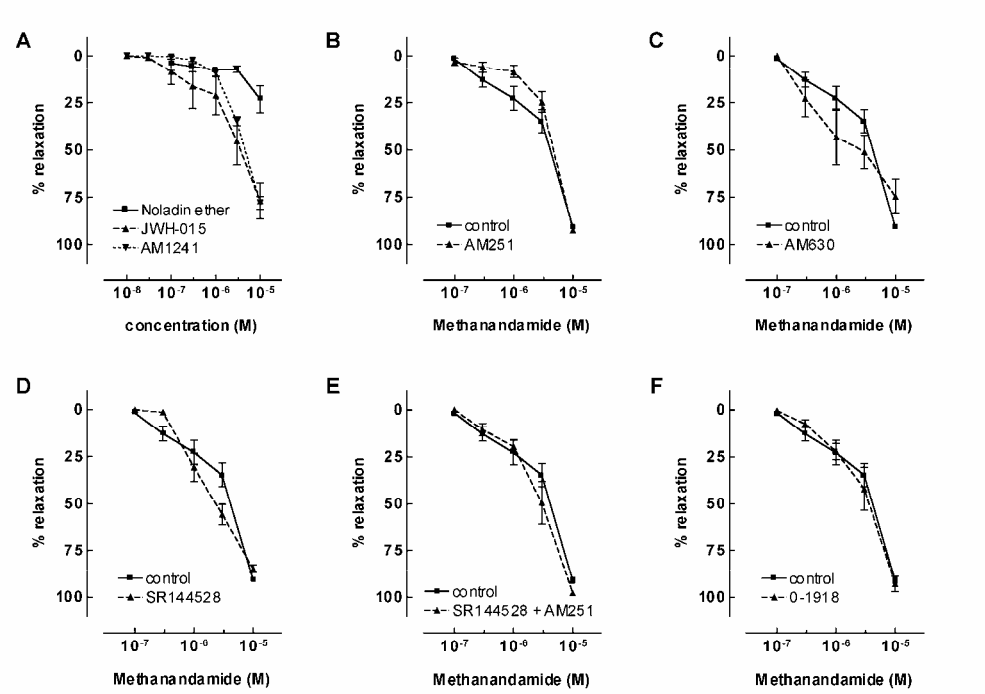

Figure 2: *Role of cannabinoid receptors in the methanandamide response in small gastric arteries. (A) Concentration response curves for the CB1 agonist noladin ether (n=4) and for the CB2 agonists JWH-015 (n=4) and AM1241 (n=7). (B-F) Concentration-response curves for methanandamide in control conditions (n=21) and after preincubation with (B) the CB1 receptor antagonist AM251 (n=7), (C) the CB2 antagonist AM630 (n=4), (D) the CB2 antagonist SR144528 (n=12), (E) combined CB1/CB2 antagonism by SR144528 + AM251 (n=4) or (F) the non CB1/CB2 cannabinoid receptor antagonist O-1918 (n=4).*

6.3.3. Role of vanilloid ($TRPV_1$) receptors in the methanandamide-induced vasorelaxation

Addition of capsaicin, which depletes perivascular nerves by stimulating the $TRPV_1$ receptor, caused small concentration-dependent relaxations of precontracted gastric arteries, confirming the presence of perivascular

nerves in these vessels (figure 3A). However, the responses were significantly less pronounced than those to methanandamide. Nevertheless, the small relaxations induced by the vanilloid receptor agonist were significantly inhibited by preincubation of the preparations with the $TRPV_1$ antagonist capsazepine (3×10^{-6} M for 10 min; figure 3A).

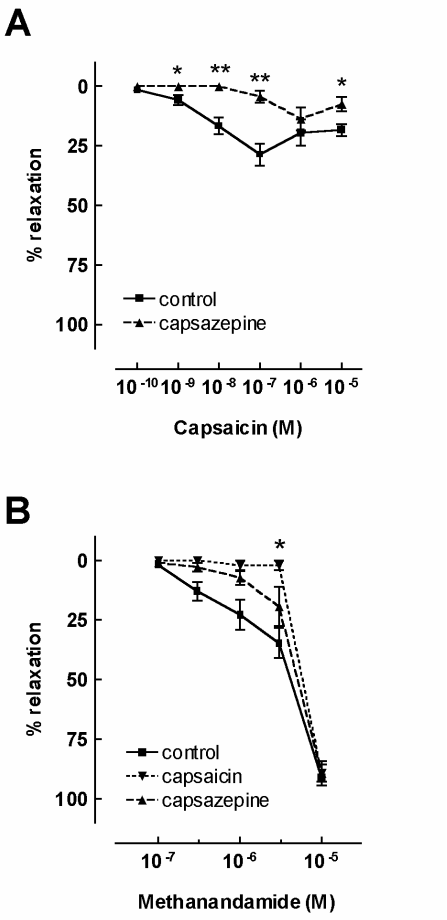

***Figure 3**: Role of $TRPV_1$ receptors in the methanandamide-induced vasorelaxation. (A) Concentration-response curves for capsaicin in control conditions (n=8) and after preincubation with capsazepine (3×10^{-6} M, n=4). (B) Concentration-response curves for the relaxation induced by methanandamide in control conditions (n=21), in the presence of capsazepine (3×10^{-6} M, n=6) and after 1h preincubation with capsaicin (10^{-5} M, n=4). (* p<0.05, **p<0.01, control versus capsaicin or capsazepine)*

As shown in figure 3B, relaxations to the smaller concentrations of methanandamide (3×10^{-7} M to 3×10^{-6} M) were slightly inhibited after depletion of the perivascular sensory nerves with capsaicin (10^{-5} M for 60 min). This effect was significant at a concentration of 3×10^{-6} M methanandamide. Relaxation to the highest dose of methanandamide, however, was not affected. Similarly, preincubation with the $TRPV_1$ receptor antagonist capsazepine (3×10^{-6} M for 10 min) tended to decrease the relaxations elicited by the lower concentrations of methanandamide while having no influence on the response to 10^{-5} M methanandamide.

6.3.4. Involvement of potassium channel activation

In a first subset of experiments, preparations were precontracted with a norepinephrine containing KRB solution supplemented with 30 mM K^+, which is known to abolish membrane hyperpolarization in response to various vasorelaxant substances. After contractions reached steady state, concentration-response curves for methanandamide and CGRP were constructed. Although a tendency was noted for the relaxations induced by the lower concentrations of methanandamide to decrease in these conditions, this did not reach statistical significance (figure 4A). On the other hand, the relaxations induced by CGRP were significantly reduced by 30 mM K^+ (figure 4D).

The involvement of K_{ATP}-channels in the relaxations induced by methanandamide and CGRP was tested by pre-treatment of the preparations with glibenclamide (10^{-5} M for 10 min), an inhibitor of K_{ATP}-channels. Pre-exposure to glibenclamide, which completely inhibited relaxations by the K_{ATP}-opener levcromakalim (data not shown), had no

influence on the relaxations induced by both methanandamide and exogenous CGRP (figure 4B and E).

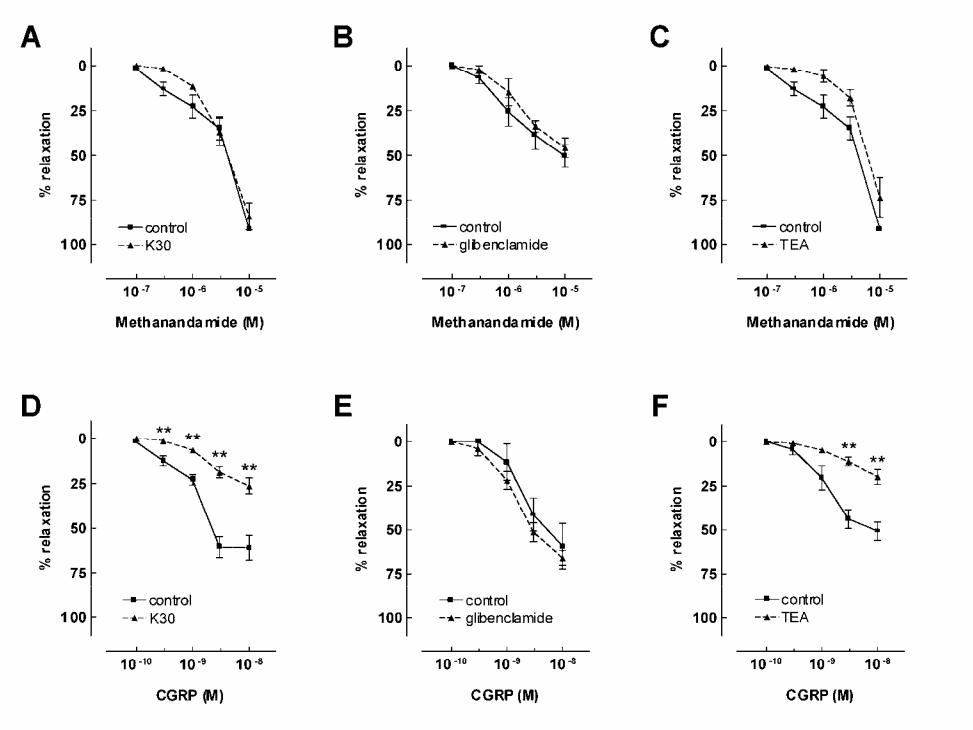

Figure 4: *Influence of an increased concentration of K^+-ions (K30) on the relaxations induced by (A) methanandamide (control: n=21; K30: n=7) and (D) CGRP (n=7). Effect of treatment with 10^{-5} M glibenclamide on relaxations elicited by (B) methanandamide (control: n=10; glibenclamide: n=5) and (E) exogenous CGRP (n=4). Influence of preincubation with 3×10^{-3} M TEA on the relaxing responses to (C) methanandamide (control: n=21; TEA: n=7) and (F) CGRP (n=5) in rat small gastric arteries (** p<0.01).*

The role of Ca^{2+} activated K^+-channels (K_{Ca}) in the responses to methanandamide and CGRP was tested by preincubation of the preparations with 3×10^{-3} M tetraethyl ammonium (TEA, 20 min). At this concentration, TEA is known to be selective for K_{Ca} channels [41]. The

relaxations induced by methanandamide were not significantly inhibited by TEA (figure 4C). The CGRP-induced responses, however, were significantly reduced (figure 4F).

6.3.5. K_{120}-induced contractions

Replacing the standard KRB by K_{120} solution resulted in a stable contraction of 8.2 ± 0.6 mN (n=20). Active tone in these conditions is increased mainly by Ca^{2+} influx through voltage-dependent Ca^{2+} channels, since the L-type Ca^{2+} channel blocker nifedipine (10^{-9} to 10^{-6} M) totally relaxed the K_{120}-preconstricted arteries, an effect counteracted by 10^{-6} M of the Ca^{2+} channel activator Bay K8644 (figure 5A). Methanandamide also caused concentration-dependent relaxation of the K_{120}-precontracted vessels (figure 5B). As shown in this figure, activation of the L-type Ca^{2+} channels with Bay K8644 was similarly able to significantly blunt the relaxant response to the higher concentrations of the cannabinoid (95.6 ± 0.5 % relaxation in the absence vs. 42.4 ± 6.0 % in the presence of Bay K8644, $p<0.005$).

Since a second norepinephrine (10^{-5} M) application was found to be unable to re-induce active tension in most arteries which had been exposed to increasing concentrations of methanandamide, we tested whether the cannabinoid also inhibited contractions elicited by 120 mM K^+. After preincubation of the vessel segments with methanandamide (10^{-5} M, 20 min), increasing K^+ to 120 mM caused an increase in active tension of 0.4 ± 0.3 mN, substantially smaller than the mean stable contraction of 5.4 ± 0.8 mN observed in these preparations before exposure to the cannabinoid (figure 5C).

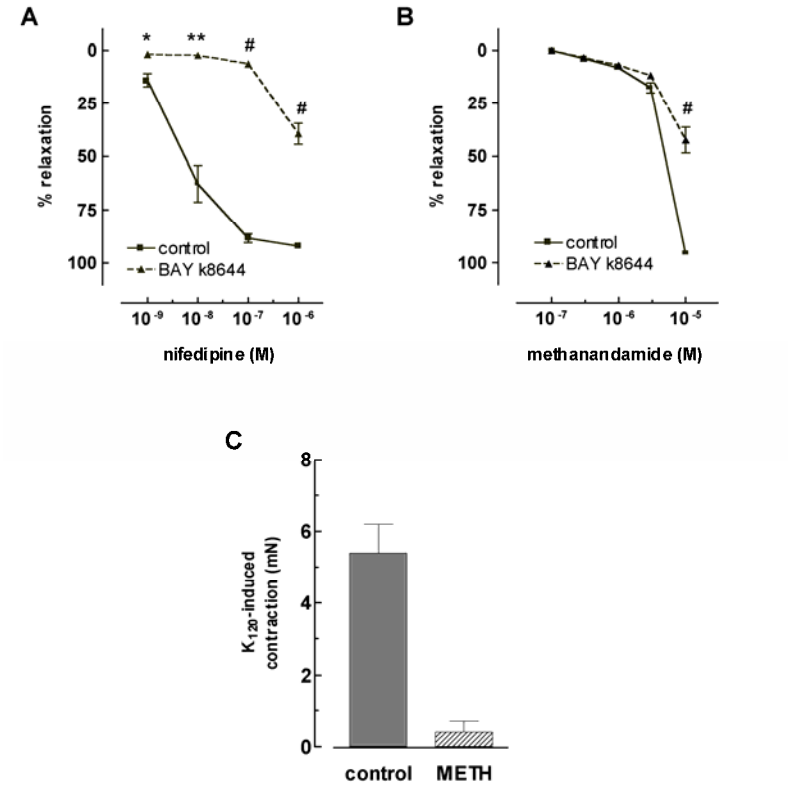

Figure 5: *Influence of treatment with 10^{-6} M (S)-(−)-Bay K8644 on the relaxations induced by (A) nifedipine (n=4) and (B) methanandamide (control: n=21; Bay K8644: n=4) in preparations contracted with K_{120}. Data are expressed as the percentage decrease of the tone induced by K_{120}. (C) Effect of preincubation with 10^{-5} M methanandamide on the K_{120}-induced contraction in small gastric arteries (n=4) (* p<0.05, ** p<0.01, # p<0.005).*

6.3.6. Influence of nifedipine-pretreatment on methanandamide-induced relaxations

Preparations were preincubated for 10 min with 10^{-6} M nifedipine. After stable contraction was reached with norepinephrine (10^{-5} M), a concentration-response curve for methanandamide was constructed. Although the relaxation induced by the lower concentrations of

methanandamide were not affected, preincubation with nifedipine significantly inhibited the responses to 10^{-5} M methanandamide (figure 6A).

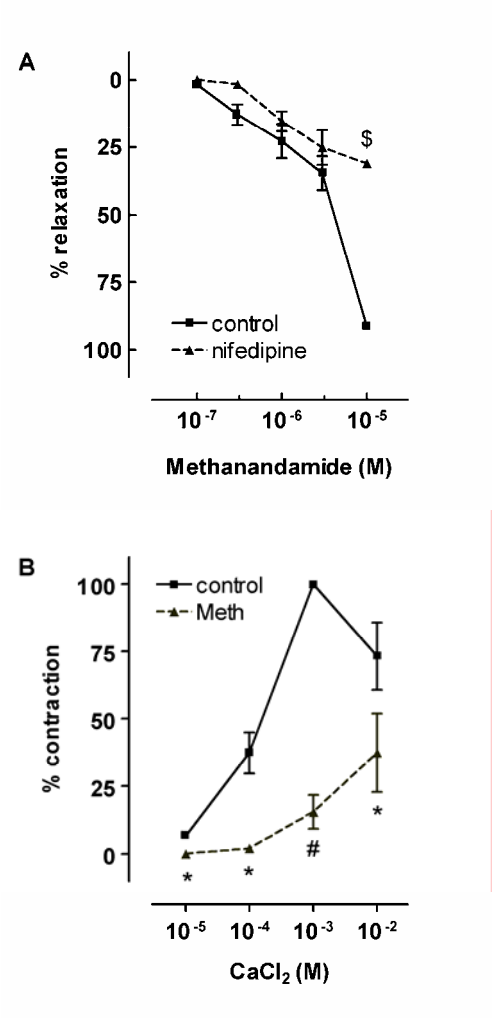

Figure 6: *(A) Influence of preincubation with 10^{-6} M nifedipine on the relaxations induced by methanandamide (n=4). (B) Influence of preincubation with 10^{-5} M methanandamide on $CaCl_2$-induced contractions in norepinephrine-stimulated vessels previously depleted of intracellular Ca^{2+} (n=4) (* p<0.05, # p<0.005; $ p<0.001).*

6.3.7. Effect of methanandamide on $CaCl_2$-contractions induced in the presence of norepinephrine

After depletion of the intracellular Ca^{2+} stores and removal of extracellular Ca^{2+}, preparations were exposed to norepinephrine (10^{-5} M) while kept in Ca^{2+}-free KRB solution. Under these conditions, readdition of $CaCl_2$ (10^{-5} to 10^{-2} M) induced concentration-dependent contractions which were maximal at 10^{-3} M. Preincubation with methanandamide (10^{-5} M), substantially inhibited contractions to $CaCl_2$ (figure 6B). Contraction to 10^{-3} M Ca^{2+} was reduced by more than 75 %.

6.4. DISCUSSION

In the present study we explored the influence and the mechanism of action of the stable endocannabinoid analogue methanandamide in gastric arteries. The main findings are that methanandamide produces concentration-dependent relaxations which are endothelium-independent and not mediated by stimulation of the known cannabinoid receptors. The responses to low concentrations of methanandamide are mediated in part by stimulation of $TRPV_1$ receptors, while relaxations to higher concentrations of the cannabinoid are independent of membrane hyperpolarization and might be due to interference with Ca^{2+} influx through voltage activated Ca^{2+} channels or a further step in the contractile activation process.

The site and precise mechanism of action of cannabinoids seem to differ among different vessels. In some vessels like the bovine coronary artery [42], the relaxant effect of anandamide is entirely dependent of the presence of a functional endothelium. Most studies, however, have shown that the

vasorelaxations caused by anandamide are completely [6] or partly [43] endothelium-independent. In the present study we found that methanandamide elicited concentration-dependent vasorelaxations of rat gastric arteries which were not inhibited by removal of the endothelium. This endothelium-independency rules out the possible role of endothelium-derived relaxing factors which have been reported to be involved in the cannabinoid induced relaxations in some isolated vascular preparations [5, 7].

The endothelium-independent pathway by which cannabinoids induce vasodilatation is still elusive. Some studies report that cannabinoids directly stimulate cannabinoid receptors on the vascular smooth muscle cells [6, 43, 44]. CB_1 receptor expression was shown in cultured human aortic smooth muscle cells [45], acutely isolated cat cerebral artery myocytes [15] and in the medial wall of rat cerebral arteries in situ [46]. In isolated cerebral artery smooth muscle cells, stimulation of the CB_1 receptor by anandamide causes relaxation by concentration-dependent inhibition of L-type Ca^{2+} channels via pertussis toxin-sensitive G-proteins. Maximal inhibition (32 %) was found with 3 x 10^{-7} M of the cannabinoid [15]. In the present study, the same concentration of methanandamide, which is slightly more selective for the CB_1 receptor, hardly produced relaxation of gastric arteries. Moreover, the potent and selective CB_1 receptor antagonist AM251 did not antagonise the relaxant effect of methanandamide, indicating that CB_1 receptors play little role. This is consistent with the relatively small relaxations observed with noladin ether, an endogenous and selective agonist of the CB_1 receptor. Moreover, two structurally unrelated selective CB_2 antagonists, AM630 and SR144528 did not antagonize the relaxations induced by methanandamide, ruling out the involvement of CB_2 receptors. The finding that even the combined presence of AM251 and SR144528 did not attenuate methanandamide induced vasorelaxation further corroborates the

conclusion that neither CB_1 nor CB_2 receptors are involved. More recent studies propose that in some vessels the vasodilator response to cannabinoids is mediated by stimulation of a novel, not yet identified, non-CB_1/CB_2 receptor located on the endothelium [10, 16, 17, 17, 47]. However, we found that methanandamide induced relaxations of gastric arteries were completely unaffected by O-1918, a selective antagonist of this novel receptor [10, 40]. Taken together with the finding that the effects of the cannabinoid are endothelium-independent, this strongly argues against the involvement of this endothelial non-CB_1/CB_2 receptor as well.

The cannabinoid anandamide has also been shown to activate $TRPV_1$ and $TRPV_4$ receptors. The $TRPV_4$ receptor is highly expressed on vascular endothelial cells, and its stimulation enhances Ca^{2+} influx, an essential trigger to release various vasoactive factors including NO, prostaglandins and the EDHF mechanism [48]. Moreover, $TRPV_4$ recently was also found in the myocytes of cerebral arteries, and its activation was shown to cause smooth muscle cell hyperpolarization via BK_{Ca} channel activation [49]. In the present study in which methanandamide was found to induce endothelium-independent relaxation, also the activation of a putative smooth muscle cell $TRPV_4$ receptor can be ruled out, however, since the non-hydrolysable analogue methanandamide was used, whereas anandamide is known to stimulate $TRPV_4$ indirectly, after conversion to its metabolite 5',6'-epoxyeicosatrienoic acid [18].

$TRPV_1$ receptors are activated by noxious stimuli including molecules with a vanilloid moiety such as capsaicin, but also by heat and protons. In the stomach, these $TRPV_1$ receptors have been shown to be localized on perivascular, primary afferent nerves. Stimulation of this receptor triggers the local release of neuropeptides from these nerve endings, the most

important of which is the powerful vasodilator CGRP [50]. The gastroprotective role of CGRP released from sensory nerves has been shown in various studies, and results from the vasodilatation and the emanating rise in mucosal blood flow [51-53]. CGRP might act directly on the vascular smooth muscle cells and/or indirectly, by stimulating the endothelial cells to release their relaxing factors [54, 55]. In the present study, application of exogenous CGRP evoked fully reproducible, concentration-dependent relaxations of gastric arteries which were totally endothelium-independent. Furthermore, preincubation with L-NA and indomethacin had no effect on the responses to CGRP, again eliminating the release of the endothelium-derived relaxing factors NO and prostacyclin and pointing to a direct relaxing influence of the peptide on the vascular smooth muscle cells. In addition, the functional presence of perivascular $TRPV_1$ containing nerves in the isolated small gastric arteries used in our study was demonstrated by the fact that exposure to capsaicin decreased norepinephrine-induced tone, an effect abolished by treatment with the $TRPV_1$ antagonist capsazepine.

Since the original observation that vasorelaxation by cannabinoids can be mediated by stimulation of $TRPV_1$ receptors on CGRP containing perivascular nerves [8], several studies have documented $TRPV_1$ stimulation by anandamide or by methanandamide, and stressed that anandamide should be considered both an endocannabinoid and an endovanilloid [56, 57]. In the present study, we found that the potency of capsaicin as a vasorelaxant was much lower than that observed for methanandamide or exogenous CGRP, suggesting a rather minor importance of the sensory nerves in our isolated preparations. Possibly, this might be related to the pre-exposures to 120 mM K^+ before the start of the experiments (see methods). Nevertheless, the vasorelaxation produced by low

concentrations of methanandamide in the present conditions was completely inhibited after depletion of the perivascular nerves by pre-exposure to capsaicin. Moreover, relaxations tended to decrease in the presence of the $TRPV_1$ antagonist capsazepine. These findings suggest, therefore, that at least the lower concentrations of methanandamide act on capsaicin sensitive $TRPV_1$ receptors on perivascular nerves in gastric arteries and stimulate the release of the vasorelaxing CGRP. The main route by which vasorelaxation is produced, however, involves another mechanism, probably located at the level of the smooth muscle. This is further corroborated by the different sensitivity to potassium channel blockers of the relaxations produced by methanandamide and by exogenous CGRP. The vasorelaxation produced by exogenous CGRP was sensitive to 30 mM extracellular K^+ and to 3×10^{-3} M TEA, but not affected by the K_{ATP} channel inhibitor glibenclamide which indicates that smooth muscle membrane hyperpolarization at least contributes to the vasodilatation induced by CGRP. Conversely, relaxations to high concentrations of methanandamide were completely unaffected by 30 mM K^+ and by the K^+ channel blockers TEA or glibenclamide, pointing to a mechanism not requiring smooth muscle cell hyperpolarization. It should be remarked, however, that for these interventions that affected the CGRP response (30 mM K^+, TEA), again a tendency was noted to diminish the vasorelaxing effect of the lower concentrations of methanandamide, although this failed to reach statistical significance.

In a recent study in gastric arteries, we found that both methanandamide and exogenous CGRP caused a hyperpolarization of the membrane potential of the smooth muscle cells [58]. Since these membrane potential changes were completely abrogated by glibenclamide, an activator of K_{ATP} channels seems to be mediating the response to both substances. The

apparent discrepancy that in the present tension measurements vasorelaxation to CGRP is sensitive to TEA and not to glibenclamide whereas in the membrane potential study hyperpolarization to CGRP was sensitive to the K_{ATP} channel blocker, suggests that the neuropeptide-activated pathway (involving cAMP and PKA, see [59]) might eventually result in the recruitment of a different K^+ channel depending on the contractile tone of the artery. Thus, while in resting gastric arteries K_{ATP} channels are opened, in norepinephrine-stimulated vessels, the higher intracellular free Ca^{2+} concentration might facilitate the opening of K_{Ca} channels by PKA dependent phosphorylation. Perhaps, this might explain some of the controversy in literature concerning the type of K^+ channel activated by CGRP [60-63]. The membrane potential-independent, direct relaxing influence of high concentrations of methanandamide might overwhelm a similar mechanism occurring at the lower concentrations.

Besides activating cannabinoid and vanilloid receptors, some cannabinoids such as anandamide and methanandamide have been shown to directly bind to other membrane proteins such as delayed rectifier K^+ channels [29, 31] and voltage activated Ca^{2+} channels [23-26], especially at higher concentrations. IC_{50} values reported for anandamide binding to different sites of the L-type Ca^{2+} channel protein, e.g., are 4, 8 and 15 μM [23, 64]. Recently, also methanandamide has been shown to inhibit dihydropyridine binding to the voltage gated Ca^{2+} channel, with an IC_{50} value of 7×10^{-6} M [65]. In mesenteric arteries of the rat, anandamide at 10^{-5} M, but not at 10^{-6} M, inhibited contractions to readdition of Ca^{2+}, directly indicating an interference with Ca^{2+} influx through voltage gated channels [26]. In the present study, the L-type Ca^{2+}-channel blocker nifedipine produced pronounced concentration-dependent relaxations of K_{120}-precontracted arteries. This was expected, since tension development in depolarizing high

K^+ solution is mediated almost entirely through opening of voltage gated Ca^{2+} channels [66]. Bay K8644 significantly inhibited these relaxations, proving its effectiveness as Ca^{2+}-channel activator. Bay K8644 also dramatically blunted the relaxations to the high concentration (10^{-5} M) of methanandamide, directly showing that activation of the Ca^{2+} channels is able to counteract at least part of the cannabinoid induced vasorelaxation. Furthermore, preincubation of the preparations with the selective L-type Ca^{2+} channel blocker nifedipine, significantly inhibited the relaxation induced by the highest concentration of methanandamide, while the responses to the lower concentrations of the cannabinoid were unaffected. This strongly argues for interference by 10^{-5} M methanandamide at the dihydropyridine binding site of the Ca^{2+} channel [65]. The fact that norepinephrine and K_{120} were unable to induce contraction in arteries pre-exposed to methanandamide, even suggests that the cannabinoid hardly dissociates from this binding site.

Further evidence for the involvement of voltage activated Ca^{2+} channels in the response to methanandamide was obtained in the experiments in which we examined the effects of methanandamide on contractions induced by cumulative readdition Ca^{2+} to norepinephrine stimulated arteries previously depleted of intracellular Ca^{2+}. In these conditions, contractions obtained with $CaCl_2$ are mainly due to Ca^{2+} influx through voltage activated Ca^{2+} channels on the vascular smooth muscle cells. Methanandamide substantially inhibited the $CaCl_2$-induced contractions, suggesting a direct action on the voltage activated Ca^{2+} channels. Taken together with the aforementioned literature reports on inhibition of L-type Ca^{2+} channels by cannabinoids, these findings strongly suggest that high concentrations of methanandamide might relax the gastric arteries by inhibition of Ca^{2+} influx in the smooth muscle cells, although interference with a further intracellular

step in the contractile activation process may not be excluded. The experiments in which methanandamide almost abolished K_{120}-induced contractions of these arteries further support this view.

We previously described the existence of endothelium-dependent hyperpolarization in rat gastric arteries [67]. The noted lack of influence of L-NA and indomethacin on the vasorelaxation elicited by acetylcholine in the present study, points to a major role of the endothelium-dependent hyperpolarization in the endothelium-dependent relaxation response to acetylcholine. As mentioned, the relaxation induced by CGRP is at least partly mediated by hyperpolarization, whereas eventual hyperpolarization induced by the highest concentration of methanandamide does not seem to be necessary to cause the relaxation by the cannabinoid. This is fully consistent with the data supporting inhibition of L-type Ca^{2+} channels by the cannabinoid, since this is a downstream mechanism and Ca^{2+} channels, once inhibited, do not respond anymore to changes in membrane potential.

In conclusion, the present study has demonstrated that methanandamide is a potent vasodilator in isolated rat small gastric arteries. The cannabinoid-induced vasorelaxation is endothelium-independent, does not involve the activation of the classical CB_1 or CB_2 receptor or the non CB_1/CB_2 receptor, and is largely independent of membrane hyperpolarization. Activation of $TRPV_1$ receptors on perivascular nerves might contribute to the relaxations induced by the lower concentrations of the cannabinoid. Higher concentrations (> 10^{-6} M) might interfere with Ca^{2+} influx into the smooth muscle cells.

6.5. ACKNOWLEDGEMENTS

We are grateful to Julien Dupont, Eric Tack, Dirk De Gruytere, Marc Gillis and Cyriel Mabilde for unfailing technical assistance.

6.6. REFERENCES

1. Devane WA, Hanus L, Breuer A, Pertwee RG, Stevenson LA, Griffin G, Gibson D, Mandelbaum A, Etinger A, Mechoulam R. Isolation and structure of a brain constituent that binds to the cannabinoid receptor. *Science.* 1992;258(5090):1946-9.

2. Hillard CJ. Endocannabinoids and vascular function. *J Pharmacol Exp Ther.* 2000;294(1):27-32.

3. Pertwee RG. Cannabinoids and the gastrointestinal tract. *Gut.* 2001;48(6):859-67.

4. Germano MP, D'Angelo V, Mondello MR, Pergolizzi S, Capasso F, Capasso R, Izzo AA, Mascolo N, De Pasquale R. Cannabinoid CB_1-mediated inhibition of stress-induced gastric ulcers in rats. *Nauny-Schmiedebergs Arch Pharmacol.* 2001;363(2):241-4.

5. Ellis EF, Moore SF, Willoughby KA. Anandamide and delta 9-THC dilation of cerebral arterioles is blocked by indomethacin. *Am J Physiol.* 1995;269(6 Pt 2):H1859-H1864.

6. Randall MD, Alexander SPH, Bennett T, Boyd EA, Fry JR, Gardiner SM, Kemp PA, McCulloch AI, Kendall DA. An endogenous cannabinoid as an endothelium-derived vasorelaxant. *Biochem Biophys Res Commun.* 1996;229(1):114-20.

7. Deutsch DG, Goligorsky MS, Schmid PC, Krebsbach RJ, Schmid HHO, Das SK, Dey SK, Arreaza G, Thorup C, Stefano G, Moore LC. Production and physiological actions of anandamide in the vasculature of the rat kidney. *J Clin Invest.* 1997;100(6):1538-46.

8. Zygmunt PM, Petersson J, Andersson DA, Chuang HH, Sorgard M, Di Marzo V, Julius D, Hogestatt ED. Vanilloid receptors on sensory

nerves mediate the vasodilator action of anandamide. *Nature.* 1999;400(6743):452-7.

9. Vanheel B, Van de Voorde J. Regional differences in anandamide- and methanandamide-induced membrane potential changes in rat mesenteric arteries. *J Pharmacol Exp Ther.* 2001;296(2):322-8.

10. O'Sullivan SE, Kendall DA, Randall MD. Heterogeneity in the mechanisms of vasorelaxation to anandamide in resistance and conduit rat mesenteric arteries. *Br J Pharmacol.* 2004;142(3):435-42.

11. Howlett AC, Barth F, Bonner TI, Cabral G, Casellas P, Devane WA, Felder CC, Herkenham M, Mackie K, Martin BR, Mechoulam R, Pertwee RG. International Union of Pharmacology. XXVII. Classification of cannabinoid receptors. *Pharmacol Rev.* 2002;54(2):161-202.

12. Howlett AC. Pharmacology of cannabinoid receptors. *Annu Rev Pharmacol Toxicol.* 1995;35:607-34.

13. Childers SR, Fleming L, Konkoy C, Marckel D, Pacheco M, Sexton T, Ward S. Opioid and cannabinoid receptor inhibition of adenylyl cyclase in brain. *Ann N Y Acad Sci.* 1992;654:33-51.

14. White R, Ho WSV, Bottrill FE, Ford WR, Hiley CR. Mechanisms of anandamide-induced vasorelaxation in rat isolated coronary arteries. *Br J Pharmacol.* 2001;134(4):921-9.

15. Gebremedhin D, Lange AR, Campbell WB, Hillard CJ, Harder DR. Cannabinoid CB_1 receptor of cat cerebral arterial muscle functions to inhibit L-type Ca^{2+} channel current. *Am J Physiol.* 1999;276(6):H2085-H2093.

16. Jarai Z, Wagner JA, Varga K, Lake KD, Compton DR, Martin BR, Zimmer AM, Bonner TI, Buckley NE, Mezey E, Razdan RK, Zimmer A, Kunos G. Cannabinoid-induced mesenteric vasodilation through an endothelial site distinct from CB_1 or CB_2 receptors. *Proc Natl Acad Sci U S A.* 1999;96(24):14136-41.

17. Ford WR, Honan SA, White R, Hiley CR. Evidence of a novel site mediating anandamide-induced negative inotropic and coronary vasodilatator responses in rat isolated hearts. *Br J Pharmacol.* 2002;135(5):1191-8.

18. Watanabe H, Vriens J, Prenen J, Droogmans G, Voets T, Nilius B. Anandamide and arachidonic acid use epoxyeicosatrienoic acids to activate $TRPV_4$ channels. *Nature.* 2003;424(6947):434-8.

19. Mackie K, Hille B. Cannabinoids inhibit N-type calcium channels in neuroblastoma glioma cells. *Proc Natl Acad Sci U S A.* 1992;89(9):3825-9.

20. Mackie K, Lai Y, Westenbroek R, Mitchell R. Cannabinoids activate an inwardly rectifying potassium conductance and inhibit Q-type calcium currents in Att20 cells transfected with rat-brain cannabinoid receptor. *J Neurosci.* 1995;15(10):6552-61.

21. Twitchell W, Brown S, Mackie K. Cannabinoids inhibit N- and P/Q-type calcium channels in cultured rat hippocampal neurons. *J Neurophysiol.* 1997;78(1):43-50.

22. Henry DJ, Chavkin C. Activation of inwardly rectifying potassium channels (Girk1) by coexpressed rat brain cannabinoid receptors in Xenopus oocytes. *Neurosci Lett.* 1995;186(2-3):91-4.

23. Johnson DE, Heald SL, Dally RD, Janis RA. Isolation, identification and synthesis of an endogenous arachidonic amide that inhibits calcium channel antagonist 1,4-dihydropyridine binding. *Prostaglandins Leukot Essent Fatty Acids.* 1993;48(6):429-37.

24. Oz M, Tchugunova YB, Dunn SMJ. Endogenous cannabinoid anandamide directly inhibits voltage-dependent Ca^{2+} fluxes in rabbit T-tubule membranes. *Eur J Pharmacol.* 2000;404(1-2):13-20.

25. Chemin J, Monteil A, Perez-Reyes E, Nargeot J, Lory P. Direct inhibition of T-type calcium channels by the endogenous cannabinoid anandamide. *EMBO J.* 2001;20(24):7033-40.

26. Ho WSV, Hiley CR. Endothelium-independent relaxation to cannabinoids in rat-isolated mesenteric artery and role of Ca^{2+} influx. *Br J Pharmacol.* 2003;139(3):585-97.

27. Nicholson RA, Liao C, Zheng J, David LS, Coyne L, Errington AC, Singh G, Lees G. Sodium channel inhibition by anandamide and synthetic cannabimimetics in brain. *Brain Res.* 2003;978(1-2):194-204.

28. Poling JS, Rogawski MA, Salem N, Vicini S. Anandamide, an endogenous cannabinoid, inhibits Shaker-related voltage-gated K^+ channels. *Neuropharmacol.* 1996;35(7):983-91.

29. Van den Bossche I, Vanheel B. Influence of cannabinoids on the delayed rectifier in freshly dissociated smooth muscle cells of the rat aorta. *Br J Pharmacol.* 2000;131(1):85-93.

30. Maingret F, Patel AJ, Lazdunski M, Honore E. The endocannabinoid anandamide is a direct and selective blocker of the background K^+ channel TASK-1. *EMBO J.* 2001;20(1-2):47-54.

31. Oliver D, Lien CC, Soom M, Baukrowitz T, Jonas P, Fakler B. Functional conversion between A-type and delayed rectifier K^+ channels by membrane lipids. *Science.* 2004;304(5668):265-70.

32. Abadji V, Lin S, Taha G, Griffin G, Stevenson LA, Pertwee RG, Makriyannis A. (R)-methanandamide: a chiral novel anandamide possessing higher potency and metabolic stability. *J Med Chem.* 1994;37(12):1889-93.

33. Lang W, Qin C, Lin S, Khanolkar AD, Goutopoulos A, Fan P, Abouzid K, Meng Z, Biegel D, Makriyannis A. Substrate specificity and stereoselectivity of rat brain microsomal anandamide amidohydrolase. *J Med Chem.* 1999;42(5):896-902.

34. Goutopoulos A, Fan P, Khanolkar AD, Xie XQ, Lin S, Makriyannis A. Stereochemical selectivity of methanandamides for the CB_1 and CB_2 cannabinoid receptors and their metabolic stability. *Bioorg Med Chem.* 2001;9(7):1673-84.

35. Holzer P. Neural emergency system in the stomach. *Gastroenterol.* 1998;114(4):823-39.

36. Mulvany MJ, Halpern W. Mechanical properties of vascular smooth muscle cells in situ. *Nature.* 1976;260(5552):617-9.

37. Gatley SJ, Gifford AN, Volkow ND, Lan R, Makriyannis A. ^{123}I-labeled AM251: a radioiodinated ligand which binds in vivo to mouse brain cannabinoid CB_1 receptors. *Eur J Pharmacol.* 1996;307(3):331-8.

38. Hosohata Y, Quock RM, Hosohata K, Makriyannis A, Consroe P, Roeske WR, Yamamura HI. AM630 antagonism of cannabinoid-stimulated [^{35}S]GTP gamma S binding in the mouse brain. *Eur J Pharmacol.* 1997;321(1):R1-R3.

39. Rinaldi-Carmona M, Barth F, Millan J, Derocq JM, Casellas P, Congy C, Oustric D, Sarran M, Bouaboula M, Calandra B, Portier M, Shire D, Breliere JC, Le Fur GL. SR 144528, the first potent and

selective antagonist of the CB_2 cannabinoid receptor. *J Pharmacol Exp Ther.* 1998;284(2):644-50.

40. Offertaler L, Mo FM, Batkai S, Liu J, Begg M, Razdan RK, Martin BR, Bukoski RD, Kunos G. Selective ligands and cellular effectors of a G protein-coupled endothelial cannabinoid receptor. *Mol Pharmacol.* 2003 March;63(3):699-705.

41. Langton PD, Nelson MT, Huang Y, Standen NB. Block of calcium-activated potassium channels in mammalian arterial myocytes by tetraethylammonium ions. *Am J Physiol*.1991;260(3 Pt 2):H927-H934.

42. Pratt PF, Hillard CJ, Edgemond WS, Campbell WB. N-arachidonylethanolamide relaxation of bovine coronary artery is not mediated by CB_1 cannabinoid receptor. *Am J Physiol.* 1998;43(1):H375-H381.

43. Chaytor AT, Martin PE, Evans WH, Randall MD, Griffith TM. The endothelial component of cannabinoid-induced relaxation in rabbit mesenteric artery depends on gap junctional communication. *J Physiol.* 1999;520 Pt 2:539-50.

44. Randall MD, Kendall DA. Involvement of a cannabinoid in endothelium-derived hyperpolarizing factor-mediated coronary vasorelaxation. *Eur J Pharmacol.* 1997;335(2-3):205-9.

45. Sugiura T, Kodaka T, Nakane S, Kishimoto S, Kondo S, Waku K. Detection of an endogenous cannabimimetic molecule, 2-arachidonoylglycerol, and cannabinoid CB_1 receptor mRNA in human vascular cells: Is 2-arachidonoylglycerol a possible vasomodulator? *Biochem Biophys Res Commun.* 1998;243(3):838-43.

46. Ashton JC, Appleton I, Darlington CL, Smith PF. Immunohistochemical localization of cerebrovascular cannabinoid CB_1 receptor protein. *J Cardiovasc Pharmacol.* 2004;44(5):517-9.

47. Mukhopadhyay S, Chapnick BM, Howlett AC. Anandamide-induced vasorelaxation in rabbit aortic rings has two components: G protein-dependent and -independent. *Am J Physiol.* 2002;282(6):H2046-H2054.

48. Yao XQ, Garland CJ. Recent developments in vascular endothelial cell transient receptor potential channels. *Circ Res.* 2005;97(9):853-63.

49. Earley S, Heppner TJ, Nelson MT, Brayden JE. $TRPV_4$ forms a novel Ca^{2+} signaling complex with ryanodine receptors and BK_{Ca} channels. *Circ Res.* 2005;97(12):1270-9.

50. Holzer P, Pabst MA. Visceral afferent neurons: role in gastric mucosal protection. *News Physiol Sci.* 1999;14:201-6.

51. Mizuguchi S, Ohno T, Hattori Y, Kamata K, Arai K, Saeki T, Saigenji K, Hayashi I, Kuribayashi Y, Majima M. Calcitonin gene-related peptide released by capsaicin suppresses myoelectrical activity of gastric smooth muscle. *J Gastroenterol Hepatol.* 2005;20(4):611-8.

52. Holzer P, Lippe IT. Stimulation of afferent nerve endings by intragastric capsaicin protects against ethanol-induced damage of gastric mucosa. *Neurosci.* 1988;27(3):981-7.

53. Kinoshita Y, Inui T, Chiba T. Calcitonin gene-related peptide: a neurotransmitter involved in capsaicin-sensitive afferent nerve-mediated gastric mucosal protection. *J Clin Gastroenterol.* 1993;17 Suppl 1:S27-S32.

54. Li YJ, Duckles SP. Effect of endothelium on the actions of sympathetic and sensory nerves in the perfused rat mesentery. *Eur J Pharmacol.* 1992;210(1):23-30.

55. Gray DW, Marshall I. Human alpha calcitonin gene-related peptide stimulates adenylate cyclase and guanylate cyclase and relaxes rat thoracic aorta by releasing nitric oxide. *Br J Pharmacol.* 1992;107(3):691-6.

56. Ralevic V. Cannabinoid modulation of peripheral autonomic and sensory neurotransmission. *Eur J Pharmacol.* 2003;472(1-2):1-21.

57. Ahluwalia J, Urban L, Bevan S, Nagy I. Anandamide regulates neuropeptide release from capsaicin-sensitive primary sensory neurons by activating both the cannabinoid 1 receptor and the vanilloid receptor 1 in vitro. *Eur J Neurosci.* 2003;17(12):2611-8.

58. Breyne J, Vanheel B. Methanandamide hyperpolarizes gastric arteries by stimulation of $TRPV_1$ receptors on perivascular CGRP containing nerves. *J Cardiovasc Pharmacol.* 2006;47(2):303-9.

59. Brain SD, Grant AD. Vascular actions of calcitonin gene-related peptide and adrenomedullin. *Physiol Rev.* 2004;84(3):903-34.

60. Quayle JM, Bonev AD, Brayden JE, Nelson MT. Calcitonin gene-related peptide activated ATP-sensitive K^+ currents in rabbit arterial smooth muscle via protein kinase A. *J Physiol.* 1994;475(1):9-13.

61. Wellman GC, Quayle JM, Standen NB. ATP-sensitive K^+ channel activation by calcitonin gene-related peptide and protein kinase A in pig coronary arterial smooth muscle. *J Physiol.* 1998;507 (Pt 1):117-29.

62. Miyoshi H, Nakaya Y. Calcitonin gene-related peptide activates the K^+ channels of vascular smooth muscle cells via adenylate cyclase. *Basic Res Cardiol.* 1995;90(4):332-6.

63. Maggi CA, Giuliani S, Zagorodnyuk V. Calcitonin gene-related peptide (CGRP) in the circular muscle of guinea-pig colon: role as inhibitory transmitter and mechanisms of relaxation. *Regul Pept.* 1996;61(1):27-36.

64. Shimasue K, Urushidani T, Hagiwara M, Nagao T. Effects of anandamide and arachidonic acid on specific binding of (+)-PN200-110, diltiazem and (-)-desmethoxyverapamil to L-type Ca^{2+} channel. *Eur J Pharmacol.* 1996;296(3):347-50.

65. Oz M, Tchugunova Y, Dinc M. Differential effects of endogenous and synthetic cannabinoids on voltage-dependent calcium fluxes in rabbit T-tubule membranes: comparison with fatty acids. *Eur J Pharmacol.* 2004;502(1-2):47-58.

66. Karaki H, Ozaki H, Hori M, MitsuiSaito M, Amano KI, Harada KI, Miyamoto S, Nakazawa H, Won KJ, Sato K. Calcium movements, distribution, and functions in smooth muscle. *Pharmacol Rev.* 1997;49(2):157-230.

67. Vanheel B, Breyne J. Endothelium-dependent hyperpolarization in small gastric arteries. *Cardiovasc Res.* 2004;63(2):331-7.

Chapter

7

Influence of the membrane potential on Ca^{2+}-oscillations in smooth muscle cells of intact mesenteric arteries of the rat

Joke Breyne, Luc Leybaert & Bert Vanheel
Department of physiology & physiopathology

Submitted

Abstract

Many cellular functions are regulated by changes in the intracellular Ca^{2+} concentration ($[Ca^{2+}]_i$). Those Ca^{2+} signals are highly organized in both time and space. It is generally accepted that modulation of $[Ca^{2+}]_i$ is a critical determinant of vascular smooth muscle tone. Using confocal microscopy and fluorescent dyes, we examined the dynamic Ca^{2+} responses in smooth muscle cells of intact small mesenteric arteries of the rat. We observed the effect of stimulation with norepinephrine and evaluated the influence of membrane potential changes on the induced Ca^{2+} oscillations. It was found that stimulation with norepinephrine ($3x10^{-6}$ M) evoked asynchronous Ca^{2+} spikes which were usually accompanied by a raise in basal fluorescence. After prolonged exposure to norepinephrine, the preparations showed a slight but significant reduction in both spiking activity and basal fluorescence. Addition of depolarizing concentrations of K^+ (15 mM) to arteries stimulated with norepinephrine resulted in the synchronization of the Ca^{2+} oscillations and significantly increased both spiking frequency and basal fluorescence. In contrast, hyperpolarization of the membrane potential with levcromakalim ($3x10^{-7}$ M) significantly reduced the spiking frequency and the level of basal fluorescence. This decline was larger than the spontaneous decrease observed in the prolonged presence of norepinephrine alone. Similar results were found with the vasodilatory neuropeptide calcitonin gene-related peptide ($3x10^{-9}$ M). Small increases in the extracellular K^+ concentration (5 mM) also significantly decreased the Ca^{2+} responses, suggesting a hyperpolarization of the membrane potential. Addition of the cannabinoid methanandamide significantly augmented the mean spiking rate and showed a slight but significant decrease of the basal fluorescence. Taken together, these findings confirm that stimulation with norepinephrine induces asynchronous Ca^{2+} oscillations in the vascular smooth muscle cells of small mesenteric arteries. Our results further suggest that depolarization is essential to synchronize these responses, while hyperpolarizing the membrane potential tends to decrease the Ca^{2+} dynamics.

7.1. INTRODUCTION

Intracellular Ca^{2+} is an important second messenger mediating a variety of vascular endothelial and smooth muscle cell functions. The regulation of hemodynamics by variations in the vascular diameter results from the contraction and relaxation of the smooth muscle cells in the vascular wall. It is generally known that vasoactive agents constrict arteries by simultaneously increasing the mean cytosolic Ca^{2+} concentration ($[Ca^{2+}]_i$) in all smooth muscle cells of the vascular wall [1-4]. Smooth muscle contraction has been thought to rely on both Ca^{2+} influx in the cell and Ca^{2+} release from intracellular stores. Contraction is initiated by Ca^{2+}-calmodulin-induced activation of myosin light chain kinase, resulting in the formation of cross bridges between actin and myosin filaments of the contractile apparatus.

Recently, it has been shown that the overall vessel Ca^{2+} concentration is not representative for the Ca^{2+} dynamics in the individual vascular smooth muscle cells [5-9]. The smooth muscle cells respond to biological activators with oscillatory and propagating rises in $[Ca^{2+}]_i$ caused by Ca^{2+} release from the sarcoplasmatic reticulum. These Ca^{2+} oscillations and Ca^{2+} waves are highly organized in both time and space and their frequency depends on the agonist concentration. Another type of Ca^{2+} signalling are Ca^{2+} sparks caused by local Ca^{2+} release events through ryanodine-sensitive Ca^{2+} release channels in the sarcoplasmatic reticulum [10-12].

Much of the knowledge about Ca^{2+} signalling in vascular smooth muscle cells has been based on studies using enzymatically isolated or cultured cells. When stimulated, isolated and cultured smooth muscle cells show elevations of the intracellular free Ca^{2+} concentration ($[Ca^{2+}]_i$), which typically progress over the entire cell length, giving it the appearance of a

wave [13]. However isolated cells display different characteristics as compared to smooth muscle cells in situ, in which intact gap junctions provide intercellular communication. The possible mechanism for the generation of agonist-induced Ca^{2+} waves in a smooth muscle cell begins with an elevation of inositoltrisphosphate (IP_3) and a rise in $[Ca^{2+}]_i$. Binding of ligands with G-protein coupled receptors stimulates phospholipase C which catalyzes the hydrolysis of membrane phosphatidylinositol 4,5-bisphosphate into IP_3. IP_3 activates the IP_3 receptors on the sarcoplasmatic reticulum and sensitizes them to Ca^{2+}. When the $[Ca^{2+}]_i$ reaches a threshold concentration, the Ca^{2+} release channels open and Ca^{2+} is set free, resulting in a Ca^{2+} spike. The resulting increase in $[Ca^{2+}]_i$ in the cytoplasm promotes the opening of adjacent channels, which gives rise to a Ca^{2+} wave which propagates down the length of the cell.

Recent advances in digital imaging techniques on the subcellular level have made it possible to study vascular cells in intact vessels and explore the spatiotemporal characteristics of Ca^{2+} spikes and waves. It has been shown that in rat tail artery, individual smooth muscle cells show asynchronous Ca^{2+} oscillations after electrical and pharmacological stimulation [14]. The Ca^{2+} oscillations are not in phase among different individual cells and oscillatory features are lost when the Ca^{2+} response was averaged. It was shown that the two sources of Ca^{2+} may work in a collaborative manner. Upon stimulation with norepinephrine, Ca^{2+} stores were released intermittently to produce Ca^{2+} oscillations. The influx of Ca^{2+} is used mainly to assist replenishment of the Ca^{2+} stores. These results have later been confirmed in the same vessel type [15] and in intact pressurized mesenteric small arteries of the rat [16]. Sometimes, especially in experiments with higher levels of activation, the Ca^{2+} oscillations in different smooth muscle cells synchronize to yield overall oscillations in intracellular Ca^{2+} and,

hence, in vascular tone, called vasomotion [7, 17]. However, the exact mechanism responsible for the conversion of asynchronous into synchronous oscillations is as yet unclear. It has been postulated that, at least in rat mesenteric arteries, Ca^{2+} released from the sarcoplasmatic reticulum activates a depolarizing current, which spreads to all smooth muscle cells [8]. When this current reaches a sufficient magnitude, it causes simultaneous depolarization of all cells [18] with subsequent synchronous influx of Ca^{2+} through voltage dependent Ca^{2+} channels. This leads to a synchronized release of Ca^{2+} from the sarcoplasmatic reticulum and hence produces synchronous Ca^{2+} oscillations. It has been shown that vasomotion or synchronous Ca^{2+} oscillations do not appear when the membrane potential is clamped and is only present with high levels of cGMP. Also, a current pulse or another brief depolarization was sufficient to synchronise cells [8].

As far as we know, only little information exists about the influence of the membrane potential on Ca^{2+} signalling in the vascular smooth muscle cells. In the present experiments we investigated the influence on the noradrenaline induced Ca^{2+} responses of levcromakalim, calcitonin gene-related peptide (CGRP) and 5 mM KCl, which have all been shown to hyperpolarize the membrane potential in several vascular preparations. We furthermore studied the effect of methanandamide on the Ca^{2+} oscillations, since we have shown in earlier reports that this cannabinoid has also a hyperpolarizing action on rat small mesenteric artery smooth muscle cells [19, 20]. Finally, we tested the influence of a depolarizing concentration of K^+-ions on the Ca^{2+} dynamics in the vascular wall.

7.2. MATERIALS AND METHODS

7.2.1. Tissue Preparation

Small mesenteric arteries from female Wistar rats (180 – 280 g) were used. The experiments were approved by the ethical committee on animal research of Ghent University. The animals were anaesthetised by a lethal dose (200 mg kg^{-1}) of pentobarbitone and killed by cervical dislocation. Branches of the small mesenteric arteries were dissected from the abdominal cavity and rapidly placed in cold (4°C) normal Krebs-Ringer bicarbonate (KRB – composition defined further) solution bubbled with a 95% O_2 – 5% CO_2 gas mixture. The arteries were cleaned from surrounding connective tissue and cut into segments of about 5 mm in length.

Subsequently, the vessel segments were cannulated with a thin glass capillary (borosilicate glass, Hilgenberg, Malsfeld, Germany) with flame polished tip that was inserted into the lumen over the entire segment length (figure 1A). The diameter of the glass capillary was slightly (~15 %) larger than the vessel lumen diameter and cannulation was done to stabilize the preparation against possible smooth muscle contractions after challenging with norepinephrine. Imaging experiments showed that the endothelium was absent in most preparations. Figure 2 shows an image of an optical section of the arterial wall, as perceived when focussing more luminally. Autofluorescence of the internal elastic lamina was observed, and no endothelial cells were detected.

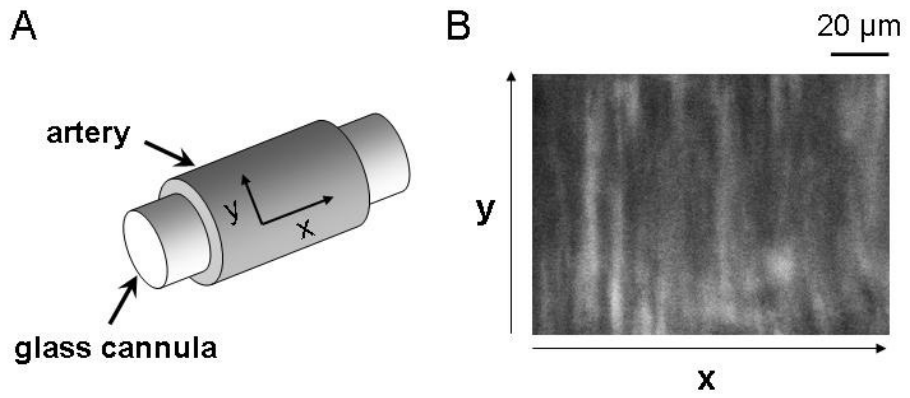

Figure 1: *Illustration of the method of recording Ca^{2+} dependent fluo-3 fluorescence in intact small mesenteric arteries of the rat. (A) Schematic diagram of an artery cannulated with a thin glass capillary. Cannulae were slightly larger than the vessel lumen diameter. The arrows labelled 'x' and 'y' indicate the plane of laser scanning. For ease of illustration, the scanning plane was drawn on the upperface of the artery. In the actual experiments, however, the bottom of the arteries was scanned. (B) Optical section of the arterial wall, as observed after fluo-3 loading, with the smooth muscle cells vertically oriented. The arrows correspond to those similarly labelled in panel A. Images were typically 123 x 93 µm.*

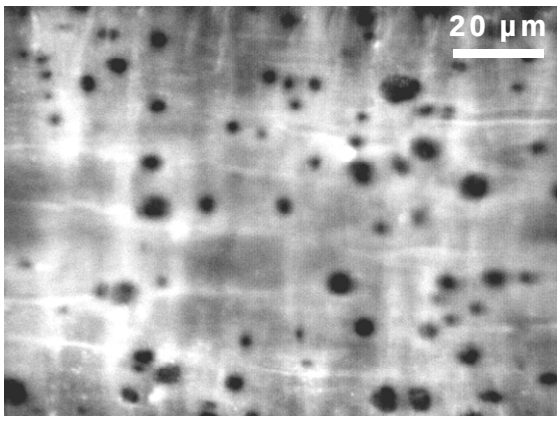

Figure 2: *Optical section of the arterial wall, showing the internal elastic lamina (IEL). The wholes in this IEL represent fenestrae, through which projections of the endothelial cells contact adjacent smooth muscle cells, allowing formation of myoendothelial gap junctions.*

7.2.2. Calcium imaging

Ca^{2+} was measured with the fluorescent Ca^{2+} probe fluo-3 in combination with laser scanning confocal microscopy. The cannulated arterial segments were loaded with the Ca^{2+} dye by incubation overnight at 4°C in a loading buffer (Hanks' balanced salt solution buffered with 25 mM HEPES (HBSS-HEPES)) containing 20 µM fluo-3-AM and 0.05 % pluronic. The morning of the experiments, the preparations were transferred to loading buffer (same fluo-3-AM concentration) now at 37°C and incubated for 90 min. The arteries were then washed in HEPES-buffered physiological salt solution (PSS, pH 7.4).

Ca^{2+} imaging was done with a custom developed real-time laser scanning microscope built around a Nikon Eclipse TE300 (Analis, Ghent, Belgium) [21] and a x40 oil immersion objective with high numeric aperture (CFI Plan Fluo, Nikon - 1.4 NA). A cannulated vessel segment was placed on a glass coverslip and immobilized by covering it with a fine nylon mesh attached to a ring. The coverslip with the vessel was placed on the stage of the inverted microscope and was continuously superfused in situ with PSS at a rate of 1 ml/min. Excitation was done with the 488 nm line of an argon-laser (type 543R-AP-A01, Melles Griot, Carlsbad, CA, U.S.A.), the dichroic mirror was a dual-wavelength type (490-550DBDR) and the emission light was bandpass filtered at 522 nm (25 nm bandwith - all filters from Omega Optical, Brattleboro, VT, U.S.A. - details can be found in [21]). Images of an optical section of the arterial wall (~ 123 µm x 93 µm and containing about 30-40 cells, figure 1B) were obtained at 2 frames s^{-1} and transferred directly to a PC equipped with an image acquisition and processing board (DT3155, Data translation, Marlboro, MA, USA). Off-line image analysis was done with software (Fluoframes) developed in Microsoft Visual C.

7.2.3. Experimental procedures and analysis

After recording 2 min (240 images) in control conditions, norepinephrine (3 x 10^{-6} M) was added to the superfusate and recording was continued for another 3 min (360 images). Thereafter, still in the presence of norepinephrine, the tissues were exposed to various pharmacological agents and the responses were monitored over another 8 min (960 images; for levcromakalim, CGRP, 5 mM KCl or methanandamide) or 3 min (360 images; for 15 mM KCl), as appropriate.

The first stage image analysis consisted of counting the number of cells showing clear Ca^{2+} responses under control conditions, in the presence of norepinephrine and in the presence of the various pharmacological substances. The responding cells were subdivided in those showing oscillatory spiking activity upon stimulation with norepinephrine and those reacting with an increase in fluorescence relative to the baseline level.

In a second stage of the analysis, the number of fluorescence peaks per cell (peaks with an amplitude of at least two times the amplitude of the noise were considered as true Ca^{2+} spikes), the spiking frequency (over the last 240 frames, expressed as spikes per minute) and the change in fluorescence relative to the baseline level was calculated (from the last 150 frames, baseline level was set to 100%). The experimental traces illustrated represent averaged fluorescence signals from the imaged vessel part in view or the fluorescence change in a single cell, as indicated in the text.

7.2.4. Solutions and drugs

The used KRB solution had the following composition (in mM): NaCl, 135; KCl, 5; $NaHCO_3$, 20; $CaCl_2$, 2.5; $MgSO_4.7H_2O$, 1.3; KH_2PO_4, 1.2; EDTA, 0.026; glucose, 10. The solution was gassed with 95% O_2 – 5% CO_2 (pH 7.4). HBSS-HEPES contained (in mM): NaCl, 137; KCl, 5.36; $Na_2HPO_4.2H_2O$, 0.18; $CaCl_2.2\ H_2O$, 0.95; $MgSO_4.7H_2O$, 0.81; KH_2PO_4, 0.44; HEPES, 25 mM; glucose, 5.55 (pH 7.4, adjusted with NaOH). PSS contained (in mM): NaCl, 130; KCl, 5; $NaH_2PO_4.\ H_2O$, 1; $CaCl_2$, 1; $MgSO_4.7H_2O$, 0.5; HEPES, 20 mM; glucose, 10 (pH 7.4, adjusted with NaOH).

Norepinephrine was purchased from Sigma-Aldrich (St. Louis, MO). Methanandamide, levcromakalim and CGRP were obtained from Tocris (Bristol, UK). Fluo-3 acetoxymethyl ester (fluo-3-AM) and pluronic were obtained from Molecular Probes (Eugene, Oregon, USA). Norepinephrine and calcitonin gene-related peptide (CGRP Rat) were dissolved in water; methanandamide in anhydrous ethanol and levcromakalim, fluo-3-AM and pluronic in anhydrous dimethyl sulfoxide. All concentrations mentioned are expressed as final molar concentrations in the experimental chamber.

7.2.5. Statistics

Results are expressed as means ± SEM. Statistical evaluation was performed using student's *t* test for paired or unpaired data, as appropriate. Values of $P<0.05$ were considered significantly different. The number of cells is indicated as *n*. When appropriate, the number of preparations was mentioned. For one single series of experiments, preparations of at least 3 different animals were used.

7.3. RESULTS

7.3.1. Influence of norepinephrine

In the 44 different vessel segments studied, on average 6.4 $\pm$ 0.7 cells per frame showed spontaneous and asynchronous Ca^{2+} spiking activity in the absence of norepinephrine. Addition of norepinephrine (3 x 10^{-6} M) significantly increased the number of spiking cells to 13.9 $\pm$ 0.9 per frame (n=44, P<0.05, figure 3). Spiking activity remained non-synchronized and was usually associated with an increase in fluo-3 fluorescence and thus $[Ca^{2+}]_i$. Typical examples of fluorescence traces in individual cells are shown in figure 4 (A-C). Figure 4 D illustrates the time course of fluorescence changes averaged over the whole frame in view. A mean fluorescence increase from 100 % in control to 107.1 ± 3.5 % in norepinephrine (P<0.05, n=44) was observed in these experiments. Because of the asynchronous nature of spiking activity, the spikes disappeared in the whole frame trace.

In a subset of these experiments we investigated the effect of prolonged (660 sec) exposure to norepinephrine. Figure 4 shows representative traces of such an experiment, and the results are summarized in figure 5 (CTRL). In these experiments, 67 cells showed oscillatory spiking activity in response to norepinephrine (figure 5A), while 58 cells showed an increase in fluorescence (figure 5B) (data from 3 different preparations). In the preparations with spiking activity, the mean number of spikes per minute was 3.4 ± 0.2 (n=67, figure 5C). The largest part (n=62) of the cells oscillating in response to addition of norepinephrine still showed spike activity after prolonged exposure. Thus, in 32 cells spiking activity was unchanged, in 12 cells it was increased, whereas it was decreased in 23 cells (figure 5A).

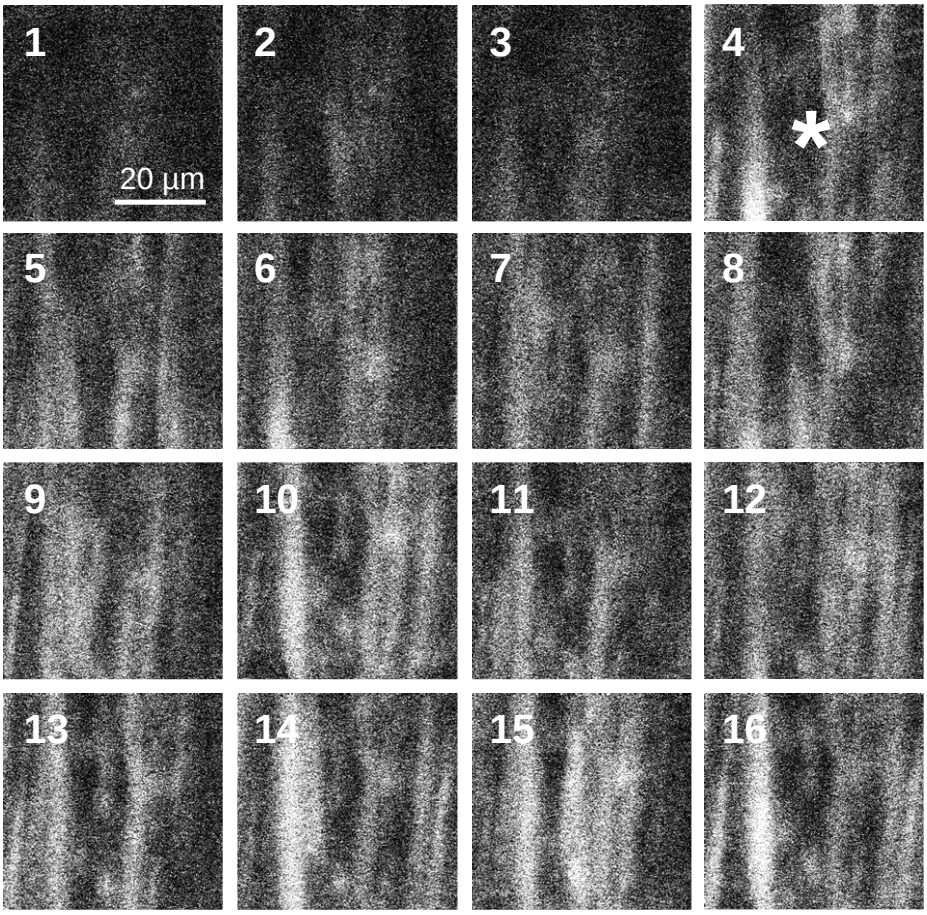

Figure 3: *Ca^{2+} responses in small mesenteric arteries of the rat in response to stimulation with 3 x 10^{-6} M norepinephrine. The images represent a detailed fragment of the original confocal images and show the fluorescence change over time in different smooth muscle cells upon stimulation with norepinephrine. The images are taken at 16 time points, with 5 seconds time difference (taken from a series of images recorded at 1 frame s^{-1}). '*' indicates the entrance of norepinephrine in the bath. In control conditions, little or no cells showed Ca^{2+} oscillations, while stimulation with norepinephrine induced asynchronous Ca^{2+} oscillations in most cells.*

However, the spiking rate slightly, but significantly decreased to 3.0 ± 0.2 spikes per minute (n=67, P<0.05). Furthermore, in 32 of the 58 cells

reacting with an increase in basal fluorescence upon stimulation with norepinephrine, the level of fluorescence decreased with exposure time. In fact, the fluorescence significantly diminished from 169.9 ± 5.2 % to 135.2 ± 5.4 % (n=58, P<0.0001, figure 5D).

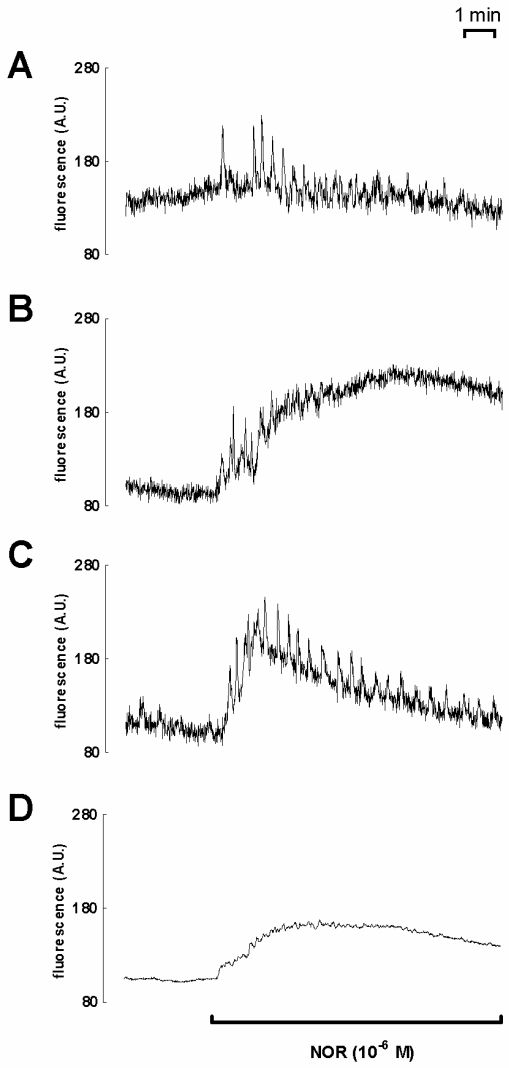

Figure 4: *Representative tracings of the fluorescence change in smooth muscle cells of rat mesenteric arteries upon addition of 3 x 10^{-6} M norepinephrine (NOR). (A-C) Representative changes in fluorescence in selected individual smooth muscle cells; (D) mean fluorescence change averaged over the whole frame in view. (A.U. = arbitrary units)*

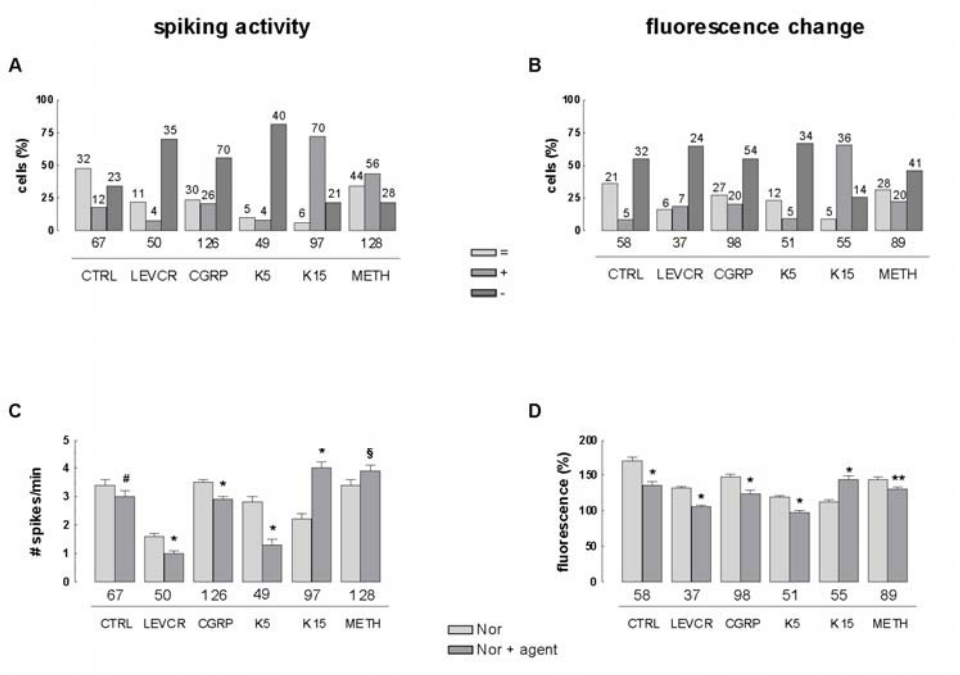

Figure 5: *(A, B) Comparison of the influence of levcromakalim (LEVCR), CGRP, 5 mM K^+ (K5), 15 mM K^+ (K15), and methanandamide (METH), administered 3 min after induction of spiking activity (A) or an increase in basal fluorescence (B), with the influence of prolonged exposure to norepinephrine alone (CTRL). The total number of cells responding to norepinephrine in each series of experiments is indicated under the bars. The numbers on top of each bar represent the number of cells showing an equal (=), an increase (+) or a decrease (-) in spiking activity (A) or basal fluorescence (B). For ease of comparison between series, Y-values were expressed as the percentage of cells. (C, D) Average number of peaks per minute (C) or absolute fluorescence (D) in the responding cells during the first 3 min after norepinephrine exposure and in the prolonged presence of norepinephrine alone (CTRL) or following addition of levcromakalim (LEVCR), CGRP, 5 mM K^+ (K5), 15 mM K^+ (K15), and methanandamide (METH). Average fluorescence is expressed relative to the fluorescence level in control conditions before exposure to norepinephrine, which is set to 100 %. * p<0.05; § p<0.01; ** p<0.005; # p<0.0001.*

7.3.2. Influence of levcromakalim

In the next series of experiments, we used levcromakalim, an opener of ATP sensitive K^+- channels (K_{ATP}), to assess the influence of

hyperpolarization of the membrane potential of the vascular smooth muscle cells on the Ca^{2+} dynamics. In this series, spiking activity in response to norepinephrine was observed in 50 cells, while 37 cells reacted with an increase in fluorescence level relative to baseline (data from 5 different preparations, figure 5). Levcromakalim ($3x10^{-7}$ M) accentuated the spontaneous small decrease in spiking rate and $[Ca^{2+}]_i$ observed in the prolonged presence of norepinephrine. Typical examples are depicted in figure 6 (A-C).

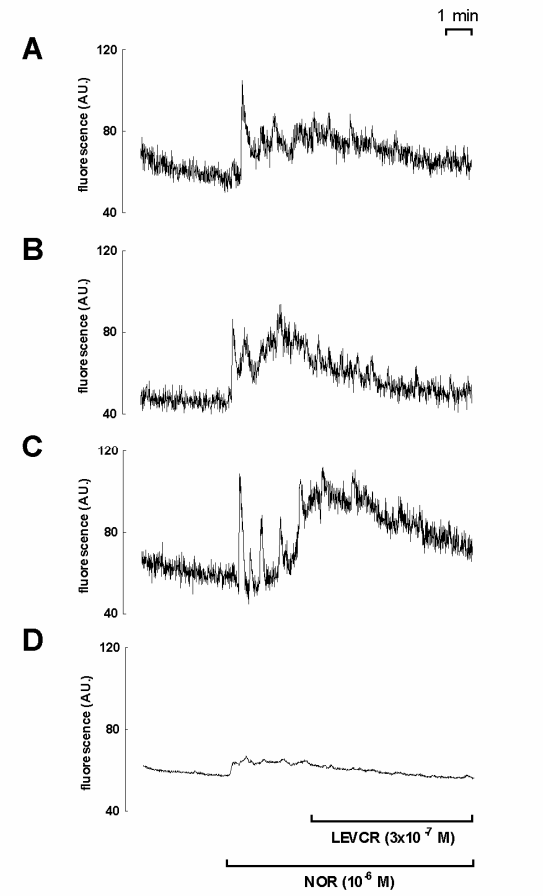

Figure 6: *Representative tracings showing the influence of levcromakalim (LEVCR) on the Ca^{2+} responses evoked by norepinephrine (NOR). (A-C) Representative changes in fluorescence in selected individual smooth muscle cells; (D) Trace of the mean fluorescence averaged from over the whole frame. (A.U. = arbitrary units)*

It can be clearly seen that in this preparation, spiking activity decreased after application of levcromakalim. From the 50 cells which oscillated in response to norepinephrine, 35 cells (70 %) showed a reduction in spike frequency, while only 4 cells (8 % of the total number of responding cells) respond with an increase (figure 5A). This ratio is much larger than in control conditions where only 34 % (23 out of 67 cells) of the responding cells showed a decrease. Additionally, the mean spike frequency significantly decreased from 1.6 ± 0.1 spikes per minute in norepinephrine to 1.0 ± 0.1 peaks per minute in the presence of levcromakalim (n=50, p<0.0001, figure 6C). Moreover, in the presence of levcromakalim, the majority of the cells (24 cells from 37) showed a decrease in fluorescence compared to the level in the presence of norepinephrine alone (figure 5B). The average fluorescence (from the entire frame) was significantly reduced from 131.6 ± 2.8 % in norepinephrine to 105.2 ± 2.8 % in levcromakalim (n=37, P<0.0001, figure 5D).

7.3.3. Influence of calcitonin gene-related peptide

Similar changes were observed with calcitonin gene-related peptide (CGRP), which is also known to cause substantial hyperpolarization in this preparation [20]. From the 126 cells oscillating in the presence of norepinephrine, 70 smooth muscle cells displayed a reduction in the spiking frequency after addition of CGRP ($3x10^{-9}$ M, figure 5A) (data from 8 different preparations). More specifically, the mean spike rate was significantly lowered from 3.5 ± 0.1 spikes per minute in norepinephrine to 2.9 ± 0.1 spikes per minute in the combined presence of norepinephrine and CGRP (n=126, P<0.0001, figure 5C). In this subset of experiments, 98 cells responded to incubation with norepinephrine with an increase in

fluorescence relative to baseline. In 54 of these cells, application of CGRP induced a lowering of the fluorescence (figure 5B). The average fluorescence was lowered from 147.3 ± 4.0 % to 123.7 ± 5.0 % (n=98, P<0.0001, figure 5D).

7.3.4. Influence of addition of 5 mM K^+

In the experiments in which we increased the KCl concentration of the KRB solution with 5 mM (yielding 10 mM K^+ in total), 49 cells oscillated in response to norepinephrine (data from 5 different preparations). Typical examples are depicted in figure 7 (A-C). After addition of 5 mM KCl, the spiking activity decreased in the majority of these cells (n=40, figure 5A, figure 7). The mean spike frequency was significantly reduced from 2.8 ± 0.2 peaks per minute in norepinephrine to 1.3 ± 0.2 peaks per minute in the presence of 5 mM K^+ (n=49, P<0.0001, figure 5C). Additionally, from the 51 cells showing an increase in fluorescence after addition of norepinephrine, this fluorescence decreased in 34 cells after incubation with 5 mM KCl (figure 5B, figure 7C). The average fluorescence significantly lowered from 119.5 ± 2.1 % to 97.4 ± 2.7 % (n=51, P<0.0001, figure 5D).

7.3.5. Influence of addition of 15 mM K^+

In a next series of experiments, we investigated the influence of the extra addition of 15 mM K^+ on the Ca^{2+} responses elicited by norepinephrine. This concentration is expected to depolarize the smooth muscle cell membrane potential by about 20 mV [22]. Incubation of the vessels with 15 mM K^+ increased spiking activity. Of the 97 cells oscillating in response to norepinephrine, 70 cells showed a higher spiking activity in the presence of

15 mM KCl (figure 5A) (data from 6 different preparations). Correspondingly, the number of spikes per minute increased significantly from 2.2 ± 0.1 in norepinephrine to 4.0 ± 0.2 in the presence of 15 mM KCl (n=97, P<0.0001, figure 5C). Individual traces are depicted in figure 8 (A-C).

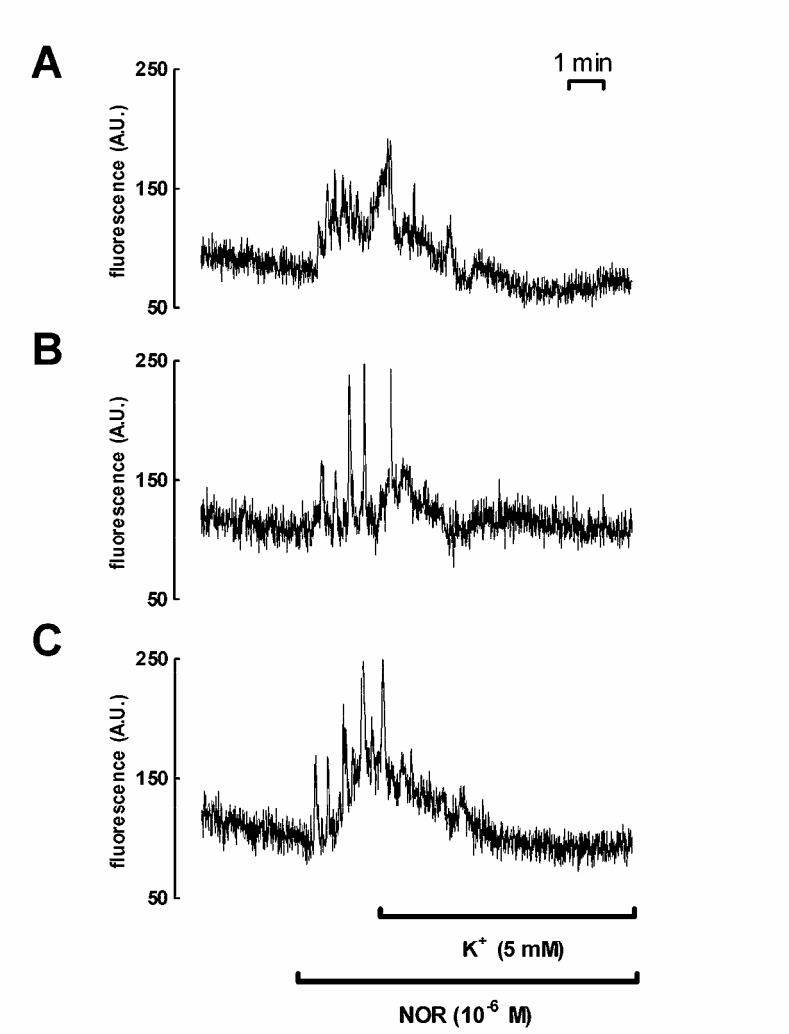

Figure 7: *Representative tracings showing the influence of an extra 5 mM K^+ on the Ca^{2+} responses evoked by norepinephrine in selected individual smooth muscle cells from the same preparation. (A.U. = arbitrary units)*

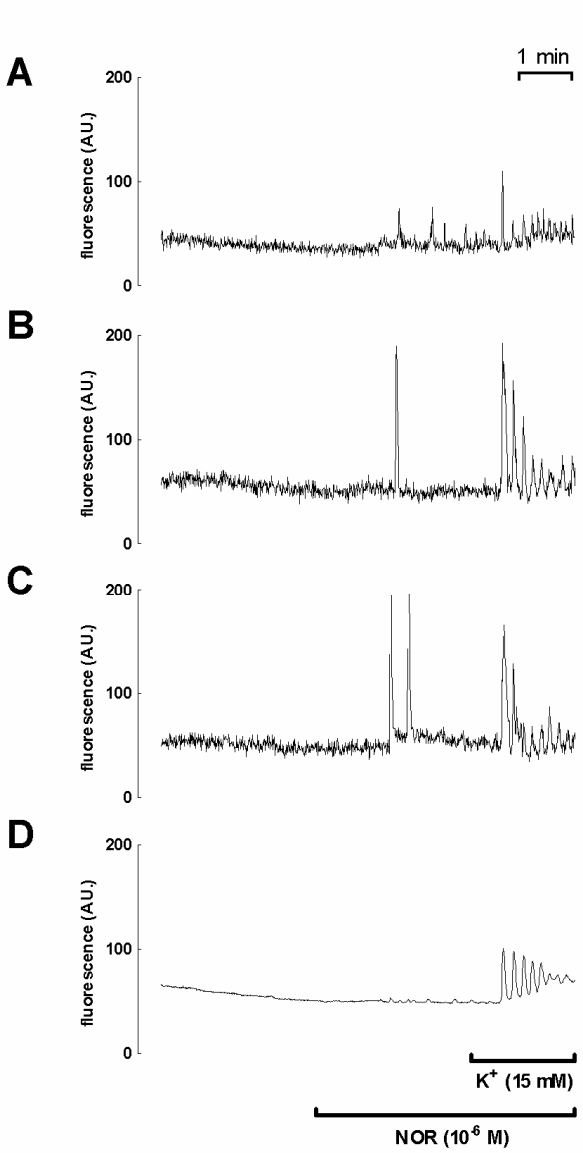

Figure 8: *Representative tracings showing the influence of 15 mM K^+ on the Ca^{2+} responses evoked by norepinephrine (NOR). (A-C) Representative changes in fluorescence in selected individual smooth muscle cells; (D) trace of the mean fluorescence averaged over the whole frame. Note that application of 15 mM K^+ synchronizes the spiking activity which is reflected in the tracing of the average fluorescence (D). (A.U. = arbitrary units*)

Furthermore, the observed oscillations became synchronized as demonstrated by the appearance of oscillations in the tracing of the average fluorescence from the entire frame, illustrated in figure 8D. The enhanced spiking activity was associated with an increase in $[Ca^{2+}]_i$. From the 55 cells responding with a increase in fluorescence to norepinephrine, 36 cells further increased fluorescence after addition of 15 mM K^+ (figure 5C). The average fluorescence significantly increased from 112.5 ± 3.2 % to 143.4 ± 5.2 (n=55, P<0.0001, figure 5D).

7.3.6. Influence of methanandamide

In the last series of experiments we tested the influence of methanandamide (10^{-5} M) on the Ca^{2+} responses. Some representative tracings of individual smooth muscle cells are depicted in figure 9 (A-C). In these preparations 128 cells oscillated in response to norepinephrine. Addition of methanandamide did not notably alter the number of oscillating cells, 56 of them responding with an increased spiking activity (data from 8 different preparations). However, as can be observed in figure 5A, the slowly decreasing trend as observed in the prolonged presence of norepinephrine was clearly reversed, although not to the same level as obtained with 15 mM K^+. Indeed, the number of cells reacting with an increase in spiking activity is twice as large as the number of cells showing a decrease (56 vs 28 cells, respectively). Moreover, the mean spike rate was significantly augmented (from 3.4 ± 0.2 spikes per minute in norepinephrine to 3.9 ± 0.2 spikes per minute in the presence of methanandamide, n=128, P<0.01, figure 5C). Apart from addition of 15 mM K^+, the application of methanandamide is the only condition in which spiking rate increases (figure 5C). In the presence of methanandamide,

oscillations remained asynchronous. The changes in spiking activity were accompanied by a small, but significant decrease in $[Ca^{2+}]_I$ as fluorescence lowered from 143.8 ± 3.5 % in norepinephrine versus 130.3 ± 3.0 % after addition of methanandamide (n=89, P<0.005, figure 5D), slightly less than observed in the prolonged presence of norepinephrine alone.

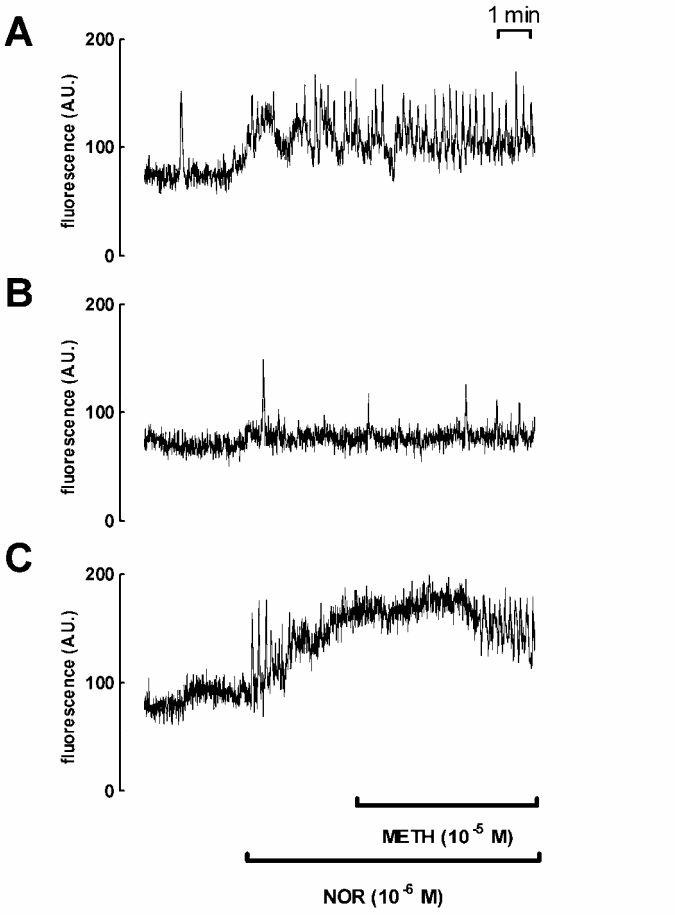

Figure 9: *Representative tracings showing the effect of methanandamide (METH) on the Ca^{2+} responses evoked by norepinephrine (NOR). The different traces (A-C) represent selected individual smooth muscle cells from the same preparation. (A.U. = artbitrary units)*

7.4. DISCUSSION

In the present study we investigated smooth muscle cell Ca^{2+} responses induced by norepinephrine and the way they were influenced by changes of the membrane potential. As far as we know, this study is the first to investigate the role of the membrane potential in the Ca^{2+} dynamics of vascular smooth muscle cells. We found that most smooth muscle cells of small mesenteric arteries of the rat showed substantial Ca^{2+} responses upon stimulation with low concentrations of norepinephrine: asynchronous spiking activity was usually accompanied by an increase in basal fluorescence. Agents known to hyperpolarize the membrane potential, such as levcromakalim and CGRP, significantly suppressed the increase in intracellular Ca^{2+} and spiking activity triggered by norepinephrine. Similarly, addition of low concentrations of extracellular K^+ tended to decrease the Ca^{2+} activity. In contrast, depolarizing concentrations of K^+ increased Ca^{2+} responses and synchronized spiking activity of the smooth muscle cells.

Vessels activated with vasoconstrictors such as norepinephrine, phenylephrine or vasopressin, show an increase in spatially averaged or whole tissue [Ca^{2+}] to a maintained level [1, 23]. However, it has recently been shown that this sustained increase of the Ca^{2+} concentration is not representative for the Ca^{2+} dynamics in the individual smooth muscle cells of both arteries and veins [5-9, 24]. In a variety of smooth muscle cells, it has now been clearly demonstrated that agonists produce cytosolic Ca^{2+} oscillations which are highly organized in both time and space. It has been shown that upon activation, the cellular Ca^{2+} level oscillates with a frequency that varies with agonist concentration and that changes in Ca^{2+} propagate as Ca^{2+} waves during exposure to the agonist [14-16]. In general,

low concentrations of an agonist elicit asynchronous Ca^{2+} oscillations and waves [6-9, 24], while high concentrations present synchronous Ca^{2+} responses and elicit vasomotion [7, 17].

The exact mechanism leading to synchronization of the Ca^{2+} responses is not yet fully understood. It has been suggested that Ca^{2+} released from the sarcoplasmatic reticulum activates a depolarizing current which can spread to the adjacent smooth muscle cells, probably through gap junctions, finally causing simultaneous depolarization of all smooth muscle cells [18]. The resulting synchronous Ca^{2+} influx through voltage dependent Ca^{2+} channels will likely result in a synchronized Ca^{2+} release from the sarcoplasmatic reticulum [25]. The Ca^{2+} waves in the individual smooth muscle cells are then synchronized, initiating vasomotion [8].

The influence of changes in the membrane potential on the Ca^{2+} responses is still elusive. Studies in rat mesenteric arteries revealed that applying a current pulse or an other brief depolarization to arteries stimulated with norepinephrine was sufficient to change the asynchronous oscillations into synchronized Ca^{2+} responses [8]. Hyperpolarizing the membrane potential with pinacidil, however, seemed to have no influence on the Ca^{2+} responses in this study.

In the present study we investigated the Ca^{2+} oscillations in vascular smooth muscle cells of mesenteric arteries of the rat. Under control conditions, in the absence of norepinephrine, only a very small fraction of the smooth muscle cells in the vascular wall exhibited spontaneous Ca^{2+} oscillations. This is consistent with previous reports in these arteries [6, 16]. Upon stimulation with norepinephrine asynchronous Ca^{2+} oscillations appeared in a significantly larger number of cells. Since asynchronous

transients do not sum, this oscillatory response was not reflected in the tracings of averaged fluorescence determined over the whole frame. Furthermore, the asynchronous spiking activity was usually accompanied by a rise in fluorescence and thus $[Ca^{2+}]_i$. However, after prolonged exposure to norepinephrine our preparations showed a decrease of the spiking activity and a slight but significant reduction of the fluorescence increase. This is consistent with other reports in smooth muscle cells of small mesenteric arteries, showing that the mean Ca^{2+} level [9, 26] and the oscillation frequency [6, 7] decreased during maintained exposure to vasoconstrictors. These effects could be due to receptor or channel desensitization.

In our experiments, addition of depolarizing concentrations of K^+ (15 mM) resulted in the synchronization of the Ca^{2+} oscillations, as observed in the traces of fluorescence averaged over the whole frame. Moreover, these high concentrations of K^+ increased the spiking frequency and further raised the fluorescence. Taken together, these results are consistent with the view that a membrane depolarization is essential to synchronize the Ca^{2+} oscillations [8].

Since depolarization and an increased Ca^{2+} influx through voltage dependent Ca^{2+} channels are able to increase oscillatory activity, it might be expected that hyperpolarization of the membrane potential could have the inverse effect. However, earlier reports had shown that hyperpolarizing the membrane potential did not influence the Ca^{2+} responses [8]. In the present study, application of levcromakalim to preparations previously stimulated with norepinephrine influenced the Ca^{2+} activity in the smooth muscle cells. In the presence of this hyperpolarizing agent, the majority of the active smooth muscle cells showed a reduction of the spiking frequency

and the fluorescence level was significantly reduced. This decline in the Ca^{2+} responses was larger than the spontaneous decrease observed in the prolonged presence of norepinephrine alone, suggesting that the induced hyperpolarization additionally attenuated the Ca^{2+} activity in the vascular smooth muscle cells. Similar results were found for calcitonin gene-related peptide (CGRP). CGRP is a powerful vasodilator in a number of vascular preparations [27, 28] and was recently demonstrated to cause substantial hyperpolarization in isolated small mesenteric and gastric arteries of the rat through the activation of K_{ATP} channels [20].

Contradicting reports have been published concerning the mechanism of action of small rises in the extracellular K^+ concentration and its effect on the vascular smooth muscle cells. Some studies in mesenteric and hepatic arteries of the rat reported that increasing the extracellular K^+ concentration with 5 mM induced a hyperpolarization of the smooth muscle membrane potential both in intact and endothelium-denuded unstimulated arteries [29-31]. Upon stimulation with phenylephrine, the K^+-induced hyperpolarizations turned endothelium-dependent and became more sensitive to gap junction uncoupling [29]. It was suggested that small increases in extracellular K^+ activate smooth muscle Na^+/K^+ ATPases and inward rectifying K^+ (K_{IR}) channels and hence induce hyperpolarization. However, stimulation of smooth muscle cells with phenylephrine, which is known to increase basal K^+ efflux from the myocytes, might saturate the Na^+/K^+ pumps and may favour the spread of endothelial hyperpolarization through myoendothelial gap junctions. Other studies in guinea-pig carotid, porcine coronary and rat gastric arteries reported, however, that small increases in the extracellular K^+ concentration had no significant hyperpolarizing effect on the membrane potential of resting arteries [32, 33]. Strikingly, in norepinephrine-stimulated rat gluteal arteries [34] non cumulative additions of small amounts of K^+ (1 to 5

mM) induced large vasorelaxations. In the present study, increasing the extracellular concentration of K^+ with 5 mM had similar effects as seen with the application of levcromakalim and CGRP. The majority of the cells responded with a significant decrease of the spiking frequency and the average basal fluorescence was significantly lowered. These results were similar to those obtained with levcromakalim and CGRP, suggesting that small amounts of K^+ may indeed hyperpolarize the membrane potential.

In a last series of experiments we tested the influence of methanandamide, a stable derivative of the endocannabinoid anandamide. Methanandamide slightly but significantly decreased the norepinephrine-induced rise in basal fluorescence but clearly reversed the decrease of the spiking rate observed in the prolonged presence of norepinephrine. Taken together with the results obtained with the hyperpolarizing agents, we can conclude that methanandamide does not substantially hyperpolarize the smooth muscle cells but, taking into account the increase in spiking activity, might have a small depolarizing effect in the present conditions. It should be noted that previous studies in the same preparation [19, 20] reported substantial hyperpolarizations of the membrane potential induced by methanandamide. This hyperpolarization was ascribed to the stimulation of $TRPV_1$ receptors on the perivascular nerves, since fully blocked in the presence of capsazepine and capsaicin. However, under the present experimental conditions only little contribution of the perivascular nerves could be expected, since prolonged incubation has been reported to deplete the perivascular nerves [35]. Therefore, these results are fully consistent with earlier results, showing that methanandamide causes a small depolarization of the membrane potential after elimination of the influence of the perivascular nerves [19, 20].

Taken together, the present study demonstrates that norepinephrine induces asynchronous Ca^{2+} spiking activity in rat mesenteric arteries, which is usually associated with a rise in the average intracellular free Ca^{2+} concentration. Hyperpolarizations induced by levcromakalim, CGRP, and presumably by small increases in the extracellular K^+ concentration diminish these responses. Finally, depolarization of the vascular smooth muscle initiates the synchronization of Ca^{2+} spiking activity.

7.5. REFERENCES

1. Meininger GA, Zawieja DC, Falcone JC, Hill MA, Davey JP. Calcium measurement in isolated arterioles during myogenic and agonist stimulation. *Am J Physiol.* 1991;261(3):H950-H959.

2. Wagner AJ, Holstein-Rathlou NH, Marsh DJ. Endothelial Ca^{2+} in afferent arterioles during myogenic activity. *Am J Physiology.* 1996;39(1):F170-F178.

3. Yip KP, Marsh DJ. $[Ca^{2+}]_i$ in rat afferent arteriole during constriction measured with confocal fluorescence microscopy. *Am J Physiol.* 1996;40(5):F1004-F1011.

4. Dora KA, Doyle MP, Duling BR. Elevation of intracellular calcium in smooth muscle causes endothelial cell generation of NO in arterioles. *Proc Natl Acad Sci U S A.* 1997;94(12):6529-34.

5. Ruehlmann DO, Lee CH, Poburko D, van Breemen C. Asynchronous Ca^{2+} waves in intact venous smooth muscle. *Circ Res.* 2000;86(4):E72-E79.

6. Zang WJ, Balke CW, Wier WG. Graded alpha(1)-adrenoceptor activation of arteries involves recruitment of smooth muscle cells to produce 'all or none' Ca^{2+} signals. *Cell Calcium.* 2001;29(5):327-34.

7. Mauban JRH, Lamont C, Balke CW, Wier WG. Adrenergic stimulation of rat resistance arteries affects Ca^{2+} sparks, Ca^{2+} waves, and Ca^{2+} oscillations. *Am J Physiol.* 2001;280(5):H2399-H2405.

8. Peng HL, Matchkov V, Ivarsen A, Aalkjaer C, Nilsson H. Hypothesis for the initiation of vasomotion. *Circ Res.* 2001;88(8):810-5.

9. Lamboley M, Schuster A, Beny JL, Meister JJ. Recruitment of smooth muscle cells and arterial vasomotion. *Am J Physiol.* 2003;285(2):H562-H569.

10. Bonev AD, Rubart M, Jaggar JH, Nelson MT. Activators of protein kinase C (PKC) decrease calcium spark frequency in cerebral artery myocytes. *Biophys J.* 1997;72(2):TU182.

11. Nelson MT, Cheng H, Rubart M, Santana LF, Bonev AD, Knot HJ, Lederer WJ. Relaxation of arterial smooth muscle by calcium sparks. *Science.* 1995;270(5236):633-7.

12. Porter VA, Bonev AD, Knot HJ, Heppner TJ, Stevenson AS, Kleppisch T, Lederer WJ, Nelson MT. Frequency modulation of Ca^{2+} sparks is involved in regulation of arterial diameter by cyclic nucleotides. *Am J Physiol.* 1998;43(5):C1346-C1355.

13. Berridge MJ, Dupont G. Spatial and temporal signaling by calcium. *Curr Opin Cell Biol.* 1994;6(2):267-74.

14. Iino M, Kasai H, Yamazawa T. Visualization of neural control of intracellular Ca^{2+} concentration in single vascular smooth muscle cells in situ. *EMBO J.* 1994;13(21):5026-31.

15. Kasai Y, Yamazawa T, Sakurai T, Taketani Y, Iino M. Endothelium-dependent frequency modulation of Ca^{2+} signalling in individual vascular smooth muscle cells of the rat. *J Physiol.* 1997;504(2):349-57.

16. Miriel VA, Mauban JRH, Blaustein MP, Wier WG. Local and cellular Ca^{2+} transients in smooth muscle of pressurized rat resistance arteries during myogenic and agonist stimulation. *J Physiol.* 1999;518(3):815-24.

17. Wier WG, Morgan KG. Alpha1-adrenergic signaling mechanisms in contraction of resistance arteries. *Rev Physiol Biochem Pharmacol.* 2003;150:91-139.

18. Hirst GD, Neild TO. An analysis of excitatory junctional potentials recorded from arterioles. *J Physiol.* 1978;280:87-104.

19. Vanheel B, Van de Voorde J. Regional differences in anandamide- and methanandamide-induced membrane potential changes in rat mesenteric arteries. *J Pharmacol Exp Ther.* 2001;296(2):322-8.

20. Breyne J, Vanheel B. Methanandamide hyperpolarizes gastric arteries by stimulation of $TRPV_1$ receptors on perivascular CGRP containing nerves. *J Cardiovasc Pharmacol.* 2006;47(2):303-9.

21. Leybaert L, de Meyer A, Mabilde C, Sanderson MJ. A simple and practical method to acquire geometrically correct images with resonant scanning-based line scanning in a custom-built video-rate laser scanning microscope. *J Microsc.* 2005;219(Pt 3):133-40.

22. Nelson MT, Quayle JM. Physiological roles and properties of potassium channels in arterial smooth muscle. *Am J Physiol.* 1995;268(4 Pt 1):C799-C822.

23. Jiang MJ, Morgan KG. Agonist-specific myosin phosphorylation and intracellular calcium during isometric contractions of arterial smooth muscle. *Pflugers Arch.* 1989;413(6):637-43.

24. Sell M, Boldt W, Markwardt F. Desynchronising effect of the endothelium on intracellular Ca^{2+} concentration dynamics in vascular smooth muscle cells of rat mesenteric arteries. *Cell Calcium.* 2002;32(3):105-20.

25. van Breemen C, Chen Q, Laher I. Superficial buffer barrier function of smooth muscle sarcoplasmic reticulum. *Trends Pharmacol Sci.* 1995;16(3):98-105.

26. Savineau JP, Marthan R. Cytosolic calcium oscillations in smooth muscle cells. *News Physiol Sci.* 2000;15:50-5.

27. Li YJ, Duckles SP. Effect of endothelium on the actions of sympathetic and sensory nerves in the perfused rat mesentery. *Eur J Pharmacol.* 1992;210(1):23-30.

28. Gray DW, Marshall I. Human alpha calcitonin gene-related peptide stimulates adenylate cyclase and guanylate cyclase and relaxes rat thoracic aorta by releasing nitric oxide. *Br J Pharmacol.* 1992;107(3):691-6.

29. Richards GR, Weston AH, Burnham MP, Feletou M, Vanhoutte PM, Edwards G. Suppression of K^+-induced hyperpolarization by phenylephrine in rat mesenteric artery: relevance to studies of

endothelium-derived hyperpolarizing factor. *Br J Pharmacol.* 2001;134(1):1-5.

30. Edwards G, Dora KA, Gardener MJ, Garland CJ, Weston AH. K^+ is an endothelium-derived hyperpolarizing factor in rat arteries. *Nature.* 1998;396(6708):269-72.

31. Edwards G, Gardener MJ, Feletou M, Brady G, Vanhoutte PM, Weston AH. Further investigation of endothelium-derived hyperpolarizing factor (EDHF) in rat hepatic artery: studies using 1-EBIO and ouabain. *Br J Pharmacol.* 1999;128(5):1064-70.

32. Quignard JF, Feletou M, Thollon C, Vilaine JP, Duhault J, Vanhoutte PM. Potassium ions and endothelium-derived hyperpolarizing factor in guinea-pig carotid and porcine coronary arteries. *Br J Pharmacol.* 1999;127(1):27-34.

33. Van de Voorde J, Vanheel B. EDHF-mediated relaxation in rat gastric small arteries: influence of ouabain/Ba^{2+} and relation to potassium ions. *J Cardiovasc Pharmacol.* 2000;35(4):543-8.

34. De Clerck I, Boussery K, Pannier JL, Van de Voorde J. Potassium potently relaxes small rat skeletal muscle arteries. *Med Sci Sports Exerc.* 2003;35(12):2005-12.

35. Zygmunt PM, Sorgard M, Petersson J, Johansson R, Hogestatt ED. Differential actions of anandamide, potassium ions and endothelium-derived hyperpolarizing factor in guinea-pig basilar artery. *Naunyn-Schmiedebergs Arch Pharmacol.* 2000;361(5):535-42.

Chapter

8

General discussion, limitations & future perspectives

8.1. GENERAL DISCUSSION

The blood supply to a given vascular bed is regulated by neuronal, humoral or local chemical mechanisms altering the diameter of the vessels of the specific tissue. It is now generally accepted that the vascular endothelium plays a crucial role in the control of blood vessel tone and blood flow. However, the endothelium is not the sole mediator of vascular tone. For example, several substances released from the perivascular nerves may also influence the cardiovascular system. In the present study we investigated the role of substances released from both the endothelium and the perivascular nerves in the reactivity of the vascular wall.

Although the role of the endothelium-dependent vasorelaxing factors NO and PGI_2 is well established, the exact mechanism involved in endothelium-dependent hyperpolarization is, despite extensive research, still a subject of intense discussion. While some studies point to a diffusible factor (EDHF) released from the endothelial cells, other reports support the idea of an electrical current or small messenger molecule being spread through myoendothelial gap junctions.

Endothelium-dependent hyperpolarization in rat gastric arteries: an important mediator of gastric mucosal blood flow?

During the search for the mechanism underlying endothelium-dependent hyperpolarization, it has become clear that there are considerable tissue and species differences [1, 2]. It has therefore been generally accepted that different hyperpolarizing mechanisms may exist in different vascular beds. Moreover some arteries such as the femoral artery of the rat even lack any

endothelium-dependent hyperpolarizing responses [3]. Thusfar, most of the membrane potential experiments in our lab were performed in small mesenteric arteries of the rat. The existence of EDHF in these arteries has been described in detail and the search for its exact mechanism of action has been a subject of many investigations. Since previous studies in our lab demonstrated endothelium-dependent, but L-NA and indomethacin resistant vasorelaxations in isolated small gastric arteries of the rat in response to acetylcholine [4], we performed membrane potential measurements to confirm the existence of an endothelium-derived hyperpolarizing factor in these vessels. Indeed, we found that acetylcholine hyperpolarizes the membrane potential of the vascular smooth muscle cells of small gastric arteries. This hyperpolarization seemed to be totally endothelium-dependent but independent of the NO or PGI_2 pathway. Since membrane potential is expected to alter vessel tone immediately, this first demonstration of endothelium-dependent hyperpolarization in gastric arteries could reveal an important and rapid regulator of gastric mucosal blood flow. However, the identity of EDHF and its mechanism of action in gastric arteries are far from revealed. We found, although, that the EDHF response in gastric arteries did not seem to rely on the stimulation of K_{IR} channels or Na^+/K^+-ATPases on the smooth muscle cells.

Endothelium-dependent hyperpolarization in rat mesenteric arteries: a story about K^+-clouds and myoendothelial gap junctions.

Since the discovery of the existence of endothelium-dependent hyperpolarizing factors, extensive research has been performed to unravel the exact mechanism of action. Several possible candidates for the EDHF have been proposed, among which K^+. In resting rat hepatic and small

mesenteric arteries it was proposed that stimulation with acetylcholine results in an IK_{Ca}- and SK_{Ca}-mediated hyperpolarization of the endothelial cells with accompanying endothelial release of K^+ in the myoendothelial space (figure 1A). It was found that the EDHF-response was significantly inhibited by the combination of Ba^{2+} and ouabain, selective inhibitors of K_{IR} channels and Na^+/K^+-ATPases, respectively. Therefore it was suggested that local transient increases in the extracellular K^+ concentration would activate Na^+/K^+ -ATPases and K_{IR} channels in the membrane of the adjacent smooth muscle cells, leading to their hyperpolarization [5, 6]. However, other studies found no evidence for the presence of K_{IR} in smooth muscle cells of rat small mesenteric arteries and suggested that these channels were restricted to the endothelial cells[7]. In the present study, no evidence was found for the involvement of K_{IR} channels in the endothelium-dependent hyperpolarization of rat small mesenteric arteries, while the involvement of Na^+/K^+-ATPases could not be completely excluded. This is somewhat different from the results obtained in gastric arteries, where the involvement of both K_{IR} channels and Na^+/K^+-ATPases could be excluded. Our results in rat mesenteric arteries rather point to the activation of an as yet unidentified, but Ba^{2+} resistant K^+ current accounting for a significant fraction of the endothelium-dependent hyperpolarization of the smooth muscle cells (figure 1A). On the other hand, we found that gap junctions play some role in the acetylcholine-induced hyperpolarization of the smooth muscle cells since carbenoxolone decreased the responses (figure 1A). This is consistent with other studies in rat mesenteric arteries, indicating that both K^+-coupling and gap junctional communication play a role in the EDHF-response.

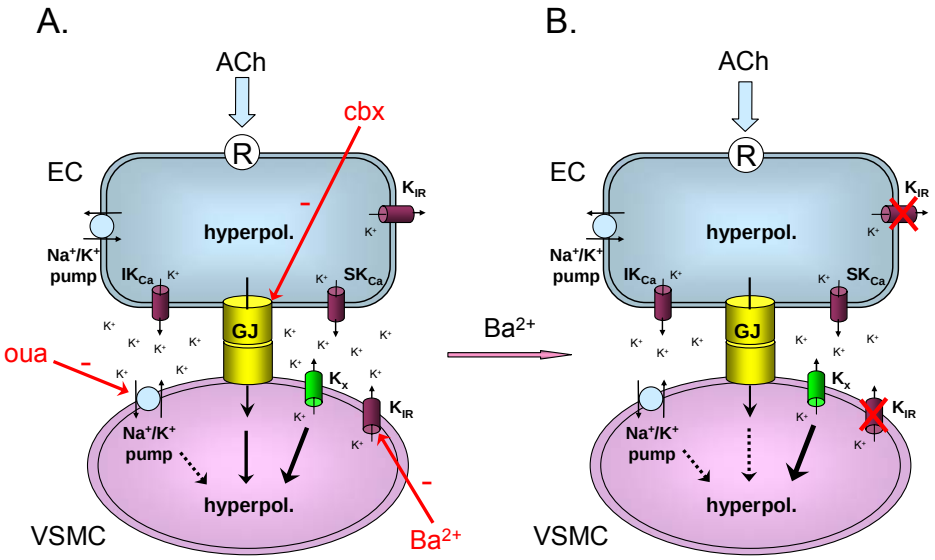

Figure 1: *Schematic presentation of the proposed pathway for the endothelium-derived hyperpolarization (EDH) in rat small mesenteric arteries. (A) In control conditions (in the presence of L-NA and indomethacin), both gap junctions (GJ) and an as yet unidentified, but Ba^{2+} resistant K^+ current (K_x) play a role in the endothelium-dependent hyperpolarization induced by acetylcholine (ACh). The involvement of Na^+/K^+-ATPases could not be completely excluded. (B) After pre-incubation with Ba^{2+}, to modulate the myoendothelial extracellular K^+ concentration, the presumed local depletion in extracellular K^+ decreases the role of GJ in the EDH-pathway and favours K^+ efflux through K_X. (oua = ouabain; cbx = carbenoxolone; K_{IR} = inwardly rectifying K^+ channel; IK_{Ca} = intermediate conductance Ca^{2+} activated K^+ channel; SK_{Ca} = small conductance Ca^{2+} activated K^+ channel; hyperpol = hyperpolarization; EC = endothelial cell; VSMC = vascular smooth muscle cell; R = receptor)*

Under basal conditions, Na^+/K^+-ATPases containing α_2- and/or α_3-subunits are suggested to be responsible for the observed K^+-induced effects [8]. Moreover, it was found that stimulation of the arteries with phenylephrine favoured the gap junctional pathway for smooth muscle hyperpolarization [6, 9]. Therefore, it was suggested that activation of the smooth muscle cells, which is known to increase K^+ efflux from the myocytes, results in a K^+ cloud in the myoendothelial spaces in these conditions [10]. This would fully activate and saturate Na^+/K^+-pumps containing α_2- and/or α_3-subunits on

the smooth muscle cells so that the acetylcholine-induced endothelium-dependent hyperpolarization would now rely more on gap junctional coupling.

If local accumulations of extracellular K^+ favour gap junctional coupling, local depletion might be expected to have the adverse effect. In the present study, we used the K_{IR} channel inhibitor Ba^{2+} to modulate the myoendothelial extracellular K^+ concentration (figure 1B). Blocking the K_{IR} channels by preincubation with Ba^{2+} might indeed be expected to reduce the steady state extracellular K^+ concentration around the smooth muscle cells. We found that under these circumstances, the endothelium-dependent hyperpolarization relies to a lesser extent on gap junctional coupling (figure 1B). This is fully consistent with the hypothesis in the mesenteric arteries that local accumulations in basal K^+ concentration would shift the acetylcholine-activated EDHF mechanism to gap junctional coupling. However, since in our experiments K_{IR} channels are not involved, the hyperpolarization of the smooth muscle cells possibly relies on another mechanism. In part, this may include Na^+/K^+-pumping. It should be noted, however, that depletions or accumulations of basal extracellular K^+ not only affect the activity of the Na^+/K^+-pumps, but are likely to affect all transmembrane K^+ fluxes.

Other evidence for the hypothesis that EDHF relies on both K^+-coupling and gap junctional communication was obtained from experiments in which the extracellular K^+ concentration was raised with a few mM. However, contradicting reports have been published concerning this topic, even in the same vessel type. Studies in hepatic and small mesenteric arteries of the rat showed that increasing the extracellular K^+ concentration with 5 mM induced a hyperpolarization of the smooth muscle membrane potential in

both intact and endothelium-denuded resting arteries [9, 10]. Upon stimulation with phenylephrine, the K^+ responses became endothelium-dependent and relied more on gap junctional coupling. This is consistent with the hypothesis of a K^+-cloud, as a result of stimulation with phenylephrine, which saturates the Na^+/K^+-pumps and makes the hyperpolarizing effects of K^+ on the endothelial cells more important. The hyperpolarization of the endothelial cells is subsequently transferred to the smooth muscle cells via myoendothelial gap junctions. Consistently, in rat gastric arteries (unpublished data) and in rat gluteal arteries [11] stimulated with norepinephrine, small increases in the extracellular K^+ concentration with 1-5 mM induced large, concentration-dependent vasorelaxations. In contrast, other studies in guinea-pig and porcine coronary arteries reported that small increases in the extracellular K^+ concentration had no significant hyperpolarizing effect on the membrane potential of resting arteries [12]. Similarly, no K^+-induced hyperpolarizations were obtained in resting rat gastric arteries [4]. In the same study, cumulative addition of K^+ (up to 15 mM) to norepinephrine precontracted arteries caused no substantial relaxation.

The present study supports the view that in rat small mesenteric arteries, a small increase in the extracellular K^+ concentration might induce a hyperpolarization of the membrane potential of the smooth muscle cells. Indeed, the results obtained with the Ca^{2+} imaging experiments also suggest a hyperpolarization of the membrane potential induced by increasing the extracellular K^+ concentration with 5 mM. Since in rat gastric and gluteal arteries, such small increases in the K^+ concentration induce potent relaxation, a membrane potential change as suggested in the present study could be the principle mediator of vasorelaxation.

Endocannabinoids: multiple pathways leading to vasodilatation.

Another candidate proposed as EDHF was the endocannabinoid anandamide [13]. However, this hypothesis has widely been argued and it is now generally accepted that anandamide is not EDHF. Besides their neurobehavioral effects, both endogenous and synthetic cannabinoids influence the cardiovascular system and have potent vasodilator effects in a number of vascular preparations [13-15]. This was confirmed in our experiments. We found that methanandamide, a stable analogue of anandamide, potently hyperpolarized the smooth muscle cells of both rat gastric and mesenteric arteries. This hyperpolarization showed a different time course and pharmacological profile as compared to the EDHF-response, excluding a role for EDHF in the membrane electrical response to cannabinoids in these preparations.

The exact mechanism by which cannabinoids induce vasodilatation is still unknown. Some studies have reported that they directly stimulate cannabinoid CB_1 or CB_2 receptors on the smooth muscle cells. [13, 14, 16]. Recently, it was suggested that in some vessels, the response to cannabinoids could be ascribed to the stimulation of a not yet identified non-CB_1/non-CB_2 receptor located on the endothelial cells. Several studies, including previous experiments in our own laboratory [17], have identified anandamide as an endovanilloid, acting by stimulation of $TRPV_1$ receptors on perivascular nerves, causing the release of vasodilator neuropeptides such as CGRP. We studied and compared the membrane electrical responses to methanandamide and exogenous CGRP. We found that methanandamide and exogenous CGRP caused similar membrane potential changes which were sensitive to the K_{ATP} channel inhibitor glibenclamide. Furthermore, hyperpolarizations induced by

methanandamide, unlike those elicited by CGRP, were sensitive to inhibition of $TRPV_1$ receptors with capsazepine. We concluded that stimulation of $TRPV_1$ receptors on perivascular CGRP containing nerves is the primary cause for the cannabinoid-induced hyperpolarization in the mesenteric and gastric arteries. The released CGRP subsequently hyperpolarizes the resting vascular smooth muscle cells through activation of K_{ATP} channels (figure 2A).

Strikingly, the Ca^{2+} imaging experiments do not point to a hyperpolarization induced by methanandamide, since the addition of methanandamide seemed to have only little direct influence on the membrane potential in the norepinephrine-stimulated arteries. Maybe a small depolarization might possibly be expected. Taken the long incubation period and the fact that the preparations were loaded at 4°C, a rather small contribution of the perivascular nerves is expected under these experimental circumstances. Indeed, it has been shown that cooling abolishes the vasodilator response to (endo)cannabinoids, probably by desensitization and/or degeneration of the perivascular nerves [18]. After desensitization of the perivascular nerves with capsaicin [17] or inhibition of the TRPV1 receptor with capsazepine (present study) in the membrane potential measurements, methanandamide was unable to induce hyperpolarization, and in some preparations even caused a small depolarization of the membrane potential. Therefore, the Ca^{2+} imaging experiments are consistent with the hypothesis that methanandamide induces hyperpolarization of the membrane potential by stimulation of the perivascular sensory nerves.

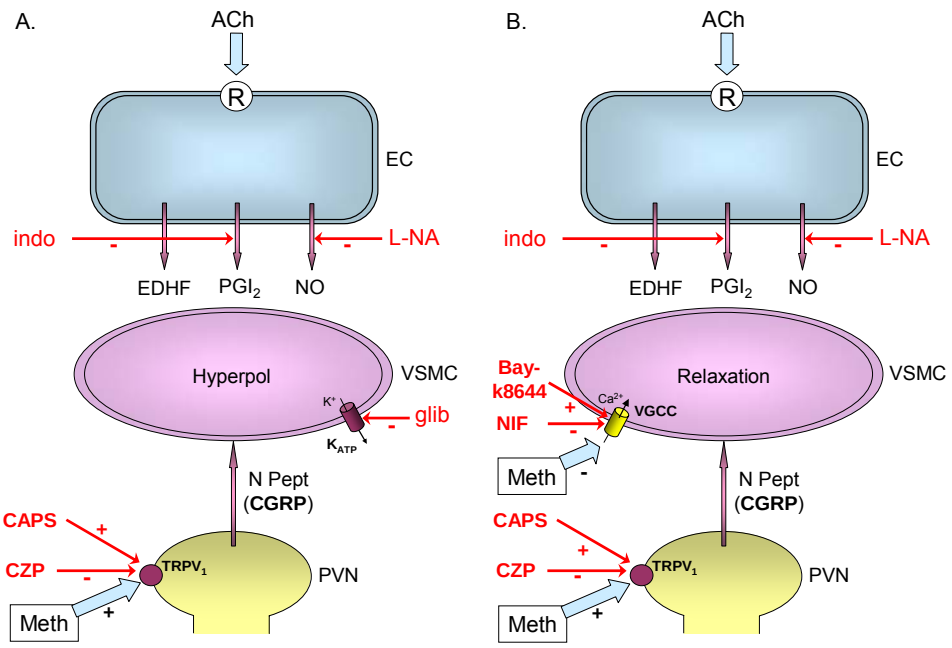

Figure 2: *Schematic presentation of the proposed pathway for the methanandamide (Meth)-induced responses. (A) Membrane potential measurements in rat gastric and mesenteric arteries (in the presence of L-NA and indomethacin (indo)) suggest that Meth stimulates $TRPV_1$ receptors on perivascular nerves (PVN), causing the release of vasodilator neuropeptides such as CGRP. CGRP subsequently hyperpolarizes (Hyperpol) the vascular smooth muscle cells (VSMC) through the activation of ATP sensitive potassium channels (K_{ATP}). (B) Tension measurements suggested that low concentrations of Meth might stimulate $TRPV_1$ receptors on the PVN, inducing the release of CGRP, followed by relaxation of the VSMC. On the other hand, higher concentrations of Meth were shown to inhibit the influx of Ca^{2+} in the VSMC through voltage gated Ca^{2+} channels (VGCC).(EC = endothelial cell; NO = nitric oxide; N Pept = neuropeptides; EDHF = endothelium-derived hyperpolarizing factor; PGI_2 = prostacyclin; glib = glibenclamide; CAPS = capsaicin; CZP = capsazepine; NIF = nifedipine)*

Since membrane hyperpolarization can be a powerful mediator of vasorelaxation, we characterized the vasorelaxing properties of cannabinoids in the gastric arteries. We found that methanandamide is also

a powerful vasorelaxant in isolated small gastric arteries of the rat. The induced vasorelaxation was endothelium-independent, consistent with reports in other arteries [13, 16]. In the present tension measurements we found no evidence that methanandamide induced relaxation through activation of one of the above mentioned cannabinoid receptors. While the hyperpolarization seemed to rely completely on activation of TRPV1 receptors on perivascular nerves (figure 2A), we found that this mechanism could not fully account for the methanandamide-induced relaxation. However, it might contribute to the relaxations induced by the lower concentrations of the cannabinoid (figure 2B).

Taken together with the results obtained from the membrane potential measurements, these findings suggest that hyperpolarization only plays a minor role in the relaxation induced by cannabinoids in norepinephrine contracted gastric arteries and that the main route by which higher concentrations produce vasorelaxation involves another mechanism. This was further corroborated by the fact that CGRP and methanandamide showed different sensitivity to potassium channel blockers. Studies with high K^+, TEA and glibenclamide showed that membrane hyperpolarization was at least involved in the vasorelaxation to exogenous CGRP, while the methanandamide-induced relaxation did not require smooth muscle cell hyperpolarization.

Interestingly, we found that higher concentrations of methanandamide might eventually relax the arteries by inhibition of Ca^{2+} influx in the smooth muscle cells (figure 2B). The former possibility is consistent with other reports about the direct inhibitory action of cannabinoids on voltage dependent Ca^{2+} channels or a further step in the excitation-contraction coupling [19-21]. In the Ca^{2+} imaging study, we found that addition of

methanandamide slightly, but significantly decreased the basal free Ca^{2+} concentration of the smooth muscle cells.

Membrane potential and Ca^{2+} oscillations.

Vasorelaxation and vasoconstriction involve changes of the mean cytosolic Ca^{2+} concentration of the smooth muscle cells in the arteriolar wall. It has been shown that the overall vessel Ca^{2+} concentration is not representative for the Ca^{2+} reactions in the individual smooth muscle cells [22-26]. Upon stimulation with vasoconstrictors, smooth muscle cells of rat tail artery and small mesenteric arteries showed asynchronous Ca^{2+} oscillations which were not reflected in the average Ca^{2+} responses [27-29]. When higher concentrations of contracting agents were used, the Ca^{2+} waves appeared synchronously between the different smooth muscle cells and give rise to oscillations in vascular tone, called vasomotion [24, 30]. It has been suggested that the switch to synchronisation of the Ca^{2+} oscillations and waves involves a simultaneous depolarization of all the smooth muscle cells. Indeed, application of a depolarizing current was sufficient to synchronise the cells [25]. In the last part of this thesis, we studied the influence of the membrane potential on norepinephrine-induced Ca^{2+} oscillations in smooth muscle cells of intact small mesenteric arteries of the rat. We found that stimulation with low concentrations of norepinephrine induces asynchronous Ca^{2+} spikes in the smooth muscle cells usually accompanied by a sustained increase of the basal fluorescence. A small reduction of the responses was seen in the prolonged presence of the vasoconstrictor. Depolarizing concentrations of K^+ increased the Ca^{2+} responses and initiated synchronization of the oscillations, confirming other reports about the initiation of vasomotion. Taken into account the effect of a

depolarization on the oscillatory behaviour, it could be expected that a hyperpolarization of the membrane potential would have inverse effects. Indeed, addition of hyperpolarizing agents such as levcromakalim significantly reduced the Ca^{2+} responses. Similar results were obtained with exogenous CGRP. It is suggested, therefore, that while methanandamide is unable to induce release of CGRP in these conditions, the exogenous application of this peptide directly acts on the vascular smooth muscle cells causing hyperpolarization. As mentioned, increasing $[K^+]_o$ with 5mM similarly causes a membrane hyperpolarization, although not as large as obtained with levcromakalim.

8.2. GENERAL CONCLUSIONS

The results of the present study emphasize the importance of EDHF in the gastrointestinal circulation. Furthermore, the mechanism by which agents derived from the endothelium or the perivascular nerves modulate the reactivity of the vessel wall is further elucidated. The main findings presented in this thesis can be summarized as follows:

- Endothelium-dependent hyperpolarization is present in mesenteric and gastric arteries and might play an important role in the regulation of the gastro-intestinal circulation.

- In mesenteric arteries, endothelium-dependent hyperpolarization involves both gap junctional coupling and activation of an as yet unidentified, but Ba^{2+}-resistant, K^+ current.

- The hyperpolarization induced by methanandamide in gastric and mesenteric arteries involves the stimulation of the $TRPV_1$ receptor on perivascular nerves and the subsequent release of CGRP.

- The relaxation induced by methanandamide in gastric arteries might involve multiple pathways: low concentrations may stimulate the $TRPV_1$ receptor on CGRP-containing perivascular nerves, while higher concentrations elicit their effects by inhibition of voltage dependent Ca^{2+} channels in the smooth muscle cells.

- Stimulation of mesenteric arteries with norepinephrine induces asynchronous Ca^{2+} oscillations in the vascular smooth muscle cells, which become synchronized upon depolarisation of the membrane potential. Hyperpolarization tends to decrease the Ca^{2+} dynamics.

8.3. LIMITATIONS OF THIS STUDY

Some limitations should be mentioned for the experiments used in this thesis. First, based on the knowledge that EDHF shows tissue and species specificity, the use of only two different arteries from a single species implies some restraints. Furthermore, it has been shown that different EDHFs might even exist within the same vascular bed, depending on the size of the arteries and the used experimental conditions. Therefore, extrapolation of the obtained results to other vessels or species, or to human level, should be done with great caution.

Second, in the present in vitro studies, the influence of neuropeptides (CGRP) released by the perivascular sensory nerves is investigated. Sensory neurons all have their cell bodies in the dorsal root ganglia, where the neuropeptides are synthesised. Upon isolation of the arteries, however,

the perivascular nerves are cut, so that after depletion, the nerve endings can not be refilled with freshly synthesised neuropeptides (CGRP). This is most likely the reason why the hyperpolarizing effect of methanandamide is not reproducible in our study. Therefore, it is very important in *in vitro* studies to pay attention to the reproducibility of a response. On the other hand, it should also be noted that, if the present *in vitro* studies point to an important role for the release of CGRP, then one could expect that its involvement would be considerably more important *in vivo*.

Third, three different techniques were used to obtain the results comprised in this thesis. The distinct techniques used in the present study were performed in totally different experimental conditions. While the results obtained with one technique were often consistent with results from another and corroborative for general conclusions, this was not always the case. The main apparent discrepancy arose from the findings that methanandamide caused substantial hyperpolarization, whereas relaxation measurements implied a minor role for this hyperpolarization because the substance apparently affected a downstream mechanism in the excitation-contraction coupling. This can be taken as a typical case for many conflicting data and discrepancies in literature. It illustrates the risks involved e.g. when extrapolating results from relaxation studies to conclusions about membrane potential, or vice versa.

8.4. FUTURE PERSPECTIVES

In this study, the importance of endothelium-dependent hyperpolarization (EDH) has been demonstrated for the first time in isolated gastric arteries of rats. Although the involvement of Na^+/K^+ ATPases and K_{IR} channels has

been ruled out, the exact mechanism by which acetylcholine hyperpolarizes the smooth muscle cells has not been elucidated yet. Therefore, additional electrophysiological and tension measurements would be useful to further investigate the exact mechanism of action of EDH in these arteries and to reveal its identity. For example, the involvement of myoendothelial gap junctions can be studied using known gap junction uncouplers such as the peptide gap-27. Furthermore, the involvement of possible EDHF candidates can be tested using specific inhibitors, such as cytochrome P450 inhibitors to assess the involvement of epoxyeicosatrienoic acids.

A second series of membrane potential experiments suggested the involvement of an as yet unidentified, but Ba^{2+}-resistant K^+ channel in the acetylcholine-response in rat mesenteric arteries. In the future, it would be interesting to further extend these results with patch clamp techniques, to learn more about the characteristics and the identity of Ba^{2+}-resistant K^+ currents accounting for a significant fraction of the endothelium-dependent hyperpolarization.

To further investigate if the suggested hypothesis of the K^+-cloud [10] is correct, the results should be extended with additional membrane potential and tension measurements. For example, we could test if indeed small increases in the extracellular K^+ concentration induce hyperpolarizations of the membrane potential of norepinephrine-stimulated vessels and could cause relaxation of small mesenteric arteries. If this is the case, the pharmacological properties of these responses should be further investigated.

Furthermore, it might be interesting to test the influence of both methanandamide and CGRP on the membrane currents of isolated smooth

muscle cells of the gastric arteries, using patch-clamp techniques. Also, further Ca^{2+} imaging experiments could be useful to clarify the exact mechanism by which methanandamide relaxes the smooth muscle cells. In this perspective, it would be useful to develop a set-up for simultaneous tension and Ca^{2+} measurements.

Finally, in the Ca^{2+} imaging experiments, glass cannulae were inserted into the lumen of the arteries to avoid motion artefacts. However, under these circumstances, it was impossible to apply intralumenal pressure and the arteries could not develop myogenic tone. Also, endothelium-dependent agonists such as acetylcholine could not be tested, because the cannulae damaged the endothelium. Therefore, experiments with pressurized and perfused arteries could be of interest for future experiments. Such an experimental set-up would allow studies on the effect of EDHF on the Ca^{2+} responses in the vascular smooth muscle cells and make it possible to investigate endothelial effects. However, this is limited to the resistance arteries since preparation depth is a limiting factor in these experiments and it would not be possible to visualise the endothelium in preparations thicker than 100 µm.

8.5. REFERENCES

1. Kemp BK, Cocks TM. Evidence that mechanisms dependent and independent of nitric oxide mediate endothelium-dependent relaxation to bradykinin in human small resistance-like coronary arteries. *Br J Pharmacol.* 1997;120(5):757-62.

2. Triggle CR, Dong H, Waldron GJ, Cole WC. Endothelium-derived hyperpolarizing factor(s): species and tissue heterogeneity. *Clin Exp Pharmacol Physiol.* 1999;26(2):176-9.

3. Sandow SL, Tare M, Coleman HA, Hill CE, Parkington HC. Involvement of myoendothelial gap junctions in the actions of endothelium-derived hyperpolarizing factor. *Circ Res.* 2002;90(10):1108-13.

4. Van de Voorde J, Vanheel B. EDHF-mediated relaxation in rat gastric small arteries: influence of ouabain/Ba^{2+} and relation to potassium ions. *J Cardiovasc Pharmacol.* 2000;35(4):543-8.

5. Edwards G, Dora KA, Gardener MJ, Garland CJ, Weston AH. K^+ is an endothelium-derived hyperpolarizing factor in rat arteries. *Nature.* 1998;396(6708):269-72.

6. Busse R, Edwards G, Feletou M, Fleming I, Vanhoutte PM, Weston AH. EDHF: bringing the concepts together. *Trends Pharmacol Sci.* 2002;23(8):374-80.

7. Crane GJ, Walker SD, Dora KA, Garland CJ. Evidence for a differential cellular distribution of inward rectifier K channels in the rat isolated mesenteric artery. *J Vasc Res.* 2003;40(2):159-68.

8. Weston AH, Richards GR, Burnham MP, Feletou M, Vanhoutte PM, Edwards G. K^+-induced hyperpolarization in rat mesenteric artery: identification, localization and role of Na^+/K^+-ATPases. *Br J Pharmacol.* 2002;136(6):918-26.

9. Edwards G, Gardener MJ, Feletou M, Brady G, Vanhoutte PM, Weston AH. Further investigation of endothelium-derived hyperpolarizing factor (EDHF) in rat hepatic artery: studies using 1-EBIO and ouabain. *Br J Pharmacol.* 1999;128(5):1064-70.

10. Richards GR, Weston AH, Burnham MP, Feletou M, Vanhoutte PM, Edwards G. Suppression of K^+-induced hyperpolarization by phenylephrine in rat mesenteric artery: relevance to studies of endothelium-derived hyperpolarizing factor. *Br J Pharmacol.* 2001;134(1):1-5.

11. De Clerck I, Boussery K, Pannier JL, Van de Voorde J. Potassium potently relaxes small rat skeletal muscle arteries. *Med Sci Sports Exerc.* 2003;35(12):2005-12.

12. Quignard JF, Feletou M, Thollon C, Vilaine JP, Duhault J, Vanhoutte PM. Potassium ions and endothelium-derived hyperpolarizing factor in guinea-pig carotid and porcine coronary arteries. *Br J Pharmacol.* 1999;127(1):27-34.

13. Randall MD, Alexander SPH, Bennett T, Boyd EA, Fry JR, Gardiner SM, Kemp PA, McCulloch AI, Kendall DA. An endogenous cannabinoid as an endothelium-derived vasorelaxant. *Biochem Biophys Res Commun.* 1996;229(1):114-20.

14. Deutsch DG, Goligorsky MS, Schmid PC, Krebsbach RJ, Schmid HHO, Das SK, Dey SK, Arreaza G, Thorup C, Stefano G, Moore LC. Production and physiological actions of anandamide in the vasculature of the rat kidney. *J Clin Invest.* 1997;100(6):1538-46.

15. Ellis EF, Moore SF, Willoughby KA. Anandamide and delta 9-THC dilation of cerebral arterioles is blocked by indomethacin. *Am J Physiol.* 1995;269(6 Pt 2):H1859-H1864.

16. Chaytor AT, Martin PE, Evans WH, Randall MD, Griffith TM. The endothelial component of cannabinoid-induced relaxation in rabbit mesenteric artery depends on gap junctional communication. *J Physiol.* 1999;520 Pt 2:539-50.

17. Vanheel B, Van de Voorde J. Regional differences in anandamide- and methanandamide-induced membrane potential changes in rat mesenteric arteries. *J Pharmacol Exp Ther.* 2001;296(2):322-8.

18. Zygmunt PM, Sorgard M, Petersson J, Johansson R, Hogestatt ED. Differential actions of anandamide, potassium ions and endothelium-derived hyperpolarizing factor in guinea-pig basilar artery. *Naunyn-Schmiedebergs Arch Pharmacol.* 2000;361(5):535-42.

19. Johnson DE, Heald SL, Dally RD, Janis RA. Isolation, identification and synthesis of an endogenous arachidonic amide that inhibits calcium channel antagonist 1,4-dihydropyridine binding. *Prostaglandins Leukot Essent Fatty Acids* 1993;48(6):429-37.

20. Chemin J, Monteil A, Perez-Reyes E, Nargeot J, Lory P. Direct inhibition of T-type calcium channels by the endogenous cannabinoid anandamide. *EMBO J* 2001;20(24):7033-40.

21. Ho WSV, Hiley CR. Endothelium-independent relaxation to cannabinoids in rat-isolated mesenteric artery and role of Ca^{2+} influx. *Br J Pharmacol.* 2003;139(3):585-97.

22. Ruehlmann DO, Lee CH, Poburko D, van Breemen C. Asynchronous Ca^{2+} waves in intact venous smooth muscle. *Circ Res.* 2000;86(4):E72-E79.

23. Zang WJ, Balke CW, Wier WG. Graded alpha(1)-adrenoceptor activation of arteries involves recruitment of smooth muscle cells to produce all or none Ca^{2+} signals. *Cell Calcium.* 2001;29(5):327-34.

24. Mauban JRH, Lamont C, Balke CW, Wier WG. Adrenergic stimulation of rat resistance arteries affects Ca^{2+} sparks, Ca^{2+} waves, and Ca^{2+} oscillations. *Am J Physiol.* 2001;280(5):H2399-H2405.

25. Peng HL, Matchkov V, Ivarsen A, Aalkjaer C, Nilsson H. Hypothesis for the initiation of vasomotion. *Circ Res.* 2001;88(8):810-5.

26. Lamboley M, Schuster A, Beny JL, Meister JJ. Recruitment of smooth muscle cells and arterial vasomotion. *Am J Physiol.* 2003;285(2):H562-H569.

27. Iino M, Kasai H, Yamazawa T. Visualization of neural control of intracellular Ca^{2+} concentration in single vascular smooth muscle cells in situ. *EMBO J.* 1994;13(21):5026-31.

28. Kasai Y, Yamazawa T, Sakurai T, Taketani Y, Iino M. Endothelium-dependent frequency modulation of Ca^{2+} signalling in individual vascular smooth muscle cells of the rat. *J Physiol.* 1997;504(2):349-57.

29. Miriel VA, Mauban JRH, Blaustein MP, Wier WG. Local and cellular Ca^{2+} transients in smooth muscle of pressurized rat resistance arteries during myogenic and agonist stimulation. *J Physiol.* 1999;518(3):815-24.

30. Wier WG, Morgan KG. Alpha1-adrenergic signaling mechanisms in contraction of resistance arteries. *Rev Physiol Biochem Pharmacol.* 2003;150:91-139.

Summary

Vascular blood flow is regulated by a complex series of mechanisms which, by altering the diameter of the vessels of a given tissue, maintain tissue homeostasis. Vasodilatation plays an important role in the regulation of the perfusion of vascular beds. The aim of this thesis was to investigate the importance and the mechanism of action of several vasodilatory substances in isolated gastric and small mesenteric arteries of the rat and to elucidate their role in gastrointestinal blood flow. We measured membrane potential changes with conventional microelectrode techniques, isometric tension changes with a wire myograph and observed the Ca^{2+} dynamics in the smooth muscle cells using confocal microscopy. These techniques are extensively described in **chapter 2**.

It is now generally accepted that the vascular endothelium plays a crucial role in the control of blood vessel tone and blood flow and the role of the endothelium-dependent vasorelaxing factors nitric oxide (NO) and prostacycline (PGI_2) is well established. However, despite extensive research, the exact mechanism involved in endothelium-dependent hyperpolarization is still a subject of intense discussion. While some studies point to a diffusible factor (EDHF) released from the endothelial cells, other reports support the idea of an electrical current or small messenger molecule spread through myoendothelial gap junctions. In **chapter 3**, we found that gap junctions indeed play some role in the endothelium-dependent hyperpolarization of rat small mesenteric arteries, while no evidence was found for the involvement of inward rectifying K^+ (K_{IR}) channels in this response. The involvement of Na^+/K^+ pumps could not be totally excluded, however, our results point to the activation of an as yet

unidentified, but Ba^{2+} resistant K^+ current accounting for a significant fraction of the endothelium-dependent hyperpolarization. We used the K_{IR} channel inhibitor Ba^{2+} to reduce the steady state extracellular K^+ concentration around the smooth muscle cells. We found that under these circumstances, the endothelium-dependent hyperpolarization relies to a lesser extent on gap junctional coupling.

During the search for the mechanism underlying endothelium-dependent hyperpolarization, it has become clear that there are considerable tissue and species differences and that various hyperpolarizing mechanisms may exist in different vascular beds. Moreover, some arteries even lack any endothelium-dependent hyperpolarizing responses. In **chapter 4**, we demonstrated the existence of an EDH(F) in rat gastric arteries stimulated with acetylcholine. The induced hyperpolarization seemed to be endothelium-dependent but independent of the NO or PGI_2 pathway and did not seem to rely on the stimulation of K_{IR} channels or Na^+/K^+ pumps. The demonstration of endothelium-dependent hyperpolarization in these arteries could reveal an important and rapid regulator of gastric mucosal blood flow.

Since the discovery of the existence of EDHF, several possible candidates have been proposed, among which the endocannabinoid anandamide. However, this hypothesis has widely been argued and it is now generally accepted that anandamide is not EDHF. This was further confirmed in **chapter 5** for rat mesenteric and gastric arteries. We found that methanandamide, a stable analogue of anandamide, potently hyperpolarized the smooth muscle cells of both rat gastric and mesenteric arteries. This hyperpolarization, however, showed a different time course and pharmacological profile as compared to the EDHF-response, excluding

a role for EDHF in the membrane electrical response to cannabinoids in these preparations. We showed that stimulation of $TRPV_1$ receptors on perivascular CGRP containing nerves is the primary cause for the cannabinoid-induced hyperpolarization in the mesenteric and gastric arteries. The released CGRP subsequently hyperpolarizes the vascular smooth muscle cells through activation of ATP sensitive K^+ (K_{ATP}) channels.

Membrane hyperpolarization is a powerful mediator of vasorelaxation. Therefore, in **chapter 6** we characterized for the first time the vasorelaxation to cannabinoids in rat gastric arteries. We showed that methanandamide is a powerful vasorelaxant in isolated rat small gastric arteries. The induced relaxation is endothelium-independent and does not involve the activation of the CB_1 or CB_2 cannabinoid receptor or the recently described non CB_1/CB_2 cannabinoid receptor. We found that activation of $TRPV_1$ receptors does not fully account for the methanandamide-induced relaxation, but might contribute to the relaxations induced by the lower concentrations of the cannabinoid. Furthermore, higher concentrations of methanandamide might possibly relax the arteries by inhibition of Ca^{2+} influx in the smooth muscle cells.

In **chapter 7** we studied the Ca^{2+} dynamics in the smooth muscle cells of rat small mesenteric arteries. More specifically, we observed the influence of hyperpolarization and depolarization of the membrane potential on norepinephrine-induced Ca^{2+} oscillations in smooth muscle cells of intact small mesenteric arteries of the rat. We confirmed that stimulation with low concentrations of norepinephrine induces asynchronous Ca^{2+} spikes in the smooth muscle cells usually accompanied by a sustained increase of the basal fluorescence. Depolarization (with 15 mM KCl) caused a significant increase in the Ca^{2+} responses and synchronized the oscillations. In

contrast, hyperpolarization (with levcromakalim, CGRP or eventually with 5 mM KCl) significantly reduced the Ca^{2+} responses.

In conclusion, the different studies compiled in this thesis further elucidate the characteristics and the mechanism of action of EDHF and endocannabinoids, both important mediators of the arterial tone. Additionally, the influence of the membrane potential on the Ca^{2+} dynamics of the smooth muscle cells was to some extent clarified.

Samenvatting

Weefseldoorbloeding wordt geregeld door een complexe reeks mechanismen die, hoofdzakelijk door het regelen van de diameter van de bloedvaten, zorgen voor het behoud van de weefselhomeostase. Vasodilatatie speelt een belangrijke rol in de regeling van de doorbloeding van een bepaald vaatbed. Het voornaamste doel van het onderzoek verricht in het kader van deze thesis, was meer te weten te komen over het belang en de werkingsmechanismen van verschillende vasodilaterende stoffen in geïsoleerde maag- en mesenterische arteriën van de rat om zo tot een beter inzicht te komen over hun rol in de gastro-intestinale doorbloeding. In dit onderzoek werd gebruik gemaakt van verschillende *in vitro* technieken op geïsoleerde bloedvaten: membraanpotentiaalmetingen met behulp van conventionele micro-elektroden, isometrische tensiemetingen met een draadmyograaf en calcium bepalingen door middel van confocale microscopie. Deze technieken werden uitvoerig beschreven in **hoofdstuk 2**.

Het is op heden algemeen aanvaard dat het vaatendotheel een belangrijke rol speelt in de controle van de vaattonus en de bloedstroom. Terwijl de rol van de endotheel-afhankelijke vasorelaxerende factoren stikstof monoxide (NO) en prostacycline (PGI_2) al grondig gekend is, heeft men het exacte mechanisme verantwoordelijk voor de endotheel-afhankelijke hyperpolarisatie nog steeds niet achterhaald. Volgens sommige studies betreft het een diffunderende factor die vrijgesteld wordt uit het endotheel (EDHF). Andere experimenten wijzen eerder op een elektrische stroom of kleine boodschappermolecule die de hyperpolarisatie van het endotheel naar de gladde spiercellen overbrengt via gap juncties. In **hoofdstuk 3**

werd aangetoond dat gap junctie inderdaad een rol spelen in de endotheel-afhankelijke hyperpolarisatie in mesenterische arteriën van de rat. Er werd geen bewijs gevonden dat K_{IR} kanalen betrokken zijn in deze respons, terwijl een rol voor de Na^+/K^+ pompen niet kon worden uitgesloten. Onze resultaten suggereren eerder dat de activering van een nog niet geïdentificeerde, Ba^{2+} resistente K^+ stroom verantwoordelijk is voor een aanzienlijk deel van de endotheel-afhankelijke hyperpolarisatie. Met behulp van Ba^{2+}, een K_{IR} inhibitor, reduceerden we de extracellulaire K^+ concentratie in de omgeving van de gladde spiercellen, wat ertoe leidde dat gap juncties minder inbreng kregen in de endotheel-afhankelijke hyperpolarisatie.

In de loop der jaren is gebleken dat endotheel-afhankelijke hyperpolarisaties heel wat weefsel- en speciesverschillen vertonen. Diverse hyperpolariserende mechanismen kunnen voorkomen in verschillende vaatgebieden, maar ze kunnen in bepaalde bloedvaten ook helemaal ontbreken. In **hoofdstuk 4** werd endotheel-afhankelijke hyperpolarisatie aangetoond in rat gastrische arteriën na toevoegen van acetylcholine. Deze hyperpolarisatie bleek volledig onafhankelijk van NO en PGI_2. Er werd aangetoond dat zowel K_{IR} als Na^+/K^+ ATPasen helemaal geen rol spelen in deze respons. Deze hyperpolarisatie zou een belangrijke en snelle regulator kunnen betekenen voor de maagdoorbloeding.

Sinds de ontdekking van EDHF zijn al uiteenlopende kandidaten naar voor geschoven, onder wie de endocannabinoid anandamide. Op heden is het echter algemeen aanvaard dat anandamide geen EDHF kan zijn. Dit werd bevestigd in **hoofdstuk 5** voor de gastrische en de mesenterische arteriën van de rat. Daarin werd aangetoond dat methanandamide, de stabielere analoog van anandamide, een sterke hyperpolarisatie veroorzaakt in de

gladde spiercellen van zowel de maag- als de mesenterische bloedvaten. Het tijdsverloop en de farmacologische eigenschappen verschillen echter zeer sterk van deze van de EDHF-respons. Uit onze resultaten bleek dat methanandamide de membraanpotentiaal hyperpolariseert door stimulatie van de $TRPV_1$ receptoren op de perivasculaire zenuwen. De daaropvolgende vrijstelling van CGRP hyperpolariseert de membraan van de gladde spiercellen door activering van ATP-gevoelige K^+ (K_{ATP}) kanalen.

Hyperpolarisatie ligt vaak aan de basis van vasorelaxatie. In **hoofdstuk 6** hebben we de relaxerende eigenschappen van cannabinoiden onderzocht in de maagarterie van de rat. Methanandamide lokte sterke endotheel-onafhankelijke relaxaties uit, maar hyperpolarisatie bleek hier slechts een beperkte rol in te spelen. Bovendien toonden we aan dat geen enkele van de beschreven cannabinoid receptoren betrokken is in deze relaxaties. Activering van de $TRPV_1$ receptor op de perivasculaire zenuwen droeg enkel bij tot de relaxaties veroorzaakt door de lagere concentraties methanandamide. Hogere concentraties van de cannabinoid zouden de arteriën kunnen relaxeren door inhibitie van de Ca^{2+} influx in de gladde spiercellen.

Tot slot hebben we in **hoofdstuk 7** de Ca^{2+} veranderingen bestudeerd in de gladde spiercellen van de mesenterische arteriën van de rat. Meerbepaald hebben we de invloed nagegaan van veranderingen in de membraanpotentiaal op Ca^{2+}-oscillaties geïnduceerd door norepinephrine. Er werd aangetoond dat stimulatie met deze agonist asynchrone Ca^{2+} spikes uitlokt in de gladde spiercellen, die meestal gepaard gaan met een toename van de basale fluorescentie. Depolarisatie van de membraanpotentiaal (met 15 mM KCl) veroorzaakte een significante toename van de Ca^{2+} responsen en leidde tot synchronisatie van de

oscillaties. Daar tegenover staat dat hyperpolarisatie (met levcromakalim, CGRP en mogelijk ook met 5 mM KCl) zorgde voor een significante afname van de responsen.

In conclusie, de verschillende studies gebundeld in deze thesis bieden meer inzicht in de eigenschappen en de werkingsmechanismen van EDHF en van cannabinoiden bij kleine bloedvaten. Daarnaast werd de rol van de membraanpotentiaal in de Ca^{2+} dynamiek van de gladde spiercellen uitgediept.

Dankwoord

Tot slot had ik een woord van dank willen richten tot alle mensen die in de afgelopen zes jaar direct of indirect hebben bijgedragen tot het verwezenlijken van mijn doctoraat. Zo zijn er de mensen waarmee ik intensief heb samengewerkt in blok B en die stuk voor stuk hebben meegeholpen aan het realiseren van alle data die zich in dit proefschrift bevinden. Maar er zijn ook heel wat mensen die steeds voor me klaarstonden met raad en daad, die voor de nodige niet-wetenschappelijke afleiding zorgden en die me oppepten en me alles leerden relativeren als het me even teveel werd… Op deze laatste pagina's hoop ik duidelijk te kunnen maken hoe elk van jullie zijn steentje heeft bijgedragen tot deze doctoraatsthesis.

Vooreerst wil ik mijn promotor *Prof. Bert Vanheel* bedanken voor de kans die ik zes jaar geleden kreeg om dit onderzoek uit te voeren en voor de hulp om het tot een goed einde te brengen. U leerde me de knepen van de elektrofysiologie en de trucjes voor het welslagen van de o zo delicate membraanpotentiaal metingen. Daarnaast waardeer ik ook uw hulp bij het uitvoeren van de experimenten, het schrijven van artikels en het presenteren van mijn onderzoeksresultaten.

Mijn bijzondere dank gaat ook uit naar *Prof. Johan Van de Voorde*, voor zijn interesse en bezorgdheid, het kritisch nalezen van manuscripten (geen dubbele spatie kon aan uw oog ontglippen!) en vooral voor de prettige samenwerking. U heeft me wegwijs gemaakt in de wereld van de relaxaties en contracties en in de periode dat de resultaten met de membraanpotentiaal metingen wat tegenvielen kon ik op de tweede

verdieping terecht voor enkele tensiemetingen. Uw enthousiasme en inzet kenden geen grenzen, wat ik enorm heb geapprecieerd.

Prof. Luc Leybaert zou ik willen bedanken voor het ter beschikking stellen van de confocale microscoop en het kritisch nalezen van artikels. U hebt me binnengeleid in de wereld van de Ca^{2+}-golven, hielp me bij het opmaken van de vele foto's en beelden en stond steeds klaar voor een woordje uitleg. Ook *Prof. Gaspard De Ley* zou ik willen bedanken voor de samenwerking tijdens de practica.

Prof. Dr. Em. J. Weyne en *Prof. Dr. J.-L. Pannier*, vakgroepvoorzitters van de vakgroep Fysiologie en Fysiopathologie, ben ik dankbaar voor het ter beschikking stellen van de middelen en het personeel van het labo. *Prof. Weyne*, u volgde mijn werk met veel enthousiasme en ik kon steeds rekenen op uw hulp en begrip.

Prof. Dr. H. Bult, Prof. Dr. G. Callewaert, Prof. Dr. W. Derave, Prof. Dr. R. Lefebvre, Prof. Dr. G. Joos, Prof. Dr. J. Van de Voorde en Prof. Dr. L. Leybaert, de leden van de examencommissie, wil ik graag bedanken voor hun kritische evaluatie van deze thesis en voor hun opbouwende suggesties.

Tijdens de jaren onderzoek die een doctoraat voorafgaan kom je heel wat verwachte en onverwachte hindernissen tegen en dankzij de hulp van heel wat mensen op het labo ben ik er in geslaagd deze stuk voor stuk te overwinnen. Indien ik alles op mijn eentje had moeten verwezenlijken, dan ben ik er steevast van overtuigd dat ik vaak zou zijn blijven steken zijn in 'onoverkomelijke' problemen. *Julien*, jij was steeds het zonnetje in blok B en zorgde voor de nodige 'entertainment'. Voor praktische probleempjes

kon ik steeds bij jou terecht: jij toverde in een handomdraai de nodige draadjes, naaldjes of buisjes tevoorschijn. Daarnaast zorgde je steeds dat iedereen voldoende energie had om zijn proeven uit te voeren: chocolade, snoepjes, koffiekoeken, ijsjes, fruit,…je legde ons echt in de watten! *Dirk*, jij stond niet alleen paraat om computer- en andere technische problemen op te lossen, maar je was ook steeds te vinden voor een gezellige babbel. Nu je op pensioen bent zullen de computerfrustraties in blok B hoogstwaarschijnlijk sterk toenemen. Ook *Cyriel* zou ik willen bedanken voor de technische hulp. *Eric* zou ik willen bedanken voor de hulp bij het uitvoeren van de tensiemetingen en het maken van oplossingen. *André* was steeds op post voor het oplossen van administratieve en organisatorische problemen en heeft menigmaal gefunctioneerd als 'telefoonboek' van blok B. *Marc* stond altijd klaar met advies en hulp bij het maken van figuren en posters en was een vaste waarde voor de practica. Graag wil ik ook *Eliane Dewulf* bedanken, die tot haar pensioen instond voor het maken van de perfusie en de vele oplossingen. Ook *Daniël* zou ik willen bedanken voor de organisatorische hulp.

Ik mag ook zeker mijn collega doctoraatsstudenten niet vergeten! De frustraties, tegenslagen en 'dipjes' verdwijnen in het niets als ik terugdenk aan de vele fijne uurtjes die we in blok B hebben beleefd. *Koen, Siska* en *Ine*, de anciens, wil ik bedanken voor de leuke koffiekletskes, de soms hilarische momenten, maar ook voor de hulp bij proeven, de steun en het luisterend oor. Daarnaast wil ik ook *Sofie* en *Nele* en de vele andere (ex)doctoraatsstudenten bedanken die mijn verblijf in het labo aangenaam gemaakt hebben.

Ook mijn *familie, schoonfamilie en vrienden* verdienen een woordje van dank voor hun nimmer aflatende steun, interesse en vooral voor de nodige afleiding na de werkuren.

Een speciaal plaatsje in dit dankwoord is voorbehouden aan mijn ouders. *Mama en papa*, het is een onmogelijke opdracht in enkele regels te omschrijven hoe groot jullie bijdrage was aan dit eindresultaat. Jullie gaven me de kans om te studeren, zorgden dat ik nooit iets tekort kwam en steunden me bij elke beslissing. Jullie leerden me door te bijten en alles te relativeren als het eens moeilijk ging. Ik kon steeds bij jullie terecht om mijn hart te luchten en jullie deelden mijn geluk. Jullie stonden ook steeds klaar voor mij en boden zoveel hulp als jullie maar konden: taxidienst, boodschappenservice, restaurant, lay-out advies, noem maar op,… Hartelijk dank daarvoor!

Kristof, mijn doctoraat is af! Ik kan je voor zoveel dingen bedanken. Ondanks je drukke praktijk en de lange werkdagen die je klopt, bleef je me door dik en dun steunen. Je luisterde naar mijn werk-frustraties, toonde begrip, overleefde mijn kuren en motiveerde mij om door te zetten in moeilijker tijden. Je zorgde voor de nodige afleiding op de momenten dat ik die nodig had. Je bent er één-uit-de-duizend!

Allemaal zeer hartelijk dank!

Joke